

INSTYTUT PODSTAWOWYCH PROBLEMÓW TECHNIKI  
POLSKA AKADEMIA NAUK



ROZPRAWA DOKTORSKA

**Modyfikacja powierzchni włókien z biodegradowalnych poliestrów alifatycznych za pomocą reakcji aminolizy i przyłączania żelatyny do zastosowań w inżynierii tkankowej**

Surface modification of biodegradable aliphatic polyester fibers using aminolysis reaction and gelatin attachment for applications in tissue engineering

mgr inż. Oliwia Jeznach

Praca wykonana w Samodzielnej Pracowni Polimerów i Biomateriałów  
pod kierunkiem Prof. dr hab. inż. Pawła Łukasza Sajkiewicza  
Promotor pomocniczy: dr inż. Dorota Kołbuk-Konieczny

WARSZAWA 2024

Badania prowadzone w ramach niniejszej pracy były częścią projektu OPUS o numerze 2016/23/B/ST8/03409 finansowanego przez Narodowe Centrum Nauki oraz projektu POWER Och! DOK o numerze POWR.03.02.00-00-1028/17-00 realizowanego w ramach Programu Operacyjnego Wiedza Edukacja Rozwój 2014-2020 oraz współfinansowanego ze środków Europejskiego Funduszu Społecznego.



Fundusze Europejskie  
Wiedza Edukacja Rozwój



Rzeczpospolita Polska

Unia Europejska  
Europejski Fundusz Społeczny



## **Składam serdeczne podziękowania**

*Panu Profesorowi Pawłowi Łukaszowi Sajkiewiczowi za opiekę merytoryczną i przekazaną wiedzę, a także za okazane wsparcie i życzliwość*

*Pani Doktor Dorocie Kołbuk-Konieczny za poświęcony czas, pozytywną motywację i inspirację w realizacji badań*

*Wszystkim koleżankom i kolegom z Samodzielnej Pracowni Polimerów i Biomaterialów za cenne wskazówki w realizacji badań i okazaną serdeczność*

*Mężowi za wsparcie, ogromną wyrozumiałość i nieoceniony humor*

*Rodzicom za motywację i przekazane wartości towarzyszące mi w realizacji pracy*

*Wszystkim Bliskim, którzy wspierali mnie w drodze do ukończenia pracy*

*Córeczce Poli*

## **Streszczenie**

Niniejsza rozprawa doktorska obejmuje badania nad modyfikacją powierzchni włókien polimerowych wykorzystywanych jako podłoża komórkowe w inżynierii tkankowej. Włókna zostały otrzymane metodą elektroprzędzenia z trzech poliestrów alifatycznych należących do najczęściej wykorzystywanych w inżynierii tkankowej: poli(kaprolaktonu), poli(L-laktydu) i poli(L-laktydu-ko-kaprolaktonu). Poliestry różniły się częstością występowania reaktywnych grup estrowych w łańcuchu makrocząsteczki, temperaturą zeszklenia i stopniem krystaliczności. Celem modyfikacji była poprawa wzrostu komórek na podłożu poprzez wprowadzenie grup aminowych na powierzchnię i przyłączenie żelatyny zawierającej sekwencję peptydową rozpoznawaną przez komórki. Takie zmiany na poziomie molekularnym skutkują zwiększeniem hydrofilowości oraz wprowadzeniem biologicznej aktywności podłożu. Pierwszym etapem modyfikacji było przeprowadzenie reakcji aminolizy, a drugim przyłączenie żelatyny za pomocą sieciowania glutaraldehydem. W ramach rozprawy wykonano badania mające na celu analizę mechanizmów modyfikacji oraz badania zmian właściwości podłożu i odpowiedzi komórkowej. Wyniki wskazały, że aminoliza prowadzona w tych samych warunkach zachodzi wolniej na włóknach niż na kontrolnych foliach poliestrowych oraz reaktywność włókien PCL jest znacznie niższa niż włókien PLCL i PLLA. Przedstawiono mechanizmy obserwowanych zależności. Wykazano też, że łagodne warunki funkcjonalizacji powodują wprowadzenie wystarczającej ilości grup aminowych do włókien na tyle, aby poprawić odpowiedź komórkową a jednocześnie zachować wyjściową morfologię włókien i bliskie wyjściowym właściwości mechaniczne. Stwierdzono pozytywny wpływ zarówno chemicznego jak i kontrolnego fizycznego przyłączania żelatyny na odpowiedź komórkową, ze wskazaniem na lepszy efekt przyłączania chemicznego i większą stabilność wiązania żelatyny w roztworze PBS. Przyczyną bardziej pozytywnego wpływu przyłączania chemicznego na odpowiedź komórek może być zarówno wyższa koncentracja żelatyny jak i jej specyficzna konformacja molekularna, zapewniająca lepszą ekspozycję sekwencji peptydowych rozpoznawanych przez komórki.

## **Abstract**

This doctoral thesis concerns research on the surface modification of polymer fibers used as cell substrates in tissue engineering. The fibers were obtained via electrospinning technique from three aliphatic polyesters, poly(caprolactone), poly(L-lactide), and poly(L-lactide-co-caprolactone), being one of the most commonly used polymers in the tissue engineering. Given polyesters differed in frequency of ester groups in macromolecule chain, glass transition temperature, and degree of crystallinity. The aim of the modification was to improve cell growth on the substrate by introducing amine groups onto the surface and immobilization of gelatin containing peptide sequence, which is recognized by cells. Such changes on the molecular level result in an increase in wettability and the introduction of the biological activity of the substrate. The first step of the modification was an aminolysis reaction, and the second one - was gelatin immobilization via glutaraldehyde crosslinking. Modification mechanism and impact on substrate properties and cell response were studied. The results indicated that aminolysis conducted in the same conditions proceeds slower on the fibers than on control polyester films. Moreover, it was observed that the reactivity of PCL fibers is significantly lower in comparison to PLCL and PLLA. Mechanisms of the observed dependence were presented. It has been shown that mild conditions of the aminolysis functionalization cause the introduction of sufficient quantities of amine groups on the fiber surface to improve cell response while fiber morphology and mechanical properties are close to the initial ones. It was found that both chemical and physical attaching the gelatin improved cell response. However, a superior effect of immobilized gelatin and its higher stability in PBS solution were demonstrated for chemical modification. The reason for a more positive effect of chemical immobilization on cell response could be a higher amount of gelatin and/or its specific molecular conformation, which provides better exposure of peptide sequences recognized by cells.

## **Spis treści**

|         |   |    |
|---------|---|----|
| 1.      | Wstęp .....   | 11 |
| 2.      | Cele pracy .....  | 16 |
| 3.      | Hipoteza badawcza .....   | 16 |
| 4.      | Materiały .....   | 17 |
| 4.1.    | Poliestry alifatyczne .....   | 17 |
| 4.2.    | Etylenodiamina .....  | 17 |
| 4.3.    | Glutaraldehyd .....   | 17 |
| 4.4.    | Żelatyna .....  | 18 |
| 5.      | Metody .....  | 18 |
| 5.1.    | Formowanie włóknin poliestrowych .....  | 18 |
| 5.2.    | Formowanie folii poliestrowych .....  | 19 |
| 5.3.    | Funkcjonalizacja włókien i folii poliestrowych za pomocą reakcji aminolizy .....  | 19 |
| 5.4.    | Przyłączenie żelatyny do powierzchni włókien poliestrowych funkcjonalizowanych za pomocą reakcji aminolizy .....                    | 19 |
| 5.5.    | Funkcjonalizacja włókien poliestrowych za pomocą reakcji hydrolizy .....  | 20 |
| 5.6.    | Funkcjonalizacja włókien poliestrowych za pomocą obróbki niskotemperaturową plazmą tlenową .....                                    | 20 |
| 5.7.    | Przyłączenie żelatyny do powierzchni włókien poliestrowych funkcjonalizowanych za pomocą reakcji hydrolizy lub obróbki plazmą ..... | 21 |
| 5.8.    | Charakteryzacja włókien poliestrowych po modyfikacji .....  | 21 |
| 5.8.1.  | Obrazowanie włókien za pomocą skaningowej mikroskopii elektronowej .....  | 21 |
| 5.8.2.  | Ocena stężenia przyłączonych grup aminowych .....   | 21 |
| 5.8.3.  | Ocena stężenia przyłączonej żelatyny .....  | 21 |
| 5.8.4.  | Ocena struktury molekularnej powierzchni próbek .....   | 22 |
| 5.8.5.  | Ocena struktury supermolekularnej próbek .....  | 22 |
| 5.8.6.  | Pomiar zwilżalności .....   | 23 |
| 5.8.7.  | Pomiar zmian mas cząsteczkowych .....   | 23 |
| 5.8.8.  | Wyznaczenie właściwości mechanicznych .....   | 23 |
| 5.8.9.  | Pomiar odczynu pH .....   | 24 |
| 5.8.10. | Wyznaczenie swobodnej energii powierzchniowej .....   | 24 |
| 5.8.11. | Ocena stabilności przyłączonej warstwy żelatyny .....   | 24 |
| 5.8.12. | Ocena odpowiedzi komórkowej .....   | 24 |

|   |    |
|---|----|
| 5.8.13 Analiza statystyczna .....   | 25 |
| 6. Publikacje włączone w cykl .....   | 26 |
| 6.1. Aminolysis of various aliphatic polyesters in a form of nanofibers and films .....   | 27 |
| 6.2. Aminolysis as a surface functionalization method of aliphatic polyester nonwovens: impact on material properties and biological response ..... | 29 |
| 6.3. Immobilization of gelatin on fibers for tissue engineering applications: a comparative study of three aliphatic polyesters .....               | 31 |
| 6.4. A comparative study of three approaches to fibre's surface functionalization .....   | 34 |
| 7. Podsumowanie i wnioski .....   | 37 |
| 8. Elementy wkładu oryginalnego .....   | 39 |
| 9. Literatura .....   | 41 |
| 10. Publikacje naukowe włączone do rozprawy.....  | 44 |

## Skróty

- ANOVA jednoczynnikowa analiza wariancji (ang. analysis of variance)
- ALD osadzanie warstw atomowych (ang. atomic layer deposition)
- ATR-FTIR fourierowska spektroskopia w podczerwieni osłabionego całkowitego odbicia (ang. attenuated total reflection–Fourier transform infrared spectroscopy)
- ATRP polimeryzacja rodnikowa z przeniesieniem atomu (ang. atom transfer radical polymerization)
- BCA kwas bicynchoninowy (ang. bicinchoninic acid)
- ECM macierz międzykomórkowa (ang. extracellular matrix)
- EDA etylenodiamina
- EDC/NHS 1-etylo-3-(3-dimetyloaminopropylo)karbodiimid/N-hydroksysukcynimid (ang. 1-Ethyl-3-(3-dimethylaminopropyl)carbodiimide/N-hydroxysuccinimide)
- GPC chromatografia żelowa (ang. gel permeation chromatography)
- L929 linia fibroblastów mysich
- MG-63 linia osteoblastopodobnych komórek ludzkich
- PBS buforowana fosforanem sól fizjologiczna (ang. phosphate-buffered saline)
- PCL poli( $\epsilon$ -kaprolakton) (ang. poly( $\epsilon$ -caprolactone))
- PGA poli(glikolid) (ang. poly(glycolic acid))
- pH ilościowa skala kwasowości i zasadowości roztworów wodnych związków chemicznych
- pI punkt izoelektryczny
- PI współczynnik polidispersyjności (ang. polydispersity index)
- PLCL poli(L-laktyd-ko-kaprolakton) (ang. poly(L-lactide-co-caprolactone))
- PLGA poli(L-laktyd-ko-glikolid) (ang. poly(L-lactide-co-glycolic acid))
- PLLA poli(L-laktyd) (ang. poly(L-lactide))

RGD sekwencja aminokwasów: arginina-glicyna-kwas asparaginowy, (ang. arginine (R), glycine (G), aspartic acid (D), Arg-Gly-Asp)

SEM skaningowa mikroskopia elektronowa (ang. scanning electron microscopy)

THF tetrahydrofuran

WAXS szerokątowe rozpraszanie rentgenowskie (ang. wide-angle X-ray scattering)

XPS rentgenowska spektrometria fotoelektronów (ang. X-ray photoelectron spectroscopy)

## **1. Wstęp**

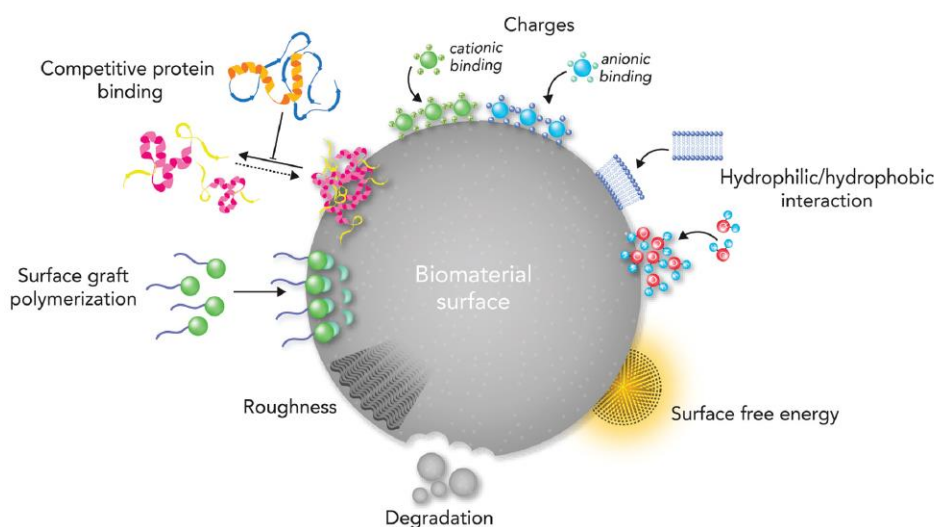
Inżynieria tkankowa jest dyscypliną, której początki przypadają na wczesne lata 90. XX wieku. W 1993 roku została zdefiniowana przez Profesora Roberta Langer i Doktora Josepha Vacantiego na łamach czasopisma *Science* jako „interdyscyplinarna dziedzina, wykorzystująca podstawy inżynierii i nauk biologicznych w celu pozyskania biologicznych zamienników, które przywracają, utrzymują lub poprawiają funkcjonowanie organu” [1]. Obecnie pod hasłem “tissue engineering” można wyszukać 89118 oryginalnych artykułów w bazie publikacji naukowych *Scopus* [2].

Należy podkreślić, że w niniejszej rozprawie pod terminem „inżynieria tkankowa” rozumie się badanie i wykorzystanie biomateriałowych biodegradowalnych podłoży wszczepianych do organizmu, mających służyć jako tymczasowe wsparcie dla wzrostu komórek regenerowanej tkanki. W literaturze termin „inżynieria tkankowa” funkcjonuje również w stosunku do rozwiązań wykorzystujących podłożą biomateriałową zasiedlaną komórkami *ex vivo* [3], a także w odniesieniu do materiałów pełniących funkcję nośników wszczepianych komórek, takich jak hydrożele [4].

Według definicji *European Society for Biomaterials* biomateriał to substancja inna niż lek lub kombinacja substancji syntetycznych lub naturalnych, która może być użyta w dowolnym czasie jako część lub całość systemu, zastępując tkankę lub organ, lub pełniąc jego funkcję [5]. Jak wspomniano wcześniej, w inżynierii tkankowej wykorzystuje się podłożą wykonane z biodegradowalnych biomateriałów, których celem jest tymczasowe zastąpienie funkcji tkanki i umożliwienie jej odbudowy. Podłożą komórkowe dla celów inżynierii tkankowej powinny charakteryzować się biozgodnością i bioaktywnością, odpowiednią strukturą przestrenną, odpowiednimi właściwościami mechanicznymi, odpowiednią szybkością biodegradacji, porowatością umożliwiającą transport substancji odżywczących, strukturą optymalną dla wzrostu komórek danej tkanki oraz powinny być sterylizowalne [6, 7].

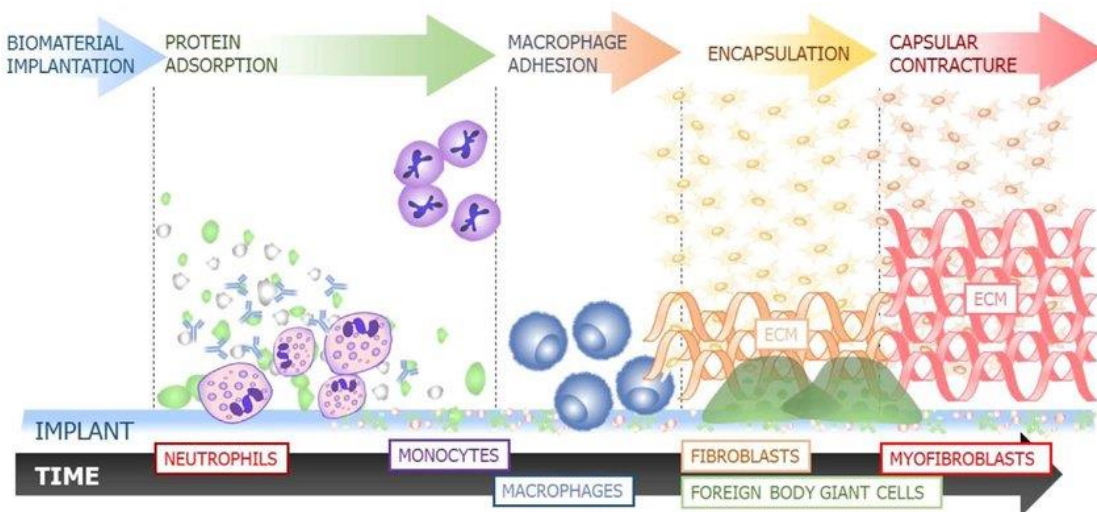
Poliestry alifatyczne, które są przedmiotem niniejszej rozprawy wykazują szereg korzystnych właściwości – są biokompatybilne, biodegradowalne i łatwo przetwarzalne za pomocą różnych technik. Formowane z nich metodą elektroprzędzenia podłożą komórkowe imitują układ włókien macierzy pozakomórkowej ECM. Jednak równocześnie, podłożą te są hydrofobowe i nieaktywne biologicznie, co jest niekorzystne z perspektywy adhezji i proliferacji komórek na podłożu. Należy zaznaczyć, że na początkowym etapie wzrostu komórek szczególne znaczenie ma ich oddziaływanie z powierzchnią podłożą, które jest zależne od zaadsorbowanych (lub wcześniej przyłączonych) białek.

Wszczepienie obcego materiału do organizmu wywołuje natychmiastową reakcję fizjologiczną obejmującą na początku adsorpcję białek (m.in. fibronektyny, fibrynogenu, albuminy) z otaczającego płynu na powierzchni materiału [8]. Adsorpcja białek jest skomplikowanym i niestabilnym procesem zależnym od właściwości otaczających płynów takich jak odczyn pH, temperatura, stężenie jonów i kompozycja medium [9], i od właściwości powierzchni materiału, np. zwilżalności, swobodnej energii powierzchniowej, polarności, ładunku i rodzaju grup funkcyjnych czy topografii (**Rys. 1.**) [10, 11]. Parametry te determinują rodzaj, ilość, orientację i konformację zaadsorbowanych białek co przekłada się na dalszą odpowiedź biologiczną. Na przykład, zaobserwowano, że powierzchnie bardzo hydrofobowe sprzyjają adsorpcji białek, ale i dochodzi na nich do ich denaturacji. Jest to spowodowane silnymi oddziaływaniami hydrofobowej powierzchni i cząsteczki białka prowadzącymi do zmian konformacji cząsteczki [10]. Może to prowadzić do utraty biologicznej aktywności białka. Z kolei powierzchnie bardzo hydrofilowe ze względu na zaadsorbowaną warstwę wody i niską energię swobodną na styku faz mogą w ogóle nie adsorbować białek co skutkuje dalej brakiem adhezji komórek na powierzchni materiału [12]. Równocześnie, adsorpcja określonych białek (np. albuminy) [13] lub zmiana konformacji przestrzennej białka na hydrofobowej powierzchni i ekspozycja danych sekwencji peptydowych może aktywować komórki żerne, makrofagi, w kierunku prozapalnym i w konsekwencji doprowadzić dotworzenia łącznotkankowej włóknistej otoczki wokół podłożu komórkowego (**Rys.2.**), i dalej braku integracji podłożu komórkowego z otaczającą tkanką [14].



**Rysunek 1.** Kluczowe właściwości powierzchni podłożu wpływające na interakcję komórka-podłoże [15].

Adhezji pożądanych komórek na powierzchni podłoża sprzyja adsorpcja lub wcześniejsze przyłączenie odpowiednich białek (np. fibronektyny). Ważne jest tutaj odtworzenie naturalnego mechanizmu połączenia komórek z włóknami macierzy pozakomórkowej. Do połączenia komórka-włókno dochodzi za pomocą rozpoznawania danych sekwencji peptydowych białek macierzy przez receptory komórki, integryny [16]. Na przykład, sekwencja peptydowa składająca się z aminokwasów argininy, glicyny i kwasu asparaginowego (Arg-Gly-Asp, RGD) znajdująca się m.in. w fibronektynie i żelatynie jest rozpoznawana przez integryny  $\alpha v\beta 3$  i  $\alpha 5\beta 1$  obecne w wielu komórkach, np. fibroblastach linii L929 [17, 18]. Na dalszych etapach, jakość połączenia komórka-podłożo wpływa na funkcjonowanie komórki, jej proliferację, produkcję macierzy ECM, sekrecję genów, itd., a także odbiór sygnałów z otoczenia komórki. Tzw. „focal adhesions”, kompleksy integrynowe powiązane zarówno z włóknami ECM, jak i z włóknami aktynowymi komórek, pozwalają na przekazywanie sygnałów mechanicznych z macierzy pozakomórkowej do komórek [19], co powoduje, np. różnicowanie się komórek macierzystych do fenotypu osteoblastów. Wytworzenie dobrego połączenia między komórkami a podłożem ma więc bardzo istotny wpływ na proces odbudowy i funkcjonowanie tkanki.



Rys. 2. Etapy reakcji organizmu na wszczepiony biomateriał z uwzględnieniem reakcji obronnej na ciało obce [20].

Obecnie, obserwuje się znaczny rozwój metod modyfikacji powierzchni materiałów polimerowych dla inżynierii tkankowej [21, 22]. Do wykorzystywanych technik należą m.in. obróbka plazmą, obróbka promieniowaniem UV, osadzanie cienkich warstw (ALD), ablacja laserowa, metody chemiczne: hydroliza, aminoliza, polimeryzacja rodnikowa ATRP itd. [23]. Celem modyfikacji jest zmiana właściwości powierzchni mających znaczenie dla adsorpcji

białek lub takich, które bezpośrednio wpływają na adhezję i funkcjonowanie komórek. Na przykład, dodatnio naładowana powierzchnia materiału może oddziaływać z ujemnie naładowaną błoną komórkową, a zmiana topografii prowadzić do zmian kształtu komórek czy kierunku różnicowania komórek macierzystych. Drugim nurtem w modyfikacji powierzchni podłoży jest pokrywanie biomolekułami, bardzo często białkami, dzięki którym podłożo stają się bioaktywne. Białka przyłączane są przy wykorzystaniu fizycznej adsorpcji lub metod chemicznych [24]. Chemiczne przyłączanie często składa się z dwóch etapów, wprowadzenia grup funkcyjnych na powierzchni podłożu komórkowego, np. grup karboksylowych za pomocą obróbki plazmą czy hydrolizy, czy grup aminowych za pomocą reakcji aminolizy, a następnie etapu wiązania przyłączonych grup funkcyjnych z białkiem, np. za pomocą sieciowania z wykorzystaniem pochodnych karbodiimidowych czy za pomocą glutaraldehydu. Kluczową kwestią jest zachowanie aktywności biologicznej cząsteczki białka po przyłączeniu do podłożu komórkowego. Metoda fizycznej adsorpcji jest łatwiejsza do przeprowadzenia i nie wymaga stosowania agresywnych odczynników chemicznych, jednak może powodować denaturację cząsteczki białka. W takiej postaci białka mogą nie spełniać swojej funkcji biologicznej [10]. W literaturze zwraca się też uwagę na to, że białka przyłączone wiązaniem fizycznym podczas kontaktu z otaczającym płynem fizjologicznym mogą być zastępowane innymi białkami na zasadzie “competitive replacement” znanego też jako efekt Vromanna [10]. Połączenie białek z podłożem wiązaniem chemicznym w większym stopniu zapewnia zachowanie danej konformacji białka i stabilność wiązania.

W rozprawie badano modyfikację powierzchni składającą się z dwóch etapów, funkcjonalizacji powierzchni poprzez wprowadzenie grup aminowych za pomocą reakcji aminolizy oraz przyłączenia żelatyny jako białka zawierającego sekwencję RGD. Dwie prace z cyklu publikacji włączonych w rozprawę dotyczą pierwszego etapu, reakcji aminolizy przeprowadzonej na foliach i włókninach poliestrowych. Reakcja aminolizy przebiega według, dość powszechnego w chemii organicznej, mechanizmu substytucji nukleofilowej. W przypadku aminolizy, nukleofilem jest amina, diamina bądź poliamina atakująca grupę estrową (-COO-) licznie występującą w łańcuchu poliestru. W niniejszej pracy reakcję aminolizy przeprowadzono stosując etylenodiaminę. W trakcie reakcji aminolizy dochodzi do zerwania wiązania estrowego poliestru i przyłączenia w tym miejscu grupy aminowej diaminy za pomocą wiązania amidowego (-CONH-) oraz powstania dodatkowych grup hydroksylowych [25]. Druga grupa aminowa diaminy pozostaje wolna i może być wykorzystana do przyłączenia cząsteczki białka. W niniejszej pracy przyłączone wolne grupy aminowe zostały powiązane z

żelatyną za pomocą reakcji z glutaraldehydem co było przedmiotem badań trzeciej publikacji z cyklu. Glutaraldehyd wiąże się jedną ze swoich grup aldehydowych z przyłączoną do poliestru wolną grupą aminową, a drugą z grupą aminową żelatyny, sieciując żelatynę z poliestrem. Grupa aldehydowa i grupa aminowa reagują ze sobą tworząc tzw. zasadę Schiffa [26]. Należy dodać, że przyłączone do podłoża komórkowego grupy aminowe mogą być wiązane również z innymi grupami funkcyjnymi biomolekuł takimi jak grupy karboksylowe, hydroksylowe czy tiolowe za pomocą odpowiednich czynników sieciujących [27]. W ostatniej z prac wchodzących w cykl publikacji rozprawy, przyłączanie żelatyny z wykorzystaniem aminolizy zostało porównane z metodami bazującymi na reakcji hydrolizy i obróbce plazmą tlenową. Obie metody powodują zrywanie wiązań estrowych poliestru i wprowadzają do łańcucha poliestru grupy karboksylowe i hydroksylowe. Przyłączenie żelatyny odbywa się wówczas za pomocą wiązania jej grup aminowych z grupami karboksylowymi podłoża z wykorzystaniem sieciowania bazującego na pochodnych karbodiimidowych, np. odczynniku EDC.

## **2. Cele pracy**

- 1) porównanie przebiegu reakcji aminolizy dla submikronowych włókien i folii poliestrowych z uwzględnieniem efektywności przyłączania grup aminowych oraz wpływu reakcji na zmiany stopnia krystaliczności, właściwości mechaniczne i zwilżalność włókien i folii,
- 2) określenie wpływu budowy chemicznej włókien z poliestrów alifatycznych na efektywność aminolizy oraz optymalizacja parametrów reakcji aminolizy prowadzonej na submikronowych włóknach poliestrowych tak, aby uzyskać poprawę odpowiedzi komórkowej bez obniżania właściwości mechanicznych i zmiany morfologii włóknin,
- 3) wykazanie wpływu efektywności aminolizy na ilość przyłączonej żelatyny do powierzchni poliestrowych włókien i ocena wpływu tej ilości na odpowiedź komórkową oraz wpływu warunków przyłączania na właściwości mechaniczne włókien,
- 4) porównanie opracowanej metody przyłączania żelatyny z dwoma innymi metodami, opartymi na hydrolizie oraz obróbce plazmą tlenową.

## **3. Hipoteza badawcza**

Specyfika struktury submikronowych włókien formowanych metodą elektroprzędzenia determinuje przebieg i efektywność procesu aminolizy inny niż w przypadku folii poliestrowych. Dodatkowo, zróżnicowanie budowy chemicznej poliestrów wpływa na przebieg aminolizy.

Mimo to, możliwy jest taki dobór warunków aminolizy, który prowadzi do odpowiedniego stężenia grup aminowych na powierzchni włókien, warunkujących przyłączenie żelatyny w stężeniu zapewniającym poprawę odpowiedzi komórkowej, pozwalając na zachowanie morfologii włókien i ich wytrzymałości mechanicznej.

## **4. Materiały**

### **4.1. Poliestry alifatyczne**

Poliestry alifatyczne są polimerami posiadającymi wiązanie estrowe ( $-C(=O)-O-$ ) w łańcuchu głównym. Wiązanie estrowe, powszechnie występujące w przyrodzie, ulega reakcji hydrolizy, dzięki czemu dochodzi do rozpadu cząsteczek pod wpływem kontaktu z wodą [28]. Podobnie, syntetyczne poliestry alifatyczne również dobrze degradują w środowisku. W inżynierii tkankowej poliestry alifatyczne znalazły zastosowanie ze względu na kilka cech: degradowalność, biozgodność, dobrą przetwarzalność i odpowiednie właściwości mechaniczne. Do najczęściej stosowanych zalicza się PLLA, PLCL, PCL, PGA, PLGA. W pracy badano folie i włókna otrzymane z trzech poliestrów: PCL, PLLA i kopolimeru laktedu i kaprolaktonu, PLCL. Polimery różniły się między sobą m.in. gęstością występowania wiązania estrowego w łańcuchu cząsteczki, będącą najwyższą dla PLLA, a najniższą dla PCL i temperaturą zeszklenia, podobnie, najwyższą dla PLLA, a najniższą dla PCL. Otrzymane z poliestrów folie i włókna różniły się między sobą stopniem krystaliczności, przy czym najwyższy wykazywały folie i włókna PCL, a najniższy - obie formy PLLA.

### **4.2. Etylenodiamina**

Etylenodiamina ( $C_2H_8N_2$ ) jest organicznym związkiem chemicznym z grupy amin. Wykorzystywana jest w przemyśle chemicznym do otrzymywania, np. żywic poliamidowych i formaldehydowo-mocznikowych, barwników, wosków syntetycznych, środków antykorozyjnych oraz jako emulgator i stabilizator gumy [29]. Dobrze rozpuszcza się m.in. w alkoholach i wodzie [25]. Diaminy, do których należy etylenodiamina, są wykorzystywane w inżynierii tkankowej w badaniach funkcjonalizacji powierzchni polimerowych podłoży komórkowych. Działanie diamin opiera się na addycji nukleofilowej do grupy karbonylowej poliestru - zerwaniu wiązania estrowego i przyłączeniu się w tym miejscu grupy aminowej diaminy. Druga z grup aminowych przyłączona do diamin pozostaje wolna, co zwykle zwiększa zwilżalność podłożu komórkowego ze względu na hydrofilowy charakter grup aminowych. Funkcjonalizacja powierzchni za pomocą diamin umożliwia także dalszą modyfikację chemiczną poprzez przyłączanie do grup aminowych biomolekuł.

### **4.3. Glutaraldehyd**

Glutaraldehyd ( $C_5H_8O_2$ ) jest organicznym związkiem chemicznym z grupy aldehydów. Stosowany jest m.in. do sterylizacji narzędzi chirurgicznych i endoskopów, garbowania skóry, utrwalania struktur biologicznych do obserwacji mikroskopowej [30, 31]. Glutaraldehyd może

sieciować białka poprzez reakcję grup aldehydowych z grupami aminowymi białek i tworzenie tzw. zasad Schiffa. Jest wykorzystany w inżynierii tkankowej do wiązania białek z grupami aminowymi przyłączonymi wcześniej do powierzchni podłoża komórkowego.

#### **4.4. Żelatyna**

Żelatynę otrzymuje się poprzez zniszczenie sieci wiązań utrzymujących naturalną nadmolekularną strukturę kolagenu [32]. Kolagen ulega denaturacji do żelatyny podczas odpowiedniej obróbki termicznej. W zależności od zastosowanych warunków reakcji otrzymuje się żelatynę typu A (punkt pI przy pH równym 8-9) w warunkach kwaśnych i żelatynę typu B (punkt pI przy pH równym 4-5) w warunkach zasadowych [33]. W odróżnieniu od kolagenu żelatyna jest rozpuszczalna w wodzie. Zniszczenie wiązań sieciujących w kolagenie powoduje, że lepiej wyeksponowana jest sekwencja peptydowa składająca się z aminokwasów argininy, glicyny i kwasu asparaginowego (Arg-Gly-Asp, RGD), która jest odpowiedzialna za wiązanie się z integrynami, receptorami komórek odpowiedzialnymi za adhezję.

### **5. Metody**

#### **5.1. Formowanie włóknin poliestrowych**

Podłoża komórkowe w postaci włóknin otrzymano za pomocą metody elektroprzedzenia. Elektroprzedzenie jest techniką formowania włókien z roztworu polimeru. Roztwór jest tłoczony z określona prędkością poprzez strzykawkę z igłą, do której przyłożone jest duże napięcie elektryczne. W komorze przedzalniczej znajduje się również kolektor, który jest uziemiony lub połączony do napięcia o przeciwnym potencjale. Występująca między igłą a kolektorem różnica napięć powoduje powstanie sił elektrostatycznych i rozciąganie kropli naładowanego roztworu polimeru do postaci tzw. stożka Taylora, z którego formuje się cienki strumień, który następnie ulega spiralnym zawijowaniom i dalszemu pocienieniu na drodze do kolektora. Równocześnie następuje też odparowywanie rozpuszczalnika i osadzanie włókien na obracającym się kolektorze.

Badane w rozprawie włókniny zostały wytworzone z roztworów poliestrów alifatycznych w odpowiednich rozpuszczalnikach. Zastosowano 15% (w/w) roztwór PCL w mieszaninie kwasów octowego i mrówkowego w stosunku 9:1 (w/w), 7% (w/w) roztwór PLCL w heksaizopropanolu, 3.5% (w/w) roztwór PLLA w heksaizopropanolu. Zastosowano horyzontalny tryb elektroprzedzenia. Dystans między igłą a kolektorem wynosił 15 cm,

kolektor obracał się z prędkością 300 rpm. Do igły przykładowano napięcie 12-15 kV w przypadku PCL i 12-14 kV dla PLCL i PLLA, a do kolektora napięcie -2 kV lub 0 kV. Wartości temperatury i wilgotności wynosiły odpowiednio: dla PCL: 24°C, 40%, dla PLCL: 38°C, 40%, dla PLLA: 24°C, 40%. Były to optymalne wartości pozwalające na formowanie włóknin o odpowiedniej morfologii. Szczegółowe informacje na temat warunków formowania włóknin poliestrowych znajdują się we wszystkich publikacjach z cyklu.

## **5.2. Formowanie folii poliestrowych**

Folie poliestrowe zostały uformowane poprzez wylanie roztworów polimerów na specjalnie przygotowane szklane podłożą, pozostawienie do odparowania i zdjęcie z podłożą. Zastosowano te same rozpuszczalniki i stężenia polimerów w roztworach jak w przypadku metody elektroprzędzenia.

## **5.3. Funkcjonalizacja włókien i folii poliestrowych za pomocą reakcji aminolizy**

Włókna poliestrowe i folie zostały poddane funkcjonalizacji za pomocą reakcji aminolizy poprzez zanurzenie w roztworze alkoholowym etylenodiaminy. W celu porównania reaktywności włókien poliestrowych i folii zastosowano takie same warunki reakcji: 6% (w/v) roztwór EDA w izopropanolu, temperaturę: 30°C, czas: 5 i 15 minut. W przypadku optymalizacji aminolizy włókien z użyciem EDA zastosowano różne warunki reakcji. Dla PCL stężenie EDA w izopropanolu wynosiło 10%, 20% lub 30% (w/v), a dla PLCL i PLLA: 2%, 6% lub 10% (w/v), zaś czasy reakcji wynosiły odpowiednio: 30 min, 6h, 24h i 72h dla PCL oraz 5 min, 10 min, 15 min i 30 min dla PLCL i PLLA. Reakcję prowadzono w temperaturze 30°C, w inkubatorze z funkcją mieszania. Po reakcji aminolizy próbki były płukane 3-krotnie w wodzie dejonizowanej, a następnie suszone pod wyciągiem. Szczegółowe informacje na temat funkcjonalizacji znajdują się w publikacjach: *Aminolysis of various aliphatic polyesters in a form of nanofibers and films i Aminolysis as a surface functionalization method of aliphatic polyester nonwovens: impact on material properties and biological response.*

## **5.4. Przyłączenie żelatyny do powierzchni włókien poliestrowych funkcjonalizowanych za pomocą reakcji aminolizy**

Do badania przyłączania żelatyny wybrano po dwa zestawy warunków reakcji aminolizy dla każdego typu włókien, dla PCL: 1) c = 10% w/v, t = 24h, 2) c = 30% w/v, t = 24h, dla PLCL: 1) c = 2% w/v, t = 5 min, 2) c = 10% w/v, t = 10 min, dla PLLA: 1) c = 2% w/v, t = 5 min, 2) c = 6% w/v, t = 10 min. Temperatura reakcji aminolizy wynosiła 30°C. Po przeprowadzeniu funkcjonalizacji za pomocą aminolizy próbki zanurzono na 2.5h w 1% (w/v)

rozworze wodnym glutaraldehydu w temperaturze 25°C. Następnie, wypłukane próbki umieszczone na 24h w 0.2% w/v roztworze wodnym żelatyny w temperaturze 38°C. Analogicznie, niefunkcjonalizowane próbki kontrolne zanurzono w roztworze żelatyny w celu przeprowadzenia fizycznej adsorpcji żelatyny. Następnie próbki płukano przez 24h w temperaturze 38°C i suszono pod wyciągiem. Szczegółowe informacje na temat przyłączania żelatyny znajdują się w publikacji: *Immobilization of Gelatin on Fibers for Tissue Engineering Applications: A Comparative Study of Three Aliphatic Polyesters*.

### **5.5. Funkcjonalizacja włókien poliestrowych za pomocą reakcji hydrolizy**

Hydroliza zasadowa włókniny PLCL została przeprowadzona poprzez jej zanurzenie w roztworze NaOH o odpowiednim stężeniu: 0.1 M, 0.25 M, 0.5 M i 1 M, na czas 3h w temperaturze 25°C. Następnie próbki zanurzono w 0.01 M roztworze HCl w celu protonacji nowo utworzonych grup COO<sup>-</sup> oraz wypłukano w wodzie i osuszono pod wyciągiem. Szczegółowe informacje na temat funkcjonalizacji znajdują się w publikacji: *A Comparative Study of Three Approaches to Fibre's Surface Functionalization*.

### **5.6. Funkcjonalizacja włókien poliestrowych za pomocą obróbki niskotemperaturową plazmą tlenową**

Do przeprowadzenia obróbki niskotemperaturową plazmą tlenową na włókninach PLCL wykorzystano urządzenie Plasma Cleaner (Diener, ZEPTO PCCE, Ebhausen, Niemcy). Zastosowano niską moc wynoszącą 1% mocy urządzenia i ciśnienie tlenu wynoszące 0.1 mBar. Czasy obróbki wynosiły 10 s i 40 s. Szczegółowe informacje na temat funkcjonalizacji znajdują się w publikacji: *A Comparative Study of Three Approaches to Fibre's Surface Functionalization*.

### **5.7. Przyłączenie żelatyny do powierzchni włókien poliestrowych funkcyjonalizowanych za pomocą reakcji hydrolizy lub obróbki plazmą**

Włókniny PLCL poddane wcześniej hydrolizie i obróbce plazmą zostały zanurzone na 1h w 0.23%/0.12% (w/w) roztworze pochodnej karbodiimidowej EDC z odczynnikiem NHS w mieszaninie etanolu i wody w stosunku 7:3. Po wypłukaniu w wodzie próbki zostały umieszczone w 0.2% (w/v) roztworze żelatyny na 20 h w temperaturze 38°C. Następnie próbki płukano w wodzie przez 24h i osuszono pod wyciągiem. Szczegółowe informacje na temat przyłączania żelatyny znajdują się w publikacji: *A Comparative Study of Three Approaches to Fibre's Surface Functionalization*.

## **5.8. Charakteryzacja włókien poliestrowych po modyfikacji**

### **5.8.1. Obrazowanie włókien za pomocą skaningowej mikroskopii elektronowej**

Obrazowanie włókien wykonano za pomocą skaningowego mikroskopu elektronowego (Jeol, JSM-6010PLUS/LV InTouchScope™, Akishima, Tokio, Japonia). Przed obrazowaniem próbki pokryto złotem. Zastosowano napięcie wiązki elektronów w zakresie 7–10 kV. Szczegółowe informacje na temat badania znajdują się w publikacjach: *Aminolysis as a surface functionalization method of aliphatic polyester nonwovens: impact on material properties and biological response* i *Immobilization of Gelatin on Fibers for Tissue Engineering Applications: A Comparative Study of Three Aliphatic Polyesters*.

### **5.8.2. Ocena stężenia przyłączonych grup aminowych**

Do oceny stężenia przyłączonych grup aminowych wykorzystano test ninhydrynowy. Test wykonano na 3 próbkach dla każdego typu materiału. Reakcję przeprowadzono poprzez zanurzenie próbki w 2% (w/v) roztworze ninhydryny w etanolu z dodatkiem kwasu octowego w stosunku 49:1. Przygotowane roztwory podgrzewano przez 10 min na płytce o temperaturze 100°C. Po dodaniu odpowiednich rozpuszczalników, próbki roztworów zostały poddane pomiarom absorbancji światła o długości 570 nm za pomocą spektrofotometru (Thermo Fisher Scientific, MultiskanGo, Waltham, MA, USA). Stężenie grup aminowych zostało obliczone na podstawie przygotowanej krzywej kalibracyjnej. Szczegółowe informacje na temat badania znajdują się w publikacjach: *Aminolysis of various aliphatic polyesters in a form of nanofibers and films* i *Aminolysis as a surface functionalization method of aliphatic polyester nonwovens: impact on material properties and biological response*.

### **5.8.3. Ocena stężenia przyłączonej żelatyny**

Stężenie przyłączonej żelatyny oceniono za pomocą kolorymetrycznego testu BCA. Roztwór BCA został przygotowany według instrukcji producenta. Test wykonano na 3 próbkach dla każdego typu materiału poprzez zanurzenie w roztworze BCA i inkubację przez 2h w temperaturze 37°C. Próbki roztworów zostały poddane pomiarom absorbancji światła o długości 562 nm za pomocą spektrofotometru (Thermo Fisher Scientific, MultiskanGo, Waltham, MA, USA). Stężenie żelatyny dla próbek zostało obliczone na podstawie krzywej kalibracyjnej otrzymanej z pomiarów roztworów żelatyny o różnym stężeniu. Szczegółowe informacje na temat badania znajdują się w publikacji: *Immobilization of Gelatin on Fibers for Tissue Engineering Applications: A Comparative Study of Three Aliphatic Polyesters*.

#### **5.8.4. Ocena struktury molekularnej powierzchni próbek**

Powierzchniowa struktura molekularna próbek została oceniona za pomocą spektroskopii ATR-FTIR przy użyciu spektrometru (Bruker, Vertex 70, Mannheim, Niemcy). Pomiary prowadzono w zakresie 4000–400 cm<sup>-1</sup>. Rozdzielcość pomiaru wynosiła 2 cm<sup>-1</sup>. Szczegółowe informacje na temat badania znajdują się w publikacjach: *Aminolysis of various aliphatic polyesters in a form of nanofibers and films i Aminolysis as a surface functionalization method of aliphatic polyester nonwovens: impact on material properties and biological response.*

Wybrane próbki, kontrolna i poddane aminolizie, zostały zbadane metodą spektroskopii XPS, za pomocą urządzenia PHI VersaProbe II (Physical Electronics, Chanhassen, MN, USA) wyposażonego w źródło monochromatycznego promieniowania Al K $\alpha$  (1486.6 eV). Moc promieniowania wynosiła 25W. Wiązka została skupiona na obszarze 100 μm. Szczegółowe informacje na temat badania znajdują się w publikacji: *Aminolysis as a surface functionalization method of aliphatic polyester nonwovens: impact on material properties and biological response.*

Wybrane próbki, kontrolna, poddana aminolizie, i z przyłączoną żelatyną, zostały zbadane metodą spektroskopii XPS, za pomocą urządzenia SPECS (GmbH, Berlin, Niemcy) przy użyciu niemonochromatycznego źródła promieniowania Mg K $\alpha$  (1253.6 eV). Szczegółowe informacje na temat badania znajdują się w publikacji: *Immobilization of Gelatin on Fibers for Tissue Engineering Applications: A Comparative Study of Three Aliphatic Polyesters.*

#### **5.8.5. Ocena struktury supermolekularnej próbek**

Pomiary metodą dyfraktometrii WAXS wykonano za pomocą dyfraktometru (Bruker, D8, Mannheim, Niemcy) wyposażonego w źródło promieniowania CuK $\alpha$ , przy napięciu wynoszącym 40 kV, i natężeniu prądu równym 20 mA. Wszystkie pomiary przeprowadzono w trybie odbicia, używając optyki Goebel do formowania wiązki: szczeliny wynoszącej 0.6 mm i kolimatora Sollera. Użyto wysoko czułego detektora Lynx Eye 1-D. Zakres kąta dyfrakcji 2 $\Theta$  wynosił między 5° a 35°. Szczegółowe informacje na temat badania znajdują się w publikacjach: *Aminolysis of various aliphatic polyesters in a form of nanofibers and films i Aminolysis as a surface functionalization method of aliphatic polyester nonwovens: impact on material properties and biological response.*

### **5.8.6. Pomiar zwilżalności**

Na próbkach poddanych aminolizie wykonano pomiary kąta zwilżania wodą za pomocą goniometru (Data Physics Instruments, OCA 15EC, Filderstadt, Niemcy). Objętość i szybkość dozowania kropli wynosiły odpowiednio 1  $\mu\text{l}$  i 2  $\mu\text{l}/\text{s}$ . Wykonano po 5 pomiarów dla każdej próbki. Szczegółowe informacje na temat badania znajdują się w publikacjach: *Aminolysis of various aliphatic polyesters in a form of nanofibers and films* i *Aminolysis as a surface functionalization method of aliphatic polyester nonwovens: impact on material properties and biological response*.

W przypadku włóknin z przyłączoną żelatyną wykonano pomiary czasu wnikania kropli wody w próbce. Wykonano po 5 pomiarów dla każdej próbki. Szczegółowe informacje na temat badania znajdują się w publikacji: *Immobilization of Gelatin on Fibers for Tissue Engineering Applications: A Comparative Study of Three Aliphatic Polyesters*.

### **5.8.7. Pomiar zmian mas cząsteczkowych**

Zmiany wagowo średniej masy cząsteczkowej  $\overline{M_w}$  i liczbowo średniej masy cząsteczkowej  $\overline{M_n}$  oraz współczynnika polidispersyjności PI zostały zmierzone za pomocą chromatografu żelowego Nexera (Shimadzu, Kyoto, Japonia). Urządzenie zaopatrzone było w pompę, kolumnę (Phenomenex, Phenogel<sup>TM</sup> 5mm 10e5° A, Torrance, CA, USA), detektor współczynnika załamania światła (Shimadzu, RID-20A, Kyoto, Japonia) i oprogramowanie LabSolutions GC (Shim-Pol, Warszawa, Polska). Próbki włóknin zostały rozpuszczone w THF. Krzywą kalibracyjną otrzymano na podstawie pomiarów próbek wzorcowych poli(styrenu) o średnich masach cząsteczkowych  $\overline{M_n}$  od 3470Da do 2520000Da (PSS Polymer Standards Service GmbH, Amherst, MA, USA). W obliczeniach mas cząsteczkowych uwzględniono odpowiednie parametry wynikające z równania Marka-Houwinka. Szczegółowe informacje na temat badania znajdują się w publikacji: *Aminolysis as a surface functionalization method of aliphatic polyester nonwovens: impact on material properties and biological response*.

### **5.8.8. Wyznaczenie właściwości mechanicznych**

Moduł Younga, naprężenie przy zerwaniu i wydłużenie przy zerwaniu zostały wyznaczone w 1-osiowej próbie rozciągania przeprowadzonej za pomocą urządzenia LloydEZ-50 (AMETEK Sensors, Test & Calibration (STC), Berwyn, PA, USA). Dla każdego typu materiału przygotowano po 3 próbki. Rozmiar próbki wynosił 5x40 mm, a pomiar zebrano z obszaru 5x20 mm. Grubość każdej z próbek zmierzono za pomocą grubościomierza.

Szczegółowe informacje na temat badań mechanicznych zawierają wszystkie publikacje z cyklu.

#### **5.8.9. Pomiar odczynu pH**

Odczyn pH został zmierzony za pomocą pH-metru CP-401 (Elmetron, Zabrze, Polska) z użyciem elektrody ERH-NS (Elmetron, Zabrze, Polska). Badanie miało na celu sprawdzenie czy zanurzenie włóknin w roztworze żelatyny powoduje zmianę odczynu pH roztworu w określonym czasie. Do badań przygotowano roztwory żelatyny o stężeniu 0.2% (w/v) w objętości 10 mL i zmierzono ich odczyn pH. Następnie w roztworach zanurzono włókniny PCL, PLCL i PLLA i umieszczone je na 20h w 38°C po czym ponownie zmierzono odczyn pH. Zastosowano 3 roztwory dla każdego typu próbki. Szczegółowe informacje na temat badania znajdują się w publikacji: *Immobilization of Gelatin on Fibers for Tissue Engineering Applications: A Comparative Study of Three Aliphatic Polyesters*.

#### **5.8.10. Wyznaczenie swobodnej energii powierzchniowej**

Swobodna energia powierzchniowa została wyznaczona dla folii poliestrowych. Za pomocą goniometru wyznaczono kąty zwilżania folii dla 3 cieczy: wody, formamidu i dijodometanu. Dla każdej próbki wykonano po 5 pomiarów. Swobodną energię powierzchniową wyznaczono za pomocą oprogramowania SCA20 (Data Physics Instruments GmbH, Filderstadt, Niemcy) z wykorzystaniem modelu Owensa-Wendta-Rabelanda-Kaelble'a. Szczegółowe informacje na temat badania znajdują się w publikacji: *Immobilization of Gelatin on Fibers for Tissue Engineering Applications: A Comparative Study of Three Aliphatic Polyesters*.

#### **5.8.11. Ocena stabilności przyłączenia żelatyny**

Stabilność przyłączonej warstwy żelatyny oceniono porównując stężenie żelatyny na powierzchni włókien PCL przed i po inkubacji w roztworze PBS. Dla każdego typu materiału badano po 3 próbki. Test prowadzono przez 90 dni mierząc stężenie żelatyny w kilku punktach pomiarowych. Stężenie żelatyny wyznaczono za pomocą kolorymetrycznego testu BCA. Szczegółowe informacje na temat badania znajdują się w publikacji: *Immobilization of Gelatin on Fibers for Tissue Engineering Applications: A Comparative Study of Three Aliphatic Polyesters*.

#### **5.8.12. Ocena odpowiedzi komórkowej**

Do oceny odpowiedzi komórkowej użyto dwóch typów komórek: mysich fibroblastów linii L929 (SigmaAldrich, Saint Louis, MO, USA) i ludzkich komórek osteblastopodobnych

linii MG-63 (SigmaAldrich, Saint Louis, MO, USA). Próbki włóknin były sterylizowane poprzez zanurzenie w 70% roztworze etanolu i poprzez ekspozycję na promieniowanie UV. Hodowla komórek na włókninach była prowadzona w 48-dołkowych płytach hodowlanych z użyciem medium odpowiedniego dla danych komórek. Hodowla przebiegała w temperaturze 37°C, przy 5% zawartości CO<sub>2</sub> przez 3 lub 5 dni. Do oceny aktywności metabolicznej komórek użyto testu PrestoBlue™ (Thermo Fisher Scientific, Waltham, MA USA). Morfologia komórek została zobrazowana przy pomocy skaningowej mikroskopii elektronowej i mikroskopii fluorescencyjnej. Wszystkie wyniki zostały odniesione do hodowli kontrolnej na płytce hodowlanej z poli(styrenu). Szczegółowe informacje na temat badania odpowiedzi komórkowej znajdują się w publikacjach: *Aminolysis as a surface functionalization method of aliphatic polyester nonwovens: impact on material properties and biological response*, *Immobilization of Gelatin on Fibers for Tissue Engineering Applications: A Comparative Study of Three Aliphatic Polyesters* i *A Comparative Study of Three Approaches to Fibre's Surface Functionalization*.

#### **5.8.13 Analiza statystyczna**

Wyniki odpowiednich badań zostały poddane analizie statystycznej za pomocą testu t dla prób zależnych i analizy wariancji ANOVA z odpowiadającymi im testami post-hoc. Do analizy wykorzystano oprogramowanie Statistica 13 (StatSoft Polska, Kraków, Polska). Istotność statyczna została ustalona na poziomie p<0.05. Szczegółowe informacje na temat analizy statystycznej znajdują się w publikacjach: *Aminolysis as a surface functionalization method of aliphatic polyester nonwovens: impact on material properties and biological response* i *Immobilization of Gelatin on Fibers for Tissue Engineering Applications: A Comparative Study of Three Aliphatic Polyesters*.

## **6. Publikacje włączone w cykl**

- 1.** Jeznach O., Kołbuk D., Sajkiewicz P., Aminolysis of various aliphatic polyesters in a form of nanofibers and films, *Polymers*, Vol.11, No.10, pp.1669-1-16, 2019.
- 2.** Jeznach O., Kołbuk D., Marzec M., Bernasik A., Sajkiewicz P., Aminolysis as a surface functionalization method of aliphatic polyester nonwovens: impact on material properties and biological response, *RSC Advances*, Vol.12, No.18, pp.11303-11317, 2022.
- 3.** Jeznach O., Kołbuk D., Reich T., Sajkiewicz P., Immobilization of Gelatin on Fibers for Tissue Engineering Applications: A Comparative Study of Three Aliphatic Polyesters, *Polymers*, Vol.14, No.19, pp.4154-1-21, 2022.
- 4.** Dulnik J., Jeznach O., Sajkiewicz P., A Comparative Study of Three Approaches to Fibre's Surface Functionalization, *Journal of Functional Biomaterials*, Vol.13, No.4, pp.272-1-23, 2022.

**Tab.1.** Dane bibliograficzne publikacji włączonych w rozprawę.

| <b>Numer publikacji</b> | <b>Rok wydania publikacji</b> | <b>IF (2022)</b> | <b>Punkty MNiSW (2023)</b> | <b>Liczba cytowań (Scopus)</b> | <b>Liczba cytowań (Web of Science)</b> |
|-------------------------|-------------------------------|------------------|----------------------------|--------------------------------|--|
| 1.                      | 2019                          | 5.000            | 100                        | 36                             | 32                                     |
| 2.                      | 2022                          | 3.900            | 100                        | 13                             | 12                                     |
| 3.                      | 2022                          | 5.00             | 100                        | 4                              | 3                                      |
| 4.                      | 2022                          | 4.800            | 100                        | 2                              | 2                                      |

## **6.1. Aminolysis of various aliphatic polyesters in a form of nanofibers and films**

Celem pracy rozpoczynającej cykl publikacyjny było porównanie przebiegu reakcji aminolizy na włóknach i foliach polimerowych dla trzech rodzajów poliestrów należących do najczęściej wykorzystywanych w inżynierii tkankowej: poli(kaprolaktonu), poli(L-laktydu-kaprolaktonu) i poli(L-laktydu). Motywacją do przeprowadzenia badań był brak w literaturze przedmiotu analizy możliwych różnic w reaktywności włókien i folii poliestrowych. Dodatkowym wkładem pracy jest uwzględnienie różnic w reaktywności różnych poliestrów. Większość dotychczasowych prac na temat wykorzystania aminolizy do modyfikacji powierzchniowej odnosiła się do folii polimerowych. Równocześnie brakowało systematycznych informacji w odniesieniu do włókien, zwłaszcza formowanych za pomocą elektroprzедzenia. Należy wspomnieć, że to włókniny mają potencjał zastosowania w inżynierii tkankowej natomiast folie polimerowe traktowane są jako ‘model’ do oceny przebiegu funkcjonalizacji. Podejmując badania zakładano, że reakcja aminolizy będzie bardziej efektywna na włóknach niż na foliach polimerowych ze względu na ich większe rozwinięcie powierzchni, a więc większy kontakt z roztworem diaminy.

W pracy zbadano trzy rodzaje poliestrów w formie elektroprzедzionych włókien i folii otrzymanych metodą odlewania z roztworu. Zastosowano dwa zestawy parametrów z krótszym i dłuższym czasem reakcji przy stałym stężeniu diaminy i temperaturze reakcji. Badania kolorometryczne przeprowadzone z użyciem testu ninhydrynowego wykazały, że:

- 1) zastosowanie tych samych warunków aminolizy skutkuje wprowadzeniem większej ilości grup aminowych w przeliczeniu na powierzchnię materiału w przypadku folii niż włókien,
- 2) zarówno dla folii jak i włókien te same warunki aminolizy prowadzą do przyłączenia największej ilości grup aminowych w przypadku poli(L-laktydu) i najmniejszej dla poli(kaprolaktonu), przy czym w przypadku włókien z poli(kaprolaktonu) nie ujawniono w ogóle grup aminowych,
- 3) dłuższy czas reakcji prowadzi do przyłączenia większej ilości grup aminowych.

Spektroskopia ATR-FTIR potwierdziła jakościowo zajście reakcji aminolizy na próbkach poprzez obecność drgań pochodzących od pierwszo- i drugorzędowych wiązań amidowych.

Metoda WAXS pozwoliła ocenić zmiany stopnia krystaliczności badanych materiałów. Założono, że obserwowana niższa podatność włókien na aminolizę w porównaniu do folii może

wynikać z wyższego stopnia krystaliczności, zwłaszcza na powierzchni, co jest związane ze specyfiką struktury powstającej w procesie elektroprzędzenia. Poprzeczny gradient struktury z bardziej krystalicznym naskórkiem i amorficznym rdzeniem jest opisany w literaturze dla klasycznych włókien formowanych za pomocą metody *high-speed spinning*. Wynika on z bardziej efektywnego porządkowania się makrocząsteczek na powierzchni włókna ze względu na niższą temperaturę stopu bądź szybsze odparowywanie rozpuszczalnika z roztworu co prowadzi do wyższego przechłodzenia czy odpowiednio przesycenia roztworu. Wyższe średnice klasycznych włókien pozwalają na wykazanie efektu otoczka-rdzeń doświadczalnie. W przypadku włókien elektroprzędzonych nie ma na ten temat danych empirycznych, jednakże, na podstawie zbliżonych lub wyższych prędkości przędzenia można wnioskować o analogii mechanizmu krystalizacji. Dostępność reaktywnych grup estrowych jest dużo mniejsza w fazie krystalicznej w porównaniu do fazy amorficznej ze względu na wolniejszą dyfuzję diamin w strukturze krystalicznej. W ten sposób krystaliczny naskórek włókna może tworzyć barierę dla dyfuzji diamin i zajścia aminolizy. W przypadku folii, gdzie ze względu na wolniejsze odparowywanie rozpuszczalnika nie występuje ten efekt, aminoliza będzie zachodzić szybciej. Z kolei zróżnicowanie podatności włókien z różnych poliestrów na aminolizę wynika z różnej częstości grup estrowych w łańcuchu makrocząsteczk, najwyższej dla PLLA, a najniższej dla PCL. Wpływ na to może mieć także najwyższy stopień krystaliczności włókien PCL oraz najwyższy stopień rekombinacji wolnych grup NH<sub>2</sub> wynikający z prowadzenia aminolizy w temperaturze (30°C) dużo powyżej temperatury zeszklenia włókien PCL (-60°C), zapewniającej dużą mobilność łańcuchów makrocząsteczek. Dla wszystkich próbek wykazujących obecność grup aminowych zaobserwowano wzrost stopnia krystaliczności w porównaniu do próbek wyjściowych. Widoczny był również wzrost stopnia krystaliczności próbek wraz ze wzrostem czasu reakcji. Wyższy stopień krystaliczności po funkcjonalizacji wynika z przerwania łańcuchów makrocząsteczek poliestru, co sprzyja ich uporządkowaniu i dodatkowej krystalizacji. Pomiary wielkości krystalitów w różnych kierunkach krystalograficznych wykazały z kolei tendencję do ich zmniejszania w procesie aminolizy. Powstające kryształy są niedoskonałe i małe ze względu na trudną kinetycznie krystalizację przy dużym już stopniu krystaliczności co zmniejsza mierzony średni rozmiar kryształu. W przypadku PCL, spadek wielkości krystalitów może być pośrednim dowodem na słabe zachodzenie reakcji aminolizy.

Wpływ aminolizy na strukturę włókien widoczny był też w wynikach 1-osiowej próby rozciągania. Zaobserwowano tendencję do spadku naprężenia przy zerwaniu po

funkcjalizacji, przy czym były to zarówno niewielkie spadki, wynoszące 7%, jak w przypadku folii PCL o mniejszym stężeniu grup aminowych jak i bardzo duże spadki, wynoszące 78%, jak w przypadku folii PLCL o mniejszym stężeniu grup aminowych. Za spadek naprężenia przy zerwaniu odpowiada skracanie łańcuchów makrocząsteczek spowodowane aminolizą, co prowadzi do zmniejszenia gęstości splatań łańcuchów, a w konsekwencji łatwiejszych przemieszczeń łańcuchów względem siebie, skutkujących obniżeniem naprężenia zrywającego. W pracy przytoczono równanie opracowane przez P. J. Flory'ego wiążące naprężenie przy zerwaniu ze średnią masą cząsteczkową  $\overline{M_n}$ . Dla niektórych próbek zaobserwowano duże spadki wydłużenia przy zerwaniu.

Pomimo obecności hydrofilowych grup aminowych zwilżalność próbek zwiększyła się w małym stopniu lub pozostała bez zmian. Największy spadek kąta zwilżania zaobserwowano dla próbek folii PCL (25°). Wyniki zwilżalności próbek nie korelowały z ilością wprowadzonych grup aminowych. W przypadku próbek włóknistych, należy wziąć pod uwagę wpływ efektu kapilarnego i powietrza znajdującego się w porach próbki na obserwowany kąt zwilżania. Za brak poprawy zwilżalności może też odpowiadać ekspozycja hydrofobowego łańcucha diaminy w kontakcie z wodą.

## **6.2. Aminolysis as a surface functionalization method of aliphatic polyester nonwovens: impact on material properties and biological response**

Celem niniejszej pracy było zbadanie wpływu aminolizy na właściwości materiałowe i odpowiedź komórek i na tej podstawie dobór optymalnych warunków funkcjalizacji elektroprzедzionych włókien za pomocą aminolizy. Motywacją do badań był brak systematycznych danych w literaturze przedmiotu na temat aminolizy submikrowłókien poliestrowych. Tak jak w poprzedniej pracy, zbadano włókna otrzymane z trzech rodzajów poliestrów: PCL, PLCL i PLLA.

Aminoliza włókien została przeprowadzona w szerokim zakresie parametrów z zastosowaniem 12 punktów pomiarowych ze zmiennym stężeniem etylenodiaminy i czasem reakcji. Zaobserwowano dużo wyższą podatność włókien PLLA i PLCL na aminolizę w porównaniu do włókien PCL, przy czym włókna PCL wymagały zastosowania dużo wyższego stężenia etylenodiaminy i czasów reakcji dla uzyskania stężenia grup aminowych tego samego rzędu. Najwyższą reaktywność wykazano dla włókien PLLA. Wpływ na to mają wspomniane we wcześniejszej pracy czynniki: stosunek reaktywnych grup estrowych do alkilowych w

łańcuchu makrocząsteczkii, temperatura zeszklenia, stopień krystaliczności i gradientowy rozkład struktury. Analiza XPS wykonana dla wybranej próbki (PLCL) poddanej aminolizie przy stężeniu EDA równym 10% i czasie reakcji 15 minut wykazała stężenie azotu (na powierzchni) równe 1.1at%. Dla tej samej próbki badanie profilowe stężenia wiązań chemicznych nie wykazało zmian stężenia azotu do głębokości ok. 370 nm, co wskazuje na zajście reakcji w całej objętości włókna. Badania za pomocą chromatografii GPC wykazały spadki średnich mas cząsteczkowych  $\overline{M_w}$  i  $\overline{M_n}$  dla wszystkich próbek poddanych aminolizie wynikające ze skracania łańcuchów przy zajściu reakcji. W przypadku PCL i PLCL zastosowanie odpowiednich, łagodnych parametrów reakcji pozwalało zachować masy cząsteczkowe bliskie wyjściowym masom  $\overline{M_w}$  (odpowiednio 99% i 93%). W przypadku PLLA dochodziło do bardzo gwałtownego spadku mas cząsteczkowych do 63% wyjściowej masy  $\overline{M_w}$  nawet przy najniższym stężeniu roztworu EDA i najkrótszym czasie reakcji, co koresponduje z najwyższą reaktywnością włókien PLLA. Uzyskane wyniki zmian mas cząsteczkowych potwierdzają wyniki badania profilowego XPS wskazując na zajście reakcji aminolizy w całej objętości włókna.

Ocena morfologii włóknin za pomocą mikroskopii SEM wskazuje, że w przypadku łagodnych warunków reakcji zachowana jest ich wyjściowa struktura. Przy wysokich stężeniach i czasach reakcji obserwowano kruche pękanie włókien niezależnie od typu poliestru, przy czym najbardziej intensywne zmiany zaobserwowano dla włókien PLLA. Podobnie jak w pierwszej publikacji z cyklu, pomiary kątów zwilżania wodą wykazały jedynie niewielkie wzrosty zwilżalności, nie przekraczające kilku % wyjściowej wartości kąta zwilżania.

Do dalszej części badań wytypowano po dwie próbki dla każdego rodzaju poliestru, o różnym poziomie stężenia przyłączonych grup aminowych. Dla badanych próbek, wyniki uzyskane metodą WAXS wskazują na wzrost stopnia krystaliczności po funkcjonalizacji, szczególnie duży dla włókien PLLA. Wynika to ze skracania łańcuchów makrocząsteczek w reakcji aminolizy i ich dodatkowej krystalizacji. Wyniki 1-osiowej próby rozciągania, w której wyznaczono naprężenie i wydłużenie przy zerwaniu, nie były jednoznaczne. Obserwowano zarówno brak zmian jak i wzrost i spadek naprężenia przy zerwaniu. Było to spowodowane wpływem na naprężenie przy zerwaniu przeciwnych czynników, skracania łańcuchów makrocząsteczek i erozji powierzchniowej prowadzących do jego spadku i wzrostu stopnia krystaliczności wpływającego na jego wzrost. Dla próbek wszystkich poliestrów z wyższym stężeniem przyłączonych grup aminowych zaobserwowano bardzo duży spadek wydłużenia

przy zerwaniu, odpowiednio wynoszący 82% wartości wyjściowej dla PCL, 96% dla PLCL i 59% dla PLLA. Tak duże spadki wynikały ze skrócenia łańcuchów makrocząsteczek, a co za tym idzie zmniejszenia gęstości splatań łańcuchów. W przypadku niższych stężeń grup aminowych, wydłużenie przy zerwaniu nie zmieniło się bądź wzrosło.

Wyniki badań *in vitro* z użyciem komórek fibroblastów linii L929 wskazywały na poprawę ich morfologii, większe rozpraszczenie komórek w porównaniu do próbek kontrolnych i widoczne filopodia świadczące o poprawie interakcji komórek z materiałem dla wszystkich próbek. Nie zaobserwowano wyraźnych różnic między próbками z różnym stężeniem grup aminowych, przy czym komórki wykazywały najbardziej korzystną morfologię na próbках PLCL. Z kolei badania *in vitro* z użyciem komórek linii MG-63 wykazały większe rozpraszczenie komórek dla próbek PCL i PLCL w porównaniu do próbek wyjściowych, natomiast dla próbki PLLA obserwowano pogorszenie morfologii komórek. Wyniki testu aktywności metabolicznej komórek PrestoBlue™ nie korespondowały z obserwacjami morfologii komórek. Zaobserwowano duży wzrost aktywności komórek L929 na próbках PCL, brak zmian na próbках PLCL i spadek na próbках PLLA. W przypadku komórek MG-63 stwierdzono spadek aktywności metabolicznej dla wszystkich próbek z niższym stężeniem grup aminowych i brak zmian (dla PCL i PLLA) lub poprawę (dla PLCL) dla próbek z wyższym stężeniem grup aminowych. Powyższe wyniki mogą wskazywać, że funkcjonalizacja pozytywnie wpłynęła na poprawę adhezji komórek, co jest widoczne w morfologii komórek, natomiast nie zawsze powodowała poprawę proliferacji komórek widoczną w wynikach aktywności metabolicznej.

### **6.3. Immobilization of gelatin on fibers for tissue engineering applications: a comparative study of three aliphatic polyesters**

Celem pracy było porównanie procesu przyłączania żelatyny do powierzchni funkcjonalizowanych włókien otrzymanych z trzech poliestrów pod kątem efektywności i wpływu na odpowiedź komórkową oraz właściwości mechaniczne. Motywacją do przeprowadzenia badań było usystematyzowanie wiedzy w zakresie przyłączania żelatyny do włókien funkcjonalizowanych metodą aminolizy.

Ponownie zbadano włókna PCL, PLCL i PLLA. Wykorzystano włókna o dwóch różnych stężeniach przyłączonych grup aminowych aby ocenić ich wpływ na efektywność wiązania żelatyny. W pracy zastosowano chemiczne przyłączanie żelatyny do wolnych grup

aminowych po uprzedniej reakcji z glutaraldehydem. Wyniki badań odniesiono do przypadku fizycznej adsorpcji żelatyny przeprowadzonej na próbkach niepoddanych funkcjonalizacji. Na podstawie obserwacji za pomocą mikroskopii SEM nie stwierdzono wpływu immobilizacji żelatyny poprzedzonej reakcją z glutaraldehydem na morfologię. Wyniki uzyskane za pomocą kolorymetrycznego testu BCA wskazywały na efektywne przyłączanie żelatyny do powierzchni wszystkich włókien, również niepoddanych funkcjonalizacji. Jednakże, próbki poddane aminolizie wykazywały wyższe ilości żelatyny, co było najbardziej widoczne dla włókien PCL. Dodatkowo, na przykładzie włókien PLCL, wykonano bardziej szczegółowe pomiary ilości przyłączonej żelatyny dla kilku próbek o różnym stężeniu przyłączonych grup aminowych. W zakresie małych stężeń grup aminowych, poniżej  $5 \cdot 10^{-8}$  mol/mg, zaobserwowano zmniejszenie ilości przyłączonej żelatyny ze wzrostem stężenia grup aminowych; dopiero powyżej tej wartości stwierdzano wzrost ilości przyłączanej żelatyny ze wzrostem stężenia grup aminowych. Na tej podstawie stwierdzono, że przy małych stężeniach grup aminowych dużą rolę w procesie przyłączania odgrywa fizyczna adsorpcja, a aminoliza prawdopodobnie zaburza ten proces. Analiza struktury chemicznej wybranych próbek PCL wykonana za pomocą spektroskopii XPS wykazała obecność azotu dla próbek z żelatyną wynoszącą 5at% i 8at%, odpowiednio dla próbek poddanym fizycznemu- oraz chemicznemu przyłączaniu, potwierdzając wyniki uzyskane za pomocą metody BCA. Porównując te wartości z ilością azotu w czystej żelatynie (16at%) stwierdzono, że warstwy przyłączonej żelatyny są grubością mniejszą od głębokości wnikania wiązki XPS, a więc 10 nm. Analiza udziału procentowego grup funkcyjnych dla próbek z przyłączoną żelatyną wskazywała na zmiany w kierunku rozkładu wiązań dla próbki żelatyny.

Wszystkie próbki z przyłączoną żelatyną wykazywały całkowitą zwilżalność, co wskazuje na dobrą ekspozycję hydrofilowych grup żelatyny. Dodatkowo, na obserwowaną zwilżalność wpływał efekt kapilarny powodujący wnikanie wody w głąb włókniny. Czasy absorpcji kropli wody były widocznie skorelowane z ilością przyłączonej żelatyny na powierzchni próbek. Duża zwilżalność ma znaczenie przy transporcie składników odżywczych z medium hodowanego przez włókninę, a także może przyspieszać hydrolityczną degradację materiału *in vivo*. Wyniki 1-osiowej próby rozciągania wskazywały na niewielkie spadki (do 15%) lub brak zmian naprężenia przy zerwaniu dla wszystkich włókien z fizycznie zaadsorbowaną żelatyną lub chemicznie przyłączoną do powierzchni próbek o niskim stężeniu grup aminowych. Dla wszystkich poliestrów wystąpił bardziej znaczny spadek naprężenia przy zerwaniu w przypadku próbek z większą ilością grup aminowych, najmniejszy dla włókien

PCL. Spadek naprężenia jest spowodowany skróceniem łańcuchów makrocząsteczek w procesie funkcjonalizacji. W przypadku wydłużenia przy zerwaniu tylko dla próbek PLCL i PLLA z większą ilością grup aminowych zaobserwowano duże spadki (96% i 85% wartości wyjściowej), natomiast wyniki dla włókien PCL wykazały dużo mniejszy spadek (19% wartości wyjściowej). Wyniki testu stabilności przyłączonej warstwy żelatyny w roztworze PBS przeprowadzone dla włókien PCL wskazywały na większą stabilność warstw przyłączonych chemicznie. Spadki masy przyłączonej żelatyny do 14 dnia inkubacji w roztworze wynosiły odpowiednio 37%, 2.4% i 17% dla próbki z fizycznie przyłączoną żelatyną i odpowiednio, próbek o mniejszym i większym stężeniu grup aminowych z chemicznie przyłączoną żelatyną. Od 14 dnia obserwowano ustabilizowanie uwalniania żelatyny do roztworu. Dla jednej z funkcjonalizowanych próbek duży udział w spadku ilości żelatyny może mieć desorpcja fizycznie przyłączonych cząsteczek. Należy mieć również na uwadze, że w warunkach *in vivo*, przy udziale degradacji enzymatycznej proces uwalniania żelatyny z powierzchni próbek mógłby być dużo bardziej dynamiczny.

Na wszystkich próbkach z przyłączoną żelatyną zaobserwowano poprawę morfologii komórek linii L929. Obserwacje za pomocą mikroskopii SEM wskazywały na dużo większe rozpraszczenie komórek na wszystkich próbkach z przyłączoną żelatyną, przy czym dla próbek PCL i PLCL wyraźniej dla próbek modyfikowanych chemicznie. Potwierdziły to obserwacje za pomocą mikroskopii fluorescencyjnej, gdzie uwidoczniono bardziej rozwinięty szkielet aktynowy dla powyższych próbek. Wyniki aktywności metabolicznej komórek po 5 dniach hodowli wskazywały na stopniowy wzrost od próbki z fizycznie przyłączoną żelatyną do próbki o wyższym stężeniu grup aminowych dla włókniny PCL. W przypadku PLCL i PLLA nie zaobserwowano wzrostu aktywności metabolicznej dla próbek z fizycznie przyłączoną żelatyną. Dla PLCL wyższa aktywność metaboliczna wystąpiła dla obu próbek z chemicznie przyłączoną żelatyną, a dla PLLA wyraźnie wyższą zaobserwowano dla próbki z wyższą ilością grup aminowych. Zarówno obserwacje mikroskopowe jak i wyniki badań aktywności metabolicznej wskazują na większy wpływ modyfikacji chemicznej na poprawę odpowiedzi komórkowej. Wyniki badań wykazały, że dla wszystkich włókien możliwe jest takie dobranie warunków modyfikacji chemicznej, które nie wpływa znacznie na naprężenie i wydłużenie przy zerwaniu i prowadzi do poprawy morfologii komórek L929, a w przypadku włókien PCL i PLCL również aktywności metabolicznej.

#### **6.4. A comparative study of three approaches to fibre's surface functionalization**

Celem pracy było porównanie trzech metod przyłączania żelatyny do powierzchni włókien PLCL pod kątem wpływu na wybrane właściwości, ze szczególnym uwzględnieniem odpowiedzi komórek linii L929.

W badaniach zastosowano trzy metody przyłączania żelatyny, oparte na aminolizie, hydrolizie zasadowej z użyciem NaOH i obróbce niskotemperaturową plazmą tlenową, które należą do najczęściej wykorzystywanych metod funkcjonalizacji poliestrowych włókien w inżynierii tkankowej. Zastosowano badaną wcześniej metodę przyłączania żelatyny za pomocą aminolizy i sieciowania glutaraldehydem oraz metody wykorzystujące funkcjonalizację hydrolizą oraz niskotemperaturową plazmą tlenową i sieciowanie mieszaniną EDC/NHS. W odróżnieniu od aminolizy, pozostałe dwie metody funkcjonalizacji wprowadzają na powierzchnię włókien grupy karboksylowe -COOH. Są one związane z grupami aminowymi białka za pomocą środka sieciującego EDC.

W pierwszej części pracy przedstawiono wyniki optymalizacji funkcjonalizacji włókien za pomocą hydrolizy i niskotemperaturowej plazmy tlenowej oraz dokonano porównania z aminolizą. Wybrano trzy zestawy parametrów reakcji aminolizy zapewniające brak zmian morfologii i różną ilość przyłączonych grup aminowych. Poszczególne metody funkcjonalizacji w różny sposób wpływały na zwilżalność włóknin. W wybranym zakresie parametrów aminoliza nie powodowała zmian zwilżalności włókien PLCL. Z kolei, zastosowanie hydrolizy i obróbki plazmą prowadziło do ich całkowitej zwilżalności. Dla większości wybranych warunków tych dwóch funkcjonalizacji obserwowano wniknięcie kropli we włókninę w ciągu 30s. Zaobserwowało również różny wpływ każdej z metod funkcjonalizacji na morfologię włókien, świadczący o odmiennym mechanizmie reakcji. W przypadku hydrolizy widoczne było „łuszczenie się” powierzchni włókien, a dla najwyższych stężeń roztworu NaOH i czasu reakcji - także ich sklejanie. Jak wskazano we wcześniejszej pracy z cyklu, aminoliza przy zastosowaniu wysokich parametrów reakcji prowadzi z kolei do kruchego pękania włókien. Dla włókien funkcjonalizowanych za pomocą obróbki plazmą przy zastosowanych parametrach nie uwidoczniono zmian morfologii. Wyniki uzyskane za pomocą chromatografii żelowej wskazywały, że zarówno aminoliza jak i obróbka plazmą prowadzą do spadku masy cząsteczkowej polimeru, przy czym dla wybranych warunków funkcjonalizacji spadki były większe w przypadku aminolizy. Wskazuje to na wpływ aminolizy i obróbki plazmą na strukturę chemiczną całej objętości materiału, nie tylko jego powierzchni. W odróżnieniu do nich, na chromatogramach próbek poddanych hydrolizie obserwowano

praktycznie niezmieniony pik główny oraz dodatkowy pik odpowiadający bardzo małym masom cząsteczkowym (do 5 kDa). Uzyskane wyniki wraz z mikroskopowymi obserwacjami stopniowego łuszczenia się włókien wskazują na fakt, że działanie hydrolizy jest ograniczone do powierzchni włókien ze względu na wolną dyfuzję roztworu NaOH w głąb włókna.

W drugiej części pracy zbadano przyłączanie żelatyny do powierzchni funkcjonalizowanych próbek. Wyniki spektroskopii ATR-FTIR wykazały obecność drgań pochodzących od pierwszo- i drugorzędowych wiązań amidowych, potwierdzając obecność żelatyny na powierzchni włókien modyfikowanych każdą z trzech metod. Wyniki uzyskane za pomocą kolorymetrycznego testu BCA wskazywały na najwyższą ilość przyłączonej żelatyny na próbce poddanej hydrolizie w najwyższym 1M stężeniu roztworu NaOH. Jednak duże uwolnienie żelatyny z powierzchni próbki w ciągu 1. dnia inkubacji w roztworze PBS świadczyło o dużym udziale fizycznie zaadsorbowanej żelatyny. Ponadto, biorąc pod uwagę pocienienie próbki i zmianę morfologii włókien, ograniczające praktyczne zastosowanie wybranych warunków funkcjonalizacji, próbka ta została zbadana jedynie w celach porównawczych. Pozostałe warunki wszystkich metod funkcjonalizacji zapewniały wysoką stabilność przyłączonej warstwy żelatyny, o czym świadczą jedynie nieznaczne spadki ilości żelatyny w ciągu 7 dni inkubacji w roztworze PBS. Najwyższe wyjściowe stężenie żelatyny wykazano dla jednej z próbek poddanych obróbce plazmą (9.38 µg/mg), a najniższe dla jednej z próbek poddanych hydrolizie (6.21 µg/mg). Intensyfikacja warunków obróbki plazmą i hydrolizy prowadziła do stopniowego wzrostu ilości przyłączonej żelatyny. W przypadku aminolizy nie zaobserwowano znaczących zmian ilości żelatyny dla wybranych parametrów reakcji. Przyłączenie żelatyny prowadziło do całkowitej zwilżalności wszystkich próbek, co wskazuje na ekspozycję hydrofilowych grup żelatyny wraz z działaniem efektu kapilarnego. Wyniki 1-osiowej próby rozciągania wykazały spadki naprężenia przy zerwaniu wszystkich próbek, przy czym dla wybranych parametrów modyfikacji udało się zachować jego dość wysoki poziom. Najmniejszy spadek (10% wartości wyjściowej) zaobserwowano dla próbki poddanej aminolizie w najbardziej łagodnych warunkach. W przypadku hydrolizy najmniejszy spadek wyniósł 19% wartości wyjściowej, a dla obróbki plazmą - 24% wartości wyjściowej. Dla większości próbek nie zaobserwowano znaczących spadków wydłużenia przy zerwaniu.

Na podstawie badań *in vitro* z udziałem fibroblastów linii L929 wykazano brak cytotoksyczności dla wszystkich próbek z przyłączoną żelatyną. Nie zaobserwowano jednak jednoznacznego trendu w zmianach aktywności metabolicznej komórek hodowanych na modyfikowanych próbках. Po 3 dniach hodowli, największy wzrost aktywności metabolicznej

komórek w stosunku do próbki kontrolnej wykazano dla jednej z próbek poddanych obróbce plazmą i próbki poddanej hydrolizie w najbardziej agresywnych warunkach. Pozostałe próbki wykazywały zarówno brak zmian jak i mniejszy wzrost lub spadek aktywności metabolicznej komórek. Obserwacje wykonane za pomocą mikroskopii SEM i mikroskopii fluorescencyjnej wykazały poprawę morfologii komórek linii L929 dla wszystkich próbek z przyłączoną żelatyną, przy czym próbki modyfikowane w najbardziej intensywnych warunkach obróbki plazmą i hydrolizy, o największym stężeniu żelatyny, wykazywały najbardziej rozwinięte filopodia i lamellipodia, struktury komórki wskazujące na jej bardzo dobry kontakt z danym podłożem.

Na podstawie uzyskanych wyników należy stwierdzić, że każda z badanych metod może prowadzić do poprawy odpowiedzi komórkowej, przy czym kluczowym jest dobór parametrów modyfikacji ze względu na zmiany właściwości podłoża takie jak morfologia włóknin, właściwości mechaniczne (naprężenie i wydłużenie przy zerwaniu) czy średnia masa cząsteczkowa, a także stabilność przyłączonej warstwy żelatyny i ich wpływ na funkcjonowanie włókniny w danym zastosowaniu. Duże znaczenie mogą mieć też kwestie technologiczne. Przykładowo, metoda obróbki plazmą może nie zapewnić równomiernego przyłączenia grup funkcyjnych do bardziej przestrzennych niż włókniny podłoży komórkowych takich jak podłoża otrzymywane metodą druku 3D.

## **7. Podsumowanie i wnioski**

Niniejsza rozprawa doktorska pozwoliła na wykazanie że:

- Aminoliza przebiega wolniej na włókninach niż na foliach poliestrowych pomimo ich większego rozwinięcia powierzchni w przeliczeniu na masę materiału. Najprawdopodobniej jest to spowodowane wyższym stopniem krystaliczności włókien, zwłaszcza na ich powierzchni, wynikającym ze specyfiki formowania,
- Aminoliza przebiega wolniej na włóknach PCL w porównaniu do włókien PLCL i PLLA ze względu na niższączęstość występowania wiązania estrowego w łańcuchu makrocząsteczk, wyższy stopień krystaliczności oraz prawdopodobnie wyższy stopień rekombinacji wolnych grup NH<sub>2</sub>,
- Możliwa jest optymalizacja parametrów reakcji aminolizy prowadzonej na włóknach PCL, PLCL i PLLA tak aby uzyskać poprawę morfologii komórek linii L929 i MG-63 (z wyjątkiem komórek linii MG-63 dla włókien PLLA) bez obniżania właściwości mechanicznych włókien,
- Zastosowanie zbyt agresywnych warunków reakcji aminolizy prowadzi do gwałtownego spadku mas cząsteczkowych wszystkich typów badanych włókien, kruchego pękania włókien i obniżenia właściwości mechanicznych, przy czym najwyraźniej jest to obserwowane dla włókien PLLA,
- Przyłączanie żelatyny do poliestrowych włókien za pomocą reakcji aminolizy i sieciowania glutaraldehydem prowadzi do uzyskania większej ilości żelatyny na powierzchni włókien niż w przypadku fizycznej adsorpcji; na przykładzie włókien PCL wykazano również wyższą stabilność warstw żelatyny przyłączonych metodą chemiczną,
- Obserwacje mikroskopowe i wyniki badań aktywności metabolicznej wskazują na większy wpływ modyfikacji chemicznej na poprawę odpowiedzi komórkowej niż fizycznej adsorpcji żelatyny. Istotne jest, że zastosowanie łagodnych warunków funkcjonalizacji chemicznej prowadzi do małych zmian naprężenia i wydłużenia przy zerwaniu włókniny, porównywalnych do zmian po zastosowaniu fizycznej adsorpcji,
- Zastosowanie łagodnych warunków aminolizy włókien PLCL wraz z przyłączeniem do nich żelatyny za pomocą sieciowania glutaraldehydem pozwala poprawić morfologię komórek L929 hodowanych na powierzchni włókien i zachować najbliższe wyjściowemu naprężenie przy zerwaniu włókniny w porównaniu do metod opartych na hydrolizie lub plazmie niskotemperaturowej,

- Dobór metody funkcjonalizacji i przyłączania żelatyny powinien być zawsze podyktowany wymaganiami uwzględniającymi specyfikę konkretnego miejsca aplikacji.

## **8. Elementy wkładu oryginalnego**

Oryginalnym wkładem przeprowadzonych badań w literaturę przedmiotu jest uzyskanie i opracowanie wyników doświadczalnych przebiegu aminolizy w submikronowych włóknach z poliestrów alifatycznych formowanych metodą elektroprzedzenia, w procesie funkcjonalizacji ich powierzchni. Istotnym jest odniesienie uzyskanych wyników do rezultatów aminolizy w foliach polimerowych i wykazanie wyraźnych różnic w przebiegu aminolizy zależnie od formy materiału. Dotychczasowe prace odnoszące się do efektywności aminolizy dotyczyły przede wszystkim aromatycznych poliestrów (niedegradowalnych) w postaci folii i stosunkowo grubych włókien formowanych metodą klasycznego przedzenia [27, 34, 35]. W literaturze przedmiotu brakowało usystematyzowanych informacji odnoszących się do aminolizy submikronowych włókien z poliestrów alifatycznych. W momencie rozpoczęcia badań, aminoliza włókien dla inżynierii tkankowej stawała się jedną z najczęściej wykorzystywanych metod modyfikacji powierzchniowej. W literaturze pojawiały się doniesienia, że aminoliza zachodzi wolniej na włóknach elektroprzedzionych niż na foliach, jednak tematyka ta nie była podjęta w żadnym porównawczym badaniu [36]. W pracy będącej częścią rozprawy nie tylko usystematyzowano wiedzę w tym zakresie ale i przedstawiono możliwe przyczyny obserwowanych różnic. Oryginalnym wkładem jest również zbadanie przebiegu i wpływu aminolizy w szerokim zakresie parametrów na właściwości różnych włókien poliestrowych. Zauważono, że w niektórych pracach wykorzystywano aminolizę jako etap pośredni w przyłączaniu molekuł do powierzchni włókien bez sprawdzenia efektywności zajścia reakcji aminolizy. W rozprawie pokazano, że może to prowadzić do takiej sytuacji jak dla włókien PCL, w przypadku których badania wstępne nie potwierdziły zajścia reakcji aminolizy dla powszechnie stosowanego zestawu parametrów, a wykazano, że przyłączanie białka może zachodzić na drodze fizycznej adsorpcji. W rozprawie wykazano, że taka fizyczna adsorpcja nie zapewnia uzyskania stabilnych warstw materiału finalnie przyłączanego do powierzchni włókien. Praca przyniosła też wyniki uzupełniające wiedzę na temat aminolizy włókien elektroprzedzionych z uwzględnieniem m.in. różnic w efektywności reakcji między poliestrami oraz wpływem reakcji na średnią masę cząsteczkową poliestrów, właściwości mechaniczne czy odpowiedź komórkową. Oryginalnym elementem badań jest porównanie przebiegu przyłączania żelatyny do funkcjonalizowanych włókien elektroprzedzionych otrzymanych z różnych poliestrów, o różnym stężeniu grup aminowych oraz odniesienie tych wyników do fizycznej adsorpcji żelatyny. Systematyczne zbadanie procesu, uwzględniające m.in. stabilność warstwy i wpływ na odpowiedź komórek, jest ważne ze względu na duże

wykorzystanie metody w badaniach modyfikacji powierzchniowej włókien. W rozprawie dokonano również porównania badanej metody przyłączania żelatyny z dwoma innymi, równie często wykorzystywanyimi metodami, bazującymi na hydrolizie i obróbce plazmą. Praca uzupełniła informacje na temat różnic między metodami, zwłaszcza we wpływie metod funkcjonalizacji na właściwości mechaniczne i odpowiedź komórek.

## 9. Literatura

- [1] Langer, R., Vacanti, J.P. (1993). Tissue engineering. *Science*, 260, 920–926.
- [2] Pobrane z: www.scopus.com (26.03.2024).
- [3] Bianco, P., Robey, P. G. (2001). Stem cells in tissue engineering. *Nature*, 414(6859), 118-121.
- [4] De Pieri, A., Rochev, Y., Zeugolis, D. I. (2021). Scaffold-free cell-based tissue engineering therapies: Advances, shortfalls and forecast. *NPJ Regenerative Medicine*, 6(1), 18.
- [5] Williams, D. F., Black, J., Doherty, P. J. (1992). Biomaterial-tissue interfaces. W: Proceedings of the Ninth European Conference on Biomaterials (s. 9-11).
- [6] Chung, S., King, M. W. (2011). Design concepts and strategies for tissue engineering scaffolds. *Biotechnology and Applied Biochemistry*, 58(6), 423-438.
- [7] AA, M. A. (2020). Scaffolds in tissue engineering. *Annals of RSCB*, 24(1), 142-152.
- [8] Dave, K., Gomes, V. G. (2019). Interactions at scaffold interfaces: Effect of surface chemistry, structural attributes and bioaffinity. *Materials Science and Engineering: C*, 105, 110078.
- [9] Rabe, M., Verdes, D., Seeger, S. (2011). Understanding protein adsorption phenomena at solid surfaces. *Advances in Colloid and Interface Science*, 162(1-2), 87-106.
- [10] Stewart, C., Akhavan, B., Wise, S. G., Bilek, M. M. (2019). A review of biomimetic surface functionalization for bone-integrating orthopedic implants: Mechanisms, current approaches, and future directions. *Progress in Materials Science*, 106, 100588.
- [11] Katti, D. S., Vasita, R., Shanmugam, K. (2008). Improved biomaterials for tissue engineering applications: surface modification of polymers. *Current Topics in Medicinal Chemistry*, 8(4), 341-353.
- [12] Wang, Y. X., Robertson, J. L., Spillman, W. B., Claus, R. O. (2004). Effects of the chemical structure and the surface properties of polymeric biomaterials on their biocompatibility. *Pharmaceutical Research*, 21, 1362-1373.
- [13] Godek, M. L., Michel, R., Chamberlain, L. M., Castner, D. G., Grainger, D. W. (2009). Adsorbed serum albumin is permissive to macrophage attachment to perfluorocarbon polymer surfaces in culture. *Journal of Biomedical Materials Research Part A*, 88(2), 503-519.
- [14] Khandwekar, A. P., Patil, D. P., Hardikar, A. A., Shouche, Y. S., & Doble, M. (2010). In vivo modulation of foreign body response on polyurethane by surface entrapment technique. *Journal of Biomedical Materials Research Part A*, 95(2), 413-423.
- [15] Rahmati, M., Silva, E. A., Reseland, J. E., Heyward, C. A., Haugen, H. J. (2020). Biological responses to physicochemical properties of biomaterial surface. *Chemical Society Reviews*, 49(15), 5178-5224.

- [16] Cai, S., Wu, C., Yang, W., Liang, W., Yu, H., & Liu, L. (2020). Recent advance in surface modification for regulating cell adhesion and behaviors. *Nanotechnology Reviews*, 9(1), 971-989.
- [17] Davidenko, N., Schuster, C. F., Bax, D. V., Farndale, R. W., Hamaia, S., Best, S. M., Cameron, R. E. (2016). Evaluation of cell binding to collagen and gelatin: a study of the effect of 2D and 3D architecture and surface chemistry. *Journal of Materials Science: Materials in Medicine*, 27, 1-14.
- [18] Le, P., Mai-Thi, H. N., Stoldt, V. R., Tran, N. Q., Huynh, K. (2021). Morphological dependent effect of cell-free formed supramolecular fibronectin on cellular activities. *Biological Chemistry*, 402(2), 155-165.
- [19] Ahmad Khalili, A., Ahmad, M. R. (2015). A review of cell adhesion studies for biomedical and biological applications. *International Journal of Molecular Sciences*, 16(8), 18149-18184.
- [20] Barr, S., Hill, E. W., Bayat, A. (2017). Functional biocompatibility testing of silicone breast implants and a novel classification system based on surface roughness. *Journal of the Mechanical Behavior of Biomedical Materials*, 75, 75-81.
- [21] Hu, X., Wang, T., Li, F., & Mao, X. (2023). Surface modifications of biomaterials in different applied fields. *RSC Advances*, 13(30), 20495-20511.
- [22] Cai, S., Wu, C., Yang, W., Liang, W., Yu, H., & Liu, L. (2020). Recent advance in surface modification for regulating cell adhesion and behaviors. *Nanotechnology Reviews*, 9(1), 971-989.
- [23] Hetemi, D., Pinson, J. (2017). Surface functionalisation of polymers. *Chemical Society Reviews*, 46(19), 5701-5713.
- [24] Richbourg, N. R., Peppas, N. A., Sikavitsas, V. I. (2019). Tuning the biomimetic behavior of scaffolds for regenerative medicine through surface modifications. *Journal of Tissue Engineering and Regenerative Medicine*, 13(8), 1275-1293.
- [25] Zhu, Y., Mao, Z., Shi, H., Gao, C. (2012). In-depth study on aminolysis of poly ( $\epsilon$ -caprolactone): Back to the fundamentals. *Science China Chemistry*, 55, 2419-2427.
- [26] Subasi, N. T. (2022). Overview of Schiff Bases. W: T. Akitsu (red.) *Schiff Base in Organic, Inorganic and Physical Chemistry*. Londyn: IntechOpen.
- [27] Albertsson, A. C., Varma, I. K. (2002). Aliphatic polyesters: Synthesis, properties and applications. W: A.C. Albertsson (red.) *Degradable aliphatic polyesters* (s. 1-40). Berlin, Heidelberg: Springer.
- [28] Zieliński, M., Twardowska, E., Bonczarowska, M. (2019). Etylenodiamina: metoda oznaczania w powietrzu na stanowiskach pracy z zastosowaniem wysokosprawnej chromatografii cieczowej z detekcją spektrofotometryczną. *Podstawy i Metody Oceny Środowiska Pracy*, 1(99), 29-44.

- [29] Zhu, Y., Mao, Z., Shi, H., & Gao, C. (2012). In-depth study on aminolysis of poly ( $\epsilon$ -caprolactone): Back to the fundamentals. *Science China Chemistry*, 55, 2419-2427.
- [30] Śmiechowski, K., Żarłok, J. (2022). Wpływ zagarbowania aldehydem glutarowym i natłuszczania na sucho na wybrane właściwości skór garbowanych bezchromowo. *Przegląd Włókienniczy-Włókno, Odzież, Skóra*, 5, 32-37.
- [31] Krzywicka, H. (1970) Bakteriobójcze działanie aldehydu glutarowego w stosunku do form wegetatywnych bakterii. *Roczn. PZH*, 21(1), 87-92.
- [32] Sionkowska, A., Lewandowska, K. (2016). Biopolimery.
- [33] Gómez-Guillén, M. C., Giménez, B., López-Caballero, M. A., Montero, M. P. (2011). Functional and bioactive properties of collagen and gelatin from alternative sources: A review. *Food Hydrocolloids*, 25(8), 1813-1827.
- [34] Aflori, M., Drobota, M., Timpu, D., Barboiu, V. (2008). Studies of amine treatments influence on poly (ethyleneterephthalate) films. *Optoelectronics and Advanced Materials-Rapid Communications*, 2, 291-295.
- [35] Ohe, T., Yoshimura, Y. (2012). Reactions of PET Fibers with Ethylenediamine in a Water Solution Containing Surfactants. *Sen'i Gakkaishi*, 68(9), 253-258.
- [36] Fukatsu, K. (1992). Mechanical properties of poly (ethylene terephthalate) fibers imparted hydrophilicity with aminolysis. *Journal of Applied Polymer Science*, 45(11), 2037-2042.

**PUBLIKACJE NAUKOWE  
WŁĄCZONE DO ROZPRAWY**

Article

# Aminolysis of Various Aliphatic Polyesters in a Form of Nanofibers and Films

Oliwia Jeznach <sup>\*</sup>, Dorota Kolbuk and Paweł Sajkiewicz

Institute of Fundamental Technological Research, Polish Academy of Sciences, Pawinskiego 5B, 02-106 Warsaw, Poland; dorotakolbuk@gmail.com (D.K.); plsajkiewicz@gmail.com (P.S.)

\* Correspondence: oliwia.jeznach@gmail.com

Received: 17 September 2019; Accepted: 11 October 2019; Published: 14 October 2019



**Abstract:** Surface functionalization of polymer scaffolds is a method used to improve interactions of materials with cells. A frequently used method for polyesters is aminolysis reaction, which introduces free amine groups on the surface. In this study, nanofibrous scaffolds and films of three different polyesters—polycaprolactone (PCL), poly(lactide-*co*-caprolactone) (PLCL), and poly(L-lactide) (PLLA) were subjected to this type of surface modification under the same conditions. Efficiency of aminolysis was evaluated on the basis of ninhydrin tests and ATR–FTIR spectroscopy. Also, impact of this treatment on the mechanical properties, crystallinity, and wettability of polyesters was compared and discussed from the perspective of aminolysis efficiency. It was shown that aminolysis is less efficient in the case of nanofibers, particularly for PCL nanofibers. Our hypothesis based on the fundamentals of classical high speed spinning process is that the lower efficiency of aminolysis in the case of nanofibers is associated with the radial distribution of crystallinity of electrospun fiber with more crystalline skin, strongly inhibiting the reaction. Moreover, the water contact angle results demonstrate that the effect of free amino groups on wettability is very different depending on the type and the form of polymer. The results of this study can help to understand fundamentals of aminolysis-based surface modification.

**Keywords:** aminolysis; polyester; electrospinning; nanofibers; film; surface chemical modification

## 1. Introduction

The interactions between scaffolds and cells are determined primarily by surface properties of materials, such as roughness and topography, chemical structure and functional groups, types and density of electrical charges, balance between hydrophilicity and hydrophobicity, and surface free energy [1–9]. To date, many methods have been proposed to induce changes of the surface physico-chemical properties in a way that makes it attractive for a specific application [10]. According to the literature, common strategies of polymer surface modification for biological applications include: Plasma [11] and laser treatment [12], wet chemical methods such as aminolysis [13], hydrolysis [14], ion implantation [15], blending with hydrophilic pluronic, segregating at the surface [16], and various approaches of protein immobilization [17–19].

Electrospinning is a method that allows to obtain fibers with nano and sub-micro diameters from polymer solution. This technique is commonly used to produce fibrous scaffolds mimicking the extracellular matrix (ECM) (e.g., [20]). From a technical point of view, electrospinning is a relatively simple method; however, from a physical perspective, the process is quite complex, leading to the formation of non-equilibrium structures. Such structures are very different from the structures formed using classical methods, raising new problems; for instance, related to the structure/properties radial gradients, which can be essential from the perspective of surface modifications.

Aliphatic polyesters, such as polyesters–polycaprolactone (PCL), poly(lactide-*co*-caprolactone) (PLCL), and poly(L-lactide) (PLLA) belong to the class of polymers commonly used in biomedical applications, due to their biocompatibility and degradability in human body conditions. Their advantages also include easily-tunable physical and mechanical properties, as well as ease of processing. It is worth noting that aliphatic polyesters are excellent materials to enhance surface properties using chemical methods like aminolysis because of the presence of ester bonds in the polymer chain. These, provided defined conditions, undergo rupture easily, causing, in the case of aminolysis, the formation of hydroxyl and amino groups at the material surface. In such a case, only one of the amino groups is consumed during the chain scission at the polymer surface, being converted to an amide group, while the second amine group remains free. This method is based on simple treating of the polymer scaffold in diamine solution (e.g., 1,6-hexanediamine [21], 1,2-ethanediamine [22], Fmoc-PEG-diamine [23], etc.) and was previously considered for improving the dyeing process and moisture regain in the textile industry [24–26]. In tissue engineering, aminolysis of polyesters is usually applied as the final [14,27] or the intermediate step in the biomolecule immobilization process [28]. In many papers, surface modification with aminolysis reaction is reported for polycaprolactone [14,29–35]. A smaller number of studies is related to the surface functionalization of other polyesters, such as polylactide [36–38] and poly(lactide-*co*-caprolactone) [19,39–41]. Moreover, in the case of PLLA meshes, aminolysis is frequently used as a method of fiber fragmentation [42–46]. The aim of our paper is to explain the different efficiency of the aminolysis at the same processing conditions for various aliphatic polyesters in the form of nanofibers and films. In the literature, there is a lack of such comparison. In our opinion, considering the extensive use of aminolysis for surface modification of polyester materials, a systematic study of the reaction efficiency and its impact on material properties is necessary. The polyesters were chosen regarding the glass transition temperature, being related to molecular mobility, which is expected to be crucial from the point of view of the possible free amine recombination process. We hypothesize that the difference between the efficiency of aminolysis is due to the structure peculiarities in fibers and films, which result from the difference in formation (crystallization) conditions.

## 2. Materials and Methods

### 2.1. Materials

Three types of polymers were used for fabrication of nanofibers and films: Poly(caprolactone) (PCL) (Sigma-Aldrich (Saint Louis, MO, USA), Mw = 80,000 g/mol, Tg = –60 °C), poly(L-lactide) (PLLA) (PL49, Corbion (Amsterdam, The Netherlands,)), inherent viscosity = 4.9 dL/g, Tg = 58 °C, and poly(L-lactide-*co*-caprolactone) (PLCL) 70:30 (Resomer® LC703S, Evonik (Weiterstadt, Germany), inherent viscosity = 1.3–1.8 dL/g, Tg = 32–42 °C). Solvents—acetic acid (AA) (purity degree 99.5%), formic acid (FA) (purity degree ≥ 98%), and hexafluoroisopropanol (HFIP) (purity degree 98.5%) were purchased from Poch (Gliwice, Poland), Sigma-Aldrich (Saint Louis, MO, USA), and Iris Biotech GmbH (Marktredwitz, Germany), respectively. Ethylenediamine (purity degree 99.5%), isopropanol (purity degree 99.8%), ninhydrin (purity degree 99%), and ethanol (purity degree 99.8%) were purchased from Chempur (Piekary Śląskie, Poland). For PCL and PLLA, glass transition temperatures were determined experimentally. Glass transition temperature of PLCL was assumed as stated by the producer.

### 2.2. Fabrication of PCL, PLCL, and PLLA Nanofibrous Scaffolds and Films

Three polymer solutions were used for electrospinning: 15% w/w solution of PCL in mixed solution of acetic acid and formic acid at 9:1 ratio, 7% w/w PLCL solution in HFIP, and 3.5% w/w solution of PLLA in HFIP. The electrospinning equipment (Bioinicia, Valencia, Spain) was operated in a horizontal mode. Solutions were pumped through a stainless steel needle placed at a distance of 15 cm from the collector rotating at a speed of 300 rpm. The applied voltage and ambient conditions were chosen to form nonwovens with appropriate morphology. The positive voltage applied to the needle was 13–15 kV for PCL and PLCL, and 13 kV for PLLA. The collector was maintained at the electrical potential of

–2 kV in the case of PCL and PLCL and 0 kV for PLLA. Temperature and humidity conditions during electrospinning process were 26 °C, 36% for PCL, 38 °C, 40% for PLCL, and 24 °C, 35% for PLLA, respectively. The films were solution cast from the same solutions as the electrospun nanofibers and air-dried under the hood at room temperature.

### 2.3. Aminolysis Treatment

Samples were immersed in 6% *w/v* solution of 1,2-ethandiamine (ED) in isopropanol (app. sample/diamine solution ratio: 1.5 mg/mL) at 30 °C for 5 and 15 min with shaking at 100 rpm. Then, samples were washed three times with copious amount of water, followed by vacuum drying overnight.

### 2.4. Ninhydrin Assay

Effectiveness of the aminolysis was evaluated from concentration of free amino groups using ninhydrin staining. For quantitative tests, samples were transferred to a glass vial and 0.5 mL of 2% *w/v* ninhydrin solution was added. Then, they were heated for 10 min using a hot plate at 100 °C. After that, 1 mL of isopropanol (for PLLA and PLCL) or isopropanol/dioxane 1/1 solution (for PCL) was added. Absorbance of the samples was measured at 570 nm. The amount of free amino groups was calculated on the basis of the absorbance calibration curve with known concentration of ED in isopropanol solution. For visualization of staining, samples were placed onto glass dish, wetted with 0.2% *w/v* solution of ninhydrin in ethanol using a Pasteur pipette, and incubated at 40 °C for 15 min.

### 2.5. ATR–FTIR

Surface molecular structure of samples was analyzed using attenuated total reflectance Fourier transform infrared (ATR–FTIR) spectrometer Bruker Vertex 70 (Mannheim, Germany), in absorbance mode, in 4000–400 cm<sup>−1</sup> range. The resolution of measurement was 2 cm<sup>−1</sup>.

### 2.6. WAXS

Wide angle X-ray scattering (WAXS) was applied for analysis of the supermolecular structure. WAXS measurements were performed using Bruker D8 Discover diffractometer Mannheim, Germany) with CuK $\alpha$  radiation operated at a voltage of 40 kV, and a current of 20 mA. All measurements were performed in reflection mode, using Goebel optics for beam formation: A 0.6 mm slit and Soller collimator. Highly sensitive Lynx Eye 1-D silicon strip detector was used. The range of diffraction angle, 2 $\theta$ , was between 5° and 35°, with a step of 0.01° and a time of data accumulation at angular point of 0.2 s. The “empty” scan without a sample was subtracted and the default function of subtracting background was applied. Then, the WAXS profiles were deconvoluted numerically using PeakFit software assuming Pearson VII and Gauss functions for the crystal diffraction peaks from the amorphous halo, respectively. The degree of crystallinity was determined as the ratio of the area of all the crystalline diffraction peaks to the overall area of the profile. The full width at half maximum (FWHM) was used in determination of the relative mean crystal size, L, without correction for instrumental broadening, from the Scherrer equation:

$$L = K\lambda/\beta\cos\theta \quad (1)$$

where K is the dimensionless Scherrer shape factor, assumed as 0.9,  $\beta$  is the line broadening at FWHM,  $\lambda$  is the X-rays wavelength, and  $\theta$  is the Bragg angle.

### 2.7. Mechanical Testing

Mechanical properties were measured using uniaxial testing machine Lloyd EZ-50 (New York, USA) equipped with handles for thin and delicate samples with a 50 N load cell for nanofibrous scaffolds and 100 N for polymer films under cross-head speed of 5 mm/min. For each type of material, three 10 × 40 mm dry samples were used (10 × 25 mm—actual area of testing). Sample thickness was

measured with a thickness gauge. Mechanical properties—Young's modulus, stress at break, and strain at break were determined from stress-strain curves.

### 2.8. Water Contact Angle

The wettability of the matrices was determined by water contact angle measurements using goniometer Data Physics OCA 15EC (Filderstadt, Germany). The results are reported as mean value  $\pm$  standard deviation evaluated on five repetitions.

## 3. Results

### 3.1. Ninyhydrin Staining of Free Amino Groups

The amount of  $\text{NH}_2$  groups on the aminolyzed polymer nanofibers and films was measured by ninhydrin assay on the basis of previously obtained calibration curve (Figure 1). Presence of free amino groups was confirmed for all samples, except PCL nanofibers. This observation indicates that aminolysis at these conditions is not effective for PCL nanofibers, contrary to other investigated polyesters as well as to PCL films. This trend of more effective aminolysis for films as compared to nanofibers was also observed in results for PLLA and PLCL. Concentration of amino groups for films was considerably higher than for nanofibers—for example in the case of PLCL it reached  $5.43 \times 10^{-8} \pm 9.0 \times 10^{-9}$  M/mg for nanofibers and  $4.72 \times 10^{-7} \pm 1.45 \times 10^{-8}$  M/mg for film after 5 min of aminolysis. It is worth noting that effectiveness of the aminolysis was significantly lower for PCL film than for PLCL and PLLA film samples. Additionally, for each type of material, an increase in concentration of  $\text{NH}_2$  groups with reaction time was observed.

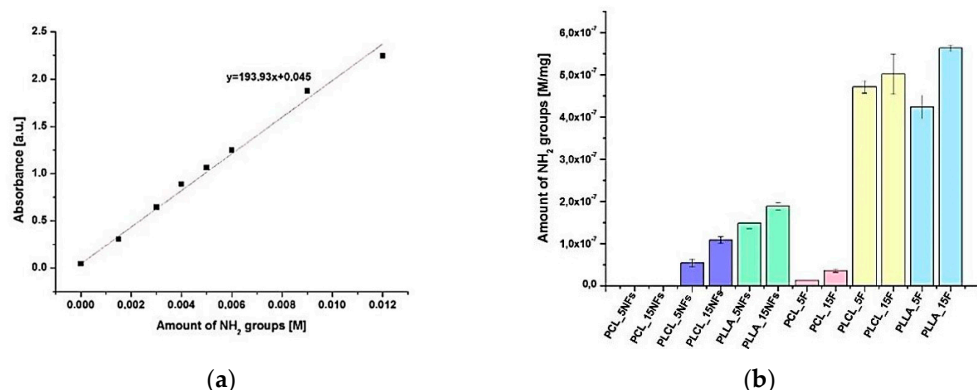


**Figure 1.** (a) Calibration curve used for amino groups quantification. (b) Amount of amino groups on modified nanofibers and films.

Figure 2 illustrates the qualitative results of ninhydrin staining. Among aminolyzed samples, only PCL nanofibers were unstained, what is in agreement with quantitative results (Figure 1b). In the case of PLLA film, highly effective aminolysis was accompanied by degradation, which is manifested by higher brittleness.



**Figure 2.** Representative images of samples after ninhydrin staining.

### 3.2. Molecular Structure from ATR–FTIR Analysis

Figure 3 shows the ATR–FTIR spectra of PCL, PLCL, and PLLA nanofibers and films before and after the aminolysis. There are two amide bands resulting from nucleophilic attack of diamine on the carbonyl group, which may be treated as evidence of aminolysis reaction. The first band in the range 1510–1580 cm<sup>−1</sup> is assigned to amide II, being mainly associated with N–H bending vibrations; the second one in the range 1600–1700 cm<sup>−1</sup> corresponds to amide I, being mainly associated with C=O (carbonyl) stretching vibration (70–85%) and C–N group vibrations (10–20%). In the case of PCL (Figure 3a), the amide II band is observed for films after the treatment, which confirms the ninhydrin results, indicating the occurrence of aminolysis. Contrary to this, there are no amide peaks for PCL nanofibers after the aminolysis treatment, which is in agreement with ninhydrin staining results (Figure 2), indicating no aminolysis for PCL nanofibers. For modified PLCL films, broad peaks from the amide, mostly amide II bands, were observed (Figure 3b). In the case of PLCL nanofibers, the amide peaks were observed after 15 min of the treatment, only. The lack of amide peaks for PLCL nanofibers after 5 min of the treatment is most probably due to too low of a concentration of amine groups to be detected by the ATR–FTIR method. In the case of PLLA (Figure 3c), both amide I and II bands and for both nanofibers and films are observed, indicating that aminolysis is very effective for this polyester.

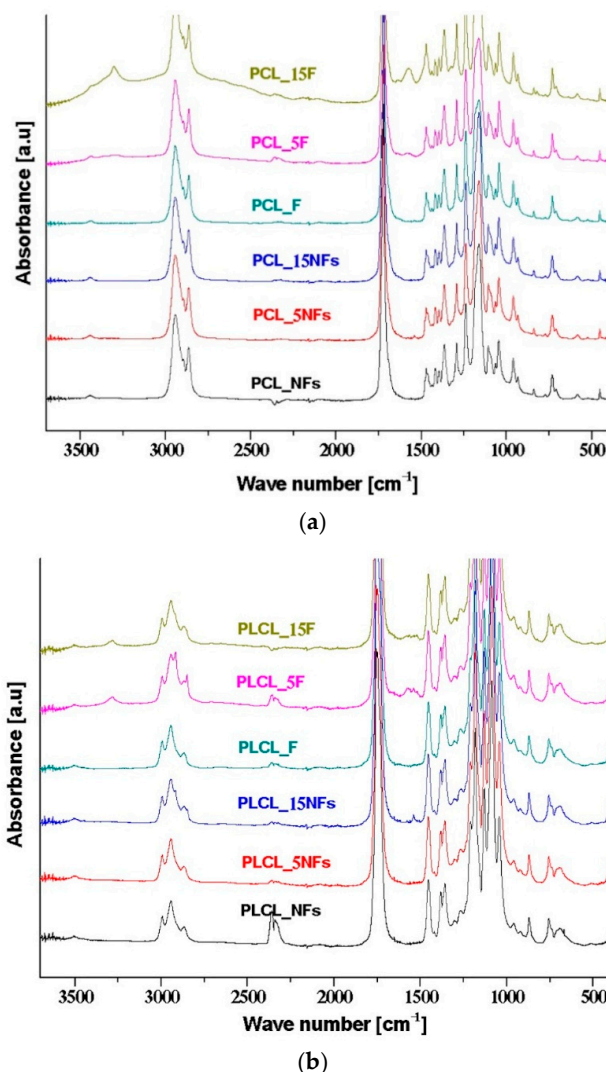


**Figure 3. Cont.**

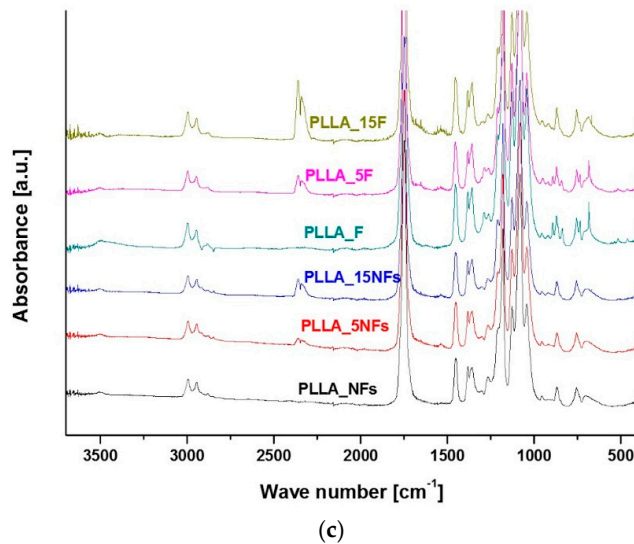


**Figure 3.** ATR-FTIR spectra of (a) PCL, (b) PLCL, and (c) PLLA nanofibers and films before and after the aminolysis treatment.

### 3.3. Supermolecular Structure (Crystallinity) from WAXS

WAXS profiles of PCL, PLLA, and PLCL films and nanofibers, before and after 5 min of the aminolysis treatment, are shown in Figure 4. Detailed information on the degree of crystallinity and crystal size/order are presented in Figure 5.

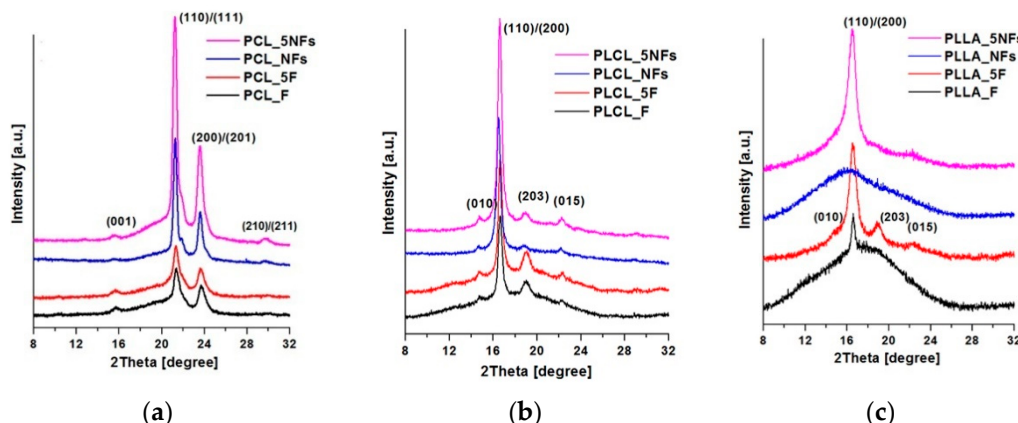


**Figure 4.** WAXS profile of casted films and fibers before and after the aminolysis treatment: (a) PCL, (b) PLCL, (c) PLLA.

WAXS profiles of PCL indicate diffraction from crystal structure with strongest maximum at  $2\theta = 15.6$  deg, 21.3 deg, 23.6 deg, and 29.7 deg corresponding to (001), (110)/(111), (200)/(201), and (210)/(201) lattice planes, respectively, and the maximum of the amorphous halo at  $2\theta = 21$  deg (Figure 4a). This is in agreement with our previous studies [47,48].

Samples of PLCL show peaks at  $2\theta = 14.7$  deg, 16.6 deg, 19 deg, and 22.4 deg (Figure 4b) corresponding to the (010), (110)/(200), (203), and (015) lattice planes, respectively [49].

The WAXS profile of PLLA is composed of a broad scattering peak from amorphous phase and small or zero intensity peaks from the crystal phase (Figure 4c). It may be seen that the aminolysis treatment leads to increase of PLLA crystallinity, making peaks at  $2\theta = 14.7$  deg, 16.5 deg, 18.9 deg, and 22.3 deg, corresponding to the (010), (110)/(200), (203), and (015) lattice planes, evident [49,50].

The results shown in Figure 5 clearly indicate an increase of crystallinity with time of the aminolysis treatment for all polyesters films, as well as for PLLA and PLCL nanofibers. This increase

in crystallinity is a result of molecular degradation leading to higher mobility of shorter molecules during the aminolysis treatment. The largest crystallinity increase is for PLLA and the lowest for PCL films, what is correlated with the ninhydrin results. No change in crystallinity is observed for treated PCL nanofibers (Figure 5a), for which the aminolysis treatment was found ineffective. A decrease of average crystal size with time of the treatment observed for PCL, PLCL, and PLLA nanofibers and films (Figure 5b,d,f) is most probably caused by formation of additional small crystals for most materials or disruption of existing crystals in the case of PCL nanofibers.

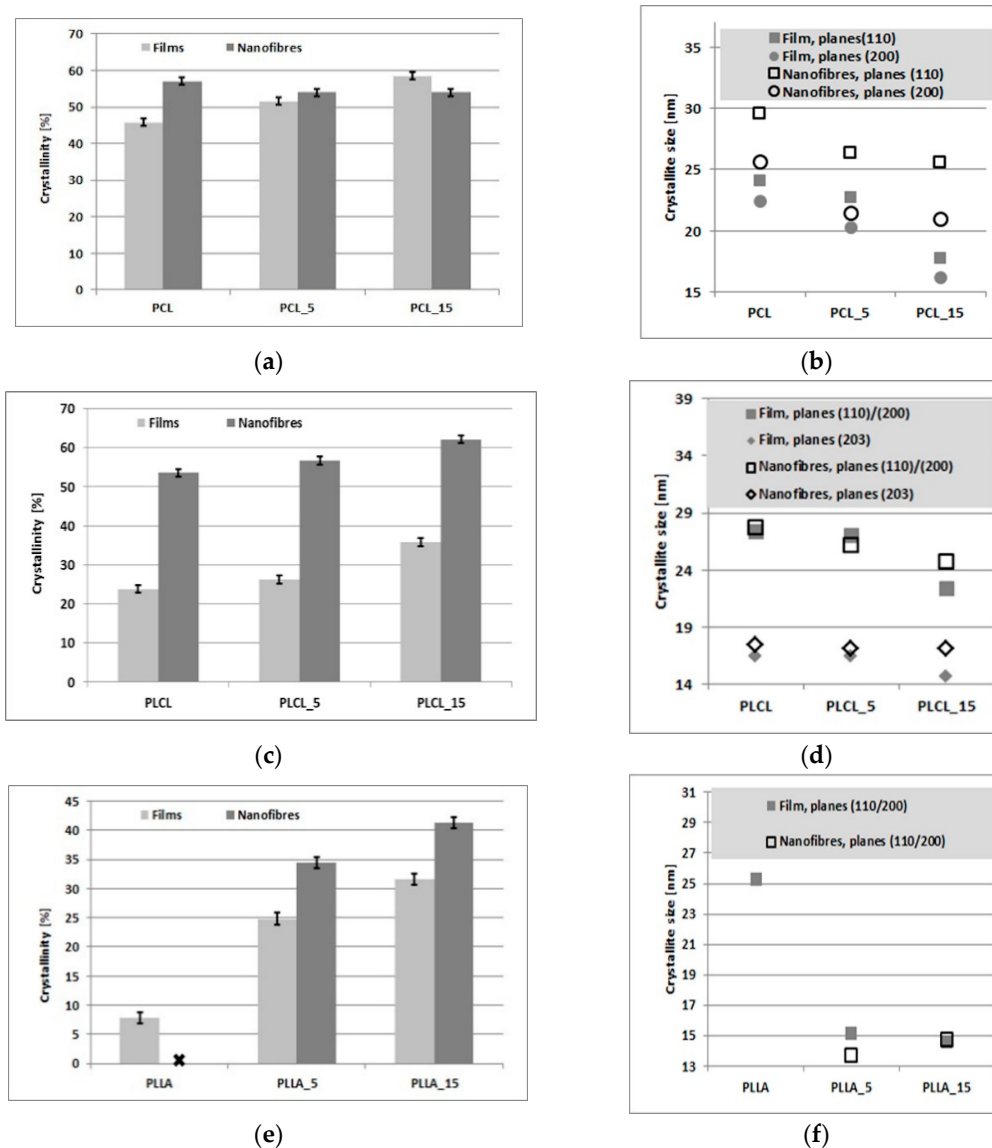


**Figure 5.** Crystallinity and crystal size of: (a,b) PCL, (c,d) PLCL, (e,f) PLLA.

### 3.4. Mechanical Properties

Figure 6 shows mechanical properties of samples before and after the aminolysis treatment. The changes of Young's modulus (Figure 6a) were not informative from the perspective of aminolysis because of no simple correlation with crystallinity, as was expected. We anticipate that other factors like erosion of surface after the aminolysis treatment can influence the registered Young's modulus. An increase in modulus with the treatment time correlated with increase in crystallinity was observed for PCL films, only. For other samples, no essential changes or even reduction of Young's modulus with the treatment time was observed, with no correlation with crystallinity changes.

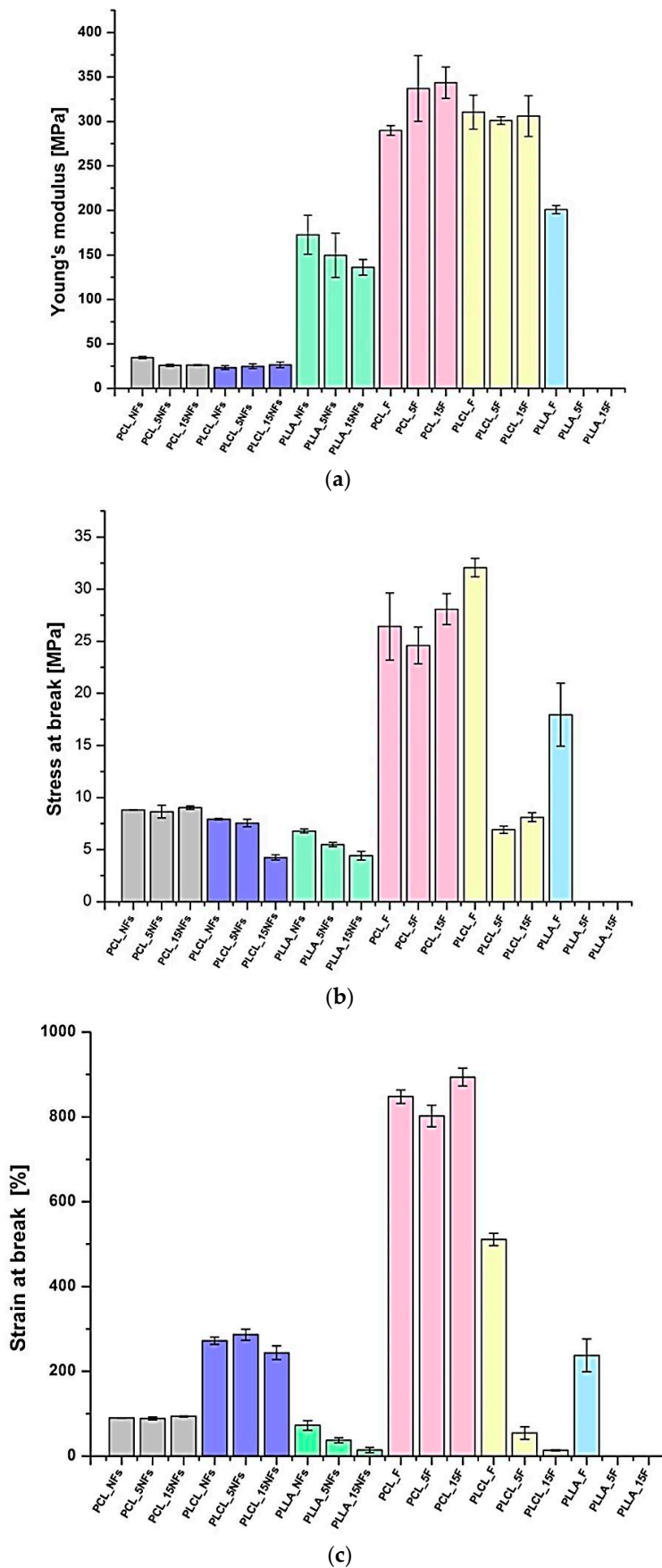


**Figure 6.** Mechanical properties of nanofibers and cast films before and after the aminolysis treatment: (a) Young's modulus, (b) stress at break, (c) strain at break. For PLLA films after the treatment, there are no results because of complete degradation.

More direct information on the efficiency of the aminolysis can be drawn from analysis of the stress at break, which is molecular weight-dependent. An empirical equation, which combines the tensile strength,  $\sigma$ , with polymer molecular weight, has been proposed by Flory to predict variation of the stress at break with the polymer number-average molecular weight  $M_n$  [51]. This equation can be presented as:

$$\sigma = \sigma_\infty - B/M_n, \quad (2)$$

where  $\sigma_\infty$  is the fracture strength at infinite molecular weight, and  $B$  is a constant derived from the relationship, discussed by Bersted and Anderson as:

$$B = K\sigma_\infty M_c, \quad (3)$$

where  $K$  is a constant value between 2 and 3 and  $M_c$  is the critical molecular weight for entanglements [52].

Drop of the stress at break was noticed by us for all samples except PCL nanofibers and films, with a tendency to be more significant for longer times of the aminolysis treatment (Figure 6b). This stress at break reduction is a result of effective aminolysis, as evidenced directly by ninhydrin tests. The trends in the stress at break correspond with changes in the strain at break, with most visible reduction after the aminolysis treatment for PLLA nanofibers and PLCL films being as dramatic as from  $511 \pm 14.41\%$  for PLCL\_F to  $13.6 \pm 1.55\%$  for PLCL\_15F (Figure 6c).

### 3.5. Water Contact Angle

Figure 7 shows results of water contact angle (WCA) measurements. For PCL and PLCL nanofibers, a slight decrease in WCA after the aminolysis treatment was observed. In the case of PCL—from  $140.55 \pm 1.21^\circ$  for pristine to  $133.18 \pm 2.21^\circ$  for 5 min and  $131.51 \pm 4.67^\circ$  for 15 min of the treatment. For PLCL nanofibers, the values of water contact angle were as follow:  $134.27 \pm 2.04^\circ$ ,  $126.46 \pm 0.64^\circ$ , and  $128.95 \pm 2.55^\circ$  for pristine and treated for 5 and 15 min samples, respectively. For PLLA nanofibers, 5 min of the treatment led to even an increase in WCA from  $132.9 \pm 2.48^\circ$  for the pristine sample to  $137.52 \pm 1.92^\circ$ . The general observation is that water contact angles are generally lower for film samples. After the treatment, a significant decrease of water contact angle was visible for PCL films. In the case of PLCL film, the values were almost unchanged. For PLLA films, it was impossible to measure water contact angle due to complete degradation.

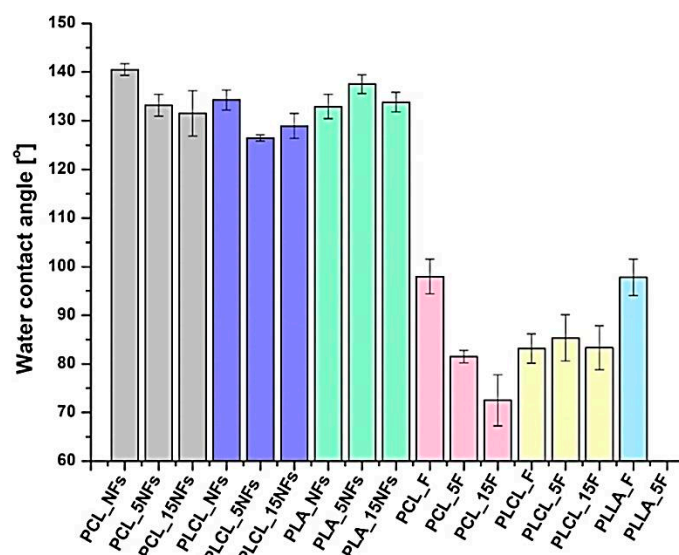


**Figure 7.** Water contact angle measurements for samples before and after the aminolysis treatment. For PLLA films after the treatment, there are no results because of complete degradation.

#### 4. Discussion

In this study we analyze the effects of the aminolysis treatment for three types of polyesters in the form of nanofibers and films.

The efficiency of the aminolysis for PCL, PLCL and PLLA samples was quantitatively measured by the amount of free amino groups using ninhydrin staining. The susceptibility of investigated polymer to aminolysis was the highest for PLLA, leading even to complete degradation of films, medium for PLCL, and the lowest for PCL. For example, after 5 min of the treatment, the amount of amino groups was about 35 times higher for PLCL in comparison with PCL film. As was expected, in the case of effective aminolysis treatment, the amount of free amino groups increased with the time of the treatment, which has already been reported [53,54]. The reactions under the same conditions turned out to be much more efficient in films as compared to nanofibers, despite the higher surface area to volume ratio for nanofibrous samples. The aminolysis treatment was ineffective for PCL nanofibers. We performed an additional experiment for PCL nanofibers with the aminolysis treatment at the same concentration and temperature conditions, but with the time extended to 144 h. However, morphology of nanofibers was unchanged and the amount of amine groups was only ca.  $8.2 \times 10^{-8}$  M/mg.

We provide additional results by the direct method of the ATR–FTIR technique and the indirect methods of WAXS and mechanical tensile tests. In the case of ATR–FTIR, the efficiency of the aminolysis treatment is confirmed by the appearance of the absorbance of the amide II and amide I bands.

The results of the ninhydrin tests are well correlated with the WAXS analysis of crystallinity. It is evident that crystallinity increases with the treatment time for all the samples, except PCL nanofibers. This crystallinity increase is due to chain scission, an effect of the ester bond cleavage resulting in higher molecular mobility allowing for additional crystallization. In the case of PCL nanofibers showing the aminolysis treatment as ineffective, there is also no increase in crystallinity as measured by WAXS. A reduction in the average crystal size with the treatment time observed for PCL, PLLA, and PLCL nanofibers and films is most probably a result of either formation of additional small crystals, in the case of the effective aminolysis for most materials, or disruption of existing crystals, in the case of PCL nanofibers.

The confirmation of the results of ninhydrin staining by the results of mechanical tensile tests is based on the molecular degradation, which accompanies the aminolysis process. Chain scission causes a decrease of the stress and strain at break. It is a well-known fact that reduction of chain length via aminolysis results in lower resistance against tension [55]. In our study, this process seems to be most intense in the case of PLLA nanofibers and films, as well as PLCL films. In the literature, there are many examples of reduction in mechanical properties, such as tensile strength, elongation at break, and even Young's modulus, as a result of aminolysis process [14,56,57]. It should be noted that there are also studies in which authors observed an increase of tensile strength or elastic modulus after reaction [32]. In our work, we also noticed a small increase of mechanical properties for PCL films after the aminolysis treatment. This phenomenon was explained by Ganjalinia et al. as formation of cross-links between hydroxyl molecular chains of polymer and NH<sub>2</sub>-terminated groups of reactant [55]. Summarizing the problem of various susceptibility of investigated polyesters to aminolysis, we can conclude that it is most probably associated with:

- Various ratios of ester to alkyl groups being the lowest for PCL and the highest for PLLA.
- Different crystallinity, being the highest for PCL and the lowest for PLLA. It is known that the availability of ester groups for aminolysis depends on the supermolecular organization, being lower for the crystal phase than for the amorphous one.
- Different rates of NH<sub>2</sub> recombination after aminolysis, being dependent on the position of the aminolysis temperature in relation to glass transition temperature. It is anticipated that in the case of PCL with glass transition temperature far below aminolysis temperature, the free amine recombination rate should be much higher than for PLCL with T<sub>g</sub> = 32–42 °C, and particularly for PLLA, for which aminolysis is performed below glass transition temperature.

The non-trivial problem is related to the effect of the form of material on the aminolysis effectiveness. Our results clearly indicate that aminolysis reaction turned out to be much easier in the case of films. Our hypothesis is that the reason is related to the radial distribution of structure in the case of nanofibers with more crystalline skin, which inhibits the reaction. There are some works regarding the fundamentals of polymer aminolysis, where it is claimed that aminolysis is a highly selective process, attacking primarily ester bonds in the amorphous regions, which is detected as a rapid drop in polymer molar mass and weight [26,47,58]. The less intensive attack of crystallites occurs at the further stage of the reaction. Considering the large differences in the effectiveness of aminolysis of film and electrospun nanofibers, we should return to the basics of fiber formation in classical processes of spinning from solution and melt. Relatively thick fibers formed in classical spinning processes allow to investigate experimentally the details of the internal structure, including its radial distribution. It was shown theoretically [59,60] that the crystallization driving force is higher at the fiber surface due to two reasons. The first one being of a thermodynamic nature is related to lower temperature at the jet surface in the case of melt spinning, or to a higher polymer concentration caused by surface solvent evaporation at the jet surface in the case of solution spinning. In both cases there is higher thermodynamic force at the jet surface because of higher supercooling or supersaturation. The second reason for the higher crystallization driving force at the jet surface is related to higher stress because of higher solution viscosity caused by lower temperature or higher polymer concentration. It leads to more effective molecular orientation at the surface, resulting in faster crystallization. Both factors are responsible for higher crystallinity at the fiber surface, as evidenced experimentally [61,62]. This radial distribution of structure with higher crystallinity at the surface compared to that at the core is narrower the higher the spinning rate [53]. For instance, the crystallinity of PET fibers spun at 5400 m/min and analyzed directly using localized electron scattering show well-pronounced crystallinity near the fiber surface with a practically amorphous fiber core [55]. This direct crystallinity analysis corresponds to measurements of radial variation of birefringence and Lorentz density [55]. It should be taken into account that the typical velocity of the jet during electrospinning, as measured directly using a moving substrate and high-speed camera, as well as laser Doppler velocimetry, is between 300 and 900 m/min [63–65], which is comparable to traditional dry spinning. Estimations of the electrospinning velocity based on the mass of the collected nanofibers range from 6000 m/min to an astonishing 60,000 m/min [66–70], so is the same order or even higher as for the processes of high speed spinning. However, it should be made aware that the estimation of the velocity from the mass of the collected nanofibers can be loaded with an error due to the splitting of the electrospinning jet or multiple electrospinning jets from the spinneret [71]. So, it is expected that in the case of solution electrospinning, there will be a similar rate of solvent evaporation resulting in similar crystallinity radial distribution in both processes, high speed spinning and electrospinning, allowing to transfer the conclusions from the high-speed spinning process to electrospinning. Some authors use the term skin/core morphology for this kind of structure radial distribution of fibers. In the case of electrospinning, there is no experimental evidence of such radial distribution of crystallinity because of extremely small diameter of fibers compared to those formed by classical spinning. There are only speculations using some experimental results on the possibility of the existence of the skin–core morphology, for instance in electrospun nylon-6 fibers [72]. Summarizing the problem, it is expected that the crystallinity of skin is much higher than for core of fibers, forming an effective barrier for aminolysis processing of nanofibers. In the case of casted films, we do not expect such gradient of crystallinity across the film thickness because of a much slower evaporation rate. An extreme example is the case of PCL nanofibers, for which aminolysis reaction is completely inefficient at given conditions.

The needs of harder reaction conditions for PCL nanofibers than for membranes was discussed by Piai et al. [73], who associated the problem with the high hydrophobicity of PCL nonwovens. However, our results show that the PLCL and PLLA nanofibers, which have very similar water contact angles to the PCL, are reactive at the same conditions, indicating that this is no problem of hydrophobicity. Our WAXS crystallinity measurements before aminolysis clearly show that bulk crystallinity of nanofibers

is considerably higher than that of films, reaching 57% for PCL which is ca. 10% higher compared to PCL films. In the case of PLCL and PLLA nanofibers, crystallinity before aminolysis is lower compared to PCL, reaching 53%, while PLLA nanofibers remain practically amorphous. This very high bulk crystallinity of PCL nanofibers, together with highly probable crystallinity radial distribution, lets us suppose that surface PCL nanofibers' crystallinity is extremely high, forming a strong barrier against aminolysis reaction.

According to the literature, additional information about aminolysis comes from water contact angle measurements, because introducing hydrophilic free amino groups on the surface should result in enhancement of wettability. Indeed, in the case of PCL film, we observed a significant decrease of water contact angle for modified samples, and the value was lower as time increased (25° drop for 15 min of aminolysis). Surprisingly, we also observed a slight decrease for PCL nanofibers, for which we did not detect any amino groups on the surface. However, this effect could be associated with the change of roughness after immersing in ED/isopropanol solution or surface hydrophilization with alcohol [74]. For the PLCL nanofibers, the observed decrease was also very slight being up to 9 degrees. Moreover, for the PLLA nanofibers and PLCL film, we did not observe any enhancement of wettability, or even a slight increase of water contact angle. Despite commonly emphasized improvement of wettability after aminolysis [75,76], this phenomenon seems to be much more complex. According to the literature, frequently only a slight decrease of water contact angle is observed [14,50,77]. Monnier et al. reported for PLLA film a similar observation to ours, for which water contact angle slightly increased with the time of aminolysis [78]. The authors proposed two mechanisms, which could be responsible for this phenomenon. Firstly, they proved appearing of double grafting during aminolysis, which means that two amine groups of diamine can react with ester bonds of polymer and, in this case, there is no free hydrophilic amino group. Indeed, in the literature there are reports of using diamines for cross-linking of polyester macromolecules [79]. According to the authors, another cause of contact angle increase could be related to the effect of hydrophobic alkyl chains of diamine, which can dominate the impact of free NH<sub>2</sub> groups. A similar explanation was presented in the work of Bakry et al. [50], where identical values of advancing contact angle for pristine and aminated PLLA film were assigned to re-orientation of the hydrophobic parts of grafted amine.

## 5. Conclusions

In these studies, we analyzed—using various methods, both direct and indirect—the efficiency of aminolysis under the same processing conditions for various aliphatic polyesters (PCL, PLCL, and PLLA) in the form of nanofibers and films. Considering the type of polymer, the order of aminolysis efficiency from highest to lowest is as follows: PLLA, PLCL, and PCL. Our explanation of this sequence of polymer susceptibility to aminolysis is related to different ratios of ester to alkyl groups, primary crystallinity, and NH<sub>2</sub> recombination rate. Taking into account the form of the material, aminolysis reaction turned out to be much easier in the case of films. Our hypothesis is that the reason is related to the radial distribution of the structure, particularly of the supermolecular structure, with more crystalline skin in the case of nanofibers, strongly inhibiting the reaction. Our results of the amine group concentration analysis correspond to a change of crystallinity and mechanical properties, especially stress and strain at break after the aminolysis process. These results provide an important basis for the future research on the use of aminolysis for surface functionalization of polymers.

**Author Contributions:** Conceptualization, methodology, validation, writing—original draft preparation, visualization: O.J., D.K. and P.S.; supervision: P.S. D.K., project administration: P.S.

**Funding:** This research was funded by the POLISH NATIONAL SCIENCE CENTER (NCN), grant number 2016/23/B/ST8/03409.

**Conflicts of Interest:** The authors declare no conflicts of interest.

## References

1. Ma, Z.; Mao, Z.; Gao, C. Surface modification and property analysis of biomedical polymers used for tissue engineering. *Colloid Surf. B Biointerfaces* **2007**, *60*, 137–157. [[CrossRef](#)]
2. Vasita, R.; Shanmugam, I.K.; Katt, D.S. Improved Biomaterials for Tissue Engineering Applications: Surface Modification of Polymers. *Curr. Top. Med. Chem.* **2008**, *8*, 341–353. [[CrossRef](#)]
3. Wang, Y.X.; Robertson, J.L.; Spillman, W.B., Jr.; Claus, R.O. Effects of the Chemical Structure and the Surface Properties of Polymeric Biomaterials on Their Biocompatibility. *Pharm. Res.* **2004**, *21*, 1362–1373. [[CrossRef](#)]
4. Budnicka, M.; Szymaniak, M.; Kołbuk, D.; Ruśkowski, P.; Gadomska-Gajadhur, A. Biominerization of poly-l-lactide spongy bone scaffolds obtained by freeze-extraction method. *J. Biomed. Mater. Res. Part B Appl. Biomater.* **2019**, in press. [[CrossRef](#)] [[PubMed](#)]
5. Kołbuk, D.; Urbanek, O.; Denis, P.; Choińska, E. Sonochemical coating as an effective method of polymeric nonwovens functionalization. *J. Biomed. Mater. Res. Part A* **2019**, in press.
6. Jeznach, O.; Gajc, M.; Korzeb, K.; Kłos, A.; Orliński, K.; Stępień, R.; Krok-Borkowicz, M.; Rumian, Ł.; Pietryga, K.; Reczyńska, K.; et al. New calcium-free  $\text{Na}_2\text{O}-\text{Al}_2\text{O}_3-\text{P}_2\text{O}_5$  bioactive glasses with potential applications in bone tissue engineering. *J. Am. Ceram. Soc.* **2018**, *101*, 602–611. [[CrossRef](#)]
7. Heljak, M.K.; Moczulska-Heljak, M.; Choińska, E.; Chlenda, A.; Kosik-Koziół, A.; Jaroszewicz, T.; Jaroszewicz, J.; Swieszkowski, W. Micro and nanoscale characterization of poly(DL-lactic-co-glycolic acid) films subjected to the L929 cells and the cyclic mechanical load. *Micron* **2018**, *115*, 64–72. [[CrossRef](#)]
8. Ju, J.; Peng, X.; Huang, K.; Li, L.; Liu, X.; Chitrakar, C.; Chang, L.; Gu, Z.; Kuang, T. High-performance porous PLLA-based scaffolds for bone tissue engineering: Preparation, characterization, and in vitro and in vivo evaluation. *Polymer* **2019**, *180*, 121707. [[CrossRef](#)]
9. Lin, J.; Zhou, W.; Han, S.; Bunpitch, V.; Zhao, K.; Liu, C.; Yin, Z.; Ouyang, H. Cell-material interactions in tendon tissue engineering. *Acta Biomater.* **2018**, *70*, 1–11. [[CrossRef](#)]
10. Neděla, O.; Slepčík, P.; Švorčík, V. Surface Modification of Polymer Substrates for Biomedical Applications. *Materials* **2017**, *10*, 1115. [[CrossRef](#)]
11. Kooshki, H.; Ghollasi, M.; Halabian, R.; Kazemi, N.M. Osteogenic differentiation of preconditioned bone marrow mesenchymal stem cells with lipopolysaccharide on modified poly-l-lactic-acid nanofibers. *J. Cell. Physiol.* **2019**, *234*, 5343–5353. [[CrossRef](#)] [[PubMed](#)]
12. Wismayer, K.; Mehrban, N.; Bowen, J.; Birchall, M. Improving cellular migration in tissue-engineered laryngeal scaffolds. *J. Laryngol. Otol.* **2019**, *133*, 135–148. [[CrossRef](#)]
13. Zhu, Y.; Mao, Z.; Gao, C. Aminolysis-based surface modification of polyesters for biomedical applications. *RSC Adv.* **2013**, *3*, 2509–2519. [[CrossRef](#)]
14. De Luca, A.C.; Terenghi, G.; Downes, S. Chemical surface modification of poly- $\epsilon$ -caprolactone improves Schwann cell proliferation for peripheral nerve repair. *J. Tissue Eng. Regen. Med.* **2014**, *8*, 153–163. [[CrossRef](#)] [[PubMed](#)]
15. Chen, X.; Zhang, X.; Zhu, Y.; Zhang, J.; Hu, P. Surface modification of polyhydroxyalkanoates by ion implantation. Characterization and cytocompatibility improvement. *Polym. J.* **2003**, *35*, 148–154. [[CrossRef](#)]
16. Birhanu, G.; Akbari Javar, H.; Seyedjafari, E.; Zandi-Karimi, A.; Dusti Telgerd, M. An improved surface for enhanced stem cell proliferation and osteogenic differentiation using electrospun composite PLLA/P123 scaffold. *Artif. Cells Nanomed. Biotechnol.* **2018**, *46*, 1274–1281. [[CrossRef](#)] [[PubMed](#)]
17. Sadeghi, A.R.; Nokhasteh, S.; Molavi, A.M.; Khorsand-Ghayeni, M.; Naderi-Meshkin, H.; Mahdizadeh, A. Surface modification of electrospun PLGA scaffold with collagen for bioengineered skin substitutes. *Mater. Sci Eng. C Mater. Biol. Appl.* **2016**, *66*, 130–137. [[CrossRef](#)] [[PubMed](#)]
18. Khademi, F.; Ai, J.; Soleimani, M.; Verdi, J.; Mohammad Tavangar, S.; Sadroddiny, E.; Massumi, M.; Mahmoud Hashemi, S. Improved human endometrial stem cells differentiation into functional hepatocyte-like cells on a glycosaminoglycan/collagen-grafted polyethersulfone nanofibrous scaffold. *J. Biomed. Mater. Res. B* **2017**, *105*, 2516–2529. [[CrossRef](#)]
19. Pan, H.; Zheng, Q.; Yang, S.; Guo, X. Effects of functionalization of PLGA-[Asp-PEG]n copolymer surfaces with Arg-Gly-Asp peptides, hydroxyapatite nanoparticles, and BMP-2-derived peptides on cell behavior in vitro. *J. Biomed. Mater. Res. A* **2014**, *102*, 4526–4535. [[CrossRef](#)]
20. Jun, I.; Han, H.S.; Edwards, J.R.; Jeon, H. Electrospun Fibrous Scaffolds for Tissue Engineering: Viewpoints on Architecture and Fabrication. *Int. J. Mol. Sci.* **2018**, *19*, 745. [[CrossRef](#)]

21. Krithica, N.; Natarajan, V.; Madhan, B.; Sehgal, P.K.; Mandal, A.B. Type I Collagen Immobilized Poly(caprolactone) Nanofibers: Characterization of Surface Modification and Growth of Fibroblasts. *Adv. Eng. Mater.* **2012**, *4*, B149–B154. [[CrossRef](#)]
22. Cao, L.; Yu, Y.; Wang, J.; Werkmeister, J.A.; McLean, K.M.; Liu, C. 2-N, 6-O-sulfated chitosan-assisted BMP-2 immobilization of PCL scaffolds for enhanced osteoinduction. *Mater. Sci. Eng. C Mater. Biol. Appl.* **2016**, *74*, 298–306. [[CrossRef](#)] [[PubMed](#)]
23. Hsieh, Y.F.; Sahagian, K.; Huang, F.; Xu, K.; Patel, S.; Li, S. Comparison of plasma and chemical modifications of poly-L-lactide-co-caprolactone scaffolds for heparin conjugation. *Biomed. Mater.* **2017**, *12*, 065004. [[CrossRef](#)] [[PubMed](#)]
24. Liu, K.; Chen, L.; Huang, L.; Lai, Y. Evaluation of ethylenediamine-modified nanofibrillated cellulose/chitosan composites on adsorption of cationic and anionic dyes from aqueous solution. *Carbohydr. Polym.* **2016**, *151*, 1115–1119. [[CrossRef](#)]
25. Ohe, T.; Yoshimura, Y. Reaction of PET fibers with ethylenediamine in a water solution containing surfactants. *Sen'i Gakkaishi* **2012**, *68*, 253–258. [[CrossRef](#)]
26. Fukatsu, K. Mechanical Properties of Poly(ethylene terephthalate) Fibers Imparted Hydrophilicity with Aminolysis. *J. Appl. Polym. Sci.* **1992**, *45*, 2037–2042. [[CrossRef](#)]
27. Zhao, Y.; Tan, K.; Zhou, Y.; Ye, Z.; Tan, W.S. A combinatorial variation in surface chemistry and pore size of three-dimensional porous poly( $\epsilon$ -caprolactone) scaffolds modulates the behaviors of mesenchymal stem cells. *Mater. Sci. Eng. C Mater. Biol. Appl.* **2016**, *59*, 193–202. [[CrossRef](#)]
28. Zhu, Y.; Gao, C.; Liu, X.; He, T.; Shen, J. Immobilization of Biomacromolecules onto Aminolyzed Poly(L-lactic acid) toward Acceleration of Endothelium Regeneration. *Tissue Eng.* **2004**, *10*, 53–61. [[CrossRef](#)]
29. Aguirre-Chagala, Y.E.; Altuzar, V.; León-Sarabia, E.; Tinoco-Magaña, J.C.; Yañez-Limón, J.M.; Mendoza-Barrera, C. Physicochemical properties of polycaprolactone/collagen/elastin nanofibers fabricated by electrospinning. *Mater. Sci. Eng. C Mater. Biol. Appl.* **2017**, *76*, 897–907. [[CrossRef](#)]
30. Amirian, J.; Lee, S.Y.; Lee, B.T. Designing of Combined Nano and Microfiber Network by Immobilization of Oxidized Cellulose Nanofiber on Polycaprolactone Fibrous Scaffold. *J. Biomed. Nanotechnol.* **2016**, *12*, 1864–1875. [[CrossRef](#)]
31. Song, M.-J.; Amirian, J.; Linh, N.T.B.; Lee, B.-T. Bone morphogenetic protein-2 immobilization on porous PCL-BCP-Col composite scaffolds for bone tissue engineering. *J. Appl. Polym. Sci.* **2017**, *134*, 45186. [[CrossRef](#)]
32. Bhattacharjee, P.; Naskar, D.; Kim, H.-W.; Maiti, T.K.; Bhattacharya, D.; Kundu, S.C. Non-mulberry silk fibroin grafted PCL nanofibrous scaffold: Promising ECM for bone tissue engineering. *Eur. Polym. J.* **2015**, *71*, 490–509. [[CrossRef](#)]
33. Kosmala, A.; Fitzgerald, M.Z.; Moore, E.C.; Stam, F. Evaluation of a Gelatin Modified Poly( $\epsilon$ -Caprolactone) Film as a Scaffold for Lung Disease. *Anal. Lett.* **2017**, *50*, 219–232. [[CrossRef](#)]
34. Patel, J.J.; Flanagan, C.L.; Hollister, S.J. Bone Morphogenetic Protein-2 Adsorption onto Poly- $\epsilon$ -caprolactone Better Preserves Bioactivity In Vitro and Produces More Bone In Vivo than Conjugation Under Clinically Relevant Loading Scenarios. *Tissue Eng. Part C Methods* **2015**, *21*, 489–498. [[CrossRef](#)]
35. Stevens, J.S.; De Luca, A.C.; Downes, S.; Terenghi, G.; Schroeder, S.L.M. Immobilisation of cell-binding peptides on poly- $\epsilon$ -caprolactone (PCL) films: A comparative XPS study of two chemical surface functionalisation methods. *Surf. Interface Anal.* **2014**, *46*, 673–678. [[CrossRef](#)]
36. Pellegrino, L.; Cocchiola, R.; Francolini, I.; Lopreiato, M.; Piozzi, A.; Zanoni, R.; Scotto d'Abusco, A.; Martinelli, A. Taurine grafting and collagen adsorption on PLLA films improve human primary chondrocyte adhesion and growth. *Colloids Surf. B Biointerfaces* **2017**, *158*, 643–649. [[CrossRef](#)]
37. Xu, F.J.; Yang, X.C.; Li, C.Y.; Yang, W.T. Functionalized Polylactide Film Surfaces via Surface-Initiated ATRP. *Macromolecules* **2011**, *44*, 2371–2377. [[CrossRef](#)]
38. Zhang, K.; Zheng, H.; Liang, S.; Gao, C. Aligned PLLA Nanofibrous Scaffolds Coated with Graphene Oxide for promoting neural cell growth. *Acta Biomater.* **2016**, *37*, 131–142. [[CrossRef](#)]
39. Li, C.; Wang, L.; Yang, Z.; Kim, G.; Chen, H.; Ge, Z. A Viscoelastic Chitosan-Modified Three-Dimensional Porous Poly(L-lactide-co- $\epsilon$ -caprolactone) scaffold for cartilage tissue engineering. *J. Biomater. Sci. Polym. Ed.* **2012**, *23*, 405–424. [[CrossRef](#)]
40. Zhu, Y.; Chian, K.S.; Chan-Park, M.B.; Mhaisalkar, P.S.; Ratner, B.D. Protein bonding on biodegradable poly(L-lactide-co-caprolactone). *Biomaterials* **2006**, *27*, 68–78. [[CrossRef](#)] [[PubMed](#)]

41. Zhu, Y.; Leong, M.F.; Ong, W.F.; Chan-Park, M.B.; Chian, K.S. Esophageal epithelium regeneration on fibronectin grafted poly(L-lactide-co-caprolactone) (PLLC) nanofiber scaffold. *Biomaterials* **2007**, *28*, 861–868. [[CrossRef](#)] [[PubMed](#)]
42. Ahmad, T.; Lee, J.; Shin, Y.M.; Shin, H.J.; Madhurakat Perikamana, S.K.; Park, S.H.; Kim, S.W.; Shin, H. Hybrid-spheroids incorporating ECM like engineered fragmented fibers potentiate stem cell function by improved cell/cell and cell/ECM. *Acta Biomater.* **2017**, *64*, 161–175. [[CrossRef](#)] [[PubMed](#)]
43. Castro, A.G.; Lo Giudice, M.C.; Vermonden, T.; Leeuwenburgh, S.C.; Jansen, J.A.; van den Beucken, J.J.; Yang, F. A Top-Down Approach for the Preparation of Highly Porous PLLA Microcylinders. *ACS Biomater. Sci. Eng.* **2016**, *2*, 2099–2107. [[CrossRef](#)]
44. Castro, A.G.B.; Polini, A.; Azami, Z.; Leeuwenburgh, S.C.G.; Jansen, J.A.; Yang, F.; van den Beucken, J.J.P. Incorporation of PLLA micro-fillers for mechanical reinforcement of calcium-phosphate cement. *J. Mech. Behav. Biomed. Mater.* **2017**, *71*, 286–294. [[CrossRef](#)]
45. Xie, Z.; Buschle-Diller, G. Functionalized Poly(L-lactide) nanoparticles from electrospun nanofibers. *J. Biomater. Sci. Polym. Ed.* **2011**, *22*, 1331–1341. [[CrossRef](#)]
46. Polini, A.; Petre, D.G.; Iafisco, M.; de Lacerda Schickert, S.; Tampieri, A.; van den Beucken, J.; Leeuwenburgh, S.C.G. Polyester fibers can be rendered calcium phosphate-binding by surface functionalization with bisphosphonate groups. *J. Biomed. Mater. Res. A* **2017**, *105*, 2335–2342. [[CrossRef](#)]
47. Dulnik, J.; Denis, P.; Sajkiewicz, P.; Kołbuk, D.; Choińska, E. Biodegradation of bicomponent PCL/gelatin and PCL/collagen nanofibers electrospun from alternative solvent system. *Polym. Degrad. Stab.* **2016**, *130*, 10–21. [[CrossRef](#)]
48. Kołbuk, D.; Guimond-Lischer, S.; Sajkiewicz, P.; Maniura-Weber, K.; Fortunato, G. The Effect of Selected Electrospinning Parameters on Molecular Structure of Polycaprolactone Nanofibers. *Int. J. Polym. Mater. Polym. Biomater.* **2015**, *64*, 365–377. [[CrossRef](#)]
49. Li, J.; Xiao, P.; Li, H.; Zhang, Y.; Xue, F.; Luo, B.; Huang, S.; Shang, Y.; Wen, H.; de Claville, C.J.; et al. Crystalline structures and crystallization behaviors of poly (L-lactide) in poly (L-lactide)/graphene nanosheet composites. *Polym. Chem.* **2015**, *6*, 3988–4002. [[CrossRef](#)]
50. Xu, H.; Zhong, G.J.; Fu, Q.; Lei, J.; Jiang, W.; Hsiao, B.S.; Li, Z.M. Formation of shish-kebabs in injection-molded poly(L-lactic acid) by application of an intense flow field. *ACS Appl. Mater. Interfaces* **2012**, *4*, 6774–6784. [[CrossRef](#)] [[PubMed](#)]
51. Flory, P.J. Tensile Strength in Relation to Molecular Weight of High Polymers. *J. Am. Chem. Soc.* **1945**, *67*, 2048–2050. [[CrossRef](#)]
52. Bersted, B.H.; Anderson, T.G. Influence of molecular weight and molecular weight distribution on the tensile properties of amorphous polymers. *J. Appl. Polym. Sci.* **1990**, *39*, 499–514. [[CrossRef](#)]
53. Yang, Z.; Zhengwei, M.; Huayu, S.; ChangYou, G. In-depth study on aminolysis of poly(e-caprolactone): Back to the fundamentals. *Sci. China Chem.* **2012**, *55*, 2419–2427. [[CrossRef](#)]
54. Bech, L.; Meylheuc, T.; Lepoittevin, B.; Roger, P. Chemical surface modification of poly (ethylene terephthalate) fibers by aminolysis and grafting of carbohydrates. *J. Polym. Sci. Pol. Chem.* **2007**, *45*, 2172–2183. [[CrossRef](#)]
55. Ganjalinia, A.; Akbaria, S.; Solouk, A. PLLA scaffolds surface-engineered via poly(propylene imine) dendrimers for improvement on its biocompatibility/controlled pH biodegradability. *Appl. Surf. Sci.* **2017**, *394*, 446–456. [[CrossRef](#)]
56. Bakry, A.; Darwish, M.S.A.; El Naggar, A.M.A. Assembling of hydrophilic and cytocompatible three-dimensional scaffolds based on aminolyzed poly(L-lactide) single crystals. *New J. Chem.* **2018**, *42*, 16930–16939. [[CrossRef](#)]
57. Antonova, L.V.; Seifalian, A.M.; Kutikhin, A.G.; Sevostyanova, V.V.; Krivkina, E.O.; Mironov, A.V.; Burago, A.Y.; Velikanova, E.A.; Matveeva, V.G.; Glushkova, T.V.; et al. Bioabsorbable Bypass Grafts Biofunctionalised with RGD Have Enhanced Biophysical Properties and Endothelialisation Tested In vivo. *Front. Pharmacol.* **2016**, *7*, 136. [[CrossRef](#)]
58. Holmes, S.A. Aminolysis of poly(ethylene terephthalate) in aqueous amine and amine vapour. *J. Appl. Polym. Sci.* **1996**, *61*, 255–260. [[CrossRef](#)]
59. Shimizu, J.; Okui, N.; Kikutani, T. Fine Structure and Physical Properties of Fibers Melt-Spun at High-Speeds from Various Polymers. In *High-Speed Fiber Spinning, Science and Engineering Aspects*; Ziabicki, A., Kawai, H., Eds.; John Wiley & Sons: Hoboken, NJ, USA, 1985; Chapter 15.
60. Shimizu, J.; Kikutani, T.; Takaku, A. Structure Developments in High-Speed Spinning. In Proceedings of the International Symposium Fiber Science and Technology, Hakone, Japan, 20–24 August 1985.

61. Perez, G. Some effects of the rheological properties of polyethylene terephthalate) on spinning line profile and structure developed in high speed spinning. In *High-Speed Fiber Spinning, Science and Engineering Aspects*; Ziabicki, A., Kawai, H., Eds.; John Wiley & Sons: Hoboken, NJ, USA, 1985; Chapter 12.
62. Perez, G.; Jung, E. High Speed Melt Spinning: Fiber Structure and Properties. In Proceedings of the International Symposium Fiber Science and Technology, Hakone, Japan, 20–24 August 1985.
63. Kameoka, J.; Craighead, H.G. Fabrication of oriented polymeric nanofibers on planar surfaces by electrospinning. *Appl. Phys. Lett.* **2003**, *83*, 371–373. [[CrossRef](#)]
64. Kameoka, J.; Orth, R.; Yang, Y.; Czaplewski, D.; Mathers, R.; Coates, G.W.; Craighead, H.G. A scanning tip electrospinning source for deposition of oriented nanofibers. *Nanotechnology* **2003**, *14*, 1124–1129. [[CrossRef](#)]
65. Buer, A.; Ugbolue, S.C.; Warner, S.B. Electrospinning and Properties of Some Nanofibers. *Text. Res. J.* **2001**, *71*, 323–328. [[CrossRef](#)]
66. Filatov, Y.; Budyk, A.; Kirichenko, V. *Connecticut, Electrospinning of Micro- and Nanofibers: Fundamentals and Applications in Separation and Filtration Process*; NH Begell House: New York, NY, USA, 2007.
67. Fennessey, S.F.; Farris, R.J. Fabrication of aligned and molecularly oriented electrospun polyacrylonitrile nanofibers and the mechanical behaviour of their twisted yarns. *Polymer* **2004**, *45*, 4217–4225. [[CrossRef](#)]
68. Behler, K.; Havel, M.; Gogotsi, Y. New solvent for polyamides and its application to the electrospinning of polyamides 11 and 12. *Polymer* **2007**, *48*, 6617–6621. [[CrossRef](#)]
69. Wang, X.; Cao, J.; Hu, Z.; Pan, W.; Liu, Z. Jet Shaping Nanofibers and the Collection of Nanofiber Mats in Electrospinning. *J. Mater. Sci. Technol.* **2006**, *22*, 536.
70. Reneker, D.H.; Yarin, A.L. Electrospinning jets and polymer nanofibers. *Polymer* **2008**, *49*, 2387–2425. [[CrossRef](#)]
71. Reneker, D.H.; Yarin, A.L.; Fong, H.; Koombhongse, S. Bending instability of electrically charged liquid jets of polymer solutions in electrospinning. *J. Appl. Phys.* **2000**, *87*, 4531–4547. [[CrossRef](#)]
72. Wang, C.; Tsou, S.Y.; Lin, H.S. Brill transition of nylon-6 in electrospun nanofibers. *Colloid Polym. Sci.* **2012**, *290*, 1799–1809. [[CrossRef](#)]
73. Piai, J.F.; da Silva, M.A.; Martins, A.; Torres, A.B.; Faria, S.; Reis, R.L.; Muniz, E.C.; Neves, N.M. Chondroitin sulfate immobilization at the surface of electrospun nanofiber meshes for cartilage tissue regeneration approaches. *Appl. Surf. Sci.* **2017**, *403*, 112–125. [[CrossRef](#)]
74. Molisak-Tolwinska, H.; Wencel, A.; Figaszewski, Z. The Effect of Hydrophilization of Polypropylene Membranes with Alcohols on Their Transport Properties. *J. Macromol. Sci. A* **1998**, *35*, 857–865. [[CrossRef](#)]
75. Castro, A.G.B.; Yang, F.; van den Beucken, J.J.P.; Jansen, J.A. *Handbook of Intelligent Scaffolds for Tissue Engineering and Regenerative*; Khang, G., Ed.; Pan Stanford Publishing: Singapore, 2017; Chapter 18; p. 489.
76. Shahidi, S.; Wiener, J.; Ghoranneviss, M. *Eco-Friendly Textile Dyeing and Finishing*; Gunay, M., Ed.; IntechOpen: London, UK, 2013; Chapter 2; p. 44.
77. Causa, F.; Battista, E.; Della, M.R.; Guarnieri, D.; Iannone, M.; Netti, P.A. Surface Investigation on Biomimetic Materials to Control Cell Adhesion: The Case of RGD conjugation on PCL. *Langmuir* **2010**, *26*, 9875–9884. [[CrossRef](#)] [[PubMed](#)]
78. Monnier, A.; Al Tawil, E.; Nguyen, Q.T.; Valleton, J.M.; Fatyeyeva, K.; Deschrevel, B. Functionalization of poly (lactic acid) scaffold surface by aminolysis and hyaluronan immobilization: How it affects mesenchymal stem cell proliferation. *Eur. Polym. J.* **2018**, *107*, 202–217. [[CrossRef](#)]
79. Pavlinec, J.; Lazar, M. Cross-linking of poly (methyl methacrylate) by aminolysis of ester functions with diamines. *J. Appl. Polym. Sci.* **1995**, *55*, 39–45. [[CrossRef](#)]



© 2019 by the authors. Licensee MDPI, Basel, Switzerland. This article is an open access article distributed under the terms and conditions of the Creative Commons Attribution (CC BY) license (<http://creativecommons.org/licenses/by/4.0/>).



Cite this: RSC Adv., 2022, 12, 11303

## Aminolysis as a surface functionalization method of aliphatic polyester nonwovens: impact on material properties and biological response†

Oliwia Jeznach, <sup>a</sup> Dorota Kołbuk, <sup>a</sup> Mateusz Marzec, <sup>b</sup> Andrzej Bernasik <sup>b</sup> and Paweł Sajkiewicz <sup>\*a</sup>

It is reported in the literature that introducing amino groups on the surface improves cellular behaviour due to enhanced wettability and the presence of the positive charge. In this work, electrospun fibers were subjected to aminolysis under various conditions to investigate the impact of reaction parameters on the concentration of free NH<sub>2</sub> groups, change of fiber properties, and the response of L929 cells. Three types of electrospun nonwovens obtained from poly(caprolactone) (PCL), poly(L-lactide-co-caprolactone) (PLCL) 70 : 30 and poly(L-lactide) (PLLA) were investigated. For all polymers, the concentration of NH<sub>2</sub> groups increased with the diamine concentration and time of reaction. However, it was observed that PCL fibers require much stronger conditions than PLCL and PLLA fibers to reach the same level of introduced amine groups. X-ray photoelectron spectroscopy results clearly demonstrate that an aminolysis reaction is not limited to the surface of the material. Gel permeation chromatography results support this conclusion indicating global molecular weight reduction. However, it is possible to reach a compromise between the concentration of introduced amine groups and the change of mechanical properties. For most of the investigated conditions, aminolysis did not significantly change the water contact angle. Despite this, the change of L929 and MG63 cell shape to being more spread confirmed the positive effect of the presence of the amine groups.

Received 25th January 2022  
 Accepted 2nd April 2022

DOI: 10.1039/d2ra00542e  
[rsc.li/rsc-advances](http://rsc.li/rsc-advances)

### 1. Introduction

In recent years there has been a growing interest in the modification of material surface properties in biomaterials science. There is a big advantage in modulating material surface without altering bulk properties since cell–material interaction mainly refers to the interface.<sup>1</sup> Scaffolds, drug delivery systems, and implants are modified in different ways depending on the form and chemistry of the material and application site. In the case of polymer scaffolds commonly used methods are plasma treatment,<sup>2,3</sup> wet chemistry (hydrolysis, aminolysis),<sup>4</sup> layer by layer technique,<sup>5</sup> surface graft polymerization,<sup>6</sup> coating with inorganic particles<sup>7,8</sup> and biomolecule immobilization.<sup>9,10</sup> Most frequently, these modifications concern changing wettability, surface energy, topography, or surface elasticity or introducing charged groups or bioactive motives. These features can influence the body's response to biomaterials *via* determining protein adsorption (specificity, adsorption rate, protein

conformation, exposure or not of the cell-binding region)<sup>11–14</sup> and then modulating cell adhesion and their functioning, *e.g.* secretion and deposition of extracellular matrix. Several recent reviews discuss in details findings in impact of material surface properties on cells behaviour and present updated conclusion and future perspectives.<sup>1,15,16</sup>

In this study, we investigated aminolysis as a surface modification method of electrospun fibers made of three types of aliphatic polyesters used commonly in tissue engineering: poly(caprolactone), poly(L-lactide-co-caprolactone) and poly(L-lactide). Polymers differ from each other in the ratio of the ester to alkyl groups, crystallinity, and glass transition temperature, which could be essential from the reaction perspective.<sup>17</sup> All obtained nonwovens have a hydrophobic nature.

The reaction between polyesters and diamines is frequently used as an effective method for introducing NH<sub>2</sub> groups on the scaffold surface.<sup>18,19</sup> Its application is not limited to tissue engineering. Aminolysis is used in the textile industry to enhance fibers dyeing ability.<sup>20</sup> Improved adsorption of dyes by amine-functionalized fibers is also investigated for the removal of pollutants present in water.<sup>21</sup> Another studied application is improving the interfacial adhesion between aminated fibers and polymer matrixes.<sup>22</sup> It is worth mention that aminolysis can be used for the degradation of PET fibers and bottles waste.<sup>23,24</sup>

<sup>a</sup>Institute of Fundamental Technological Research, Polish Academy of Sciences, Pawinskiego 5B, 02-106 Warsaw, Poland. E-mail: psajk@ippt.pan.pl

<sup>b</sup>AGH University of Science and Technology, al. Adama Mickiewicza 30, 30-059 Cracow, Poland

† Electronic supplementary information (ESI) available. See <https://doi.org/10.1039/d2ra00542e>



Aminolysis proceeds *via* a nucleophilic attack on the carbonyl carbon of polyester.<sup>25</sup> One amino group reacts with the ester group forming an amide bond and leading to chain scission, while another one remains free. Moreover, hydroxyl groups are also created as a result of chain-breaking (Scheme 1). Aminolysis can be exploited as a single-step approach to enhance cell response as a result of improved wettability and/or presence of positive charge.<sup>4,6,26</sup> On the other hand, the aminolysis technique is frequently used as an intermediate step before further physical or chemical immobilization of biomacromolecules.<sup>27,28</sup> There are also other approaches to introduce free amine groups on the material surface. One of them is plasma treatment using ammonia ( $\text{NH}_3$ ) or nitrogen ( $\text{N}_2$ ) gases, or amine monomers with most common exploited allylamine.<sup>29</sup> Plasma treatment is a cost-effective and relatively simple method. However, generation of active species inside of the scaffold and alteration of modifying depth have to be taken into consideration.<sup>30</sup> Another method is incorporation of amine-functionalized PEG-dendrimers,<sup>31</sup> poly(ethyleneimine),<sup>32</sup> which is rich in primary amine groups, using *e.g.* EDC/NHS cross-linking or poly(dopamine), which is easily deposited by direct immersion of scaffold in dopamine solution.<sup>33</sup> However, it is rather a way to further conjugation of biomolecules with incorporated free  $-\text{NH}_2$  groups as these substances are known for suppression of protein adsorption and some cell adhesion, mainly due to its high hydrophilicity. Hence, these coatings are exploited in manufacturing of hemocompatible scaffolds.<sup>34–36</sup> Aminolysis, which is kind of wet chemical method, is a simple way to homogeneously introduce primary amine groups on the scaffold surface without complete change of surface chemistry.

It is reported that protein adsorption on hydrophobic surfaces can lead to their denaturation, which can make them unable to bind cells.<sup>37</sup> It was experimentally found that too high hydrophilicity could also be unfavourable for cell attachment.<sup>38</sup> Hence, it appears that moderate wettability provides the proper amount of adsorbed proteins as well as unchanged conformation, which results in good cell response.<sup>39</sup> From this perspective, it is important that aminolysis can cause an increase of wettability.<sup>40</sup> Considering charge of surface, it was experimentally proved that a positively charged surface has a beneficial impact on cell behaviour, most probably due to electrostatic interactions allowing effective adhesion of negatively charged proteins present in serum, as well as direct interaction with the charged surface of the cell membrane.<sup>41,42</sup> Lamas E. *et al.* used amine surface ( $-\text{NH}_3^+$ ) in computational modelling of

fibronectin adsorption and showed that in contrast to uncharged surface, protein adsorption on positively charged surface is relatively rapid and site-specific.<sup>13</sup>

Although diamine-based surface modification of polyesters was fundamentally studied by others, the vast majority of experimental results referred to solvent-casted membranes.<sup>22,43–47</sup> Currently, aminolysis is frequently used as direct or indirect functionalization of ECM-mimicking electrospun fibers<sup>22,48–53</sup> and there is no comprehensive study in the literature that concerns the optimization of this reaction for various polyester fibers.

In the previous paper, we discussed reasons for different susceptibility of electrospun fibers and solvent-casted films to aminolysis.<sup>15</sup> In this work, the aminolysis of three types of aliphatic polyester fibers is investigated more detailed in a wide range of conditions. We focus on fundamental characterization and comparison of materials in terms of surface characterization including XPS and amino groups concentration, impact of the modification on fibers morphology, molecular weight, wettability, mechanical properties and crystallinity, as well as interaction of materials with L929 and MG63 lines cells.

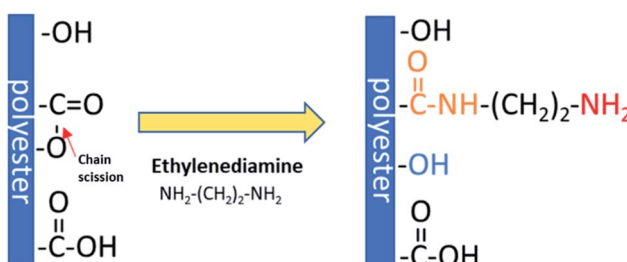
## 2. Experimental

### 2.1. Materials

Three types of polyesters were used: PCL (Sigma-Aldrich, USA,  $M_w = 108$  kDa,  $M_n = 78$  kDa,  $T_g = -60$  °C), PLCL 70 : 30 (Resomer® LC703S, Evonik, Germany,  $M_w = 88$  kDa,  $M_n = 59$  kDa, inherent viscosity = 1.3–1.8 dl g<sup>-1</sup>,  $T_g = 32$ –42 °C) and PLLA (PL49, Corbion, Netherlands,  $M_w = 338$  kDa,  $M_n = 197$  kDa, inherent viscosity = 4.9 dl g<sup>-1</sup>,  $T_g = 58$  °C). Solvents used in electrospinning process—acetic acid (AA) (purity degree 99.5%), formic acid (FA) (purity degree ≥ 98%), and hexafluoroisopropanol (HFIP) (purity degree 98.5%) were purchased from Poch (Poland), Sigma-Aldrich (USA), and Iris Biotech GmbH (Germany), respectively. Ethylenediamine (EDA) (purity degree 99.5%), isopropanol (purity degree 99.8%), ninhydrin (purity degree 99%), ethanol (purity degree 99.8%), glutaraldehyde (conc. 25%) and tetrahydrofuran (THF) (for HPLC) were purchased from Chempur (Poland). Chloroform (LiChrosolv®, for liquid chromatography) was procured from Sigma-Aldrich (USA). For all polymers,  $M_w$  and  $M_n$  were determined experimentally.

### 2.2. Preparation of electrospun fibers

Three types of nonwovens were fabricated using electrospinning equipment (Bioinicia, Spain) in horizontal mode. Solutions (15% w/w solution of PCL in a mixed solution of acetic acid and formic acid at 9 : 1 ratio, 7% w/w PLCL solution in HFIP, and 3.5% w/w solution of PLLA in HFIP) were pumped through two stainless steel needles with a speed of 6 ml h<sup>-1</sup> (3 ml h<sup>-1</sup> per needle). Other process parameters were: distance needle-collector: 15 cm, collector rotating speed: 300 rpm, voltage applied to collector: –2 kV, voltage applied to needles: PCL: 13–15 kV, PLCL: 12–14 kV, PLLA: 12–14 kV, temperature and humidity conditions: PCL: 24 °C, 40%, PLCL: 38 °C, 40%,



Scheme 1 Mechanism of aminolysis reaction.



PLLA: 24 °C, 40%, volume of solution used to obtain 12 cm × 31 cm nonwoven – PCL: 13 ml, PLCL: 18 ml, PLLA: 39 ml.

### 2.3. Aminolysis treatment

Samples of 5.5 × 5.5 cm size were immersed in 80 ml of ethylenediamine in isopropanol solution. Solutions concentrations were: 10, 20, 30% w/v for PCL and 2, 6, 10% w/v for PLCL and PLLA. Time points were: 30 min, 6 h, 24 h, 72 h for PCL and 5 min, 10 min, 15 min, 30 min for PLCL and PLLA. The temperature of the reaction was set at 30 °C. The process was conducted in an orbital shaker-incubator. After that, aminolysis samples were washed three times in deionized water and dried under vacuum overnight. Sample designations were set as the name of polymer\_EDA conc.\_reaction time, e.g. PCL\_20%\_72 h or as the name of polymer\_Control for control, unmodified samples.

### 2.4. Surface characterization

#### 2.4.1. Detection and quantification of amino groups.

Ninhydrin colorimetric test was used to quantify the concentration of amine groups grafted during aminolysis. Three samples of weight in the range of 10–30 mg, depending on the type of polymer and reaction conditions, were used. Each sample was put into a glass vial, and 0.5 ml of 2% w/v ninhydrin in ethanol/acetic acid (49 : 1 v/v) solution was added. Vials were heated for 10 min using a hot plate set at 100 °C. After that, 1 ml of isopropanol (in the case of PLCL and PLLA) or 0.5 ml of isopropanol and 0.5 ml of dioxane (in the case of PCL) were added. The absorbance of tested solutions was measured at 570 nm. The concentration of amine groups was calculated on the basis of the calibration curve obtained for a known concentration of ethylenediamine in isopropanol solution. In the case of PCL, the volume of dissolved material was included in the calculation. Results were presented as a concentration of amino groups in moles per mg of fibrous sample.

**2.4.2. XPS analysis.** Five chosen samples were analyzed using XPS: PLCL\_Control, PLCL\_2%\_15 min, PLCL\_6%\_15 min, PLCL\_6%\_30 min and PLCL\_10%\_15 min. XPS analyses were performed using a scanning XPS system (PHI VersaProbe II, USA) equipped with monochromatic Al K $\alpha$  (1486.6 eV) radiation. The power X-ray source was about 25 W. X-rays beam were focused to a 100  $\mu\text{m}$  spot which determined the area of analysis. The measurement time of the spectrum of one element was about 7 minutes. A dual beam charge compensation with 7 eV Ar $^+$  ions and 1 eV electrons were used to maintain a constant sample surface potential. All XPS spectra were referenced to the unfunctionalized, saturated carbon (C-C) C1s peak at binding energy (BE) equal to 284.8 eV. Concentration of elements and their chemical states on various depth of PLCL fiber were measure by sputtering with Argon Gas Cluster Ion Beam (Ar-GCIB). Sputtering parameters were set to 10 kV beam voltage and 30 nA current with approx. 4000 argon atoms per cluster. The size of the sputtered area was set to 3 × 3 mm. During the sputtering Zalar rotation was applied. The sputtering rate was determined in a separate experiment using a 450 nm thick PLCL layer and was set at 4.1 nm min $^{-1}$ . The

analysis of the fiber composition was performed on the surface and after consecutive 15 minute sputtering cycles.

### 2.5. SEM imaging

Scanning electron microscopy (SEM, Jeol JSM-6010PLUS/LV InTouchScope™) was used for sample imaging. Before imaging, samples were coated with gold. The acceleration voltage was in the range of 7–10 kV.

### 2.6. Wettability

The water contact angle (WCA) was determined for aminolyzed samples using goniometer Data Physics OCA 15EC (Germany). The dosing volume and dosing rates were 1  $\mu\text{l}$  and 2  $\mu\text{l s}^{-1}$ , respectively. Measurements were repeated 5 times for each sample.

### 2.7. Change of average molecular weight

Change of weight average molecular weight ( $\overline{M}_w$ ), number average molecular weight ( $\overline{M}_n$ ), and polydispersity index (PI) were measured using gel permeation chromatography (GPC, Shimadzu). PCL and PLCL samples were solubilized in THF at a concentration of 3 mg ml $^{-1}$ . PLCL granules and all PLLA samples were solubilized in chloroform due to poor solubility in THF at a concentration of 1 mg ml $^{-1}$ , respectively. THF was used as a mobile phase. The temperature was set at 40 °C. All solutions were filtered by 0.22  $\mu\text{m}$  syringe filters (Biosens). THF flow rate was equal to 1 ml min $^{-1}$ . Polystyrene standards with  $\overline{M}_n$  from 3470 Da to 2 520 000 Da (PSS Polymer Standards Service GmbH) were used to create a calibration curve. GPC equipment consisted of a pump, column (Phenogel™ 5  $\mu\text{m}$  10e5Å, Phenomenex), refractive index detector (RID-20A, Shimadzu) and LabSolutions GPC software. In the case of PLLA samples, the calculation of  $\overline{M}_w$  and  $\overline{M}_n$  were conducted using OriginPro 8.0 and PeakFit 4.12 software due to disturbance resulting from incomplete solubility of PLLA in chloroform. The Mark-Houwink equation parameters were as follow  $\alpha = 0.7$ ,  $K = 14.1 \times 10^{-5}$  dl g $^{-1}$  for polystyrene standard polymer,  $\alpha = 0.786$ ,  $K = 13.95 \times 10^{-5}$  dl g $^{-1}$  for PCL according to Sinnwell S. *et al.*<sup>54</sup>,  $\alpha = 0.68$ ,  $K = 4.84 \times 10^{-4}$  dl g $^{-1}$  for PLCL and  $\alpha = 0.65$ ,  $K = 0.001$  for PLLA according to Nuutila M. *et al.*<sup>55</sup>

Sets of the two aminolyzed samples for each type of polymer were chosen for further analysis including mechanical testing, WAXS analysis and cell response. The first sample was selected as having a lower concentration of amine groups ((1.42–3.18) × 10 $^{-8}$  mol mg $^{-1}$ ) and the second as having a higher concentration of amine groups ((1.65–1.75) × 10 $^{-7}$  mol mg $^{-1}$ ).

### 2.8. Mechanical testing

Uniaxial testing machine Lloyd EZ-50 (USA) was used to determine Young's modulus, stress at break and strain at break. Three samples (5 × 40 mm, testing area: 5 × 20 mm) for each type of material were tested. Thickness of each sample was measured with a thickness gauge. Machine was equipped with



handles for thin and delicate samples with a 50 N load cell. Cross-head speed was set at  $5 \text{ mm min}^{-1}$ .

### 2.9. WAXS analysis

Wide angle X-ray scattering (WAXS) was applied for analysis of the supermolecular structure. WAXS measurements were performed using Bruker D8 Discover diffractometer (Mannheim, Germany) with CuK $\alpha$  radiation operated at a voltage of 40 kV, and a current of 20 mA. All measurements were performed in reflection mode, using Goebel optics for beam formation: a 0.6 mm slit and Soller collimator. Highly sensitive Lynx Eye 1-D silicon strip detector was used. The range of diffraction angle,  $2\theta$ , was between  $5^\circ$  and  $35^\circ$ , with a step of  $0.01^\circ$  and a time of data accumulation at angular point of 0.2 s. The “empty” scan without a sample was subtracted and the default function of subtracting background was applied. Then, the WAXS profiles were deconvoluted numerically using PeakFit software assuming Pearson VII and Gauss functions for the crystal diffraction peaks from the amorphous halo, respectively. The degree of crystallinity was determined as the ratio of the area of all the crystalline diffraction peaks to the overall area of the profile.

### 2.10. ATR-FTIR analysis

Surface molecular structure of samples was analyzed using attenuated total reflectance Fourier transform infrared (ATR-FTIR) spectrometer Bruker Vertex 70 (Mannheim, Germany). Absorbance mode in  $4000\text{--}400 \text{ cm}^{-1}$  range was applied. The resolution of measurement was equal to  $2 \text{ cm}^{-1}$ .

### 2.11. Cell response

Mouse fibroblast cells (L929, Sigma Aldrich) and osteoblast-like cells (MG63, Sigma Aldrich) were chosen to investigate cell response. For L929 cells culture, Dulbecco's Modified Eagle Medium (DMEM, Thermo Fisher Scientific) was supplemented with fetal bovine serum (FBS, Thermo Fisher Scientific) to the concentration of 10% v/v and penicillin/streptomycin (Thermo Fisher Scientific) to the concentration of 1% v/v. For MG63 cells culture, 1% v/v of gentamicin (Thermo Fisher Scientific) was added to the media.

Cells were cultured in an incubator at  $40^\circ\text{C}$  in a 5% CO<sub>2</sub>. Samples of nonwovens were sterilized using 70% – solution of ethanol in water and 30 min-exposure to UV light on each side. Samples were placed in a 48-well culture plate – three samples for cell metabolic activity test, and two samples for SEM observation for each type of material.  $2 \times 10^3$  cells were seeded per well. Cells were cultured in an incubator for 5 days.

PrestoBlue™ (Thermo Fisher Scientific) test was chosen to evaluate cell metabolic activity. After removing the culture medium, each sample was rinsed with phosphate-buffered saline (PBS, Thermo Fisher Scientific). Then 180  $\mu\text{l}$  of PBS and 20  $\mu\text{l}$  of PrestoBlue™ reagent in the PBS solution was added to each well. PrestoBlue reagent was also added to pure PBS as a control. The plate with samples was further put into an incubator for 40 min to enable reaction. After that, 100  $\mu\text{l}$  of

each solution was placed in a 96-well plate. Emission of light was measured using Fluoroskan Ascent (Thermo Scientific) at an excitation light wavelength of 530 nm and emission light wavelength of 620 nm. Results were then calculated to percentage metabolic activity using tissue culture polystyrene as a 100% control.

Samples used for SEM observation were gently rinsed with PBS twice and then fixed with 2.5% glutaraldehyde/PBS overnight. Samples were further dehydrated using ethanol in water solution series (30, 40, 50, 60, 70, 80, 90, 100 ( $\times 2$ )% v/v), hexamethyldisilazane (HDMS, Sigma Aldrich)/ethanol solutions (1 : 2 and 2 : 1 v/v), and pure HDMS. Each ethanol solution was removed after 20 minutes, and HDMS was left overnight.

Fluorescence microscopy imaging was performed after immunohistochemical staining. Cells were washed once with phosphate buffered saline (PBS), fixed in 4% paraformaldehyde, kept in 0.1% Triton-X for 5 min and washed again with PBS. Then the actin skeleton and nucleus were stained with ActinGreen™ and NucBlue™ reagent (Thermo Scientific), respectively. All samples in comparison to TCP (Tissue Culture Plastic) were illustrated using a fluorescent microscope (Leica DMI3000B, Leica Microsystems).

### 2.12. Statistical analysis

One-way analysis of variance (ANOVA) followed by NIR *post hoc* test, or Kruskal-Wallis one-way analysis of variance was performed on WCA, stress and strain at break, and cell metabolic activity data test using Statistica 13 software. Significance was set at  $p < 0.05$ .

Results are presented as the mean value  $\pm$  SD.

## 3. Results

Fig. 1 shows the results of the ninhydrin test, which allowed to measure NH<sub>2</sub> groups introduced to samples subjected to aminolysis. The first observation is that the concentration of NH<sub>2</sub> groups on the surface increases for all polyesters with ethylenediamine concentration and reaction time. For PLCL and PLLA the same conditions were applied, and it was observed that PLLA fibers were more susceptible to aminolysis. For instance, in the conditions of 10% EDA concentration and 30 min time of reaction, the concentration of NH<sub>2</sub> groups for PLCL was  $(3.57 \pm 0.01) \times 10^{-7} \text{ mol mg}^{-1}$  and for PLLA  $(7.75 \pm 0.26) \times 10^{-7} \text{ mol mg}^{-1}$ . The results obtained for PCL fibers are even more contrasting. In the case of this polyester, there was a need to use much higher concentrations of EDA and reaction times, which was concluded on the basis of preliminary studies.<sup>17</sup> However, even for extreme conditions (30%, 72 h) of PCL aminolysis, the concentration of NH<sub>2</sub> groups is still lower than in the case of the most reacted PLLA.

Nitrogen detection using the XPS method was possible for the PLCL\_10%\_15 min sample. The concentration was measured to be equal to 1.1 at%. In the case of other aminated samples, nitrogen atomic concentration was too low to be detected by XPS. Fig. 2 presents a depth profile of the atomic concentration of the detected chemical bonds for the



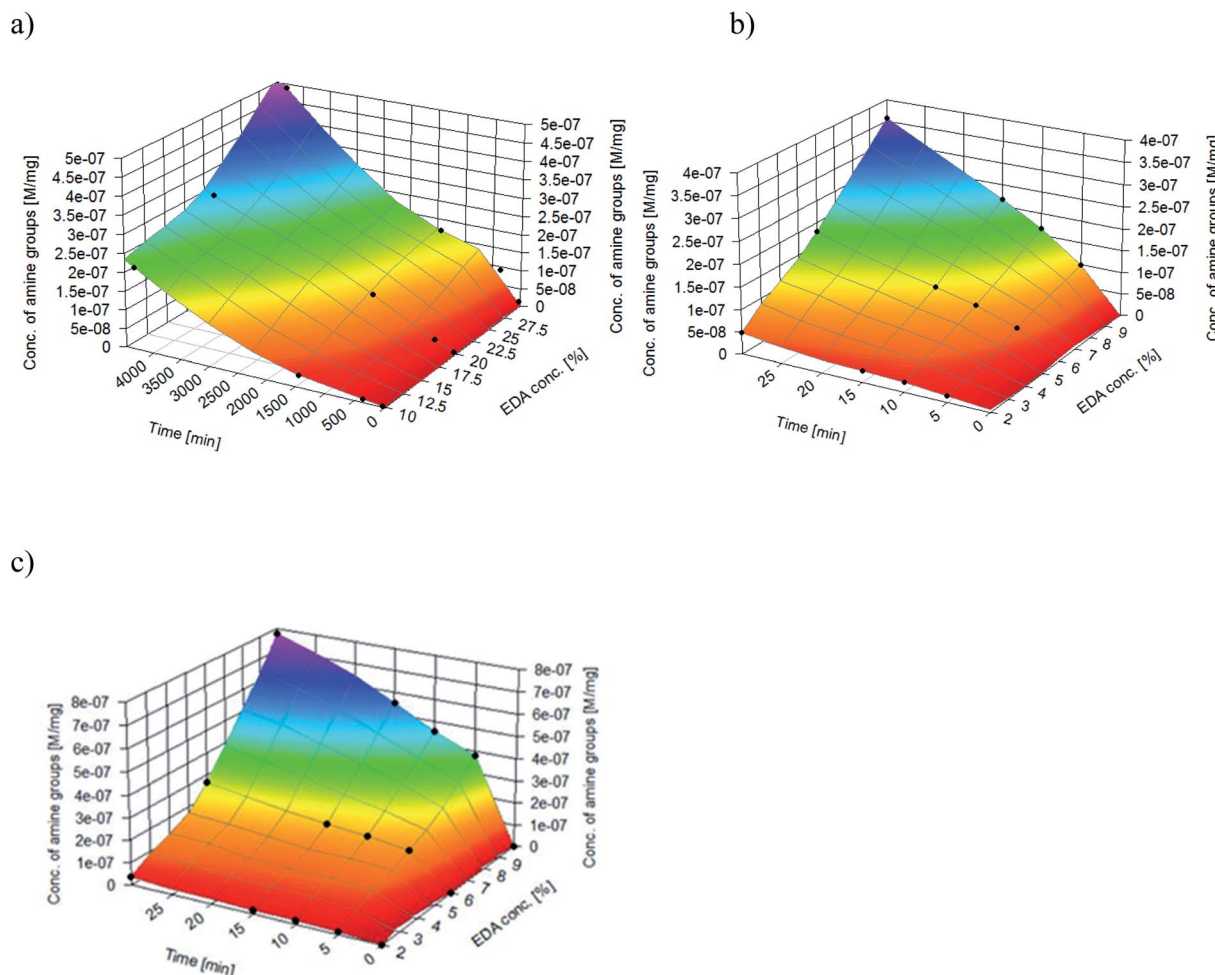


**Fig. 1** Concentrations of  $\text{NH}_2$  groups on the surface of (a) PCL, (b) PLCL, (c) PLLA fibers subjected to aminolysis at  $30\text{ }^\circ\text{C}$ .

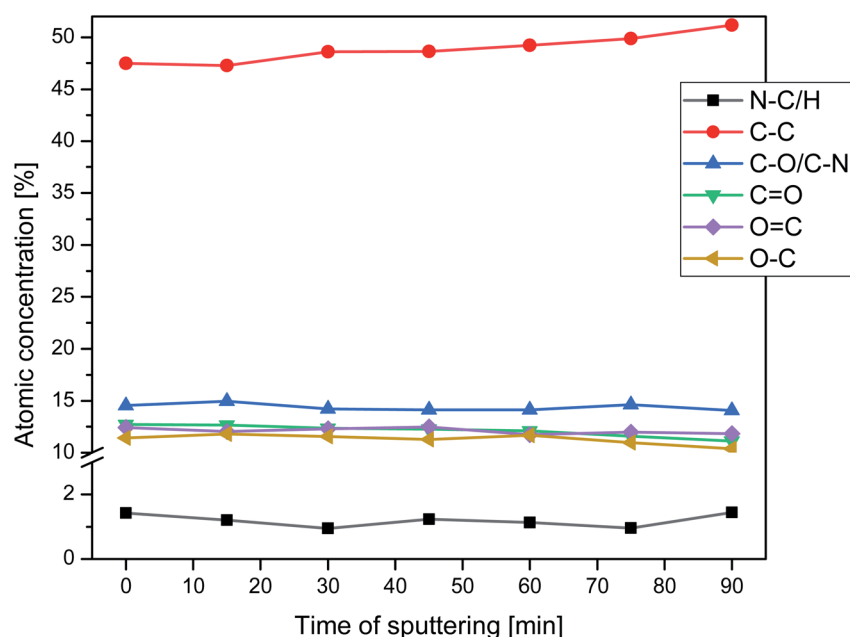


**Fig. 2** Atomic concentration of the detected chemical bonds for PLCL\_10%\_15 min sample vs. sputtering time.



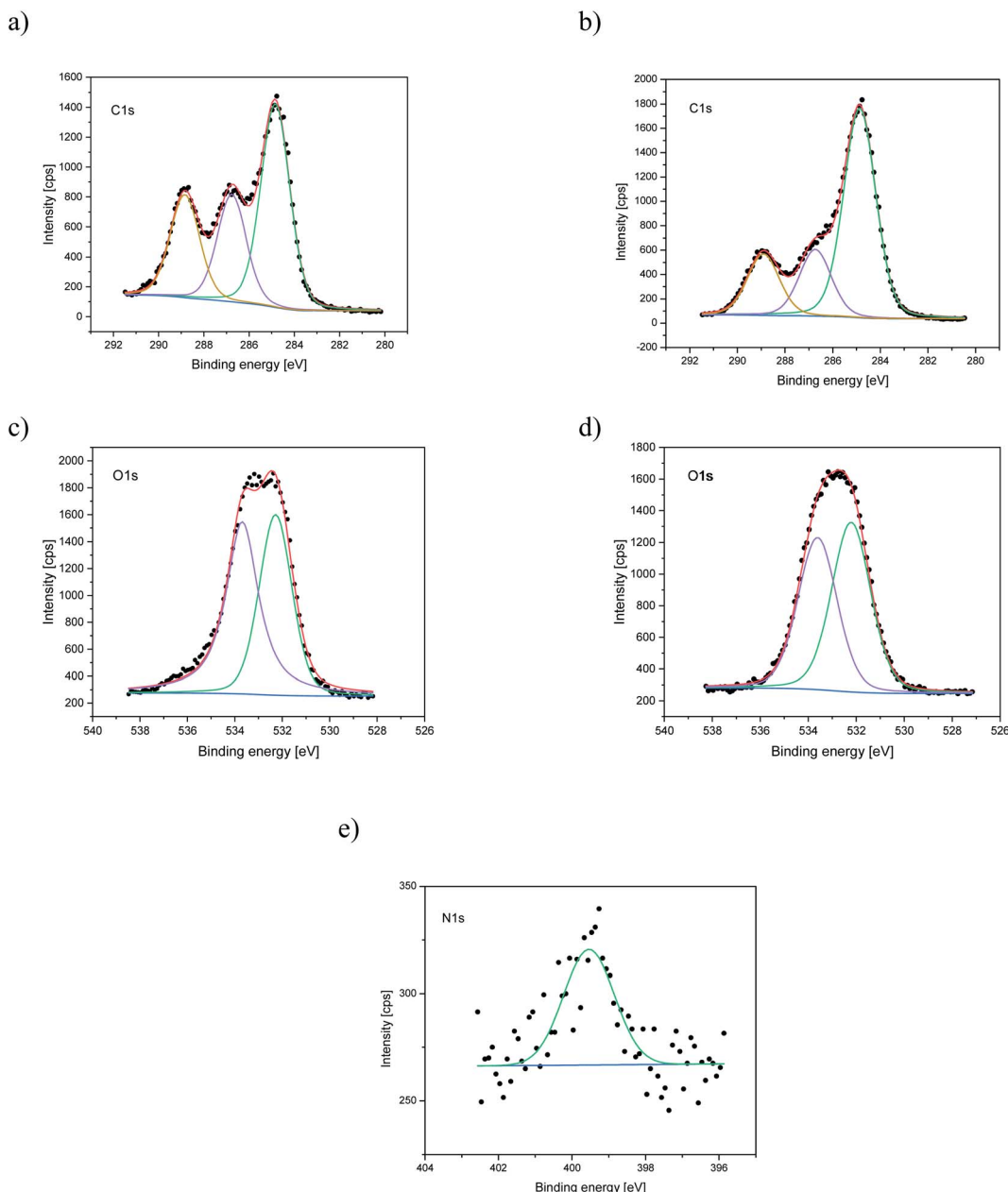


Fig. 3 XPS spectra of the C1s, O1s, N1s for PLCL\_Control (a, c) and PLCL\_10%\_15 min (b, d, e) samples.

PLCL\_10%\_15 min. Taking into account sputtering rate, time of 90 minutes corresponds to the depth of about 370 nm. There were no significant changes in atomic concentration of all

chemical bonds on the studied depth. Fig. 3 shows C1s, O1s, and N1s spectra for PLCL\_Control and PLCL\_10%\_15 min. Table 1 presents atomic concentration and the relative intensity

**Table 1** The atomic concentration and the relative intensity of the C1s peaks measured by XPS on the surface of PLCL\_Control and PLCL\_10%\_15 min (before sputtering)

| Sample          | Concentration of amine groups<br>[mol mg <sup>-1</sup> ] | Atomic concentration [%] |      |     | Relative intensity [%] |      |      |
|-----------------|--|--------------------------|------|-----|------------------------|------|------|
|                 |  | C                        | O    | N   | C—C                    | C—N  | C=O  |
|                 |  |                          |      |     | —                      | —    | —    |
| PLCL_Control    | 0  | 69.6                     | 30.4 | —   | 48.1                   | 25.6 | 26.3 |
| PLCL_10%_15 min | (2.16 ± 0.15) × 10 <sup>-7</sup>                         | 73.1                     | 25.8 | 1.1 | 61.1                   | 19.6 | 19.3 |



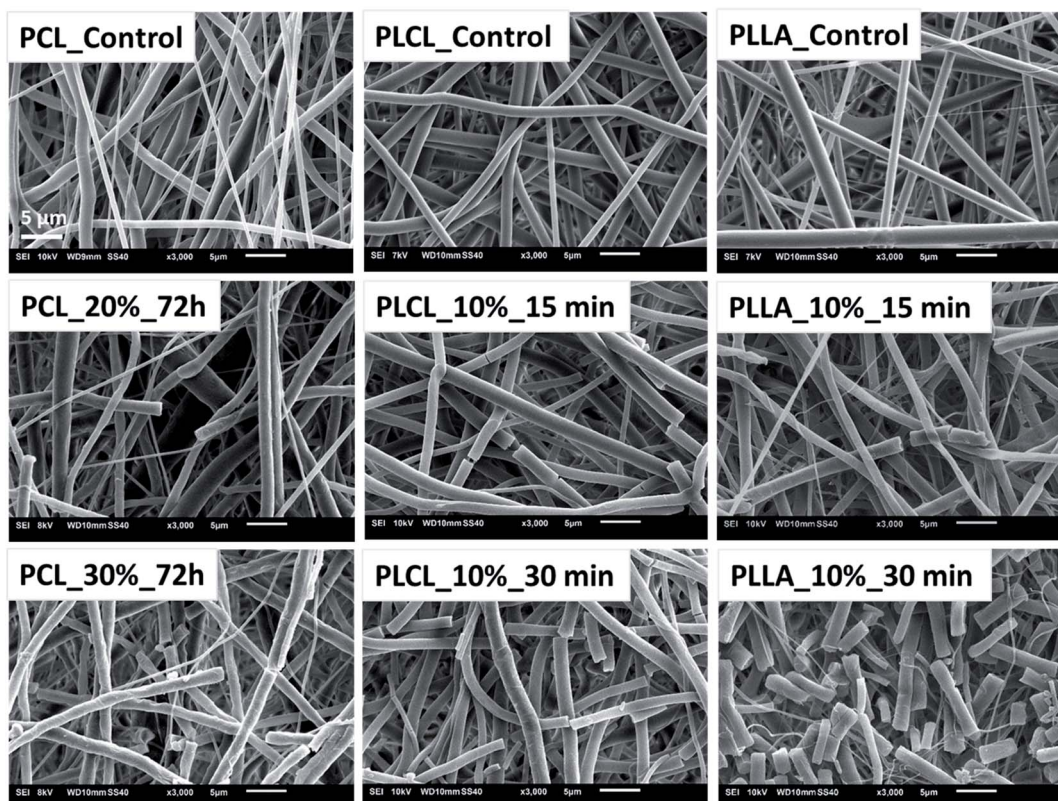


Fig. 4 SEM images of fibers breaking as a result of aminolysis under most aggressive conditions.

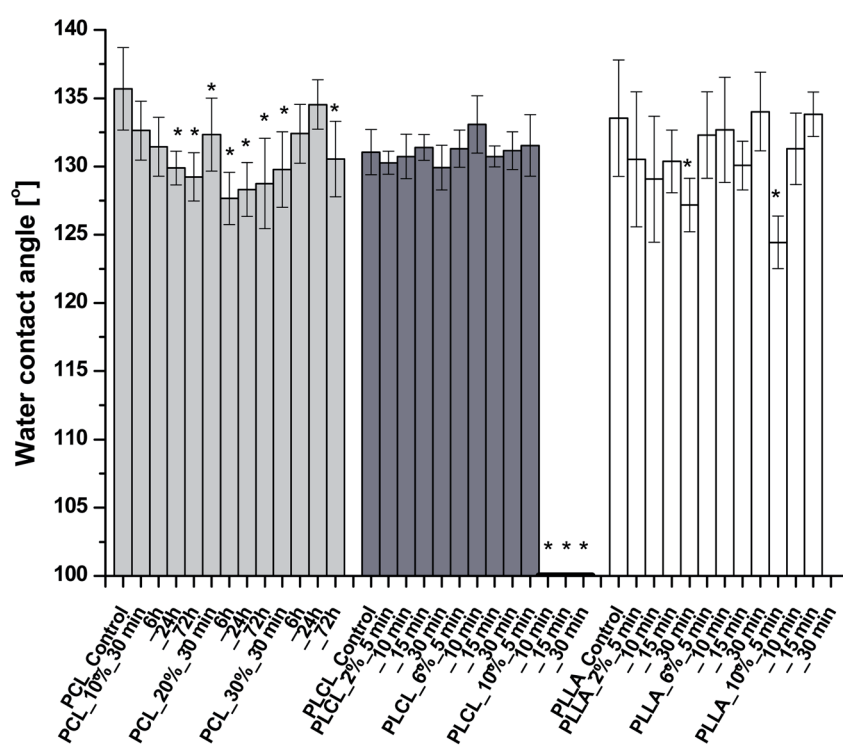


Fig. 5 Water contact angles of aminolysed samples. WCAs of three last PLCL samples were equal to 0°. No data for PLLA\_10%\_30 min due to sample degradation. Statistically significant difference between control and modified sample was marked as \* ( $p < 0.05$ ).



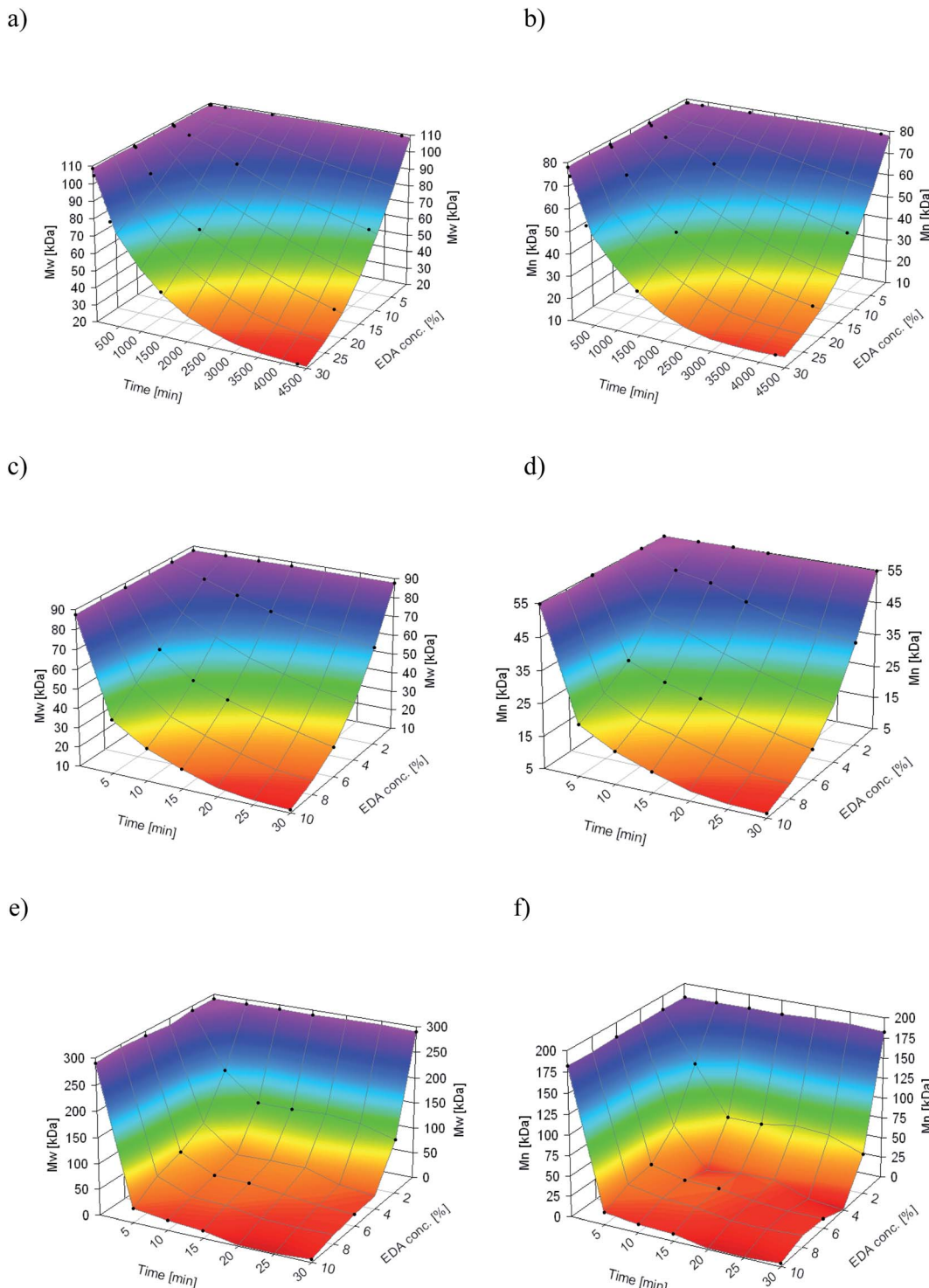


Fig. 6 Change of  $\overline{M}_w$  of (a) PCL, (c) PLCL, and (e) PLLA, and  $\overline{M}_n$  of (b) PCL, (d) PLCL, and (f) PLLA vs. EDA concentration and reaction time.

of the C1s peaks measured by XPS on the surface of PLCL\_Control and PLCL\_10%\_15 min. A detailed analysis of the C1s spectra allowed to determine the concentration of the C-C (BE: 284.8 eV), C-O/C-N (BE: 286.6 eV), and C=O (BE: 288.8 eV) bonds. Whereas the C-O and C-N bond energies differ

slightly and also that the nitrogen concentration is low, both chemical states have been fitted with one peak.

Additionally, we performed ATR-FTIR analysis. We observed a small signal around  $1530\text{ cm}^{-1}$  for aminolyzed samples, the intensity of which increases with the time of aminolysis.



**Table 2** Conc. of amine groups, molecular weights, and polydispersity of electrospun fibers

| Sample         | Conc. of NH <sub>2</sub> groups [mol mg <sup>-1</sup> ] | $\overline{M}_w$ [kDa] | $\overline{M}_n$ [kDa] | $\overline{M}_w/\overline{M}_n$ | Sample          | Conc. of NH <sub>2</sub> groups [mol mg <sup>-1</sup> ] | $\overline{M}_w$ [kDa] | $\overline{M}_n$ [kDa] | $\overline{M}_w/\overline{M}_n$ |
|----------------|---|------------------------|------------------------|---------------------------------|-----------------|---|------------------------|------------------------|---------------------------------|
| POL_Control    | 0   | 108.8                  | 78.1                   | 1.39                            | PCL_6%_15 min   | (1.09 ± 0.08) × 10 <sup>-7</sup>                        | 38.8                   | 23.0                   | 1.69                            |
| POL_10%_30 min | (1.81 ± 0.62) × 10 <sup>-9</sup>                        | 107.9                  | 77.0                   | 1.40                            | PCL_6%_30 min   | (1.79 ± 0.13) × 10 <sup>-7</sup>                        | 25.5                   | 14.4                   | 1.77                            |
| POL_10%_6 h    | (8.76 ± 0.38) × 10 <sup>-9</sup>                        | 104.0                  | 72.7                   | 1.43                            | PCL_10%_5 min   | (9.86 ± 0.44) × 10 <sup>-8</sup>                        | 37.8                   | 20.7                   | 1.82                            |
| POL_10%_24 h   | (3.18 ± 0.31) × 10 <sup>-8</sup>                        | 91.8                   | 64.3                   | 1.43                            | PCL_10%_10 min  | (1.65 ± 0.15) × 10 <sup>-7</sup>                        | 26.7                   | 15.2                   | 1.76                            |
| PCL_10%_72 h   | (2.18 ± 0.43) × 10 <sup>-7</sup>                        | 66.9                   | 44.1                   | 1.52                            | PCL_10%_15 min  | (2.16 ± 0.15) × 10 <sup>-7</sup>                        | 20.0                   | 11.4                   | 1.75                            |
| PCL_20%_30 min | (6.28 ± 1.00) × 10 <sup>-9</sup>                        | 108.2                  | 77.1                   | 1.40                            | PCL_10%_30 min  | 3.57 × 10 <sup>-7</sup>                                 | 11.6                   | 6.5                    | 1.80                            |
| POL_20%_6 h    | (3.01 ± 0.66) × 10 <sup>-8</sup>                        | 94.3                   | 65.6                   | 1.44                            | PLLA_Control    | 0   | 290.4                  | 182.4                  | 1.59                            |
| POL_20%_24 h   | (1.18 ± 0.03) × 10 <sup>-7</sup>                        | 66.6                   | 44.1                   | 1.51                            | PLLA_2%_5 min   | (1.36 ± 0.13) × 10 <sup>-8</sup>                        | 182.2                  | 121.0                  | 1.51                            |
| POL_20%_72 h   | (3.04 ± 0.31) × 10 <sup>-7</sup>                        | 35.9                   | 23.3                   | 1.54                            | PLLA_2%_10 min  | (1.78 ± 0.24) × 10 <sup>-8</sup>                        | 129.2                  | 60.9                   | 2.12                            |
| POL_30%_30 min | (1.28 ± 0.53) × 10 <sup>-8</sup>                        | 104.9                  | 74.3                   | 1.41                            | PLLA_2%_15 min  | (1.95 ± 0.24) × 10 <sup>-8</sup>                        | 128.4                  | 61.1                   | 2.10                            |
| POL_30%_6 h    | (9.30 ± 1.32) × 10 <sup>-8</sup>                        | 80.1                   | 53.9                   | 1.49                            | PLLA_2%_30 min  | (3.66 ± 0.49) × 10 <sup>-8</sup>                        | 106.5                  | 36.7                   | 2.17                            |
| POL_30%_24 h   | (1.75 ± 0.20) × 10 <sup>-7</sup>                        | 45.5                   | 29.7                   | 1.53                            | PLLA_6%_5 min   | (1.49 ± 0.12) × 10 <sup>-7</sup>                        | 74.8                   | 32.4                   | 2.31                            |
| POL_30%_72 h   | (5.05 ± 0.81) × 10 <sup>-7</sup>                        | 21.4                   | 14.7                   | 1.45                            | PLLA_6%_10 min  | (1.75 ± 0.22) × 10 <sup>-7</sup>                        | 42.7                   | 21.8                   | 1.96                            |
| PCL_2%_5 min   | 0   | 87.5                   | 55.0                   | 1.59                            | PLLA_6%_15 min  | (1.89 ± 0.09) × 10 <sup>-7</sup>                        | 40.6                   | 20.6                   | 1.97                            |
| PCL_2%_10 min  | (1.42 ± 0.08) × 10 <sup>-8</sup>                        | 81.3                   | 49.8                   | 1.48                            | PLLA_6%_30 min  | (2.63 ± 0.18) × 10 <sup>-7</sup>                        | 22.6                   | 12.4                   | 1.82                            |
| PCL_2%_15 min  | (2.23 ± 0.21) × 10 <sup>-8</sup>                        | 75.9                   | 47.8                   | 1.59                            | PLLA_10%_5 min  | (3.80 ± 0.37) × 10 <sup>-8</sup>                        | 27.5                   | 15.0                   | 1.83                            |
| PCL_2%_30 min  | (2.57 ± 0.32) × 10 <sup>-8</sup>                        | 70.5                   | 43.7                   | 1.61                            | PLLA_10%_10 min | (4.53 ± 0.25) × 10 <sup>-8</sup>                        | 19.0                   | 10.8                   | 1.76                            |
| PCL_6%_5 min   | (4.87 ± 0.30) × 10 <sup>-8</sup>                        | 61.1                   | 36.9                   | 1.65                            | PLLA_10%_15 min | (5.53 ± 0.39) × 10 <sup>-8</sup>                        | 13.8                   | 8.4                    | 1.65                            |
| PCL_6%_10 min  | (5.43 ± 0.90) × 10 <sup>-8</sup>                        | 58.4                   | 30.6                   | 1.9                             | PLLA_10%_30 min | (7.75 ± 0.26) × 10 <sup>-8</sup>                        | 5.9                    | 3.8                    |                                 |

According to the literature, this signal can be attributed to the amide II band originating from N–H stretch vibrations in primary amines and from a mixed vibration of N–H bending and C–N stretching in secondary amides.<sup>56</sup> It corresponds well with the situation where one of the diamine ends is anchored to the polymer substrate, mimicking thus the existence of primary amine with only one free end. The FTIR data were attached as ESI (Fig. S1†).

The aminolysis process did not cause the visible change of fibers morphology in most of the samples. However, for each type of polyester, fractured fibers were observed for the most aggressive aminolysis conditions corresponding to the highest concentration of amine groups (Fig. 4). Fragmented fibers were observed for PCL\_20%\_72 h, PCL\_30%\_72 h, PLCL\_10%\_15 min, PLCL\_10%\_30 min, PLLA\_10%\_15 min and PLLA\_10%\_30 min. The intensity of fragmentation was different depending on the type of polymer.

The results of WCA measurements are shown in Fig. 5. Despite the hydrophilic nature of amine groups, there is no significant change of WCA for most of the functionalized samples. Slight differences in water contact angle, which were observed, can originate from the nature of fibrous samples like variability in density and coverage of polymer fibers on the substrate, leading to masking of the wettability itself. In the case of PCL, the largest WCA decrease was only 8 degrees, for PLLA – 9 degrees. PLCL samples also remained hydrophobic with almost the same WCA as a native sample, except the three samples treated most aggressively, which manifest complete hydrophilicity in time of  $293.10 \pm 78.71$  s,  $25.08 \pm 8.34$  s, and  $7.17 \pm 3.08$  s, respectively. It is worth mentioning that the fibers in two of these samples were strongly fragmented.

As aminolysis is a kind of degradation due to the cleavage of ester bonds, the study of molecular weight change is an important input into its investigation. Fig. 6 shows 3D plots of weight and number average molecular weights, as a function of time and diamine concentration for all investigated polymers. Additionally, Table 2 contains source molecular weight data together with polydispersity index and corresponding amine concentration. Comparing three studied nonwovens, it is evident that the rate of drop in molecular weight is the slowest in the case of PCL and the fastest for PLLA.

In Fig. 7, a correlation between the concentration of introduced amine groups and the molecular weight is presented. Considering the same concentration of attached amine groups, the lowest drop in  $\overline{M}_w$  was observed for PCL and the highest for PLLA.

In Fig. 8 data of  $\overline{M}_n$  were compiled with stress and strain at break, and crystallinity for two chosen samples of each type of fibers after mild and strong aminolysis treatment. A noticeable drop of stress at break is observed only for PLCL\_10%\_10 min. A significant decrease of strain at break was noticed for all samples after strong aminolysis. In general, the changes of stress at break are not correlated with  $\overline{M}_n$  – for instance there is a strong reduction of  $\overline{M}_n$  for PLLA without any essential changes of stress at break. Regarding mechanical properties, there is a better correlation between strain at break and  $\overline{M}_n$ , particularly evident for the most aggressive aminolysis conditions (Fig. 8b).

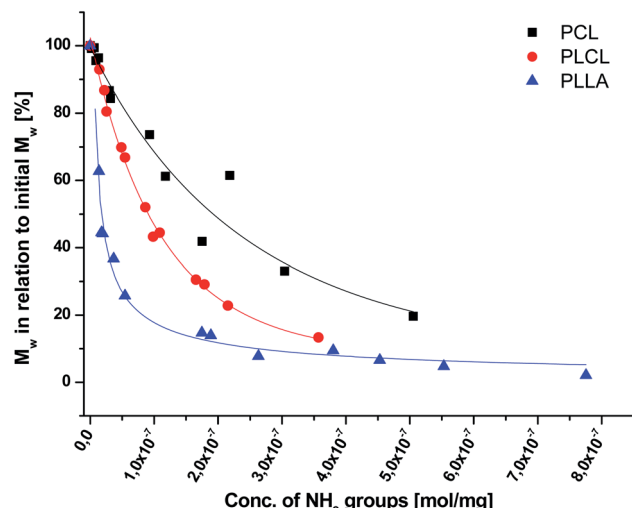


Fig. 7 Relative change of weight average molecular weight,  $\overline{M}_w$ , for PCL, PLCL, and PLLA fibers vs. grafted  $\text{NH}_2$  groups concentration. For PCL and PLCL, data were fitted with exponential curves, and for PLLA with an allometric curve.

A decrease of number average molecular weight was clearly correlated with an increase of crystallinity. We have added exemplary WAXS profiles as ESI (Fig. S2 and S3†).

Effect of aminolysis treatment on cell response to materials was studied on two chosen samples of each type of fibers. Fibroblast L929 cells and osteoblast-like MG63 cells were cultured on them for 5 days. In Fig. 9a, there are SEM images of L929 cells morphology. Cells seeded on unmodified (control) fibers have rather an unfavourable round shape compared to TCPS. Cells morphology has changed to be more spread in the case of all aminolyzed samples. It was especially observed in the case of PLCL\_10%\_10 min; however, it should be taken into account that initially, PLCL fibers promote the best cell morphology among control samples. In Fig. 9b, there are SEM images of MG63 cells morphology. For PCL and PLCL fibers after aminolysis, improvement of cell morphology is observed. In the case of PLLA fibers, control samples provide sufficient conditions for material–cells interaction. It seems that in that case aminolysis treatment causes slight deterioration of cell morphology.

In Fig. 10 there are FM images of MG63 cells cultured on studied materials. Greater spreading of actin skeleton is particularly noticeable for PCL samples after aminolysis in comparison to PCL\_Control. In the case of PLCL and PLLA fibers, proper cells morphology without significant differences between samples was observed.

In Fig. 11a, the change of metabolic activity of L929 cells was shown. We observed gradual improvement of metabolic activity in the case of PCL samples after aminolysis. Metabolic activity increases up to  $235.36 \pm 56.94\%$  and  $278.08 \pm 18.90\%$  of PCL\_Control value for a lower and higher concentration of amine groups, respectively. In the case of PLCL samples, both unmodified and modified, metabolic activity was on the same

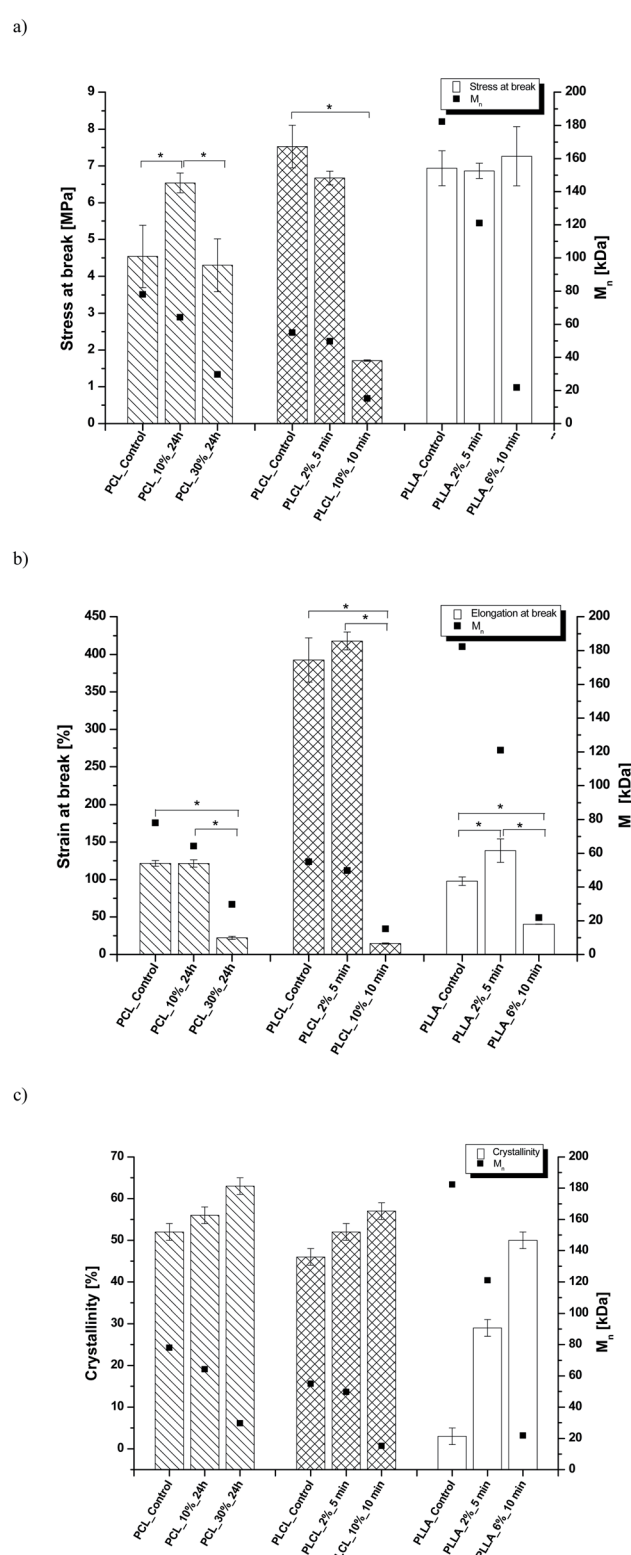


Fig. 8 (a) Stress and (b) strain at break, and (c) crystallinity of studied fibers in the function of  $\overline{M}_n$  mass. Statistically significant differences were marked as \* ( $p < 0.05$ ).



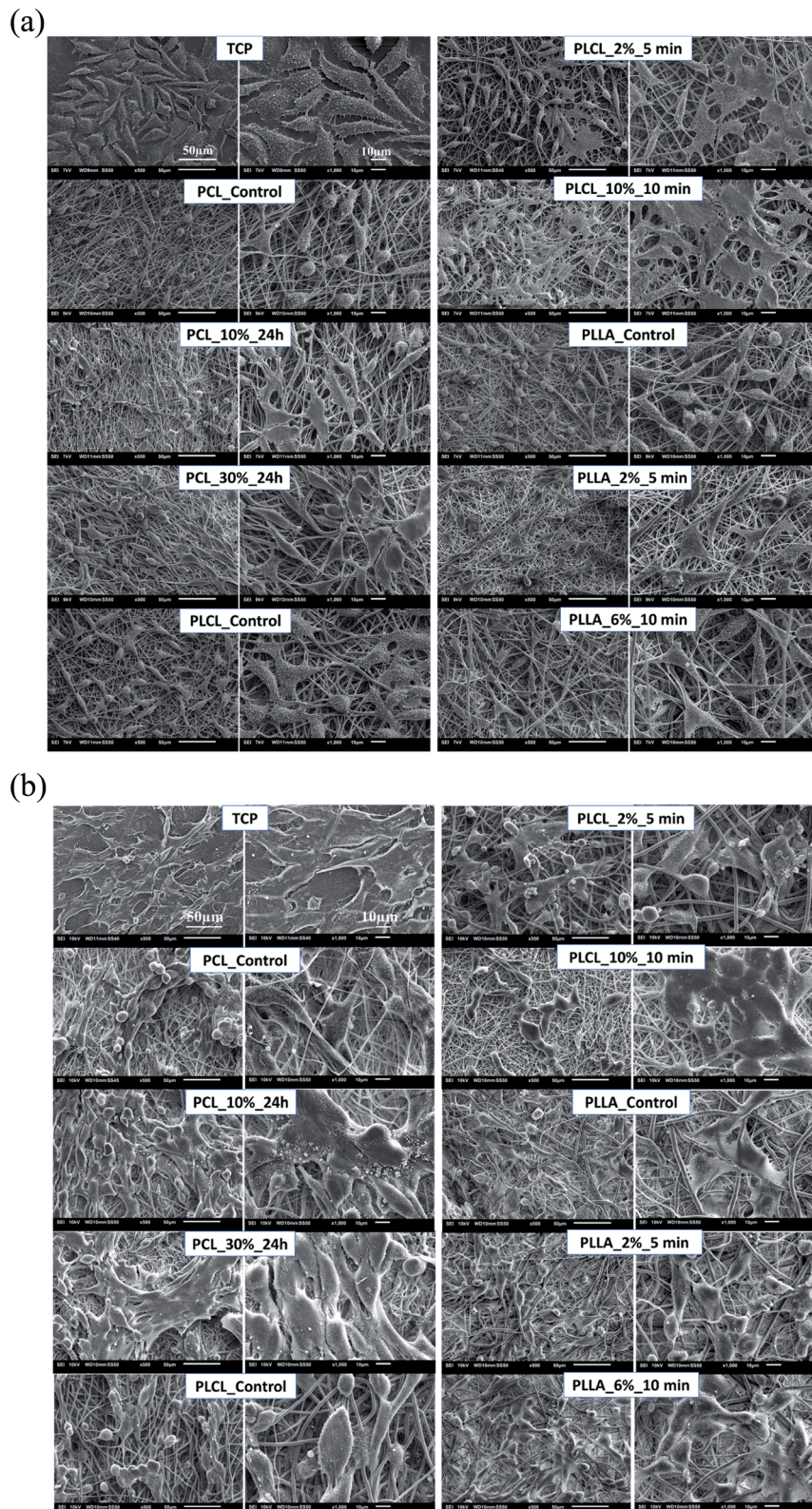


Fig. 9 SEM images of (a) L929 cells and (b) MG63 cells cultured by 5 days on control and modified fibers and TCP.

level, indicating that aminolysis does not change the metabolic activity of cells seeded on PLCL fibers. In the case of PLLA samples, we observed a decrease in metabolic activity for modified samples. In Fig. 11b, the change of metabolic activity

of MG63 cells was shown. There is only a slight increase for samples of each polymer with higher concentration of amine groups. For samples with lower amine groups concentration, a decrease of metabolic activity was observed.



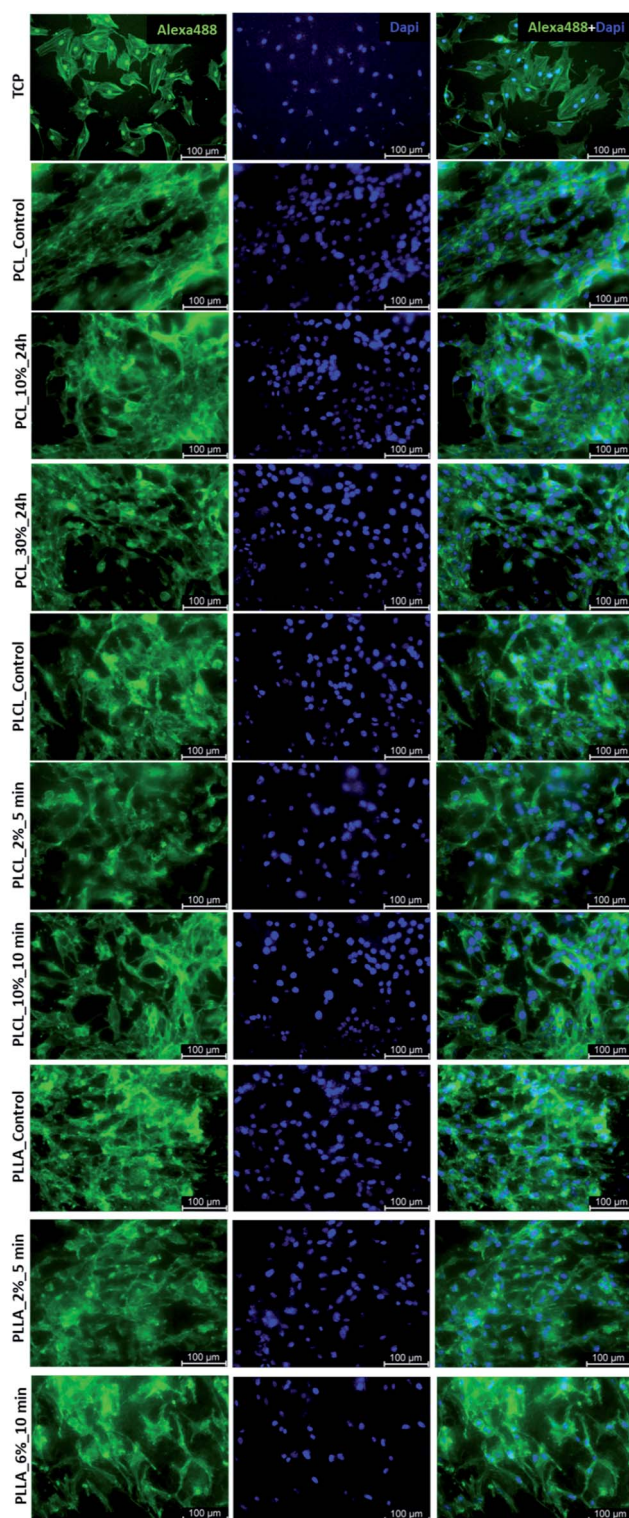
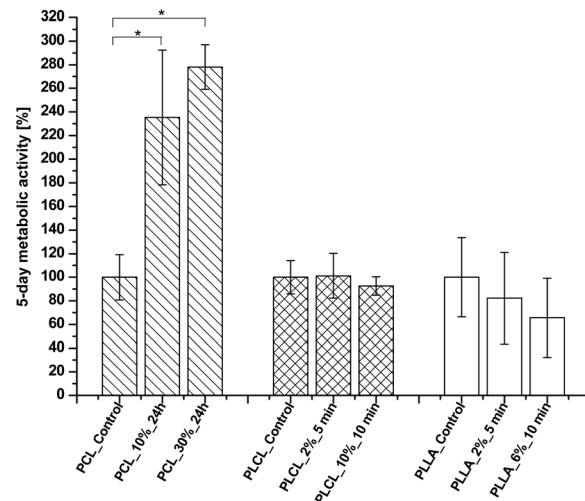


Fig. 10 FM images MG63 cells cultured by 5 days on control and modified fibers and TCP.

a)



b)

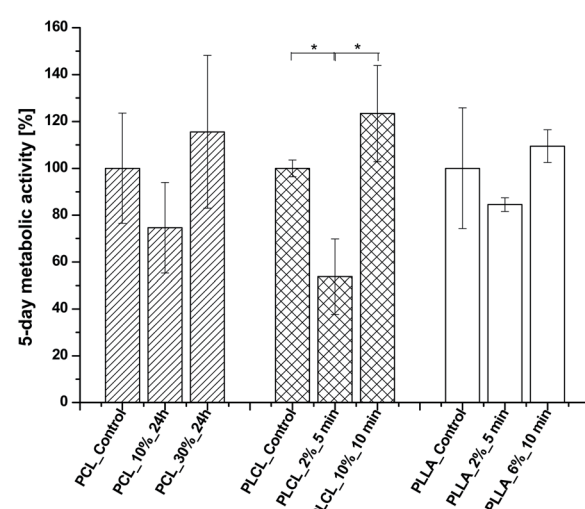


Fig. 11 Metabolic activity of (a) L929 cells and (b) MG-63 cells after 5 days of culture on control and modified fibers. Statistically significant differences were marked as \* ( $p < 0.05$ ).

## 4. Discussion

Based on the ninhydrin test results, the susceptibility of the investigated fibers to aminolysis can be presented as PLLA > PLCL  $\gg$  PCL. PCL fibers require a much higher concentration of EDA and time of reaction to reach the same level of attached amine groups as PLCL and PLLA fibers. We explain such a difference by a combination of several factors – the differences in ester bond density, glass transition temperature, and crystallinity (surface crystallinity). The ratio of reactive ester groups to alkyl groups is the highest for PLLA and the lowest for PCL. Additionally, in the case of PCL, glass transition temperature ( $-60^{\circ}\text{C}$ ) is far below the temperature of aminolysis, which provides high chain mobility and could result in free amine recombination reducing effective concentration of amine groups. Considering crystallinity, it is well known that the

availability of ester groups for aminolysis is lower for the crystal phase with a dense package of molecules, hindering the diffusion of diamines.<sup>57</sup> In our previous work, we showed differences in bulk crystallinity of these polyester fibers being the highest for PCL and the lowest for PLLA, together with a hypothesis of an additional factor related to the radial distribution of fiber structure with the more crystalline surface, which can hinder additionally aminolysis reaction for PCL.<sup>17</sup> Contrary to some other works, a decrease of the amount of attached NH<sub>2</sub> groups after a certain time threshold was not observed in our study.<sup>43,45</sup>

XPS results clearly indicate that aminolysis covers the entire volume of the fiber and not only the fiber's surface. Such conclusion can be drawn considering that the atomic concentration of the N–C/H bond is stable up to the depth of the 370 nm for the PLCL\_10%\_15 min. For the PLCL\_Control, the measured carbon and oxygen content is close to the stoichiometric composition of the polymer, whose atomic concentration ratio C/O should be equal to 2.0. Relative intensities of the C–O and C=O bonds are also consistent with the stoichiometric composition of the analyzed compound. Differences observed for sample after aminolysis can be a result of the change of group orientation as aminolysis lead to chain scission.

Fragmentation of fibers that we observed for extreme aminolysis reaction conditions was explained by Polini A. *et al.* and Kim T. G. *et al.* as a result of chains scission, additional crystallization of shortened chains, and then the formation of a specific arrangement of alternate amorphous and crystalline domains.<sup>58,59</sup> According to the authors, transverse fiber fragmentation can be caused by the easy breaking down of amorphous spaces present between crystalline regions under stress conditions.<sup>58</sup> In our case, fragmentation could be favoured by sample handling. In the literature, there are many studies in which this fragmentation is desirable as aminolysis or other techniques are used for producing fibrous "particles", especially from the PLLA nonwovens, that can be exploited as hydrogel fillers.<sup>60–63</sup>

In the literature, aminolysis is as an example of a method that improves the wettability (WCA) of material due to the hydrophilic character of amine groups.<sup>46</sup> However, studies on aminolysis show that sometimes there is a lack of wettability improvement or changes are not significant.<sup>17,49,64</sup> It was proposed by Monnier A. *et al.* that such a lack of improved wettability could be associated with the domination of the hydrophobic alkyl chain of diamine over the hydrophilic amine group.<sup>64</sup> In our study, we have not observed a clear trend in the change of the WCA values. It should also be taken into consideration that WCA results are affected by roughness.<sup>65</sup>

The results of GPC analysis indicate clearly that the whole fiber, not only its surface, underwent an aminolysis reaction, which corresponds to the XPS analysis data. In chromatograms, we observed only one peak with its gradual shifting to the lowest molecular weight for all aminated samples. In the case of reaction limited to the surface, a new peak for lower molecular weights would be expected to appear in the chromatogram in addition to the peak related to the fibers' unchanged interior. This is consistent with some fundamental studies showing that

aminolysis, contrary to hydrolysis, is not a surface-limited reaction.<sup>66,67</sup> There are also other papers, in which authors presented a significant decrease in molecular weight after aminolysis.<sup>68,69</sup> However, as it was shown in our study, aminolysis of both, PCL and PLCL, allows obtaining relatively high amine concentration at the surface, maintaining a still reasonable level of molecular weight.

As it was proposed by Flory, the reduction of number average molecular weight,  $\overline{M}_n$ , leads to a decrease of fracture strength,  $\sigma$ , according to the equation:

$$\sigma = \sigma^\infty - B/\overline{M}_n,$$

where  $\sigma^\infty$  is the fracture strength at infinite molecular weight, and  $B$  is a constant dependent on chains' entanglements.<sup>70</sup> In our study, in the case of PLCL sample with a significant reduction of  $\overline{M}_n$ , a noticeable drop of stress at break was observed. This is not the case of PCL and PLLA, for which there is practically no change or even increase of stress at break. Additional factor for stress at break reduction in the case of PLCL is breaking and cracking of fibers due to aggressive aminolysis conditions. Another factor affecting mechanical properties is the additional crystallization caused by the presence of shorter, more mobile chains. This effect is most important for PLLA with large degradation leading to essential crystallization from practically amorphous state to crystallinity 50% in the case of PLLA\_6%\_10 min. In general, an increase of crystallinity is expected to be responsible for increase of stress at break, leading to disturb the correlation of stress at break with  $\overline{M}_n$ , as observed by us. Evident reduction of elongation at break with reduction of  $\overline{M}_n$ , can be explained by the loss of elastic properties with reduction of molecular entanglement density at lower molecular weight.

In the case of all aminated samples, even with a lower level of attached amine groups, change of L929 shape to more spread was noticed. The same effect was observed for MG63 cells cultured on PCL and PLCL samples. Most probably, it is related to the positive charge of introduced amine groups as it was reported previously.<sup>4,71</sup> Especially in the case of PLCL\_10%\_10 min, a lot of well-spread L929 cells with the formed filopodia were observed, which could be additionally associated with the fact that this sample was completely hydrophilic. Despite the improvement of cell morphology, results of metabolic activity tests did not show a clear correlation with the presence of amine groups for all polymers. Indeed, in the case of PCL, gradual improvement was observed, and taking into account that all PCL samples were hydrophobic, it is most probably associated with the effect of the positively-charged surface. However, general observations lead to the conclusion that introducing amine groups on the surface of the fibers leads in all cases to the proper cells morphology but is not sufficient for improvement of their metabolic activity. In other words, there is no clear correlation between improvement in cells morphology and their metabolic activity. There is little literature supporting these observations. For instance, Shin J. W. *et al.* show that 4-fold changes in scaffold stiffness, provoked by changes in the molecular structure, increase cellular spreading



without significant impact on cell number and cellular viability.<sup>72</sup> Despite many scientific inquiries, there is still no clear relation between cell viability, metabolic activity, and shape in the literature.<sup>73</sup> We suppose that the observed SEM and FM morphology of cells is mostly affected by the quality of cellular adhesion to the fibers while the metabolic activity reflects further, post-adhesion stages of cells behaviour associated with their growth, migration and proliferation.

## 5. Conclusions

In this study, the aminolysis of three types of aliphatic polyester fibers in a wide range of conditions was investigated. It was shown that achieving the same level of amine concentration requires a much higher concentration of diamine and time of reaction in the case of PCL electrospun fibers compared to PLCL and PLLA. This phenomenon can be explained by the difference in ester bonds density, crystallinity (including surface crystallinity), and glass transition temperature. Despite the hydrophilic nature of amine groups, most of the samples remained hydrophobic. X-ray photoelectron spectroscopy results clearly demonstrate that an aminolysis reaction is not limited to the surface of the material. This observation is supported by GPC results showing bulk molecular weight decrease, which indicates that the reaction is not limited to the fiber surface, but it proceeds in the whole cross-section of the fiber.

Molecular degradation is much stronger for PLLA than for PLCL and PCL, leading to the favorable situation that for PCL and PLCL an effective concentration of amine groups is achieved at relatively weak degradation. Another effect of aminolysis is an increase of crystallinity as a result of shortening the chains and their additional arrangement. A decrease of molecular weight, as well as an increase of crystallinity, led to the change of mechanical properties. For the strongest treated samples, cracking and fragmentation of fibers were observed, affecting additional mechanical properties. However, our study shows that it is possible to reach a compromise between the concentration of introduced amine groups and change of fibers properties. Amine groups introduced in two different concentrations caused improvement of L929 and MG63 cells morphology to more spread. Taking into account that the low concentration of NH<sub>2</sub> groups on the fiber surface was sufficient to improve the morphology of cells allowing at the same time to maintain relatively high molecular weight and hence mechanical strength, we recommend using aminolysis conditions that are relatively mild for a particular type of fibrous polymer scaffold.

## Conflicts of interest

There are no conflicts to declare.

## Acknowledgements

This research was funded by the Polish National Science Center (NCN), grant number 2016/23/B/ST8/03409.

## References

- H. Amani, H. Arzaghi, M. Bayandori, A. S. Dezfuli, H. Pazoki-Toroudi, A. Shafiee and L. Moradi, *Adv. Mater. Interfaces*, 2019, **6**, 1900572.
- R. Morent, N. De Geyter, T. Desmet, P. Dubruel and C. Leys, *Plasma Processes Polym.*, 2011, **8**, 171–190.
- J. Czwartos, B. Budner, A. Bartnik, W. Kasprzycka and H. Fiedorowicz, *eXPRESS Polym. Lett.*, 2020, **14**, 1063–1077.
- A. Bakry, *J. Appl. Polym. Sci.*, 2020, **138**, 49643.
- Ch. Xie, X. Lu, K. Wang, H. Yuan, L. Fang, X. Zheng, Ch. Chan, F. Ren and C. Zhao, *ACS Biomater. Sci. Eng.*, 2016, **2**, 920–928.
- Y. Liu, M. C. Munisso, A. Mahara, Y. Kambe, K. Fukazawa, K. Ishihara and T. Yamaoka, *Biomater. Sci.*, 2018, **6**, 1908–1915.
- D. Kołbuk, O. Urbanek, P. Denis and E. Choińska, *J. Biomed. Mater. Res., Part A*, 2019, **107**, 2447–2457.
- M. Budnicka, M. Szymaniak, D. Kołbuk, P. Ruśkowski and A. Gadomska-Gajadhur, *J. Biomed. Mater. Res., Part B*, 2020, **108**, 868–879.
- L. Chambre, Z. Martín-Moldes, R. N. Parker and D. L. Kaplan, *Adv. Drug Delivery Rev.*, 2020, **160**, 186–198.
- M. A. Elnaggar, H. A. El-Fawal and N. K. Allam, *Mater. Sci. Eng.*, 2021, **119**, 111550.
- M. Binazadeh, H. Zeng and L. D. Unsworth, in *Biomaterials Surface Science*, ed. T. J. F. Mano and J. C. Rodríguez-Cabello, Wiley-VCH Verlag GmbH & Co. KGaA, Weinheim, Germany, 2013, ch. 13, pp. 1–17.
- A. Zaszczyńska, P. Ł. Sajkiewicz, A. Gradyś, R. Tymkiewicz, O. Urbanek and D. Kołbuk, *Bull. Pol. Acad. Sci.: Tech. Sci.*, 2020, **68**, 627.
- E. Liamas, K. Kubiak-Ossowska, R. A. Black, O. R. Thomas, Z. J. Zhang and P. A. Mulheran, *Int. J. Mol. Sci.*, 2018, **19**, 3321.
- S. Metwally and U. Stachewicz, *Mater. Sci. Eng., C*, 2019, **104**, 109883.
- M. Rahmati, E. A. Silva, J. E. Reseland, C. A. Heyward and H. J. Haugen, *Chem. Soc. Rev.*, 2020, **49**, 5178–5224.
- H. Fan and Z. Guo, *Biomater. Sci.*, 2020, **8**, 1502–1535.
- O. Jeznach, D. Kołbuk and P. Sajkiewicz, *Polymers*, 2019, **11**, 1669.
- A. L. M. M. Toledo, B. S. Ramalho, P. H. S. Picciani, L. S. Baptista, A. M. B. Martinez and M. L. Dias, *Int. J. Polym. Mater.*, 2020, **70**, 1258–1270.
- C. Li, L. Wang, Z. Yang, G. Kim, H. Chen and Z. Ge, *J. Biomater. Sci., Polym. Ed.*, 2012, **23**, 405–424.
- T. Ohe, Y. Yoshimura, I. Abe, M. Ikeda and Y. Shibutani, *Text. Res. J.*, 2007, **77**, 131–137.
- M. Jabli, N. Tka, G. A. Salman, A. Elaissi, N. Sebeia and M. Hamdaou, *J. Mol. Liq.*, 2017, **242**, 272–283.
- J. Hu, X. Feng, Z. Liu, Y. Zhao and L. Chen, *Surf. Interface Anal.*, 2017, **49**, 640–646.
- V. Popescu, A. Muresan, O. Constandache, G. Lisa, E. I. Muresan, C. Munteanu and I. Sandu, *Ind. Eng. Chem. Res.*, 2014, **53**, 16652–16663.



- 24 C. N. Hoang and Y. H. Dang, *Polym. Degrad. Stab.*, 2013, **98**, 697–708.
- 25 T. I. Croll, A. J. O'Connor, G. W. Stevens and J. J. Cooper-White, *Biomacromolecules*, 2004, **5**, 463–473.
- 26 A. C. de Luca, G. Terenghi and S. Downes, *J. Tissue Eng. Regener. Med.*, 2014, **8**, 153–163.
- 27 J. Amirian, S. Y. Lee and B. T. Lee, *J. Biomed. Nanotechnol.*, 2016, **12**, 1864–1875.
- 28 M. J. Song, J. Amirian, N. T. B. Linh and B. T. Lee, *J. Appl. Polym. Sci.*, 2017, **134**, 45186.
- 29 G. Aziz, N. De Geyter and R. Morent, in *Advances in Bioengineering*, ed. P. A. Serra, IntechOpen, London, UK, 2015, ch. 2.
- 30 Y. Wan, Ch. Tu, J. Yang, J. Bei and S. Wang, *Biomaterials*, 2006, **27**, 2699–2704.
- 31 J. Ward, J. Kelly, W. Wang, D. I. Zeugolis and A. Pandit, *Biomacromolecules*, 2010, **11**, 3093–3101.
- 32 L. R. Jaidev and K. Chatterjee, *Mater. Des.*, 2019, **161**, 44–54.
- 33 Y. H. Dinga, M. Florenab and W. Tan, *Biosurf. Biotribol.*, 2016, **2**, 121–136.
- 34 D. Grafarend, K. H. Heffels, M. V. Beer, P. Gasteier, M. Möller, G. Boehm, P. D. Dalton and J. Groll, *Nat. Mater.*, 2011, **10**, 67–73.
- 35 J. K. Tessmar and A. M. Göpferich, *Macromol. Biosci.*, 2007, **7**, 23–39.
- 36 M. Erol, H. Du and S. Sukhishvili, *Langmuir*, 2006, **22**, 11329–11336.
- 37 Y. Moskovitz and S. Srebnik, *Phys. Chem. Chem. Phys.*, 2014, **16**, 11698–11707.
- 38 Y. Arima and H. Iwata, *Biomaterials*, 2007, **28**, 3074–3082.
- 39 Z. Ma, Z. Mao and C. Gao, *Colloids Surf., B*, 2007, **60**, 137–157.
- 40 C. Holmes and M. Tabrizian, in *Stem cell biology and tissue engineering in dental sciences*, ed. A. Vishwakarma, P. S. Songtao and S. M. Ramalingam, Academic Press, 2015, ch. 14, pp. 187–206.
- 41 J. H. Lee, H. W. Jung, I. K. Kang and H. B. Lee, *Biomaterials*, 1994, **15**, 705–711.
- 42 Y. Zhang, J. Luan, S. Jiang, X. Zhou and M. Li, *Composites, Part B*, 2019, **172**, 397–405.
- 43 Y. Zhu, C. Gao, X. Liu and J. Shen, *Biomacromolecules*, 2002, **3**, 1312–1319.
- 44 Y. Zhu, C. Gao, T. He, X. Liu and J. Shen, *Biomacromolecules*, 2003, **4**, 446–452.
- 45 Y. Zhu, K. S. Chian, M. B. Chan-Park, P. S. Mhaisalkar and B. D. Ratner, *Biomaterials*, 2006, **27**, 68–78.
- 46 Y. Zhu, Z. Mao, H. Shi and C. Gao, *Sci. China: Chem.*, 2012, **55**, 2419.
- 47 Y. Zhu, Z. Mao and C. Gao, *RSC Adv.*, 2013, **3**, 2509.
- 48 L. Cao, Y. Yu, J. Wang, J. A. Werkmeister, K. M. McLean and C. Liu, *Mater. Sci. Eng., C*, 2017, **74**, 298–306.
- 49 P. Bhattacharjee, D. Naskar, H. W. Kim, T. K. Maiti, D. Bhattacharya and S. C. Kundu, *Eur. Polym. J.*, 2015, **71**, 490–509.
- 50 N. Krishica, V. Natarajan, B. Madhan, P. K. Sehgal and A. B. Mandal, *Adv. Eng. Mater.*, 2011, **14**, B149–B151.
- 51 J. F. Piai, M. A. da Silva, A. Martins, A. B. Torres, S. Faria, R. L. Reis, E. C. Muniz and N. M. Neves, *Appl. Surf. Sci.*, 2017, **403**, 112–125.
- 52 F. Anjum, N. A. Agabalyan, H. D. Sparks, N. L. Rosin, M. S. Kallos and J. Biernaskie, *Sci. Rep.*, 2017, **7**, 1.
- 53 B. Niemczyk, A. Gradys and P. Sajkiewicz, *Polymers*, 2020, **12**, 2636.
- 54 S. Sinnwell, A. J. Inglis, T. P. Davis, M. H. Stenzel and C. Barner-Kowollik, *Chem. Commun.*, 2008, 2052.
- 55 M. Nuuttila, Gel permeation chromatography methods in the analysis of lactide-based polymer, Master's thesis, University of Jyväskylä, 2018.
- 56 F. S. Parker, in *Applications of Infrared Spectroscopy in Biochemistry, Biology, and Medicine*, ed. F. S. Parker, Springer, Boston, USA, 1971, ch. 8, pp. 165–166.
- 57 K. Fukatsu, *J. Appl. Polym. Sci.*, 1992, **45**, 2037.
- 58 T. G. Kim and G. P. Tae, *Macromol. Rapid Commun.*, 2008, **29**, 1231–1236.
- 59 A. Polini, D. G. Petre, M. Iafisco, S. de Lacerda Schickert, A. Tampieri, J. van den Beucken and S. C. Leeuwenburgh, *J. Biomed. Mater. Res., Part A*, 2017, **105**, 2335–2342.
- 60 F. Mohabatpour, A. Karkhaneh and A. M. Sharifi, *RSC Adv.*, 2016, **6**, 83135–83145.
- 61 F. Ahadi, S. Khorshidi and A. Karkhaneh, *Eur. Polym. J.*, 2019, **118**, 265–274.
- 62 A. G. B. Castro, M. C. Lo Giudice, T. Vermonden, S. C. G. Leeuwenburgh, J. A. Jansen, J. J. J. P. van den Beucken and F. Yang, *ACS Biomater. Sci. Eng.*, 2016, **2**, 2099.
- 63 B. Niemczyk-Soczynska, J. Dulnik, O. Jeznach, D. Kolbuk and P. Sajkiewicz, *Micron*, 2021, **145**, 103066.
- 64 A. Monnier, E. Al Tawil, Q. T. Nguyen, J. M. Valleton, K. Fatyeyeva and B. Deschrevet, *Eur. Polym. J.*, 2018, **107**, 202–217.
- 65 F. Foadi, G. H. ten Brink, M. R. Mohammadizadeh and G. Palasatzas, *J. Appl. Phys.*, 2019, **125**, 244307.
- 66 M. S. Elisson, L. D. Fisher, K. W. Alger and S. H. Zeronian, *J. Appl. Polym. Sci.*, 1982, **27**, 247–257.
- 67 K. R. Carduner, M. C. Paputa Peck, R. O. Carter III and P. C. Killgoar Jr, *Polym. Degrad. Stab.*, 1989, **26**, 1–10.
- 68 N. Kasoju, A. Pátiková, E. Wawrzynska, A. Vojtíšková, T. Sedláčík, M. Kumorek, O. Pop-Georgievski, E. Sticová, J. Kříž and D. Kubies, *Biomater. Sci.*, 2020, **8**, 631–647.
- 69 Y. Zhu, Z. W. Mao, H. Y. Shi and C. Y. Gao, *Sci. China: Chem.*, 2012, **55**, 2419–2427.
- 70 P. J. Flory, *J. Am. Chem. Soc.*, 1945, **67**, 2048–2050.
- 71 P. Sangsanoh, N. Israsena, O. Suwantong and P. Supaphol, *Polym. Bull.*, 2017, **74**, 4101–4118.
- 72 J. W. Shin and D. J. Mooney, *Proc. Natl. Acad. Sci. U. S. A.*, 2016, **113**, 12126–12131.
- 73 M. Ochsner, M. Textor, V. Vogel and M. L. Smith, *PLoS One*, 2010, **5**, e9445.



## Article

# Immobilization of Gelatin on Fibers for Tissue Engineering Applications: A Comparative Study of Three Aliphatic Polyesters

Oliwia Jeznach <sup>1,\*</sup>, Dorota Kołbuk <sup>1</sup>, Tobias Reich <sup>2</sup> and Paweł Sajkiewicz <sup>1</sup>

<sup>1</sup> Institute of Fundamental Technological Research, Polish Academy of Sciences, Pawinskiego 5B, 02-106 Warsaw, Poland

<sup>2</sup> Department of Chemistry, Johannes Gutenberg University Mainz, Fritz-Strassmann-Weg 2, 55128 Mainz, Germany

\* Correspondence: ojeznach@ippt.pan.pl

**Abstract:** Immobilization of cell adhesive proteins on the scaffold surface has become a widely reported method that can improve the interaction between scaffold and cells. In this study, three nanofibrous scaffolds obtained by electrospinning of poly(caprolactone) (PCL), poly(L-lactide-co-caprolactone) (PLCL) 70:30, or poly(L-lactide) (PLLA) were subjected to chemical immobilization of gelatin based on aminolysis and glutaraldehyde cross-linking, as well as physisorption of gelatin. Two sets of aminolysis conditions were applied to evaluate the impact of amine group content. Based on the results of the colorimetric bicinchoninic acid (BCA) assay, it was shown that the concentration of gelatin on the surface is higher for the chemical modification and increases with the concentration of free NH<sub>2</sub> groups. XPS (X-ray photoelectron spectroscopy) analysis confirmed this outcome. On the basis of XPS results, the thickness of the gelatin layer was estimated to be less than 10 nm. Initially, hydrophobic scaffolds are completely wettable after coating with gelatin, and the time of waterdrop absorption was correlated with the surface concentration of gelatin. In the case of all physically and mildly chemically modified samples, the decrease in stress and strain at break was relatively low, contrary to strongly aminolyzed PLCL and PLLA samples. Incubation testing performed on the PCL samples showed that a chemically immobilized gelatin layer is more stable than a physisorbed one; however, even after 90 days, more than 60% of the initial gelatin concentration was still present on the surface of physically modified samples. Mouse fibroblast L929 cell culture on modified samples indicates a positive effect of both physical and chemical modification on cell morphology. In the case of PCL and PLCL, the best morphology, characterized by stretched filopodia, was observed after stronger chemical modification, while for PLLA, there was no significant difference between modified samples. Results of metabolic activity indicate the better effect of chemical immobilization than of physisorption of gelatin.



**Citation:** Jeznach, O.; Kołbuk, D.; Reich, T.; Sajkiewicz, P.

Immobilization of Gelatin on Fibers for Tissue Engineering Applications: A Comparative Study of Three Aliphatic Polyesters. *Polymers* **2022**, *14*, 4154. <https://doi.org/10.3390/polym14194154>

Academic Editor: Jin-Jia Hu

Received: 28 August 2022

Accepted: 23 September 2022

Published: 4 October 2022

**Publisher's Note:** MDPI stays neutral with regard to jurisdictional claims in published maps and institutional affiliations.



**Copyright:** © 2022 by the authors. Licensee MDPI, Basel, Switzerland. This article is an open access article distributed under the terms and conditions of the Creative Commons Attribution (CC BY) license (<https://creativecommons.org/licenses/by/4.0/>).

**Keywords:** gelatin; aminolysis; surface modification; electrospinning

## 1. Introduction

Understanding and improving cell–material interaction is a topic of fundamental importance in tissue engineering research [1]. At the early stage of the scaffold contact with culture medium or physiological environment, surface properties play the most significant role. Firstly, non-specific protein adsorption on the material surface occurs. This protein layer influences cell attachment, by providing or not, adhering sites for integrin-driven interaction [2,3]. Type and quantity of adsorbed proteins, and thus cell adhesion, depend on many material surface characteristics, such as charge, wettability, and electrostatic interaction [3–6]. Taking into account that cells adhere on the surface mainly via integrin-ligand binding, research effort is put into supplying the scaffolds with extracellular matrix (ECM)-originated adhesive proteins to enable specific cell attachment [7].

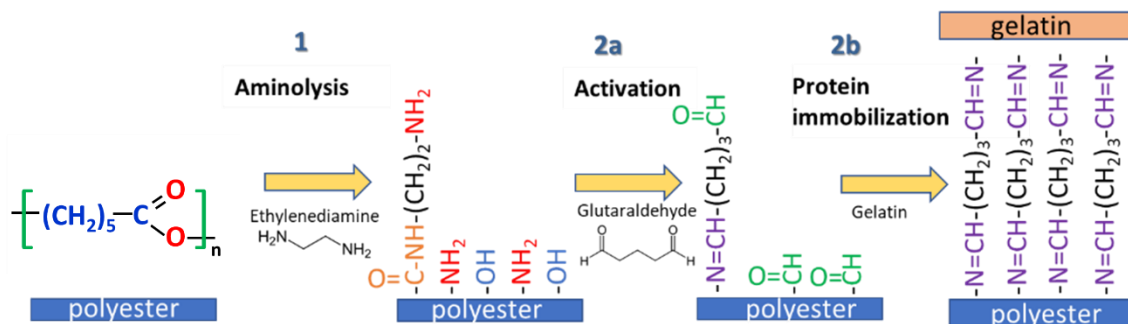
ECM molecules, such as fibronectin, vitronectin, or collagen, contain various peptide sequences that can be recognized by cell receptors. One of the most studied is the Arg-Gly-Asp (RGD) sequence, which can be provided by the denatured form of collagen-gelatin [8,9]. Depending on the type of protein, the RGD motif can be bound to different cell integrins, probably because of various spatial conformations of RGD associated with the vicinity of different amino acids or the existence of different synergistic sequences on ECM molecules [10]. In the case of gelatin, the RGD sequence is recognized by  $\alpha v\beta 3$  and  $\alpha 5\beta 1$  integrins [11]. Both integrins are present in, e.g., L929 cells [12,13]. Active integrins bound to adhesion molecules are attached to actin filaments through the focal adhesion complexes, which enable the transduction of mechanical signals from ECM to the cell [14,15]. Although specific integrin-mediated cell adhesion is widely reported in the literature of tissue engineering, there is still a need for studying factors, such as spatial conformation of ECM molecule [16,17] or so-called early cell adhesion preceding attachment of integrin to peptide sequence [18].

Currently, a lot of effort is put into the development of surface modification techniques to improve cell response to the scaffold without losing its mechanical properties or changing the degradability profile, as is observed in the case of bulk modification [19]. Electrospun nano- and submicron fibers made of aliphatic polyesters are widely studied in various tissue engineering applications (e.g., brain [20], tendon tissue regeneration [21], blood vessels [22], wound healing [23]), because of their biomimetic architecture, biocompatibility, atoxic degradation products, tunable mechanical properties, and reproducibility. However, from the perspective of the initial cell–scaffold contact, there is a problem with their hydrophobicity and lack of bioactive moieties, which could interact with cells [24]. Immobilization of biomolecules onto polyester fibers is achieved through various methods originating from chemical binding (e.g., methods based on aminolysis [25], hydrolysis [26], “click chemistry” [27]) or physical interaction between biomolecules and polymer (e.g., methods exploiting plasma treatment [28], layer-by-layer deposition [29], and simple surface entrapment [30]). In a review on recent advances in the modification of electrospun fibers, the authors pointed out many examples with a comprehensive presentation of modification method and obtained biological results [19]. Nowadays, there is a wide range of available methods, which improve cellular response, but it is important to consider their pros and cons, such as impact on bulk properties, complexity of process, etc. There is also too little information on long-term performance of the modified scaffolds under in vivo conditions. In our opinion, too little attention is also paid to fundamental understanding of mechanisms of the modification processes.

In this study, the immobilization of gelatin was investigated onto the surface of electrospun fibers made of three types of aliphatic polyesters: poly(caprolactone), poly(L-lactide-co-caprolactone), and poly(L-lactide). Aminolysis was applied in our research to introduce free amine functional groups on fibers’ surface as the “coupling sites” followed by glutaraldehyde cross-linking to chemically bind gelatin to the polymer. The polyesters used in our study differ in physicochemical properties, such as glass-transition temperature ( $T_g$ ), crystallinity, Young’s modulus, and density of ester groups. All studied polyesters are commonly used in tissue engineering. PCL and PLLA are FDA-approved polymers. Among aliphatic polyesters used, PLCL has been reported to be the most promising candidate for tissue engineering, surpassing both PLLA and PCL, in some of their properties. The most crucial point is that by the association of PLLA with PCL into PLCL, it is possible to avoid the brittle behavior of PLLA and the low stiffness of PCL [31,32], as well as to reduce the local acidification due to the degradation of PLLA [33]. In general, it may be concluded that PLCL is the most suitable polymer for various tissue engineering applications, particularly when adjustable elasticity and degradability are required. PLLA and PCL differ additionally in the kinetics of degradation, which is relatively fast for PLLA and slow for PCL. PLCL offers an adjustable degradation rate adapted to its use in tissue engineering, tailororable by changing the PCL/PLLA ratio [34].

The main aim of the research was a comparison of polyesters in terms of concentration of gelatin and nitrogen on the surface, the stability of gelatin coating, the impact of the modification on wettability and mechanical properties, and L929 cell–scaffold interaction. This type of modification was compared with the physisorption of gelatin obtained by simple immersion of nonwoven in the protein solution.

Scheme 1 illustrates the mechanism of gelatin immobilization based on aminolysis and glutaraldehyde cross-linking that was utilized in this study.



**Scheme 1.** Aminolysis-based immobilization of gelatin.

## 2. Materials and Methods

### *2.1. Materials*

Three polyesters were used: PCL (Sigma-Aldrich, St. Louis, MO, USA,  $\overline{M_w} = 108$  kDa,  $\overline{M_n} = 78$  kDa,  $T_g = -60$  °C), PLCL 70:30 (Resomer® LC703S, Evonik, Essen, Germany, inherent viscosity = 1.3–1.8 dL/g,  $\overline{M_w} = 88$  kDa,  $\overline{M_n} = 59$  kDa,  $T_g = 32$ –42 °C) and PLLA (PL49, Corbion, Amsterdam, the Netherlands, inherent viscosity = 4.9 dL/g,  $\overline{M_w} = 338$  kDa,  $\overline{M_n} = 197$  kDa,  $T_g = 58$  °C). Weight and number average molecular weights were determined by us earlier [35]. Solvents for the electrospinning process—acetic acid (AA) (purity degree 99.5%), formic acid (FA) (purity degree ≥ 98%), and hexafluoroisopropanol (HFIP) (purity degree 98.5%)—were purchased from Poch (Gliwice, Poland), Sigma-Aldrich (St. Louis, MO, USA), and Iris Biotech GmbH (Marktredwitz, Germany), respectively. Ethylenediamine (purity degree 99.5%), isopropanol (purity degree 99.8%), ninhydrin (purity degree 99%), ethanol (purity degree 99.8%), and glutaraldehyde (conc. 25%) were purchased from Chempur (Piekary Śląskie, Poland). Gelatin (G1890, type A, gel strength ~300 g Bloom), BCA assay kit (QuantiPro™, for 0.5–30 µg/mL protein conc.), and formamide ( $\geq 99.5\%$  (GC), BioReagent, for molecular biology) were procured from Sigma-Aldrich (USA). Diiodomethane (99%+, stabilized) was purchased from Acros Organics (Geel, Belgium).

## *2.2. Preparation of Electrospun Fibers*

Three types of nonwovens were obtained using electrospinning equipment (Bioinicia, Spain) in horizontal mode. Polymer solutions (15% *w/w* solution of PCL in a mixed solution of acetic acid and formic acid at 9:1 ratio, 7% *w/w* PLCL solution in HFIP, and 3.5% *w/w* solution of PLLA in HFIP) were pumped through two stainless steel needles at a speed of 6 mL/h (3 mL/h per needle). Other process parameters were as follows: distance between needle and collector 15 cm, collector rotating speed 300 rpm, voltage applied to collector –2 kV, voltage applied to needles PCL 13–15 kV, PLCL 12–14 kV, PLLA 12–14 kV, temperature and humidity conditions PCL 24 °C, 40%, PLCL 38 °C, 40%, PLLA 24 °C, 40%, volumes of polymer solution used to obtain 12 × 31 cm<sup>2</sup> nonwoven PCL 13 mL, PLCL 18 mL, and PLLA 39 mL.

### *2.3. Chemical Immobilization of Gelatin*

Two sets of aminolysis conditions, mild and strong, were applied for each type of fibers to provide different concentrations of free NH<sub>2</sub> groups and investigate their correlation.

with the concentration of immobilized gelatin. Conditions and sample designations were chosen based on our previous study on the aminolysis of electrospun fibers [35] and are shown in Table 1.

**Table 1.** Studied samples and their aminolysis parameters.

| Sample Name  | Polymer | EDA/Isopropanol Conc [% w/v] | Time   | Temp [°C] | Concentration of NH <sub>2</sub> Groups [mol/mg] [35] |
|--------------|---------|------------------------------|--------|-----------|---|
| PCL_Phys     | PCL     | -                            | -      | -         | 0   |
| PCL_Chem_I   | PCL     | 10                           | 24 h   | 30        | $(3.18 \pm 0.31) \times 10^{-8}$                      |
| PCL_Chem_II  | PCL     | 30                           | 24 h   | 30        | $(1.69 \pm 0.19) \times 10^{-7}$                      |
| PLCL_Phys    | PLCL    | -                            | -      | -         | 0   |
| PLCL_Chem_I  | PLCL    | 2                            | 5 min  | 30        | $(1.42 \pm 0.08) \times 10^{-8}$                      |
| PLCL_Chem_II | PLCL    | 10                           | 10 min | 30        | $(1.65 \pm 0.15) \times 10^{-7}$                      |
| PLLA_Phys    | PLLA    | -                            | -      | -         | 0   |
| PLLA_Chem_I  | PLLA    | 2                            | 5 min  | 30        | $(1.36 \pm 0.13) \times 10^{-8}$                      |
| PLLA_Chem_II | PLLA    | 6                            | 10 min | 30        | $(1.75 \pm 0.22) \times 10^{-7}$                      |

Samples of  $5.5 \times 5.5 \text{ cm}^2$  size were immersed in 80 mL of a given solution of ethylenediamine (EDA) in isopropanol. The process was carried out in an orbital shaker-incubator. After aminolysis, samples were washed three times in deionized water. Aminolyzed samples were subjected to glutaraldehyde treatment in 1% w/v solution of the reagent in water (80 mL per sample) by 2.5 h at 25 °C. After that, they were washed three times in deionized water. Then, samples were immersed in a 0.2% w/v solution of gelatin in water (80 mL per sample). The process was conducted in an orbital shaker-incubator at 38 °C by 20 h. After this treatment, the samples were washed in deionized water at 38 °C for 24 h to remove weakly bound gelatin, and dried under a fume hood.

Unmodified samples were used as controls and are marked as Name-of-polymer\_Control.

Additionally, to examine gelatin concentration as a function of the concentration of free NH<sub>2</sub> groups, PLCL fibers were subjected to a wide range of aminolysis conditions. Three concentrations of EDA, 2, 6, and 10% (w/v), and four time points, 5, 10, 15, and 30 min, were applied. The temperature was set at 30 °C. The process of gelatin immobilization was the same as described above.

#### 2.4. Physisorption of Gelatin

In parallel to chemical immobilization, polymer samples were subjected to the physisorption of gelatin. Firstly, they were immersed in an isopropanol/water (50:50, v/v) solution for 0.5 h. Then, they were washed three times in water. After that, samples were immersed in a gelatin solution. Process parameters for gelatin immobilization were the same as in the case of chemically modified samples, including washing and drying procedures. Sample designations are presented in Table 1.

#### 2.5. Sample Imaging

Scanning electron microscopy (SEM, Jeol JSM-6010PLUS/LV InTouchScope™) was used for imaging the samples after modification. Before imaging, samples were coated with gold. The acceleration voltage was in the range of 7–10 kV.

#### 2.6. Gelatin Concentration on Fibers' Surface

The concentration of gelatin on fibers' surface was determined using BCA assay with BCA solution prepared according to producer recommendation. Three samples (1–1.3 mg) of each modified material were put into Eppendorf vials. 0.5 mL deionized water and

0.5 mL BCA solution were added. Samples were incubated for 2 h at 37 °C. To obtain a calibration curve, 0.5 mL gelatin solution (concentrations 5–30 µg/mL) was mixed with 0.5 mL BCA solution and incubated at the same conditions. The absorbance was read at 562 nm using a spectrophotometer (Thermo Fisher Scientific MultiskanGo, Waltham, MA, USA). Results were presented as the concentration of gelatin on the surface in µg/mg of fibrous sample.

### 2.7. Analysis of Chemical Structure—X-ray Photoelectron Spectroscopy

Five samples were chosen to be analyzed by X-ray photoelectron spectroscopy: PCL\_Control, PCL\_Chem\_I, PCL\_Chem\_II, PCL after stronger aminolysis corresponding to PCL\_Chem\_II reaction parameters (marked as PCL\_Am\_II), and a fibrous gelatin sample. The gelatin sample was prepared by electrospinning (parameters: 5% solution in HFIP, voltage applied to needle 10 kV, grounded collector, distance between needle and collector 15 cm, and solution flow rate 0.5 mL/h).

For XPS measurements using non-monochromatic Mg K<sub>α</sub> radiation (1253.6 eV), the samples were inserted into the spectrometer (SPECS GmbH, Berlin, Germany) without further treatment. The samples were studied under a vacuum of  $5 \times 10^{-8}$  mbar at room temperature. After measuring overview spectra of the samples at a constant analyzer pass energy ( $E_{\text{pass}}$ ) of 50 eV, individual 1s spectra of C, N, and O were recorded with higher resolution with  $E_{\text{pass}} = 13$  eV. This corresponds to a spectrometer resolution of 1.0 eV (FWHM of the Ag 3d<sub>5/2</sub> line). The electrostatic sample charging was corrected by setting the binding energy of C 1s electrons of aliphatic carbon to 285.0 eV. The XPS spectra were analyzed using the CasaXPS software package. The error of the binding energies is  $\pm 0.1$  eV. The error of relative intensities is about  $\pm 5\%$ .

### 2.8. pH Measurements

The pH was measured using a pH meter (CP-401, Elmetron, Zabrze, Poland) and electrode ERH-NS type (Elmetron, Poland). A 10 mL volume of 0.2% gelatin solution in distilled water was prepared in triplicate for measurement of pH change of blank solution and solutions with immersed PCL, PLCL, and PLLA samples. The sample size corresponded to the sample/solution ratio used in the immobilization process. For each solution, pH was measured before immersion of the sample and after 20 h of sample incubation at 38 °C.

### 2.9. Wettability

Wettability was determined using a goniometer (Data Physics OCA 15EC, Filderstadt, Germany). Waterdrop dosing volume and dosing rate were equal to 1 µL/s and 2 µL/s, respectively. Due to the complete wettability of samples, the time of waterdrop absorption was measured. Measurements were repeated 5 times for each sample.

### 2.10. Surface Free Energy

Total surface free energy and its components were calculated for polymer films. Films were obtained by solvent casting technique from the same solutions as in the case of the electrospinning process. Contact angles were measured using three liquids: distilled water, formamide, and diiodomethane. Measurements were repeated 5 times. Surface free energy was calculated using SCA20 (v.5.0.10, DataPhysics Instruments GmbH, Filderstadt, Germany) software with the Owens, Wendt, Rabel and Kaelble (OWRK) model.

### 2.11. Mechanical Testing

A uniaxial testing machine, Lloyd EZ-50 (USA), was used to determine Young's modulus, stress at break, and strain at break. Three samples ( $5 \times 40$  mm<sup>2</sup>, testing area  $5 \times 20$  mm<sup>2</sup>) for each type of material were tested. The machine was equipped with handles for thin and delicate samples with a 50 N load cell. Cross-head speed was set at 5 mm/min. The thickness of each sample was measured with a thickness gauge.

## 2.12. Stability of Gelatin Coating

Stability of the gelatin layer on the fiber surface was tested up to 90 days by incubation in phosphate-buffered saline (PBS). Taking into consideration that polymer degradation can strongly affect measurements, PCL fibers, having the longest degradation time, were chosen for the test. It was presented previously that PCL fibers do not lose their mass during 90-day immersion in PBS solution [36]. The samples were additionally weighted showing no weight loss during the incubation test. Three samples of PCL per time point were tested. Samples were immersed in 10 mL of the PBS solution with the addition of sodium azide (0.1% *w/v*) inhibiting bacteria growth. Samples were incubated at 37 °C and shaken once every few days. The stability of the gelatin layer was evaluated on the basis of gelatin concentration measurements using a BCA assay. The BCA test was conducted according to the procedure described above.

## 2.13. Cell–Scaffold Interaction

Mouse fibroblast cells (L929, Sigma Aldrich) were used to evaluate cell response. Dulbecco's modified Eagle's medium (DMEM, Thermo Fisher Scientific) was supplemented with fetal bovine serum (FBS, Thermo Fisher Scientific) to a concentration of 10% *v/v* and penicillin–streptomycin (Thermo Fisher Scientific) to a concentration of 1% *v/v*.

Samples were sterilized by immersion in 70% solution of ethanol in water and 30 min exposure to UV light on each side. Then, they were placed in a 48-well culture plate—three samples for the cell metabolic activity test and two samples for SEM observation for each type of material. A total of  $2 \times 10^3$  cells were seeded per well. Cell culture was performed in an incubator at 37 °C in 5% CO<sub>2</sub> for 3 and 5 days.

PrestoBlue™ (Thermo Fisher Scientific) test was used to investigate cell metabolic activity. The culture medium was removed, and each sample was rinsed with PBS (Thermo Fisher Scientific). Then, 180 µL of PBS and 20 µL of PrestoBlue reagent in the PBS solution were added to each well. PrestoBlue reagent was also added to pure PBS as a control. The plate with samples was put into an incubator for 40 min to enable reaction. After this time, 100 µL of each solution was transferred to a 96-well plate. The emission of light was measured using Fluoroskan Ascent (Thermo Scientific) at an excitation light wavelength of 530 nm and emission light wavelength of 620 nm. Results were calculated to percentage metabolic activity using tissue culture polystyrene as a 100% control.

Samples used for SEM observation were gently rinsed with PBS twice and then fixed with 2.5% glutaraldehyde/PBS overnight. Dehydration was performed using ethanol in water solution series (30, 40, 50, 60, 70, 80, 90, 100 ( $\times 2$ )% *v/v*), hexamethyldisilazane (HDMS, Sigma Aldrich)/ethanol solutions (1:2 and 2:1 *v/v*), and pure HDMS. Each ethanol solution was removed after 20 minutes, and HDMS was left overnight. All samples were imaged in comparison to TCP (Tissue Culture Plastic) using scanning electron microscopy (SEM, Jeol JSM-6010PLUS/LV InTouchScope™). Before imaging, samples were coated with gold. The acceleration voltage was in the range of 8–10 kV.

Fluorescence microscopy (FM) imaging was performed after immunohistochemical staining. Cells were rinsed with PBS, fixed in 4% paraformaldehyde, kept in 0.1% Triton-X for 5 min, and rinsed again with PBS. The actin skeleton and nucleus were stained with ActinGreen™ and NucBlue™ Reagent (Thermo Scientific), respectively. All samples and TCP were imaged using a fluorescent microscope (Leica DMI3000B, Leica Microsystems, Wetzlar, Germany).

## 2.14. Statistical Analysis

Dependent sample *t*-test and Wilcoxon test were performed on pH data. One-way analysis of variance (ANOVA) followed by NIR post hoc test was performed on stress and strain at break, and metabolic activity data using Statistica (v.13, Tibco Software Inc., Palo Alto, CA, USA) software. Significance was set at *p* < 0.05.

### 3. Results and Discussion

#### 3.1. Fiber Morphology

As shown in Figure 1, the process of gelatin immobilization either by physical adsorption or covalent conjugation did not result in a change in fiber morphology. It is well known that aminolysis can cause fiber cracking and fragmentation; however, on the basis of our previous study on aminolysis, conditions that maintain fiber morphology were carefully chosen [35]. It was also observed that glutaraldehyde activation and gelatin immobilization did not affect fiber morphology. The only exception is a PLCL\_Chem\_II sample, for which morphology change—single fiber breaking in some regions of the sample was recognized. It is the effect of the aminolysis reaction and mechanical stress during further treatment. In Figure 2, histograms of fiber diameter for control samples are shown. PCL and PLCL have a bimodal distribution of fiber diameter, and in the case of PLLA, the distribution is trimodal. It is evident that the low diameter fraction of the histogram dominates over the high diameter fraction for PCL with its most probable value around 600 nm. This is the opposite of the situation observed for PLLA with a large fraction of high fiber diameter. This difference in distributions implies a difference in specific surface area, which can affect the amount of immobilized gelatin.

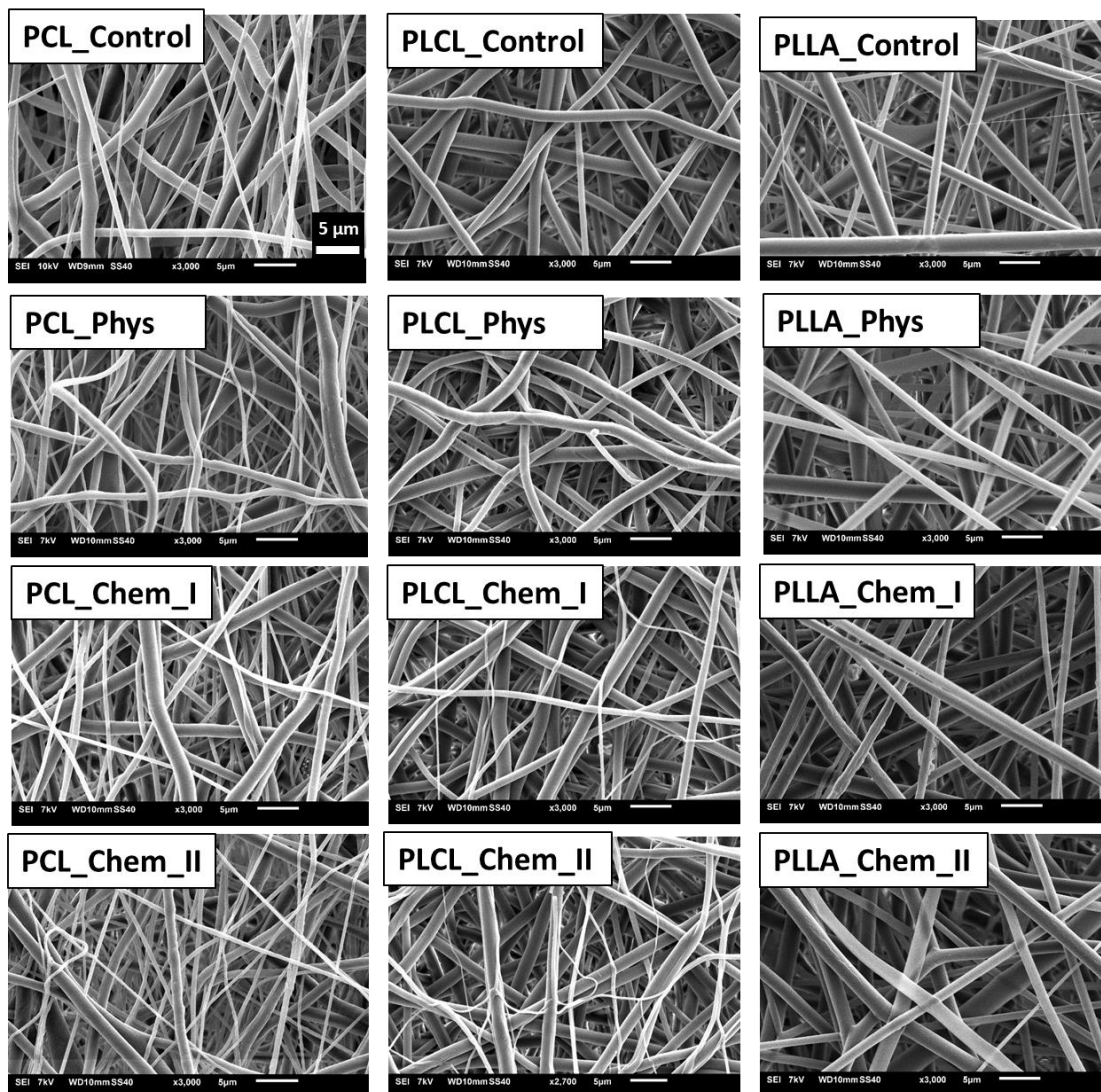


**Figure 1.** Morphology of controls and samples subjected to physisorption and chemical immobilization of gelatin.

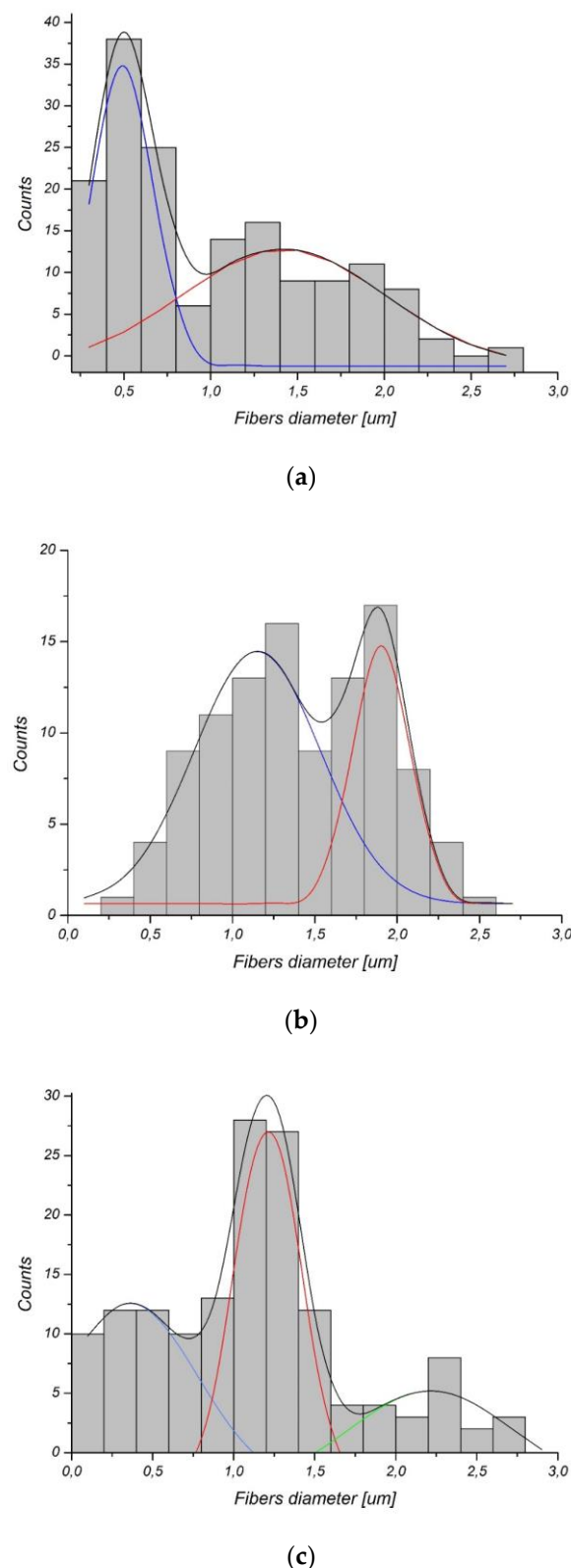


**Figure 2.** Fiber diameter histograms of (a) PCL, (b) PLCL, (c) PLLA.

### 3.2. Detection of Gelatin on Fiber Surface

Figure 3a presents the concentration of gelatin as a function of free NH<sub>2</sub> groups. The first observation is that despite similar concentrations of NH<sub>2</sub> groups, gelatin concentrations vary widely between polymers, being the highest for PCL and the lowest for PLCL.

Moreover, it is seen that the difference in gelatin concentration between polymers starts at zero of amine groups (physical adsorption). This fact together with the highest slope of the PCL curve indicates the easiest immobilization of gelatin, both physical and chemical on this polymer. This relatively high physical adsorption is consistent with previous observations by B. Atthoff, J. Hilborn who showed that spontaneous hydrolysis of degradable aliphatic polyesters surface in aqueous media is sufficient for protein adsorption [37]. The unexpectedly high physisorption of gelatin is most probably a result of various molecular interactions, including ionic and hydrophobic interactions as well as interactions with carboxyl and hydroxyl groups created on the polyester surface by spontaneous hydrolysis in an aqueous medium during gelatin immobilization. The fundamental explanation of the interactions involved in protein adsorption is included in the review of J. D. Andrade and V. Hlady [38]. Considering the simplicity of physical adsorption, this type of modification could be very attractive. On the other hand, physical adsorption could be not stable or reversible, which is confirmed by our results, presented in the following part of our study.

The pH of gelatin solution during immobilization was measured to exclude the impact of pH change due to possible polymer degradation on subsequent difference in gelatin adsorption. As shown on the Figure S1 there is no significant difference in pH before and after immobilization.

Surface energy was measured additionally for polymer films as shown in Table 2. In fact, the polar component is the lowest for PCL film, and it is observed by other authors that protein adsorption is higher on more hydrophobic surfaces [39,40]. However, it has to be taken into consideration that factors such as micro/nanoroughness, and differences in fiber diameter distribution can also influence the concentration of immobilized gelatin.

Irrespective of the highest content of immobilized gelatin on PCL due to the highest sensitivity to both physical and chemical sorption, one should be aware that the first step of modification, aminolysis, needs much more time in the case of PCL compared to PLCL and PLLA (Table 1). It can be explained by a combination of several factors—the differences in ester bond density, glass transition temperature, and crystallinity (surface crystallinity) among investigated polymers [41].

A more detailed analysis of the effect of amine groups concentration on gelatin immobilization was performed for PLCL (Figure 3b). Results support the previous observation that there is an increase of immobilized gelatin concentration with the concentration of amine groups. However, contrary to the main rising trend, there is a systematic, rather small reduction of immobilized gelatin concentration with amine concentration below  $5 \times 10^{-8}$  mol/mg of amine groups. It should be noted that most of the immobilized gelatin in the range of such small amine concentrations is due to physical adsorption, so the observed local reduction of immobilized gelatin with increasing amine concentration in this concentration range indicates some mechanisms from the side of aminolysis, which leads to reduction of the physically adsorbed layer. This observation is unexpected and needs further investigation.

Table 3 shows atomic percentages for PCL samples before modification, after aminolysis, after physical and chemical modification with gelatin, and for gelatin calculated from XPS analysis. Oxygen and carbon concentrations (atom %) for the PCL control sample agree within the experimental uncertainties with the expected stoichiometric values, which are 25% and 75%, respectively. For aminated samples, there is no evidence of N 1s peak from nitrogen, indicating that its concentration is below the detection limit of XPS. However, the introduction of NH<sub>2</sub> groups was confirmed by the ninhydrin test. The presence of nitrogen was detected in the case of PCL samples with physisorbed and chemically bound gelatin. Atomic concentrations of nitrogen are 5% for PCL\_Phys and 8% for PCL\_Chem\_II. This correlation clearly corresponds to the results obtained from the BCA test. Nitrogen concentration for the control sample of electrospun gelatin is equal to 16%, which indicates that the gelatin layer is thinner than 10 nm (depth of XPS analysis) for both PCL samples. The decomposition of C 1s and O 1s peaks is shown in Table 4. The calculated percentage of bonds for the PCL\_Control sample corresponds to the data obtained by other

authors [42,43]. Aminolysis did not change the initial contribution of bonds. In the case of samples coated with gelatin, it is evident that the contribution of bonds changes towards values adequate for the gelatin control sample. XPS spectra of studied samples are shown on Figure 4.

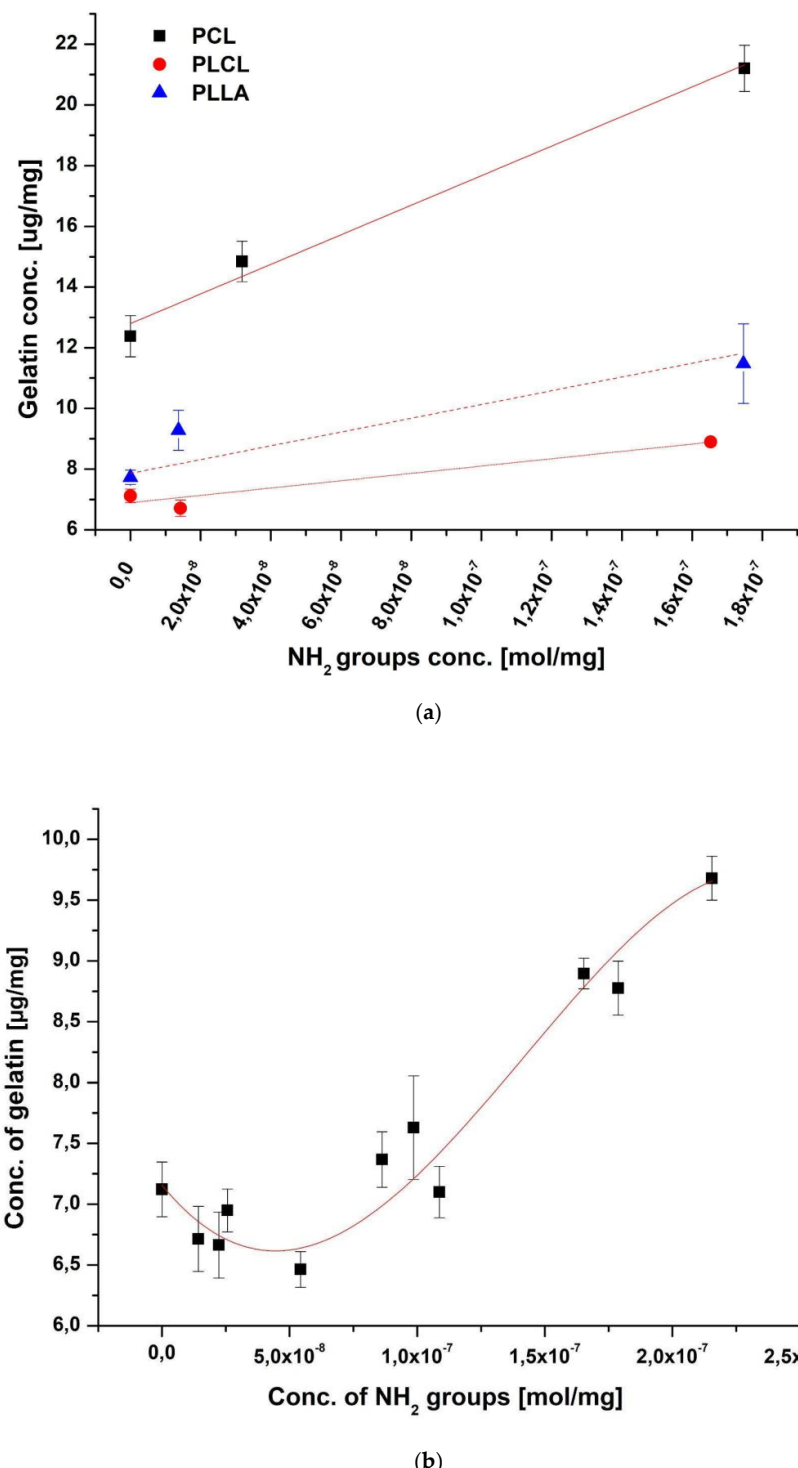


**Figure 3.** Concentrations of gelatin on the surface of the fibers as a function of free  $\text{NH}_2$  groups concentration for (a) all investigated polymers (the subsequent amine concentration points on X-axis correspond to physical adsorption, mild chemical and strong chemical immobilization) and (b) PLCL fibers.

**Table 2.** Surface free energies and their components for control samples.

|      | Dispersive Component [mN/m] | Polar Component [mN/m] | Surface Free Energy [mN/m] |
|------|-----------------------------|------------------------|----------------------------|
| PCL  | 38.25 ± 4.8                 | 0.98 ± 0.80            | 39.24 ± 4.13               |
| PLCL | 31.96 ± 1.83                | 6.98 ± 1.23            | 38.94 ± 0.93               |
| PLLA | 35.94 ± 3.75                | 4.61 ± 0.90            | 40.54 ± 3.14               |

**Table 3.** Atomic concentrations (atom-%) of oxygen, carbon and nitrogen for PCL and gelatin samples.

|   | O    | C      | N    |
|---|------|--------|------|
| PCL_Control   | 22   | 78     | 0    |
| C <sub>6</sub> H <sub>10</sub> O <sub>2</sub>                     | 25   | 75     | 0    |
| PCL (Kołbuk et al.) [44]  | 24.9 | 75.1 * | 0    |
| PCL_Am_II   | 23   | 77     | 0    |
| PCL_Phys  | 22   | 73     | 5    |
| PCL_Chem_II   | 22   | 70     | 8    |
| Gelatin   | 19   | 65     | 16   |
| C <sub>102</sub> H <sub>151</sub> O <sub>39</sub> N <sub>31</sub> | 23   | 59     | 18   |
| Gelatin (Kołbuk et al.) [44]                                      | 18.9 | 65.2 * | 15.9 |
| Gelatin (Jalaja et al.) [45]                                      | 21.5 | 67.0   | 11.5 |

\* calculated as the difference from O% and N%.

**Table 4.** Relative concentrations of functional groups for PCL and gelatin samples.

|             | C 1s   |                                     | N 1s                  |                                    | O 1s                  |                       |
|-------------|--|-------------------------------------|-----------------------|------------------------------------|-----------------------|-----------------------|
|             | C-CH <sub>x</sub> R <sub>y</sub> <sup>b</sup><br>285.0 eV <sup>a</sup> | C-OR <sup>b</sup><br>286.2–286.5 eV | C=O<br>288.1–288.9 eV | -NH <sub>2</sub><br>399.8–400.0 eV | O=R<br>531.6–532.2 eV | O-R<br>533.2–533.6 eV |
| PCL_Control | 73   | 14                                  | 13                    | -                                  | 56                    | 44                    |
| PCL_Am_II   | 69   | 16                                  | 15                    | -                                  | 53                    | 47                    |
| PCL_Phys    | 67   | 19                                  | 15                    | 100                                | 61                    | 39                    |
| PCL_Chem_II | 63   | 21                                  | 16                    | 100                                | 67                    | 33                    |
| Gelatin     | 49   | 28                                  | 23                    | 100                                | 100                   | -                     |

<sup>a</sup> This C 1s component was used to correct for electrostatic sample charging. <sup>b</sup> Hydrocarbon group.

### 3.3. Wettability

Our analysis of wettability clearly indicates that all samples with immobilized gelatin were completely wettable, contrary to the hydrophobic character of control polymer scaffolds. Water contact angles were equal to 135.69 ± 3.02°, 131.05 ± 1.66°, and 132.90 ± 2.48° for PCL, PLCL, and PLLA, respectively, as shown in our previous study [35]. In order to compare the wettability of gelatin-coated samples, the time of waterdrop absorption was measured (Figure 5). Increase of sample wettability after surface modification origins from exposed hydrophilic groups of immobilized protein. For polymer films coated with proteins, rather a decrease of water contact angle than a complete wettability is observed [46–48]. Complete wettability after protein immobilization is reported for non-wovens and appears to be additionally associated with the capillary effect of fibrous architecture [49]. It is worth noting that water absorption ability is important for nutrition transport through the scaffold [50]. It can also accelerate the hydrolytic degradation of the scaffold [51].

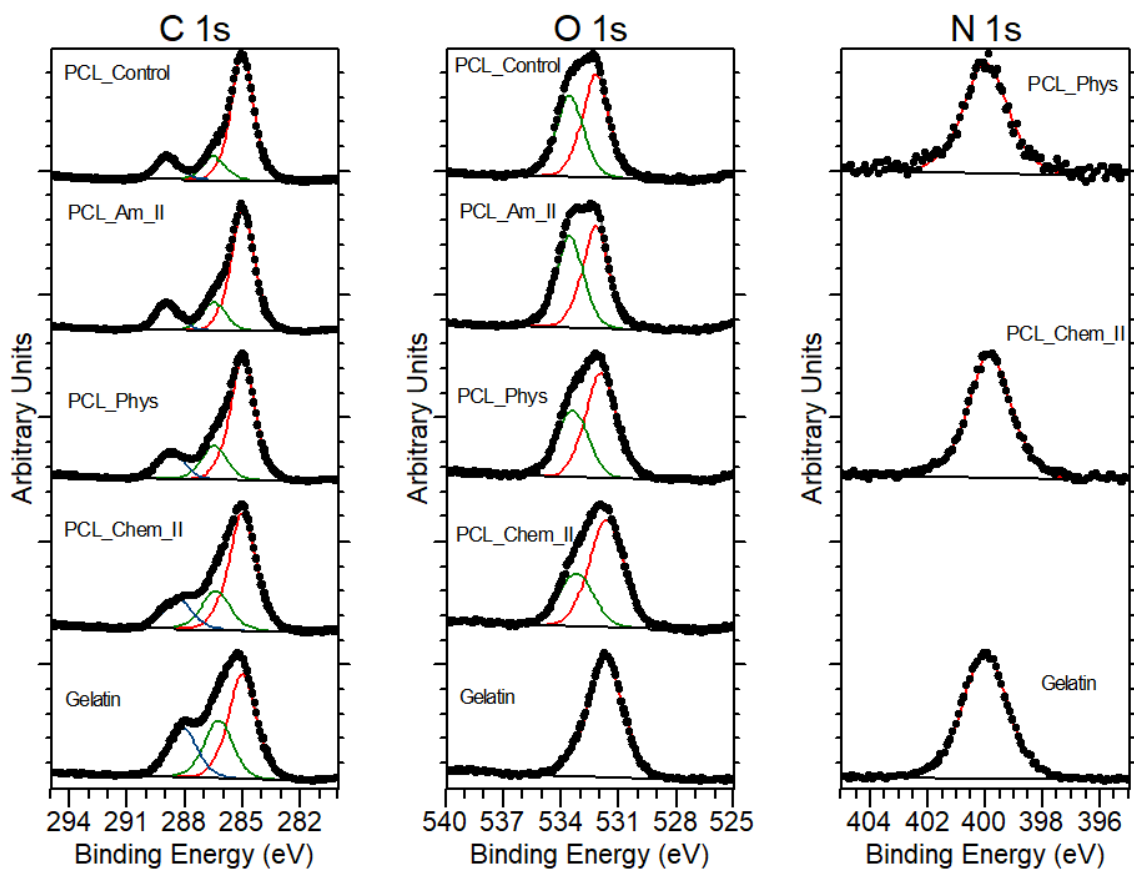


**Figure 4.** XPS spectra of PCL\_Control, PCL\_Am\_II, PCL\_Phys, PCL\_Chem\_II and gelatin.

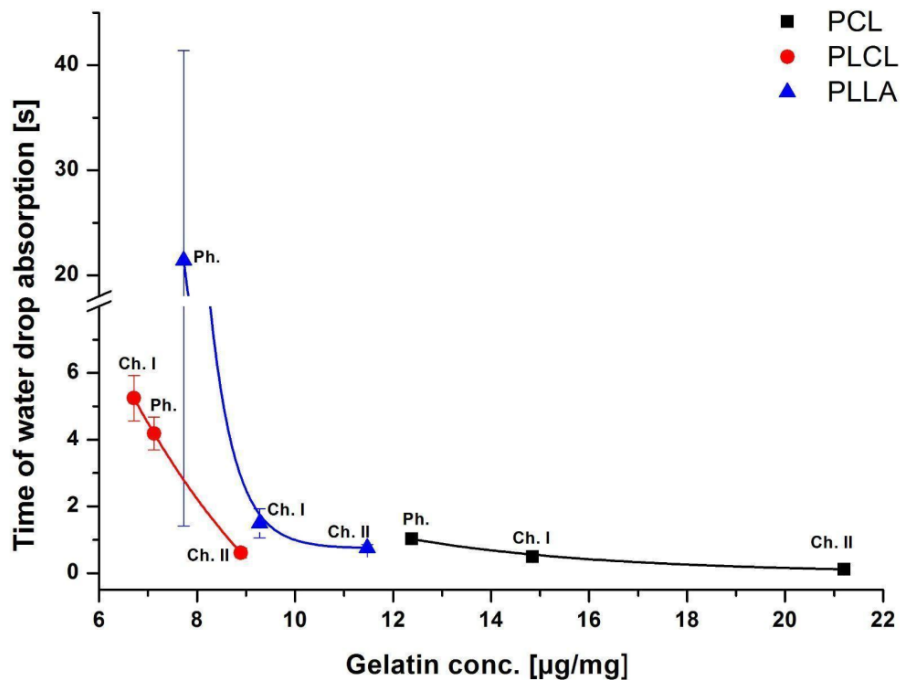


**Figure 5.** Time of waterdrop absorption as a function of gelatin concentration for physically (Ph.) and chemically (Ch. I; Ch. II) modified samples.

From our results, it is clear that for all polymers the time of absorption is correlated with the concentration of gelatin on fibers' surface being the lower the higher the gelatin concentration. In the case of PCL samples, with the highest concentrations of gelatin among all studied fibers, there was only a slight difference in time of absorption. A wide range of the absorption time values for PLLA\_Phys suggests that the physisorbed layer of gelatin could be inhomogeneously distributed on fibers, in contrast to the chemically bound coating. However, there was no such observation for PLCL or PCL fibers. Inhomogeneity of physisorbed coatings was reported previously by others [42].

#### 3.4. Mechanical Properties

Stress at break and strain at break of all samples before and after modifications were shown in Figure 6, and representative stress–strain profiles are presented in Figure S2. Only a slight decrease or no change in stress at break was observed for physisorbed and mildly chemically modified samples. A slight decrease for physically modified samples is most probably related to a slightly elevated temperature during gelatin immobilization (38 °C). For all polymers, a more significant decrease was identified in the case of a stronger chemical modification, especially for PLCL\_Chem\_II. Stress at break is clearly affected by aminolysis reaction, as discussed in our previous work [41].

Similar correlation was observed in the case of a strain at break. Only a slight decrease or no change in the strain at break was observed in the case of all samples with physisorbed gelatin or those that were mildly modified via aminolysis. The high decrease was identified for more aggressively treated samples, especially for PLCL\_Chem\_II and PLLA\_Chem\_II. It is worth noting that all PCL samples indicated a relatively low decrease in stress and strain at break.

It should be also emphasized that for all studied nonwovens, conditions that were applied in the case of mild aminolysis, enable for maintaining mechanical properties on a similar level as in the case of physisorption. Considering results for samples after stronger chemical modification, it has to be taken into account that aminolysis is also applied to obtain fragmented fibers that can be then modified with proteins and immersed in hydrogels to mimic the extracellular matrix [52,53]. In this application, their mechanical properties are not as important as in the case of fibrous scaffolds. In the case of Young's modulus, there was no common correlation between values of modulus and type of modification. In the literature, there are contradictory observations of aminolysis impact on Young's modulus [54,55].

#### 3.5. Coating Stability

An important feature that can determine the applicability of a given modification is the stability of the coating. The stability of the gelatin layer on the PCL samples after incubation in PBS solution is shown in Figure 7. For physically and strongly chemically modified samples, the most significant loss was observed up to 14 days of incubation. Then, the concentration of gelatin is stable, even after 90 days. The highest loss is observed for the sample with physisorbed gelatin approaching almost 37% after 14 days of incubation. This loss is much lower for chemically modified samples, particularly for PCL\_Chem\_I, for which 2.4% loss was noticed on the 14th day. In the case of PCL\_Chem\_II, the loss of gelatin was equal to 16.9% at this time point. It is highly probable that major loss of gelatin from the surface of chemically modified fibers originates from physisorbed gelatin. It is worth noting that there was no weight loss of PCL samples during the incubation test, which could disturb the measurements.

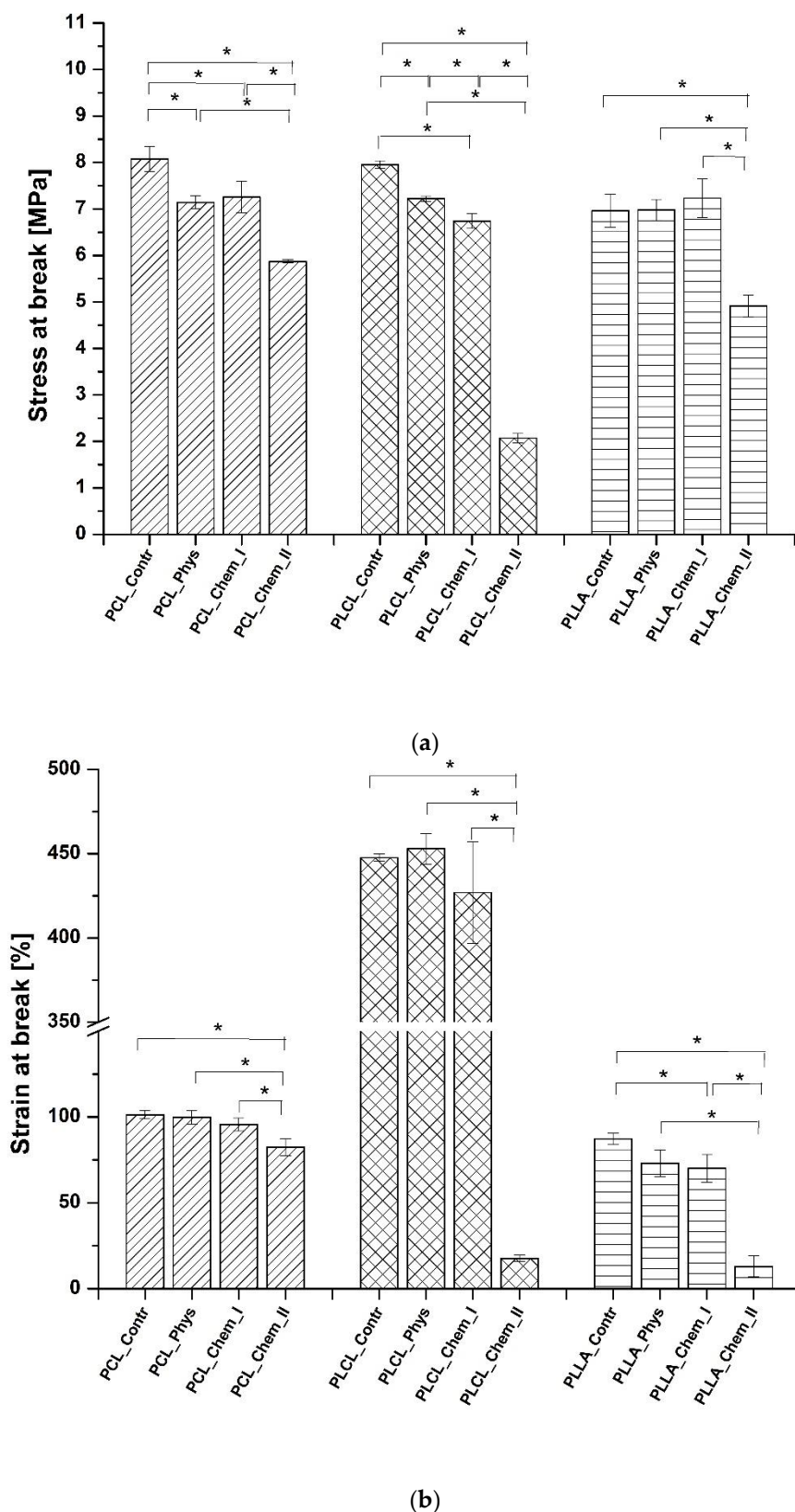


**Figure 6.** Mechanical properties: (a) stress at break, and (b) strain at break of control and gelatin-coated fibers. Statistically significant differences were marked as \* ( $p < 0.05$ ).

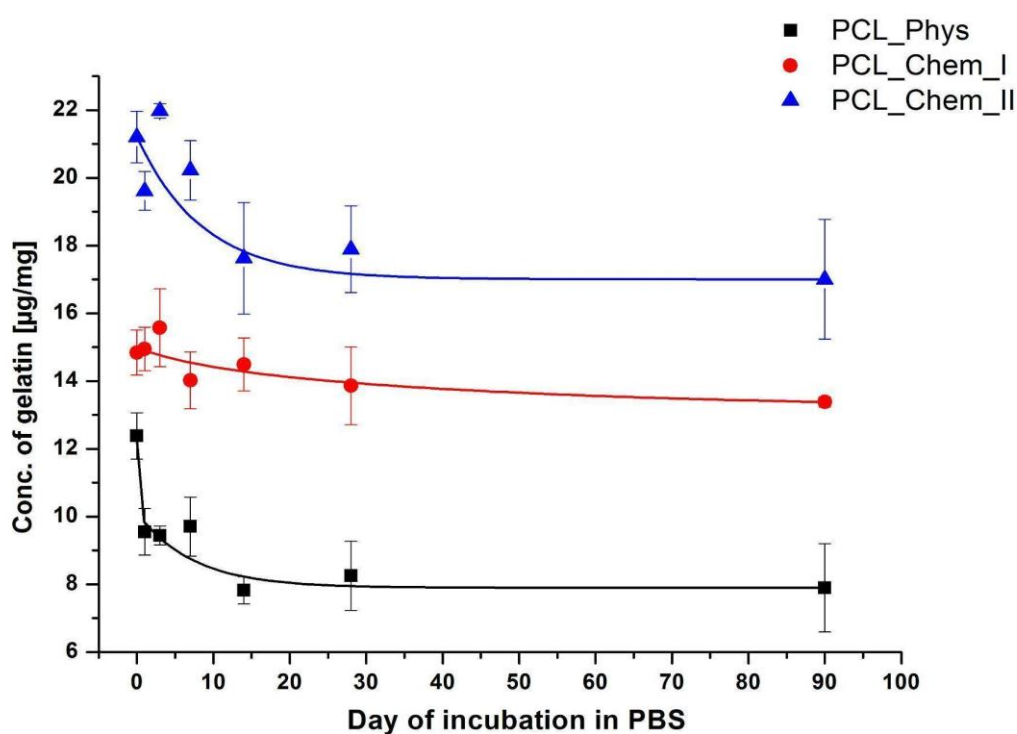


**Figure 7.** Concentration of gelatin on the PCL fibers as a function of incubation time in PBS for various time points (0; 1; 3; 7; 14; 28; 90 days).

Interestingly, even after 90 days of incubation, the gelatin layer was still present on the surface of the physically modified sample (more than 60% of initial gelatin concentration), which shows how strong are physical interactions between gelatin and polymer. In the literature, lower stability of coating is frequently pointed out as a drawback of using physisorption for protein immobilization [7]. Our results indicate saturation of desorption process after certain time. However, it may be different in *in vivo* conditions. Protein adsorption and desorption are complex processes and the mechanisms are still not completely understood [56,57]. Thus, in our opinion, coating stability should be always considered from the perspective of given biomolecule, substrate, and the application site.

### 3.6. Biological Evaluation

The morphology of L929 cells imaged with scanning electron microscopy is presented in Figure 8. For all samples, improvement of morphology after gelatin immobilization was noticed. On the control samples, rounded and not spread cells are present. In the case of both physically and chemically coated samples, expansion of cells is observed, which indicates better interaction of L929 cells with materials. In the case of PCL and PLCL, the best morphology, characterized by stretched filopodia, was observed after stronger chemical modification. For PLLA, there is no significant difference between modified samples. Fluorescence microscopy confirmed the previous observation (Figure 9). Actin spreading proves improvement of cell–material interaction after gelatin immobilization. There is also improvement in cell metabolic activity after gelatin immobilization, especially after 5 days of culture (Figure 10). Gradual increase is particularly observed for PCL samples. In addition, for PLLA\_Chem\_II enhancement of metabolic activity was observed. This increase can result from simply a higher concentration of gelatin, and/or better gelatin conformation in the case of chemically modified samples [58]. It is also worth noting that initial metabolic activity for PLCL was higher than for PCL and PLLA controls, thus the effect of gelatin immobilization could be not so significant for PLCL.

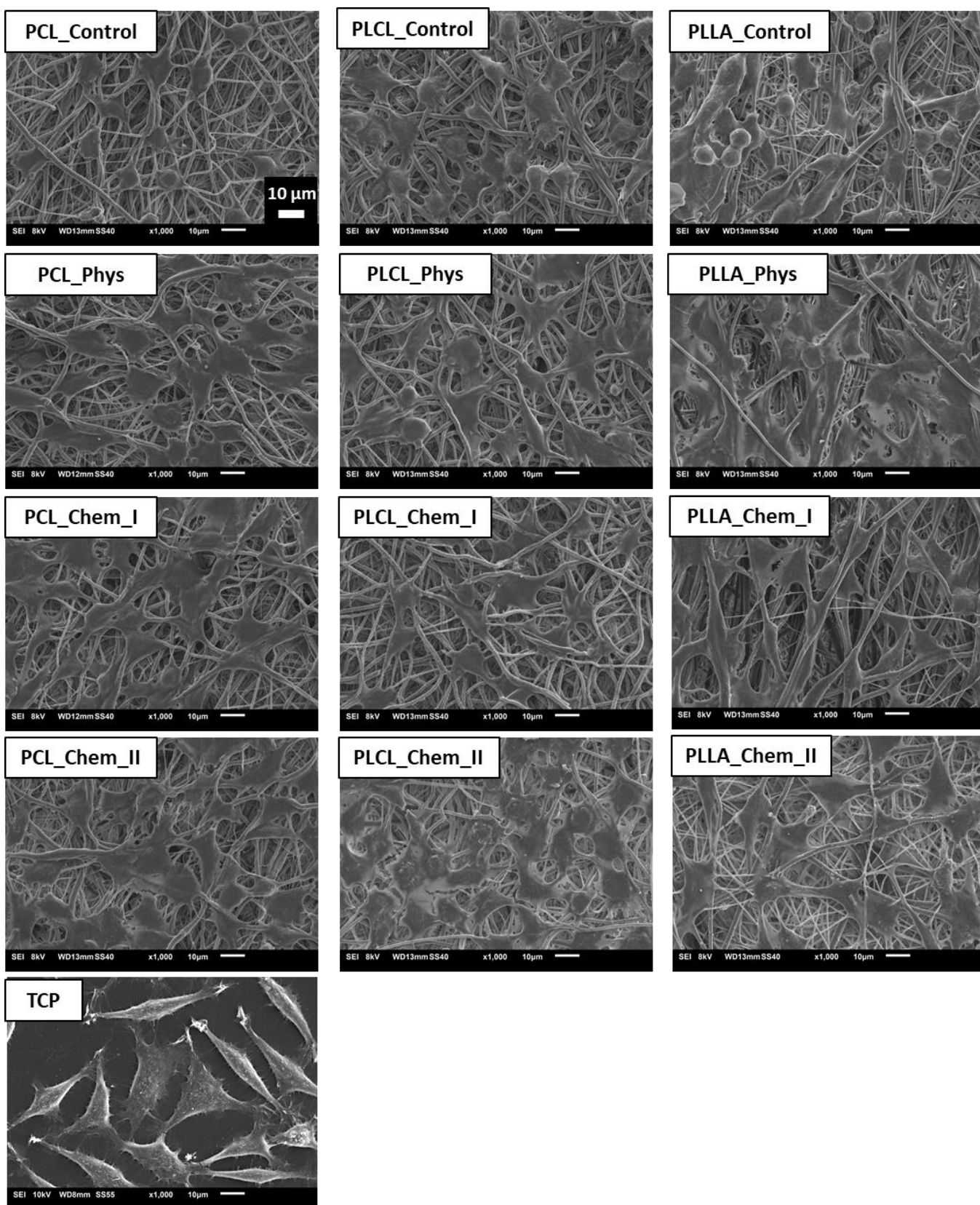


**Figure 8.** L929 cells cultured for 5 days on control and gelatin-coated samples observed with scanning electron microscopy.

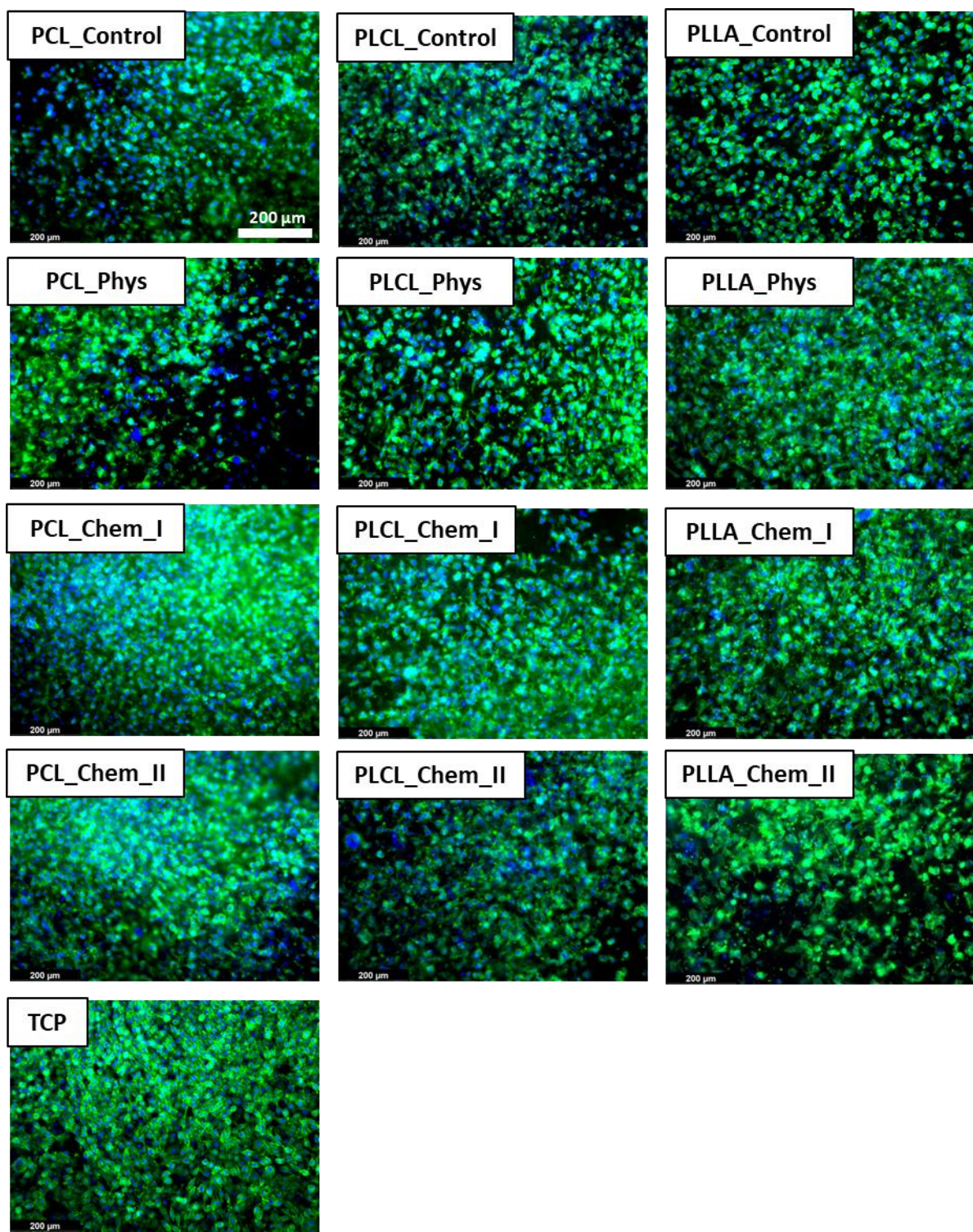
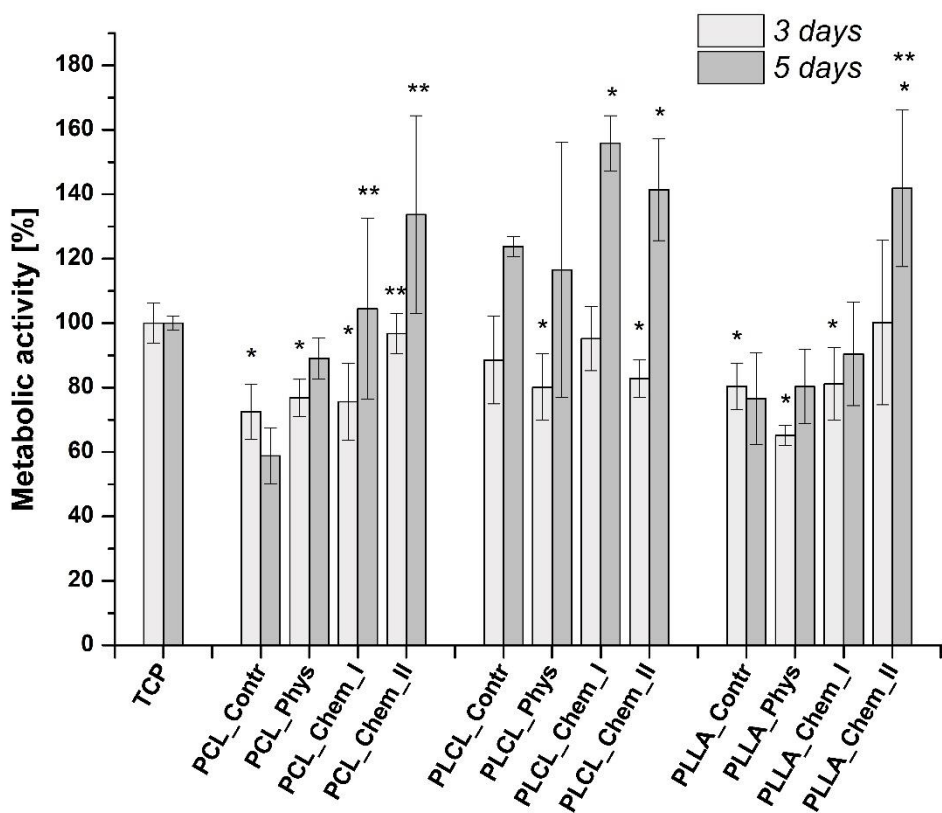


**Figure 9.** L929 cells cultured on control and gelatin-coated samples for 5 days observed with fluorescence microscopy.



\* - significant difference between TCP and given sample, ( $p < 0.05$ ), \*\* - significant difference between polymer control and given samples ( $p < 0.05$ )

**Figure 10.** Viability of L929 cells cultured on control and gelatin-coated samples.

#### 4. Conclusions

In this study, two types of modification—physisorption and chemical immobilization—of gelatin were compared for PCL, PLCL, and PLLA electrospun nonwovens. It was shown on the basis of the BCA test and the XPS analysis that chemical immobilization could provide a higher concentration of gelatin on the fiber surface. However, physisorption provides a relatively high concentration of gelatin, especially in comparison to samples subjected to mild chemical immobilization. On the basis of XPS results, the thickness of both physically and chemically bound gelatin layers was estimated to be less than 10 nm. Initially, hydrophobic samples were completely wettable after each type of modification and the time of waterdrop absorption was correlated with the gelatin concentration. Mild chemical immobilization did not change significantly mechanical properties of samples, likewise physisorption. Aminolysis conditions that were applied to provide a higher concentration of free amine groups result in a significant decrease of stress and strain at break in the case of PLCL and PLLA samples. Thus, modification method should be chosen depending on the application site and taking into account its impact on mechanical performance. It is worth emphasizing that PCL samples were much more resistant to loss of mechanical toughness than PLCL and PLLA samples. Incubation tests showed that chemically immobilized gelatin layer is more stable than physisorbed; however, for physically modified surfaces only partial desorption was observed, even after 90 days of immersion in PBS. L929 cell imaging and the results of metabolic activity test indicate a positive effect of both physical and chemical modification on cell–scaffold interaction with the better cell response on chemically modified samples, which could result from simply a higher concentration of gelatin, or better gelatin conformation. However, there is a difference in the intensity of the effect of gelatin coating on cell response between all

studied polymers. The clearest trend of improvement was observed in the case of PCL fibers. Thus, in our opinion, the immobilization method should be always considered from the perspective of given biomolecule, substrate, and type of application.

**Supplementary Materials:** The following supporting information can be downloaded at: <https://www.mdpi.com/article/10.3390/polym14194154/s1>, Figure S1. pH of the gelatin solutions before and after immersion of the polymer samples; Figure S2. Exemplary stress-strain profiles of (a) PCL, (b) PLCL, (c) PLLA.

**Author Contributions:** Conceptualization, P.S., O.J. and D.K.; methodology, O.J., D.K. and T.R.; software, O.J., D.K. and T.R.; validation, O.J., D.K., T.R. and P.S.; formal analysis, O.J., D.K., T.R. and P.S.; investigation, O.J., D.K. and T.R.; resources, P.S., O.J., D.K. and T.R.; data curation, P.S.; writing—original draft preparation, O.J., D.K., T.R. and P.S.; writing—review and editing, P.S., D.K. and T.R.; visualization, O.J., D.K. and T.R.; supervision, P.S. and D.K.; project administration, P.S.; funding acquisition, P.S. All authors have read and agreed to the published version of the manuscript.

**Funding:** This research was funded by the Polish National Science Center (NCN), grant 2016/23/B/S/T8/03409.

**Institutional Review Board Statement:** Not applicable.

**Data Availability Statement:** The raw/processed data required to reproduce these findings cannot be shared at this time due to technical or time limitations.

**Acknowledgments:** We thank the Polish National Science Center (NCN) for the funding of this research (grant 2016/23/B/S/T8/03409). We thank Jürgen Hübner (Johannes Gutenberg University Mainz) for his support during the XPS measurements.

**Conflicts of Interest:** The authors declare no conflict of interest.

## References

1. Gao, J.; Yu, X.; Wang, X.; He, Y.; Ding, J. Biomaterial–Related Cell Microenvironment in Tissue Engineering and Regenerative Medicine. *Engineering* **2022**, *13*, 31–45. [[CrossRef](#)]
2. Grafahrend, D.; Heffels, K.H.; Beer, M.V.; Gasteier, P.; Möller, M.; Boehm, G.; Dalton, P.D.; Groll, J. Degradable Polyester Scaffolds with Controlled Surface Chemistry Combining Minimal Protein Adsorption with Specific Bioactivation. *Nat. Mater.* **2011**, *10*, 67–73. [[CrossRef](#)] [[PubMed](#)]
3. Cao, B.; Peng, Y.; Liu, X.; Ding, J. Effects of Functional Groups of Materials on Nonspecific Adhesion and Chondrogenic Induction of Mesenchymal Stem Cells on Free and Micropatterned Surfaces. *ACS Appl. Mater. Interfaces* **2017**, *9*, 23574–23585. [[CrossRef](#)] [[PubMed](#)]
4. Chang, H.-I.; Wang, Y. Cell Responses to Surface and Architecture of Tissue Engineering Scaffolds. In *Regenerative Medicine and Tissue Engineering—Cells and Biomaterials*; Eberli, D., Ed.; Intech Open: Rijeka, Croatia, 2011.
5. Vohrer, U. Interfacial Engineering of Functional Textiles for Biomedical Applications. In *Plasma Technologies for Textiles: A Volume in Woodhead Publishing Series in Textiles*; Shishoo, R., Ed.; Woodhead Publishing: Cambridge, UK, 2007; pp. 202–227.
6. Kołbuk, D.; Ciechomska, M.; Jeznach, O.; Sajkiewicz, P. Effect of Crystallinity and Related Surface Properties on Gene Expression of Primary Fibroblasts. *RSC Adv.* **2022**, *12*, 4016–4028. [[CrossRef](#)]
7. Biazar, E.; Kamalvand, M.; Avani, F. Recent Advances in Surface Modification of Biopolymeric Nanofibrous Scaffolds. *Int. J. Polym. Mater. Polym. Biomater.* **2022**, *71*, 493–512. [[CrossRef](#)]
8. Hasturk, O.; Jordan, K.E.; Choi, J.; Kaplan, D.L. Enzymatically Crosslinked Silk and Silk–Gelatin Hydrogels with Tunable Gelation Kinetics, Mechanical Properties and Bioactivity for Cell Culture and Encapsulation. *Biomaterials* **2020**, *232*, 119720. [[CrossRef](#)]
9. Kołbuk, D.; Heljak, M.; Choińska, E.; Urbanek, O. Novel 3D Hybrid Nanofiber Scaffolds for Bone Regeneration. *Polymers* **2020**, *12*, 544. [[CrossRef](#)]
10. Bačáková, L.; Filová, E.; Rypáček, F.; Švorčík, V.; Starý, V. Cell Adhesion on Artificial Materials for Tissue Engineering. *Physiol. Res.* **2004**, *53*, S35–S45.
11. Davidenko, N.; Schuster, C.F.; Bax, D.V.; Farndale, R.W.; Hamaia, S.; Best, S.M.; Cameron, R.E. Evaluation of Cell Binding to Collagen and Gelatin: A Study of the Effect of 2D and 3D Architecture and Surface Chemistry. *J. Mater. Sci. Mater. Med.* **2016**, *27*, 1–14. [[CrossRef](#)]
12. Le, P.; Mai-Thi, H.N.; Stoldt, V.R.; Tran, N.Q.; Huynh, K. Morphological Dependent Effect of Cell-Free Formed Supramolecular Fibronectin on Cellular Activities. *Biol. Chem.* **2021**, *402*, 155–165. [[CrossRef](#)]
13. Lino, R.L.B.; dos Santos, P.K.; Pisani, G.F.D.; Altei, W.F.; Cominetti, M.R.; Selistre-de-Araújo, H.S. Alphavbeta3 Integrin Blocking Inhibits Apoptosis and Induces Autophagy in Murine Breast Tumor Cells. *Biochim. Biophys. Acta-Mol. Cell Res.* **2019**, *1866*, 118536. [[CrossRef](#)] [[PubMed](#)]

14. Khalili, A.A.; Ahmad, M.R. A Review of Cell Adhesion Studies for Biomedical and Biological Applications. *Int. J. Mol. Sci.* **2015**, *16*, 18149–18184. [CrossRef] [PubMed]
15. Zaszczyńska, A.; Sajkiewicz, P.; Grady, A. Piezoelectric Scaffolds as Smart Materials for Neural Tissue Engineering. *Polymers* **2020**, *12*, 161. [CrossRef] [PubMed]
16. Barberi, J.; Mandrile, L.; Napione, L.; Giovanozzi, A.M.; Rossi, A.M.; Vitale, A.; Yamaguchi, S.; Spriano, S. Albumin and Fibronectin Adsorption on Treated Titanium Surfaces for Osseointegration: An Advanced Investigation. *Appl. Surf. Sci.* **2022**, *599*, 154023. [CrossRef]
17. Sobolewski, P.; Murthy, N.S.; Kohn, J.; El Fray, M. Adsorption of Fibrinogen and Fibronectin on Elastomeric Poly(Butylene Succinate) Copolyesters. *Langmuir* **2019**, *35*, 8850–8859. [CrossRef] [PubMed]
18. Lai, Y.; Xie, C.; Zhang, Z.; Lu, W.; Ding, J. Design and Synthesis of a Potent Peptide Containing Both Specific and Non-Specific Cell-Adhesion Motifs. *Biomaterials* **2010**, *31*, 4809–4817. [CrossRef]
19. Mohammadalizadeh, Z.; Bahremandi-Toloue, E.; Karbasi, S. Recent Advances in Modification Strategies of Pre- and Post-Electrospinning of Nanofiber Scaffolds in Tissue Engineering. *React. Funct. Polym.* **2022**, *172*, 105202. [CrossRef]
20. Garrudo, F.F.F.; Mikael, P.E.; Rodrigues, C.A.V.; Udangawa, R.W.; Paradiso, P.; Chapman, C.A.; Hoffman, P.; Colaço, R.; Cabral, J.M.S.; Morgado, J.; et al. Polyaniline-Polycaprolactone Fibers for Neural Applications: Electroconductivity Enhanced by Pseudo-Doping. *Mater. Sci. Eng. C* **2021**, *120*, 111680. [CrossRef]
21. Xu, Y.; Wu, J.; Wang, H.; Li, H.; Di, N.; Song, L.; Li, S.; Li, D.; Xiang, Y.; Liu, W.; et al. Fabrication of Electrospun Poly(l-Lactide-Co-ε-Caprolactone)/Collagen Nanoyarn Network as a Novel, Three-Dimensional, Macroporous, Aligned Scaffold for Tendon Tissue Engineering. *Tissue Eng.-Part C Methods* **2013**, *19*, 925–936. [CrossRef]
22. Wang, S.; Zhang, Y.; Yin, G.; Wang, H.; Dong, Z. Electrospun Polylactide/Silk Fibroin-Gelatin Composite Tubular Scaffolds for Small-Diameter Tissue Engineering Blood Vessels. *J. Appl. Polym. Sci.* **2009**, *113*, 2675–2682. [CrossRef]
23. Joseph, B.; Augustine, R.; Kalarikkal, N.; Thomas, S.; Seantier, B.; Grohens, Y. Recent Advances in Electrospun Polycaprolactone Based Scaffolds for Wound Healing and Skin Bioengineering Applications. *Mater. Today Commun.* **2019**, *19*, 319–335. [CrossRef]
24. Richbourg, N.R.; Peppas, N.A.; Sikavitsas, V.I. Tuning the Biomimetic Behavior of Scaffolds for Regenerative Medicine through Surface Modifications. *J. Tissue Eng. Regen. Med.* **2019**, *13*, 1275–1293. [CrossRef] [PubMed]
25. Mattanavee, W.; Suwantong, O.; Puthong, S.; Bunaprasert, T.; Hoven, V.P.; Supaphol, P. Immobilization of Biomolecules on the Surface of Electrospun Polycaprolactone Fibrous Scaffolds for Tissue Engineering. *ACS Appl. Mater. Interfaces* **2009**, *1*, 1076–1085. [CrossRef] [PubMed]
26. Hartman, O.; Zhang, C.; Adams, E.L.; Farach-Carson, M.C.; Petrelli, N.J.; Chase, B.D.; Rabolt, J.F. Biofunctionalization of Electrospun PCL-Based Scaffolds with Perlecan Domain IV Peptide to Create a 3-D Pharmacokinetic Cancer Model. *Biomaterials* **2010**, *31*, 5700–5718. [CrossRef]
27. Smith Callahan, L.A.; Xie, S.; Barker, I.A.; Zheng, J.; Reneker, D.H.; Dove, A.P.; Becker, M.L. Directed Differentiation and Neurite Extension of Mouse Embryonic Stem Cell on Aligned Poly(Lactide) Nanofibers Functionalized with YIGSR Peptide. *Biomaterials* **2013**, *34*, 9089–9095. [CrossRef]
28. Nandakumar, A.; Tahmasebi Birgani, Z.; Santos, D.; Mentink, A.; Auffermann, N.; Van Der Werf, K.; Bennink, M.; Moroni, L.; Van Blitterswijk, C.; Habibovic, P. Surface Modification of Electrospun Fibre Meshes by Oxygen Plasma for Bone Regeneration. *Biofabrication* **2013**, *5*, 015006. [CrossRef]
29. Li, X.; Xie, J.; Yuan, X.; Xia, Y. Coating Electrospun Poly(ε-Caprolactone) Fibers with Gelatin and Calcium Phosphate and Their Use as Biomimetic Scaffolds for Bone Tissue Engineering. *Langmuir* **2008**, *24*, 14145–14150. [CrossRef]
30. Ghosal, K.; Thomas, S.; Kalarikkal, N.; Gnanamani, A. Collagen Coated Electrospun Polycaprolactone (PCL) with Titanium Dioxide ( $TiO_2$ ) from an Environmentally Benign Solvent: Preliminary Physico-Chemical Studies for Skin Substitute. *J. Polym. Res.* **2014**, *21*, 410. [CrossRef]
31. Vilay, V.; Mariatti, M.; Ahmad, Z.; Pasomsouk, K.; Todo, M. Characterization of the mechanical and thermal properties and morphological behavior of biodegradable poly (L-lactide)/poly (ε-caprolactone) and poly (L-lactide)/poly (butylene succinate-co-L-lactate) polymeric blends. *J. Appl. Polym. Sci.* **2009**, *114*, 1784–1792. [CrossRef]
32. Hiljanen-Vainio, M.; Karjalainen, T.; Seppala, J. Biodegradable lactone copolymers. I. Characterization and mechanical behavior of ε-caprolactone and lactide copolymers. *J. Appl. Polym. Sci.* **1996**, *59*, 1281–1288. [CrossRef]
33. Vieira, A.C.; Guedes, R.M.; Marques, A.T. Development of ligament tissue biodegradable devices: A review. *J. Biomech.* **2009**, *42*, 2421–2430. [CrossRef] [PubMed]
34. Hiljanen-Vainio, M.P.; Orava, A.; Seppala, J.V. Properties of ε-caprolactone/DL-lactide (ε-CL/DL-LA) copolymers with a minor ε-CL content. *J. Biomed. Mater. Res.* **1997**, *34*, 39–46. [CrossRef]
35. Jeznach, O.; Kołbuk, D.; Marzec, M.; Bernasik, A.; Sajkiewicz, P. Aminolysis as a Surface Functionalization Method of Aliphatic Polyester Nonwovens: Impact on Material Properties and Biological Response. *RSC Adv.* **2022**, *12*, 11303–11317. [CrossRef] [PubMed]
36. Dulnik, J.; Denis, P.; Sajkiewicz, P.; Kołbuk, D.; Choińska, E. Biodegradation of Bicomponent PCL/Gelatin and PCL/Collagen Nanofibers Electrospun from Alternative Solvent System. *Polym. Degrad. Stab.* **2016**, *130*, 10–21. [CrossRef]
37. Atthoff, B.; Hilborn, J. Protein Adsorption onto Polyester Surfaces: Is There a Need for Surface Activation? *J. Biomed. Mater. Res.-Part B Appl. Biomater.* **2007**, *80*, 121–130. [CrossRef]

38. Andrade, J.D.; Hlady, V. Protein Adsorption and Materials Biocompatibility: A Tutorial Review and Suggested Hypotheses. In *Biopolymers/Non-Exclusion HPLC. Advances in Polymer Science*; Springer: Berlin/Heidelberg, Germany, 1987; Volume 79, pp. 1–63.
39. Gonçalves, I.C.; Martins, M.C.L.; Barbosa, M.A.; Ratner, B.D. Protein Adsorption on 18-Alkyl Chains Immobilized on Hydroxyl-Terminated Self-Assembled Monolayers. *Biomaterials* **2005**, *26*, 3891–3899. [[CrossRef](#)]
40. Yadav, H.O.; Kuo, A.T.; Urata, S.; Funahashi, K.; Imamura, Y.; Shinoda, W. Adsorption Characteristics of Peptides on  $\omega$ -Functionalized Self-Assembled Monolayers: A Molecular Dynamics Study. *Phys. Chem. Chem. Phys.* **2022**, *24*, 14805–14815. [[CrossRef](#)]
41. Jeznach, O.; Kolbuk, D.; Sajkiewicz, P. Aminolysis of Various Aliphatic Polyesters in a Form of Nanofibers and Films. *Polymers* **2019**, *11*, 1669. [[CrossRef](#)]
42. Desmet, T.; Billiet, T.; Berneel, E.; Cornelissen, R.; Schaubroeck, D.; Schacht, E.; Dubrule, P. Post-Plasma Grafting of AEMA as a Versatile Tool to Biofunctionalise Polyesters for Tissue Engineering. *Macromol. Biosci.* **2010**, *10*, 1484–1494. [[CrossRef](#)]
43. Stevens, J.S.; De Luca, A.C.; Downes, S.; Terenghi, G.; Schroeder, S.L.M. Immobilisation of Cell-Binding Peptides on Poly- $\epsilon$ -Caprolactone (PCL) Films: A Comparative XPS Study of Two Chemical Surface Functionalisation Methods. *Surf. Interface Anal.* **2014**, *46*, 673–678. [[CrossRef](#)]
44. Kołbuk, D.; Guimond-Lischer, S.; Sajkiewicz, P.; Maniura-Weber, K.; Fortunato, G. Morphology and Surface Chemistry of Bicomponent Scaffolds in Terms of Mesenchymal Stromal Cell Viability. *J. Bioact. Compat. Polym.* **2016**, *31*, 423–436. [[CrossRef](#)]
45. Jalaja, K.; Naskar, D.; Kundu, S.C.; James, N.R. Fabrication of Cationized Gelatin Nanofibers by Electrospinning for Tissue Regeneration. *RSC Adv.* **2015**, *5*, 89521–89530.
46. Khorramnezhad, M.; Akbari, B.; Akbari, M.; Kharaziha, M. Effect of Surface Modification on Physical and Cellular Properties of PCL Thin Film. *Colloids Surfaces B Biointerfaces* **2021**, *200*, 111582. [[CrossRef](#)] [[PubMed](#)]
47. Zhu, Y.; Gao, C.; He, T.; Shen, J. Endothelium Regeneration on Luminal Surface of Polyurethane Vascular Scaffold Modified with Diamine and Covalently Grafted with Gelatin. *Biomaterials* **2004**, *25*, 423–430. [[CrossRef](#)]
48. Ma, Z.; Gao, C.; Ji, J.; Shen, J. Protein Immobilization on the Surface of Poly-L-Lactic Acid Films for Improvement of Cellular Interactions. *Eur. Polym. J.* **2002**, *38*, 2279–2284. [[CrossRef](#)]
49. Cui, W.; Li, X.; Chen, J.; Zhou, S.; Weng, J. In Situ Growth Kinetics of Hydroxyapatite on Electrospun Poly(DL-Lactide) Fibers with Gelatin Grafted. *Cryst. Growth Des.* **2008**, *8*, 4576–4582. [[CrossRef](#)]
50. Gao, C.; Hu, X.; Hong, Y.; Guan, J.; Shen, J. Photografting of Poly(Hydroxylethyl Acrylate) onto Porous Polyurethane Scaffolds to Improve Their Endothelial Cell Compatibility. *J. Biomater. Sci. Polym. Ed.* **2003**, *14*, 937–950. [[CrossRef](#)]
51. Wu, Y.C.; Shaw, S.Y.; Lin, H.R.; Lee, T.M.; Yang, C.Y. Bone Tissue Engineering Evaluation Based on Rat Calvaria Stromal Cells Cultured on Modified PLGA Scaffolds. *Biomaterials* **2006**, *27*, 896–904. [[CrossRef](#)]
52. Mahjoubnia, A.; Haghbin Nazarpak, M.; Karkhaneh, A. Polypyrrole-Chitosan Hydrogel Reinforced with Collagen-Grafted PLA Sub-Micron Fibers as an Electrically Responsive Scaffold. *Int. J. Polym. Mater. Polym. Biomater.* **2022**, *71*, 302–314. [[CrossRef](#)]
53. Moghadam, R.R.; Keshvari, H.; Imani, R.; Nazarpak, M.H. A Biomimetic Three-Layered Fibrin Gel/PLLA Nanofibers Composite as a Potential Scaffold for Articular Cartilage Tissue Engineering Application. *Biomed. Mater.* **2022**, *17*, 055017. [[CrossRef](#)]
54. Antonova, L.V.; Seifalian, A.M.; Kutikhin, A.G.; Sevostyanova, V.V.; Krivkina, E.O.; Mironov, A.V.; Burago, A.Y.; Velikanova, E.A.; Matveeva, V.G.; Glushkova, T.V.; et al. Bioabsorbable Bypass Grafts Biofunctionalised with RGD Have Enhanced Biophysical Properties and Endothelialisation Tested in Vivo. *Front. Pharmacol.* **2016**, *7*, 136. [[CrossRef](#)] [[PubMed](#)]
55. De Luca, A.C.; Terenghi, G.; Downes, S. Chemical Surface Modification of Poly- $\epsilon$ -Caprolactone Improves Schwann Cell Proliferation for Peripheral Nerve Repair. *J. Tissue Eng. Regen. Med.* **2014**, *8*, 153–163. [[CrossRef](#)] [[PubMed](#)]
56. Migliorini, E.; Weidenhaupt, M.; Picart, C. Practical Guide to Characterize Biomolecule Adsorption on Solid Surfaces (Review). *Biointerphases* **2018**, *13*, 06D303. [[CrossRef](#)] [[PubMed](#)]
57. Lehnfeld, J. In Pursuit of Alternatives to Poly (Ethylene Glycol) as Protein-Repellent but Cell-Adhesive Surface Coatings for Biomaterials. Ph.D. Thesis, Regensburg University, Regensburg, Germany, 2021.
58. Wahab, R.A.; Elias, N.; Abdullah, F.; Ghoshal, S.K. On the Taught New Tricks of Enzymes Immobilization: An All-Inclusive Overview. *React. Funct. Polym.* **2020**, *152*, 104613. [[CrossRef](#)]



Article

# A Comparative Study of Three Approaches to Fibre's Surface Functionalization

Judyta Dulnik , Oliwia Jeznach and Paweł Sajkiewicz \*

Laboratory of Polymers and Biomaterials, Institute of Fundamental Technological Research Polish Academy of Sciences, Pawińskiego 5b, 02-106 Warsaw, Poland

\* Correspondence: psajk@ippt.pan.pl

**Abstract:** Polyester-based scaffolds are of research interest for the regeneration of a wide spectrum of tissues. However, there is a need to improve scaffold wettability and introduce bioactivity. Surface modification is a widely studied approach for improving scaffold performance and maintaining appropriate bulk properties. In this study, three methods to functionalize the surface of the poly(lactide-co-ε-caprolactone) PLCL fibres using gelatin immobilisation were compared. Hydrolysis, oxygen plasma treatment, and aminolysis were chosen as activation methods to introduce carboxyl (-COOH) and amino (-NH<sub>2</sub>) functional groups on the surface before gelatin immobilisation. To covalently attach the gelatin, carbodiimide coupling was chosen for hydrolysed and plasma-treated materials, and glutaraldehyde crosslinking was used in the case of the aminolysed samples. Materials after physical entrapment of gelatin and immobilisation using carbodiimide coupling without previous activation were prepared as controls. The difference in gelatin amount on the surface, impact on the fibres morphology, molecular weight, and mechanical properties were observed depending on the type of modification and applied parameters of activation. It was shown that hydrolysis influences the surface of the material the most, whereas plasma treatment and aminolysis have an effect on the whole volume of the material. Despite this difference, bulk mechanical properties were affected for all the approaches. All materials were completely hydrophilic after functionalization. Cytotoxicity was not recognized for any of the samples. Gelatin immobilisation resulted in improved L929 cell morphology with the best effect for samples activated with hydrolysis and plasma treatment. Our study indicates that the use of any surface activation method should be limited to the lowest concentration/reaction time that enables subsequent satisfactory functionalization and the decision should be based on a specific function that the final scaffold material has to perform.



**Citation:** Dulnik, J.; Jeznach, O.; Sajkiewicz, P. A Comparative Study of Three Approaches to Fibre's Surface Functionalization. *J. Funct. Biomater.* **2022**, *13*, 272. <https://doi.org/10.3390/jfb13040272>

Academic Editor: Anderson de Oliveira Lobo

Received: 25 October 2022

Accepted: 30 November 2022

Published: 2 December 2022

**Publisher's Note:** MDPI stays neutral with regard to jurisdictional claims in published maps and institutional affiliations.



**Copyright:** © 2022 by the authors. Licensee MDPI, Basel, Switzerland. This article is an open access article distributed under the terms and conditions of the Creative Commons Attribution (CC BY) license (<https://creativecommons.org/licenses/by/4.0/>).

**Keywords:** surface activation; functionalization; electrospun fibres; hydrolysis; plasma; aminolysis

---

## 1. Introduction

Polymers are frequently used in tissue engineering applications due to the ease of adjusting their mechanical properties, fabrication to the desired shape, and the possibility of chemical modification [1]. Among them, aliphatic polyesters play an important role as they degrade chemically by hydrolysis, or less often, enzymatic processes without toxic products [2,3]. Lactide, caprolactone, and glycolide are the commonly used monomers to synthesise aliphatic polyesters and copolymers that are applied in tissue engineering [4]. Polymers can be manufactured using various techniques, e.g., electrospinning [5], 3D printing [6], and freeze-extraction [7]. Their bulk properties can be tailored via various methods, e.g., copolymerization [8], controlled crystallization [9], or the use of additives [10]. Thanks to the possibility of properties modification, polyester-based scaffolds are of research interest in the regeneration of a wide spectrum of tissues including skin [11], blood vessels [12], neural tissue [13], bladder tissue [14], bone [15], tendon [16], etc.

However, the functionality of polyester scaffolds in tissue engineering applications is limited by their surface properties—hydrophobicity and lack of bioactivity [3].

A few approaches are implemented to introduce missing bioactivity: using a decellularized natural extracellular matrix (ECM) as a scaffold [17–19], fabrication of scaffold from natural polymers containing adequate peptide sequences [20–22], or manufacturing synthetic-natural polymer composites [23–25]. Nowadays, a lot of attention is devoted in particular to the studies on biomolecule immobilisation on the surface of synthetic polymers to impart bioactivity and take advantage of their suitable mechanical properties and manufacturability [3].

It is well-known that cells are connected with the ECM via their receptors—integrins that recognize special peptide sequences. Up to now, a lot of sequences were found in the so-called cell adhesion molecules [26]. The accessibility of peptide sequence for given cell receptors is determined by the conformation of individual proteins and modulated by immediately adjacent amino acids [27]. One of the most examined is the Arginyl-glycyl-aspartic acid (RGD) motif, which is present mainly in fibronectin and the denatured form of collagen. RGD sequence present in gelatin is recognized by various types of cells, and in the case of L929 fibroblast cells via  $\alpha 5\beta 1$  and  $\alpha v\beta 3$  integrins [28]. Gelatin attachment to fibrous materials made of aliphatic polyesters has been shown to improve cell attachment and spreading [29].

The simplest method of surface modification by attaching a bioactive molecule like gelatin is physisorption, which is conducted by immersing the material in a biomolecule solution. In this case, electrostatic interactions, hydrogen bonds, van der Waals forces, and hydrophobic interactions are responsible for binding biomolecules with the surface [30]. Another physical approach is a layer-by-layer technique, which consists of depositing alternating layers of oppositely charged materials [31]. Mild conditions, simplicity, and applicability to a lot of materials are advantages of physical methods [23]. However, weak interactions could result in the instability of the coating. A second concern is the loss of functionality due to the conformational changes of a biomolecule, especially caused by hydrophobic interactions [32]. Chemical immobilisation is an alternative way to introduce bioactive molecules on the scaffold surface. The first step is the addition of functional groups on the surface to provide the binding site with a biomolecule. It is achieved by various methods, e.g., wet chemical methods, such as hydrolysis and aminolysis [33], photographing of poly(acrylic acid) or poly(methacrylic acid) [34], thiol bonding [35], and azide-alkyne click chemistry [36], etc. The main benefit of this kind of functionalization is a stable coating provided by covalent bonding between polymer and biomolecule. However, it should be taken into consideration that some of these methods could be destructive to materials [37,38] and by-products could exhibit cytotoxicity [39], so the method optimization toward specific materials is required.

Among the variety of biodegradable polymers commonly used in tissue engineering, poly(lactide-co- $\epsilon$ -caprolactone) PLCL has been reported to be the most promising candidate for tissue engineering. PLCL surpasses aliphatic polyester-like poly(L-lactic acid) (PLLA) and poly( $\epsilon$ -caprolactone) (PCL) in some of their properties. The most important disadvantages of PLLA and PCL are related to mechanical properties—PLLA and PLGA exhibit high strength and poor toughness, whereas PCL has good toughness but low strength [40–42].

By the association of PLLA with PCL into PLCL copolymer the advantages of both PLLA and PCL are obtained together with compensation; both the brittle behaviour of PLLA and the low stiffness of PCL [43,44] as well as the local acidification reduction due to the degradation of PLLA [45]. PLCL also offers an adjustable degradation rate adapted to its use in tissue engineering, tailorable by changing the PCL/PLLA ratio [46]. A strong shape-memory effect has also been observed for PLCL, depending on PCL/PLLA ratio [47].

In general, it may be concluded that PLCL is the most suitable polymer for various tissue engineering applications, particularly when adjustable elasticity and degradability are required. For instance, a braided PLCL scaffold (PLLA/PCL ratio = 85/15) has been recently designed for ligament tissue engineering [48].

Therefore, the main objectives of this work were to examine surface activation methods such as hydrolysis, oxygen plasma, and aminolysis acting as a first step in functionalising a

PLCL nonwoven material with gelatin and to compare the resulting material's properties. Our goal was to provide comprehensive data that could be useful to many people while deciding what method to use for their specific needs. Since gelatin has both -NH<sub>2</sub> and -COOH groups in abundance [49], in order to form a covalent bond between gelatin and fibres' surface, grafting methods such as 1-ethyl-3-(3-dimethylaminopropyl)carbodiimide hydrochloride/N-hydroxysuccinimide (EDC/NHS) coupling and glutaraldehyde crosslinking were used. Additionally, materials after physical entrapment of gelatin and immobilisation using EDC/NHS coupling without previous activation were prepared as controls. All the approaches were compared for their immobilisation effectiveness and stability, impact on fibres morphology, wettability, chemical structure, molecular weight, functionalization stability as well as mechanical properties and L929 cells response.

## 2. Materials and Methods

### 2.1. Materials

PLCL 70:30 (Resomer® LC703S, inherent viscosity = 1.3–1.8 dL/g, T<sub>g</sub> = 32–42 °C) was purchased from Evonik (Essen, Germany). Hexafluoroisopropanol (HFIP) (purity degree 98.5%) was procured from Iris Biotech GmbH (Marktredwitz, Germany). Ethylenediamine (EDA) (purity degree 99.5%), sodium hydroxide (NaOH), isopropanol (purity degree 99.8%), glutaraldehyde (GTA, conc. 25%), and tetrahydrofuran (THF) were purchased from Chempur (Piekary Śląskie, Poland). Gelatin (G1890, type A, gel strength ~300 g Bloom) and bicinchoninic acid (BCA) assay kit (QuantiPro™, for 0.5–30 µg/mL protein conc.) was supplied by Sigma-Aldrich (St Louis, MO, USA). N-hydroxysuccinimide (NHS), 1-ethyl-3-(3-dimethylaminopropyl)carbodiimide hydrochloride (EDC), Dulbecco's Modified Eagle Medium (DMEM), Phosphate-Buffered Saline (PBS) pH 7.4, Foetal Bovine Serum (FBS), Trypsin EDTA, antibiotic (Penicillin-Streptomycin 10,000 U/mL), Presto Blue, NucBlue, and ActinGreen were purchased from Thermo Fisher Scientific (Waltham, MA, USA). Mouse fibroblast L929 were purchased from Sigma-Aldrich (ATTC).

### 2.2. Electrospinning

All materials were electrospun using a Fluidnatek LE-50 electrospinning machine by Bioinicia (Valencia, Spain). The polymer solution was prepared by dissolving PLCL in HFIP with 7% *w/w* polymer concentration and stirred for 24 h at room temperature. Two needles were fed with polymer solution at a rate of 3 mL/h each and the voltage was kept in a 11–13 kV range. A drum collector ( $\phi$  5 cm) was rotating at 300 RPM speed and the distance from a needle tip to a collector's surface was set to 15 cm. Electrospinning took place in monitored air conditions set for 38 °C temperature and 40% humidity. Temperature elevated to the polymer's glass transition temperature (as provided by the manufacturer T<sub>g</sub>PLCL 32–42 °C) was used in order to avoid shrinking that happens after electrospinning of PLCL nonwoven at room temperature (20–23 °C).

After electrospinning was completed, to make sure no residual solvent was present in the fibres, nonwoven mats were kept under a fume hood overnight and then transferred to a vacuum oven set to 50 mBar for 24 h at room temperature. All surface activation/crosslinking/functionalization steps were carried out on 4.5 cm × 4.5 cm squares that electrospun materials were cut into.

### 2.3. Optimization of Surface Activation Methods

In order to determine the optimal parameters for the chosen surface activation methods, each of them was performed with a set of varying conditions (Table 1). All samples were then subjected to a series of tests to assess their morphology, physicochemical properties, and activation efficiency. This approach enabled the selection of a final set of samples with an already activated surface to undergo the next steps of functionalization.

**Table 1.** Initial set of surface activation conditions applied in the optimisation step.

| Activation Method   | Optimisation Conditions |                                     |
|---------------------|-------------------------|-------------------------------------|
|                     | Treatment Time          | Reagent Concentration               |
| Cold oxygen plasma  | 5, 10, 15, 40, 60 (s)   | -                                   |
| Alkaline hydrolysis | 10, 30, 60, 180 (min)   | 0.05, 0.1, 0.25, 0.5, 1 (M NaOH)    |
| Aminolysis          | 5, 10, 15, 30 (min)     | 2, 6, 10 (% w/v EDA in isopropanol) |

### 2.3.1. Hydrolysis

Alkaline hydrolysis experiments were performed at room temperature (25 °C). Samples were submerged in NaOH solutions with concentrations 0.05 M, 0.1 M, 0.25 M, 0.5 M, and 1 M for 10 min, 30 min, 60 min, and 180 min as mentioned in Table 1. An additional sample underwent a reaction in 1 M NaOH solution for 360 min to determine changes that occur in material subjected to extreme conditions. After appointed reaction times, samples were transferred to 0.01 M HCl solution for protonation of newly created COO- groups and subsequently to demineralised water for rinsing. Thus prepared samples were dried in a vacuum oven at room temperature. Because of the observed decrease in thickness of samples treated with higher NaOH concentrations, the samples that were chosen for functionalization were also subjected to weight and thickness measurements before and after the surface activation step.

### 2.3.2. Plasma

Cold oxygen plasma surface activation process was performed using a Plasma Cleaner (Diener, ZEPTO PCCE, Ebhausen, Germany) machine. All samples underwent plasma treatment with the same, low—1%, of instrument's power, with 0.1 mBar oxygen pressure, for a broad range of times: 5 s, 10 s, 15 s, 25 s, 40 s, and 60 s as mentioned in Table 1.

### 2.3.3. Aminolysis

This part of the experiments was based on the data collected in our previous study on aminolysis, where an increase in the amount of NH<sub>2</sub> groups with the diamine concentration and reaction time was observed and described [50]. Three concentrations—2%, 6%, and 10% w/v, and four different times—5 min, 10 min, 15 min, and 30 min were examined, as mentioned in Table 1. For this work, to provide various amounts of NH<sub>2</sub> groups on the materials' surface for the functionalization study, three different reaction conditions were chosen that result in an amount of free NH<sub>2</sub> groups on the surface equal to  $1.42 \pm 0.08 \times 10^{-8}$  mol/mg,  $5.43 \pm 0.90 \times 10^{-8}$  mol/mg, and  $8.63 \pm 1.16 \times 10^{-8}$  mol/mg for A1, A2, and A3 samples, respectively. Aminolysis was conducted by immersing samples in ethylenediamine/isopropanol solution, the temperature of the reaction was set at 30 °C. The process was conducted in an orbital shaker incubator. After aminolysis samples were washed three times in deionized water and dried under a vacuum overnight.

### 2.4. Functionalization

Gelatin immobilisation was executed via a three-step approach. First, PLCL nonwoven materials cut into 4.5 cm × 4.5 cm squares were subjected to one of the three surface activation processes: hydrolysis, cold oxygen plasma, or aminolysis. The final set of process parameters was chosen for each method based on the results of the optimization step: hydrolysis—0.1 M, 0.25 M, 0.5 M, and 1 M, for 3 h, for plasma—10 s and 40 s of treatment, for aminolysis—three sets of EDA concentration and reaction time: 2%—5 min, 2%—10 min, and 6%—5 min on the basis of the results from a previous study [50].

The next step consisted of gelatin crosslinking. Samples after surface activation with hydrolysis and plasma were placed for 1 h in w/w 0.23%/0.12% EDC/NHS solution in ethanol:water mixture with at 7:3 ratio. Simultaneously, a set of samples after aminolysis

were placed in 1% *w/v* GTA in a water solution for 2.5 h at 24 °C to compare cross-linking methods. All of the samples were thoroughly rinsed in demineralized water and right afterwards submerged in 0.2% gelatin solution for 20 h at 37 °C. Gelatin immobilisation was completed to make sure no unattached gelatin was present within the material, and samples were once again placed in demineralized water and stirred, this time for 24 h at 37 °C. Two control samples of PLCL without surface activation were prepared. One placed in an EDC/NHS solution followed by a gelatin bath, the other one only going through the last step. All functionalized sample names are specified in Table 2.

**Table 2.** Names of all samples that underwent functionalization.

| Surface Activation Method | Time   | Reagent Concentration | Crosslinking Method | Name     |
|---------------------------|--------|-----------------------|---------------------|----------|
| Hydrolysis                | 3 h    | 1 M                   | EDC/NHS             | H1       |
|                           |        | 0.5 M                 |                     | H0.5     |
|                           |        | 0.25 M                |                     | H0.25    |
|                           |        | 0.1 M                 |                     | H0.1     |
| Plasma                    | 10 s   | -                     | EDC/NHS             | P10      |
|                           | 40 s   | -                     |                     | P40      |
| Aminolysis                | 5 min  | 2% <i>w/v</i>         | GTA                 | A1       |
|                           | 10 min | 2% <i>w/v</i>         | GTA                 | A2       |
|                           | 5 min  | 6% <i>w/v</i>         | GTA                 | A3       |
| Control (no activation)   | -      | -                     | EDC/NHS             | CEN<br>C |

## 2.5. Functionalization

### 2.5.1. Water Contact Angle

Water contact angle was measured with a goniometer (Data Physics OCA 15EC, Filderstadt, Germany) using the sessile drop method. For each sample, the water contact angle was measured not less than 10 times. For each measurement, the angle was recorded at 0.5 s, 3 s, 10 s, and 30 s after placing the demineralized water drop on the surface of a sample.

### 2.5.2. Nonwovens Morphology

Scanning electron microscopy images (JSM-6010PLUS/LV InTouchScope™, JEOL, Tokyo, Japan) were taken of each sample in order to assess changes in their morphology after the surface activation process and then again after the functionalization step. Samples were sputter-coated with approx. 10 nm of gold.

### 2.5.3. Quantification of -COOH Groups

Both plasma and hydrolysis treatments were expected to increase the -COOH group density on the material's surface. Toluidine blue-O test was performed to assess how effective those processes were in various conditions. This colourimetric method works by dye-staining deprotonated carboxyl groups on fibres' surfaces through ionic interaction. Here, an adapted routine proposed by Gupta et al. [51] was used. Briefly, a 0.5 mM solution of toluidine dye with pH10 was prepared. Samples were soaked in it for 5 h at 37 °C. Afterwards, nonwovens were thoroughly rinsed with NaOH of pH 9 to remove any unattached dye. Next, the samples were transferred to acetic acid 50% *w/w* solution to detach the dye in order to measure its concentration with a UV-vis spectrophotometer at 630 nm (The Multiskan™ GO, Thermo Fisher Scientific, USA).

### 2.5.4. Fourier Transform Infrared Spectroscopy (FTIR)

A series of infrared attenuated total reflectance (ATR) spectroscopy tests were performed for two main purposes. First, during the optimization part of the work, to determine the changes that occur in the materials subjected to hydrolysis and plasma treatment, and later to assess the efficiency of gelatin attachment to the materials functionalized after

surface activation with all three types of treatment. The infrared ATR spectroscopy tests were conducted with a spectrometer Bruker Vertex 70 (Mannheim, Germany).

#### 2.5.5. Molecular Weight

Molecular weight measurements were performed using a Nexera (Shimadzu, Japan) device with THF as eluent. Gel permeation chromatography (GPC) equipment consisted of a pump, column (Phenogel™ 5  $\mu\text{m}$  10<sup>5</sup> Å, Phenomenex), refractive index detector (RID-20A, Shimadzu), and LabSolutions GPC software. All samples were dissolved in THF in 2 mg/mL concentration by vortex stirring for 24 h at room temperature and then filtered with hydrophobic polytetrafluoroethylene (PTFE) syringe filters with 0.22  $\mu\text{m}$  pore size. THF was used as a mobile phase with a flow rate equal to 1 mL/min. The temperature was set at 40 °C. The molecular weight results were calculated using a polystyrene standard (number averaged molecular weight from 3470 Da to 2,520,000 Da) calibration curve coupled with the Mark–Houwink equation where  $\alpha = 0.7$ ,  $K = 14.1 \times 10^{-5}$  dL/g for polystyrene standard polymer, and  $\alpha$  is 0.68,  $K$  is  $4.84 \times 10^{-4}$  dL/g for PLCL according to Nuuttila M. et al. [52] were used.

#### 2.5.6. Mechanical Tests

Mechanical tests were conducted using a Lloyd EZ-50 (United States of America) device. Uniaxial tensile testing was performed with a 5 mm/min extension speed. From each type of material three 50 mm × 5 mm rectangular samples were cut, their thickness was measured at the ends and the results were averaged. For testing a sample was placed in between two rubber-lined clamps, leaving the 20 mm × 5 mm part of the sample to be extended.

#### 2.5.7. Functionalization Stability

In order to determine the stability of gelatin coating on fibres' surfaces, all the samples underwent testing in conditions mimicking the environment of a living organism. Each sample (4.5 cm × 4.5 cm) was immersed in 100 mL of PBS with a pH of 7.4 and placed in an orbital shaker at 37 °C, 100 RPM (revolutions per minute). To prevent bacterial or fungi growth, sodium azide in a concentration of 0.1% was added. After 24 h and 7 days, samples were taken out and washed with demineralized water and dried with a vacuum oven.

#### 2.5.8. Quantification of Gelatin Amount on Fibres' Surfaces

The amount of protein on fibres' surfaces was measured both right away after functionalization as well as after biodegradation using a BCA assay kit (QuantiPro™, for 0.5–30  $\mu\text{g}/\text{mL}$  protein conc.). For each of the modified materials, three samples of weight  $1 \pm \text{mg}$  were investigated. Each sample was put into an Eppendorf vial and 0.5 mL of deionized water with 0.5 mL of BCA solution was added to the vial. To obtain a calibration curve, gelatin solutions of concentrations in the range of 5–30  $\mu\text{g}/\text{mL}$  were prepared. The samples, as well as calibration solutions, were incubated for 2 h at 37 °C. Absorbance was measured with a UV-vis spectrophotometer at 560 nm. Results were shown as the amount of gelatin on the surface in  $\mu\text{g}$  per mg of fibrous sample.

### 2.6. Functionalization

The mouse fibroblast L929 cell line that was used to perform all cellular tests was purchased from Sigma-Aldrich (ATTC). The culture medium used consisted of 89% Dulbecco's Modified Eagle's Medium, 10% foetal bovine serum, and 1% antibiotic (penicillin-streptomycin). For cytotoxicity on extracts and direct contact tests, nonwovens were cut into 5 mm and 10 mm discs, respectively, sterilised with 80% ethanol and UV light for 30 min for each side.

### 2.6.1. Quantitative Tests: Cytotoxicity on Extracts and Viability Test in Direct Contact

For the cytotoxicity test, material extracts were obtained by placing 5 samples (5 mm in diameter) of each nonwoven type in a 96-well plate, then 200  $\mu$ L of culture medium was added to each well, and afterwards the plate was kept at 37 °C and gently stirred for 24 h. At the same time, another 96-well plate was seeded with  $10^4$  cells/well and placed for 24 h in an incubator (37 °C, 5% CO<sub>2</sub>). After 24 h the culture medium in the cell-seeded wells was replaced with material extracts and put in the incubator for another 24 h.

To assess cell viability in direct contact with the materials, for each time point (1, 2, 3 days), 3 samples (10 mm in diameter) were placed in separate 48-well plates and seeded with a density of  $10^4$  cells/well and the plates were then put into the incubator. For the 0-day control time point, the same number of cells was seeded into 3 empty wells and the viability test was performed after 5 h so that cells had time to attach to the surface of the well bottom.

For both cytotoxicity on extracts and 0–3-day tests in direct contact, the Presto Blue method was used to assess cell metabolic activity. First, the culture medium was removed, then each well was washed with PBS, Presto Blue reagent was added with PBS in the 1:9 ratio and next the plate was put in the incubator for 40 min. After this time, 100  $\mu$ L was transferred from each well to a 96-well plate and the fluorescence was read with the excitation/emission 530/620 nm filters.

### 2.6.2. Qualitative Morphology Tests

For the purpose of assessing the morphology of cells cultured in direct contact with functionalized nonwoven surfaces, two types of qualitative observation methods were employed. The first was scanning electron microscopy (SEM) imaging and the second was observing cells' actin skeleton and nuclei with fluorescence microscopy. For these, a 5-day cell culture was performed where the materials were seeded with  $2 \times 10^3$  cells/well. Samples for SEM imaging were fixed by immersing 2.5% glutaraldehyde for 2 h and then dehydrated in a series of ethanol solutions (30–100%) followed by ethanol/hexamethyldisilazane (2:1, 1:2) mixtures. For fluorescence microscopy cells were fixed with 3% formaldehyde for 20 min, permeabilized with 0.01% triton × 100, and then stained with fluorescent dyes that attach to the cell actin skeleton (ActinGreen) and nucleus (NucBlue).

## 3. Results and Discussion

### 3.1. Optimisation of Surface Activation Methods

#### 3.1.1. Water Contact Angle

A nonwoven PLCL material, without any additional treatment, has a water contact angle of  $131.43^\circ \pm 1.94^\circ$ , which means it is hydrophobic which is typical for aliphatic polyesters [53]. The aminolysis reaction had no effect on this property as the samples A1, A2, and A3 had water contact angles equal to  $131.31^\circ \pm 1.37$ ,  $130.74^\circ \pm 1.63^\circ$ , and  $131.28^\circ \pm 0.84^\circ$ , respectively. Lack of wettability improvement or only a small change after aminolysis was reported earlier by others [54–56]. Both hydrolysis and plasma treatment lowered the water contact angle of PLCL samples.

Cold oxygen plasma proved to be an extremely time-efficient method of making PLCL fibres' surface hydrophilic. All samples treated for at least 15 s had a 0° water contact angle only 10 s after the water drop was placed on its surface (Figure 1a). Because of the nature of fibrous materials, 0° means that the drop was effectively soaked into the material.

For hydrolysed PLCL samples, the decrease in water contact angle was dependent on both reaction time and NaOH concentration. Figure 1b,c shows a comparison of water contact angle measurement results for 180 min reaction time with varying NaOH concentrations (Figure 1b) and for 1 M NaOH solution used for reaction times from 10 up to 180 min (Figure 1c).

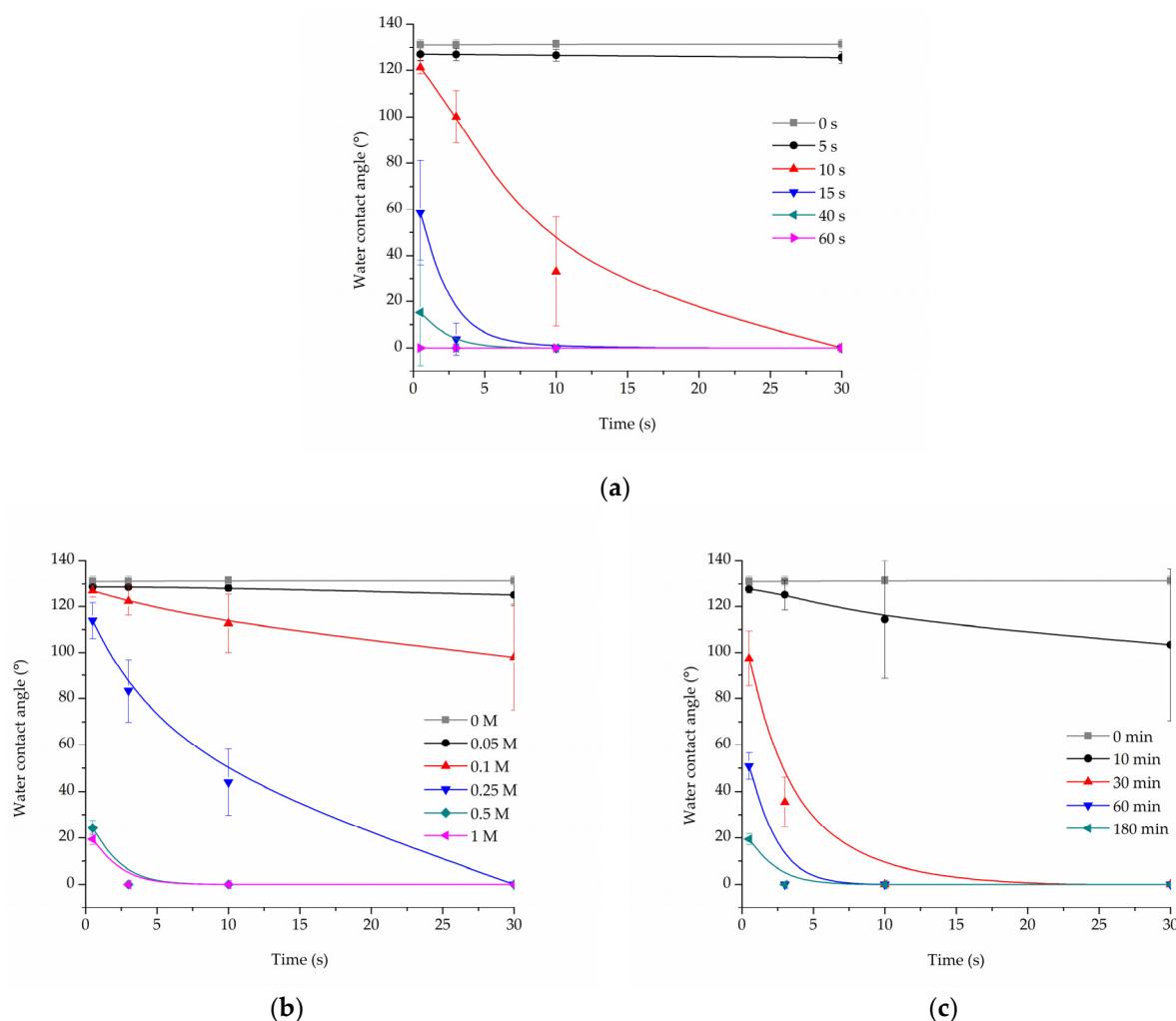


**Figure 1.** Water contact angle of PLCL nonwoven samples after surface activation with (a) oxygen plasma, (b) NaOH solutions with increasing concentrations for 3 h, (c) 1 M NaOH solution for a set of time periods up to 180 min.

From the group of samples hydrolysed for 3 h, 0.25 M, or higher NaOH concentration was needed to make materials hydrophilic, with 0.5 M and 1 M NaOH enabling a water drop to be soaked into the material within only 3 s (Figure 1b). Looking from the other side, 1 M NaOH had to be used for at least 30 min for the water contact angle to drop below 100° (Figure 1c).

### 3.1.2. Morphology

Fibres' morphology of all samples after surface activation was compared to untreated PLCL (Figure 2a). All samples treated with oxygen plasma retained the material's initial morphology whereas both hydrolysis and aminolysis did have an effect depending on activation conditions.

For hydrolysis, reaction times shorter than 3 h and concentrations lower than 0.5 M NaOH did not result in any fibres' morphology alteration. A sample placed in 0.5 M NaOH for 3 h had its fibres' surface slightly affected with small surface cracks (Figure 2b) and for the same time in 1 M concentration these changes were more pronounced as the top layer of the fibre surface seemed to be frayed, chipping off the fibres while the overall architecture is still intact (Figure 2c). The sample treated with 1 M NaOH for 6 h showed severe damage with both the surface of the fibres and the nonwoven structure being compromised (Figure 2d).

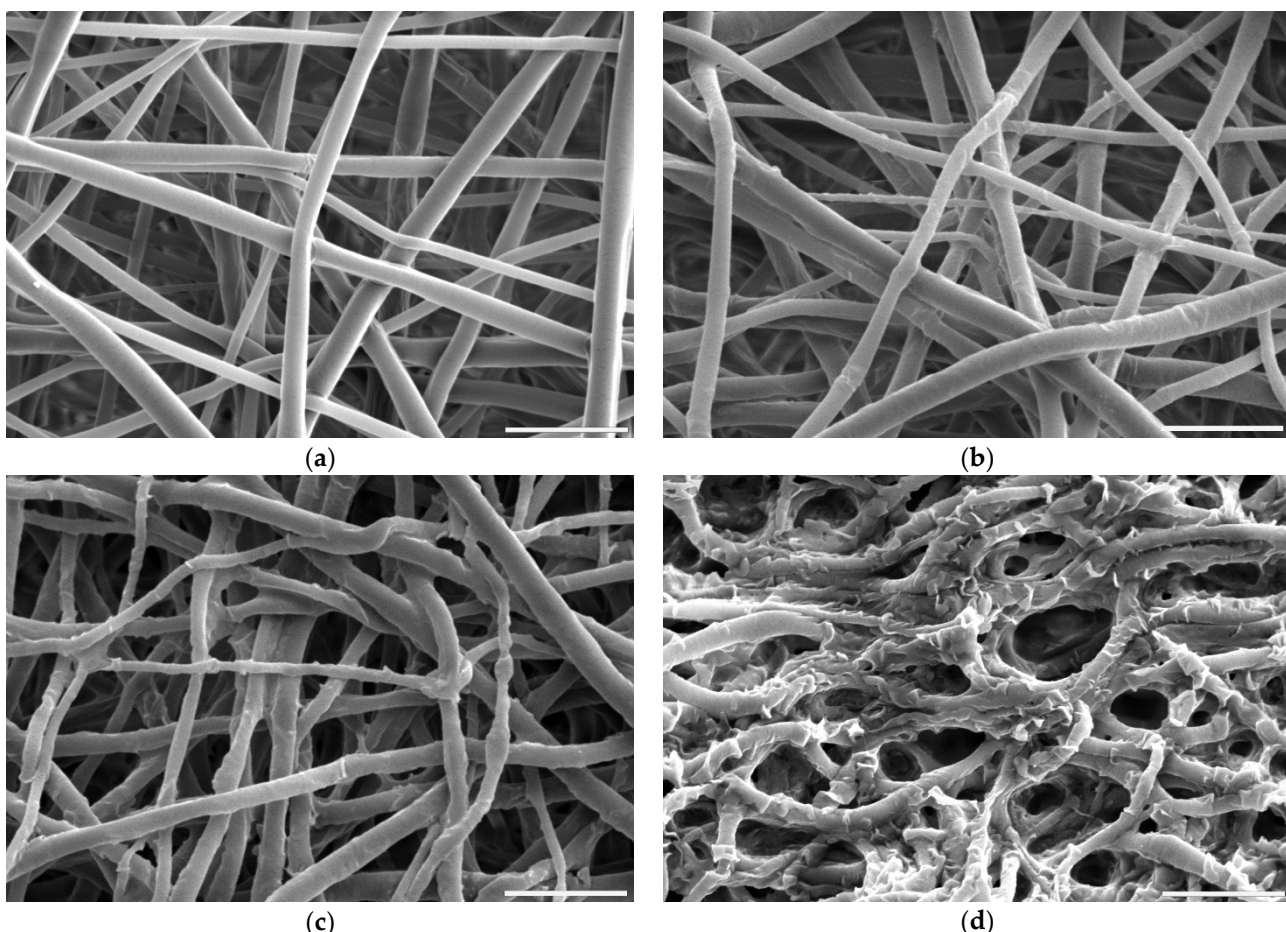


**Figure 2.** Scanning electron microscope images of PLCL nonwoven sample (a) untreated, after surface activation with (b) 0.5 M NaOH for 3 h, (c) 1 M NaOH for 3 h, (d) 1 M NaOH for 6 h. The marker is equal to 5  $\mu$ m.

In addition, measurements of both weight and thickness before and after surface activation with NaOH (Figure 3) clearly show that the hydrolysis leads to surface degradation of the polymer severe enough that the thickness and weight of the nonwovens are significantly reduced. This reduction correlates linearly with NaOH solution concentration. However, for the low 0.1–0.25 M NaOH concentrations, the drop in both values did not reach 15%, and the samples that retained 72% and 46% of their initial weight, for 0.5 M and 1 M, respectively, were visibly thinner even for the naked eye.

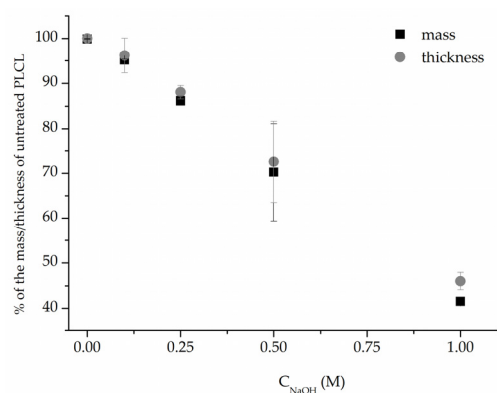


**Figure 3.** Mass and thickness change after 3 h NaOH surface activation of PLCL nonwoven.

A comparison of the fibre diameter distribution for the control PLCL sample and material treated with 1 M NaOH for 3 h (Figure 2a,c) shows how surface erosion caused by hydrolysis affected fibre thickness (Figure 4a,b). Whereas a bimodal character of the distribution for untreated PLCL is preserved in the hydrolysed sample, both of the local maxima present a lower value: 0.53  $\mu\text{m}$  and 0.95  $\mu\text{m}$  for control and 0.49  $\mu\text{m}$  and 0.78  $\mu\text{m}$  for NaOH treated material. A small percentage of fibres with a diameter below 0.3  $\mu\text{m}$  are not present in the material after hydrolysis.

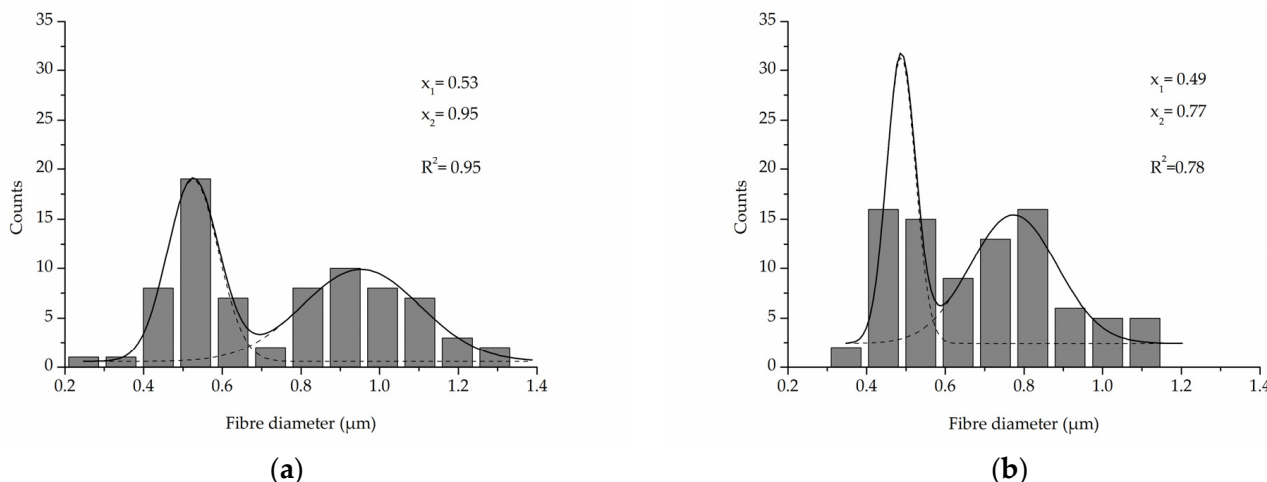


**Figure 4.** Fibre diameter distribution with local maxima and regression values of (a) an untreated PLCL sample, (b) a sample treated with 1 M NaOH for 3 h. Data were fitted with Gaussian function.

In the case of aminolysis surface activation, within the range of diamine concentration and reaction time that was chosen for this work based on our previous studies [50], no changes in fibres' morphology were observed. It is valid even for treatment with 6% diamine solution for 5 min, which was the highest chosen reaction conditions (Figure 5a). Using higher diamine concentrations and longer reaction times led to fibres being prone to brittle cracking without changing fibre diameter (Figure 5b). This effect is known and utilized to fabricate fibrous fillers, e.g., for application in composite materials [57].

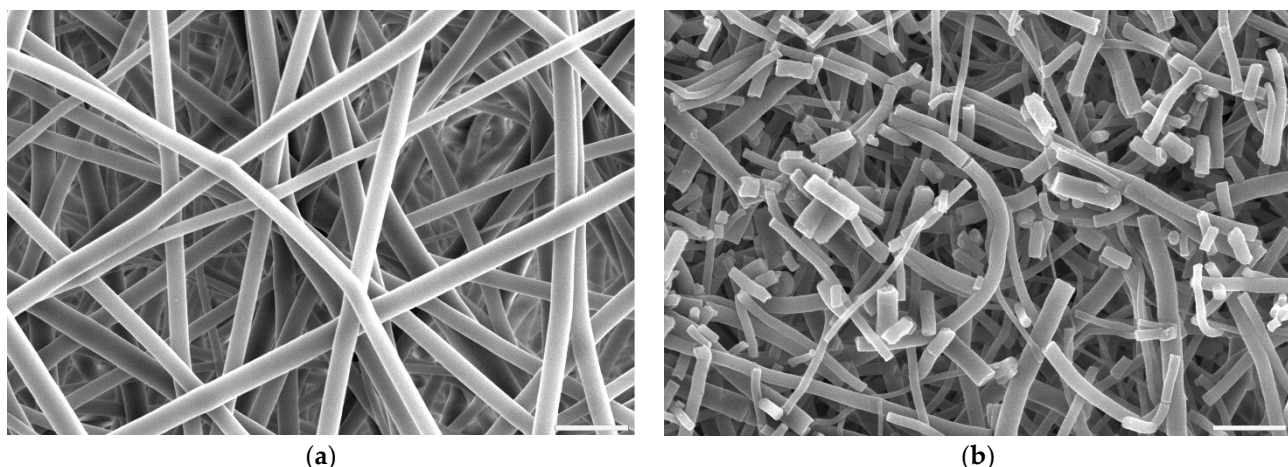


**Figure 5.** Scanning electron microscope images of PLCL nonwoven samples after surface activation at 30 °C with (a) 6% diamine for 5 min, (b) 10% diamine for 30 min. The marker is equal to 5  $\mu\text{m}$ .

### 3.1.3. The Efficacy of the -COOH Group Introduction to the Material's Surface

Both alkaline hydrolysis and oxygen plasma treatment were meant to increase -COOH group content on the surface of PLCL material to enable functionalization with gelatin

through crosslinking with EDC. Two tests were performed to assess this—Toluidine Blue O (TBO) staining and ATR-FTIR spectroscopy.

In the TBO experiment, a control untreated sample of PLCL nonwoven obtained an absorbance of 0.3 A.U. (absorbance unit). For the samples with surface activated with oxygen plasma (Figure 6a) this value increased with treatment time, reaching a plateau at 10 s time point with about 0.97 A.U. This result did not change in a significant way with longer exposure to plasma. With this method, the amount of -COOH groups on PLCL fibres' surface can be, at maximum, increased to roughly 300% of its initial content.

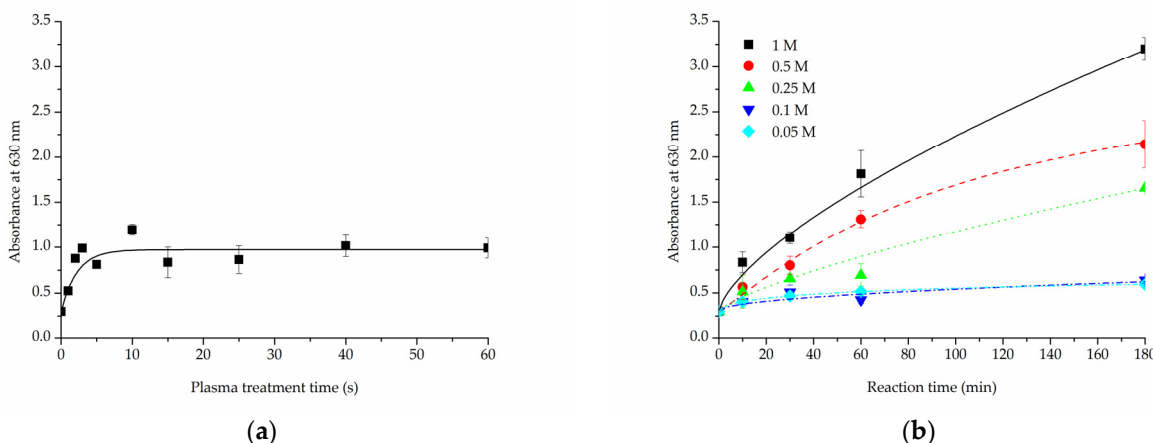


**Figure 6.** Toluidine Blue O test results for PLCL samples treated with (a) cold oxygen plasma, (b) NaOH with varying concentrations and reaction times.

The increase in -COOH groups detected on the surface of samples that underwent hydrolysis (Figure 6b) was, as predicted, relative to both NaOH concentration and reaction time. For 0.05 M and 0.1 M NaOH solutions the absorbance value increased to 0.4 A.U. after 10 min, it only reached about 0.6 A.U. even for the 3 h experiment. Much better results were achieved with solutions of higher NaOH concentrations for which the increase was more steady and steeper. For 0.5 M and 1 M NaOH solutions the absorbance measured were 7 and 10 fold, respectively, the untreated PLCL value.

For the same purpose of assessing -COOH group content on a material's surface, FTIR spectroscopy analysis was focused on C=O bond stretching vibrations. A very apparent shift can be seen for the PLCL sample subjected to extreme (1 M NaOH, 6 h) hydrolysis conditions (Figure 7). Although such conditions were not included in the final scope of experiments planned for this work, they were useful in indicating a direction of changes that could be observed with FTIR spectroscopy. A peak at  $1756\text{ cm}^{-1}$  that comes from the C=O bond that belongs to an ester group, typical for aliphatic polyesters such as PLCL, is replaced by a peak at  $1721\text{ cm}^{-1}$  that comes from the C=O bond in the -COOH group [58]. The more hydrolysed the PLCL sample is, the clearer this shift. For a sample treated with 1 M NaOH for 1 h and 3 h, an elevation indicating a  $1721\text{ cm}^{-1}$  peak is still apparent, whereas for a 0.5 M/3 h reaction the result is barely visible. Comparing these results to the TBO test it could be concluded that for a sample to show any shift in the FTIR spectrum it needs to reach at least 1.5 A.U in TBO staining. For the same reason, none of the FTIR spectra of the samples treated with oxygen plasma showed any differences in comparison to untreated PLCL material, which means this method is not as sensitive as the TBO test.

### 3.1.4. Molecular Mass Change

Each of the three surface activation methods has a different effect on the polymer's molecular weight as measured with gel permeation chromatography.

In the case of samples that underwent aminolysis and plasma treatment, a recognizable drop in molecular mass was observed. For the chosen set of reaction conditions, the plasma activation method proved to have a smaller impact on PLCL's molecular weight than

aminolysis. Oxygen plasma treatment also caused a more uniform decrease among both smaller and bigger polymer chains, whereas aminolysis induced more damage to molecules of smaller mass (Table 3, Figure 8a,b). A decrease in molecular weight after aminolysis and plasma treatment was observed by other authors [59,60].

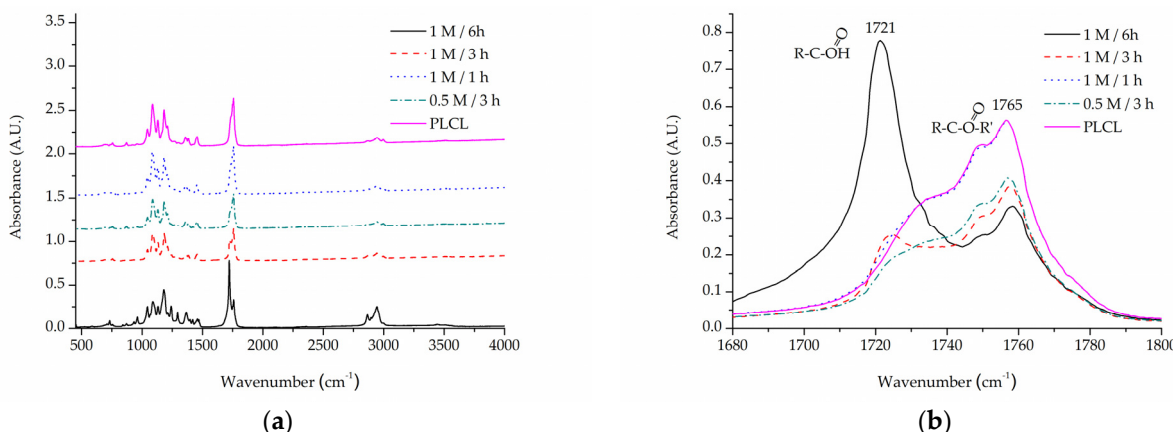


**Figure 7.** A comparison of IR spectra for PLCL samples after hydrolysis, (a) full spectrum, (b) 1680–1800  $\text{cm}^{-1}$  range that shows absorption of C=O bond stretching frequency.

**Table 3.** The changes in weight ( $M_w$ ) and number ( $M_n$ ) average molecular weight of PLCL after surface activation with different methods. Data for samples A1–A3 come from previously published work [50].

| Sample | $M_n$ (kDa) | $M_w$ (kDa) | % $M_n$ PLCL | % $M_w$ PLCL | PDI  |
|--------|-------------|-------------|--------------|--------------|------|
| PLCL   | 58.7        | 88.3        | 100%         | 100%         | 1.50 |
| A1     | 49.8        | 81.3        | 85%          | 92%          | 1.63 |
| A2     | 47.8        | 75.9        | 81%          | 86%          | 1.59 |
| A3     | 30.6        | 58.4        | 52%          | 66%          | 1.91 |
| P10    | 54.5        | 82.1        | 93%          | 93%          | 1.51 |
| P40    | 52.5        | 77.5        | 89%          | 88%          | 1.48 |
| P60    | 46.0        | 71.3        | 78%          | 81%          | 1.55 |
| H1     | 57.7        | 85.3        | 98%          | 97%          | 1.48 |
| H0.5   | 57.3        | 85.9        | 97%          | 97%          | 1.50 |
| H0.25  | 59.6        | 87.7        | 100%         | 99%          | 1.47 |
| H0.1   | 56.4        | 85.2        | 96%          | 97%          | 1.51 |
| H0.05  | 57.3        | 86.2        | 97%          | 98%          | 1.51 |

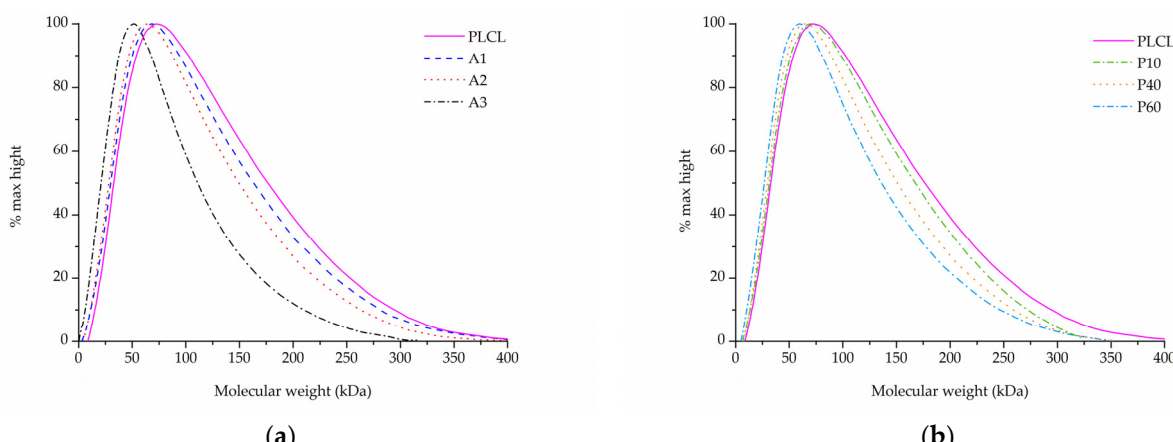


**Figure 8.** Molecular weight of PLCL treated with (a) aminolysis, (b) oxygen plasma.

In comparison to both of those methods, the surface activation with NaOH was much milder in its detrimental effect on the polymer's molecular weight when looking at the main chromatography peak (Figure 9a). However, it is important to note that hydrolysed samples lost a fraction of their mass during the activation process (Figure 3) and thus the GPC result shows the molecular mass only of the sample remaining after the hydrolysis.

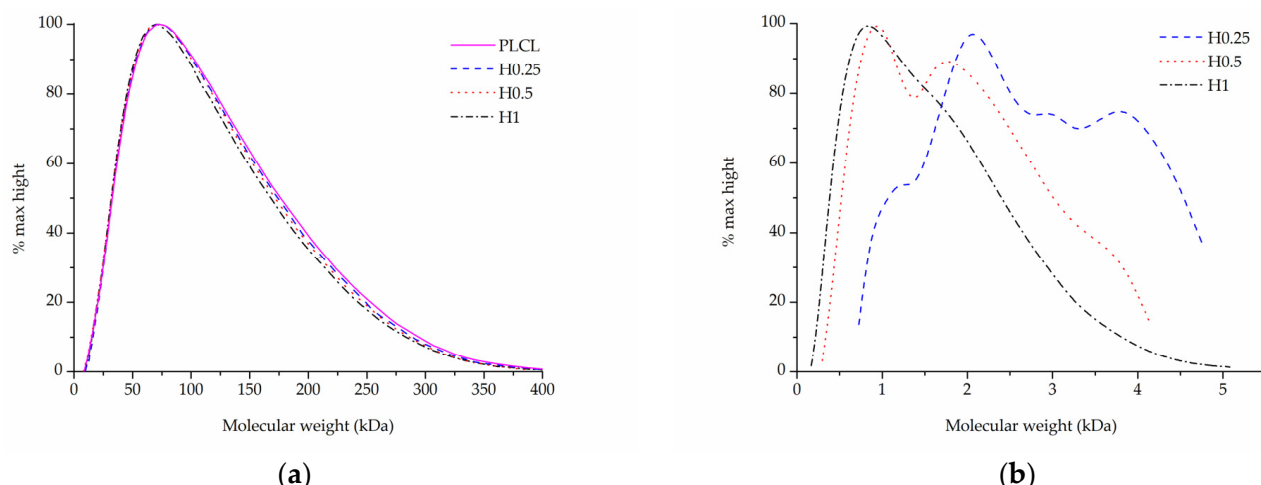


**Figure 9.** Molecular weight of PLCL treated with NaOH, (a) main peak, (b) small molecular weight peak.

Although for the highest NaOH concentration of 1 M some shortening of longer polymer chains can be seen in Figure 9a, the overall changes for both  $M_w$  and  $M_n$  are minimal for the material fraction left after hydrolysis (Table 3). Interestingly, a new second peak for very small polymer molecules can be observed for samples treated with NaOH concentrations varying from 0.25 to 1 M (Figure 9b). The higher the NaOH concentration, the smaller the molecular weight of this new peak was. It is believed that this peak shows the residues of heavily severed polymer chains that constituted the outer layers of the fibres that were degraded during hydrolysis.

Combining SEM observation of rough and frayed fibres' surface texture (Figure 2c), the mass and thickness loss of the samples (Figure 3) and a relatively small shift in molecular weight for the main chromatography peak, it was concluded that NaOH mainly affects the material's surface, leaving the core part of the fibre unscathed. In comparison, both aminolysis and oxygen plasma inflict polymer chain severing in the whole mass of the sample. For a material with a substantial molecular mass reduction ( $M_w = 11.6$  kDa,  $M_n = 6.5$  kDa) [50], fibres are prone to break, rather than fray, as can be seen in the SEM image (Figure 5d) of a sample treated with a high diamine concentrated solution for a prolonged period of time.

### 3.2. Comparison of Functionalized Materials

#### 3.2.1. Gelatin Attachment and Stability

All samples after completed functionalization underwent FTIR spectroscopy as well as BCA staining to confirm a successful attachment and measure the amount of gelatin of their surface. BCA was used then again after 1 and 7 days of stability test.

A comparison of FTIR spectra in the  $1500\text{--}1700\text{ cm}^{-1}$  range shows a clear difference between the pure PLCL sample and functionalized materials in the Amide I band region  $1600\text{--}1700\text{ cm}^{-1}$  (Figure 10). Apart from the H1 sample that has a distinct peak with a maximum of around  $1650\text{ cm}^{-1}$ , all other samples show a significant elevation in that region above the result for a pure PLCL, however, the difference between each sample is negligible. For the H1 sample, a peak in the Amide II band region is also pronounced which further proves the presence of gelatin that is attached to the surface.

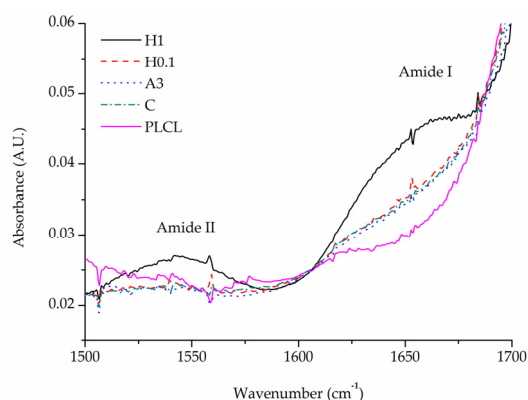


**Figure 10.** Comparison of FTIR spectra of functionalized samples.

The results of BCA staining present gelatin amounts on the fibres' surfaces at 0, 1, and 7 days of incubation in PBS and confirm what was observed in FTIR spectra analysis, that the highest gelatin amount was attached for the H1 sample (Figure 11). Much lower values were observed for other hydrolysis-activated samples with the tendency to decrease with a decline in the concentration of the solution. However, such a high value for the H1 sample could be the effect of not only the -COOH group concentration but also the high surface area of the fibre resulting from the surface fraying. There was also a positive correlation between the time of plasma treatment and the amount of gelatin. In the case of aminolysis, results are very similar for all samples without any relation between the amount of -NH<sub>2</sub> groups and the amount of gelatin. The initial amount of the gelatin on the surface of reference samples, C and CEN, was relatively high, being as high as for the P10 and P40 samples, respectively.

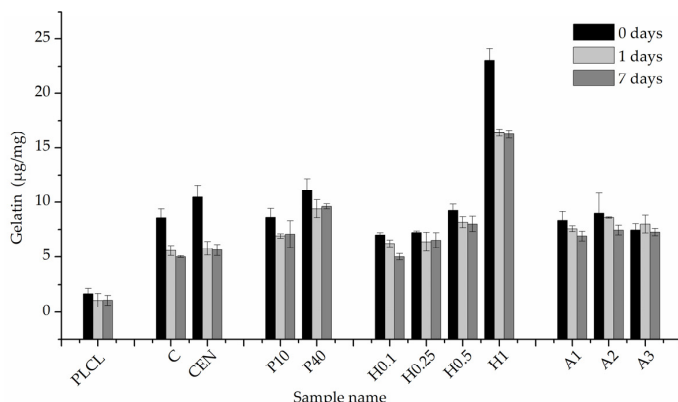


**Figure 11.** Gelatin amount on the material's surface after 0, 1 day, and 7 days of incubation in PBS.

For reference samples as well as for the H1 sample, a burst release of gelatin was observed after one day of incubation in PBS. That indicates a relatively high percentage of weakly bound absorbed gelatin, most probably due to physical interactions of polymer with gelatin molecules. In the case of the H1 sample, the likely cause of this result is its increased surface area associated with a strongly frayed surface of the fibres. For plasma-activated samples, this effect was much slighter, and even less visible for the other hydrolysed and aminolysed samples.

Results for the 7-day incubation were only slightly lower than for the 1-day incubation for all samples, which indicates the stability of gelatin coating. Except for H0.1, for all chemically modified samples, we observed higher values of gelatin amount than for both reference samples, with the highest amount equal to  $9.61 \pm 0.22 \mu\text{g}/\text{mg}$  for the P40 sample. It is worth noting that reference samples C and CEN with physically adsorbed gelatin provide 58% and 53% of the initial gelatin amount, respectively, after 7 days of incubation.

### 3.2.2. Water Contact Angle

All samples demonstrated complete ( $0^\circ$ ) wettability after functionalization with gelatin. However, there were some differences observed in the time of water drop absorption into the scaffold depending on the type of modification. The changes in wettability were also observed for some samples after the incubation in PBS.

In the case of the reference samples (Figure 12a), the initial values of contact angle were equal to  $92 \pm 21.7^\circ$  for the C sample, and  $13 \pm 29.3^\circ$  for the CEN sample, and after 7 days of incubation, the initial contact angle was close to the angle before degradation for the C sample being equal to  $80 \pm 14.13^\circ$  and increased to  $58.65 \pm 8.76^\circ$  for the CEN sample. An increase was then observed in the absorption time after 7 days of incubation for the C sample, which can be related to the degradation of the coating.

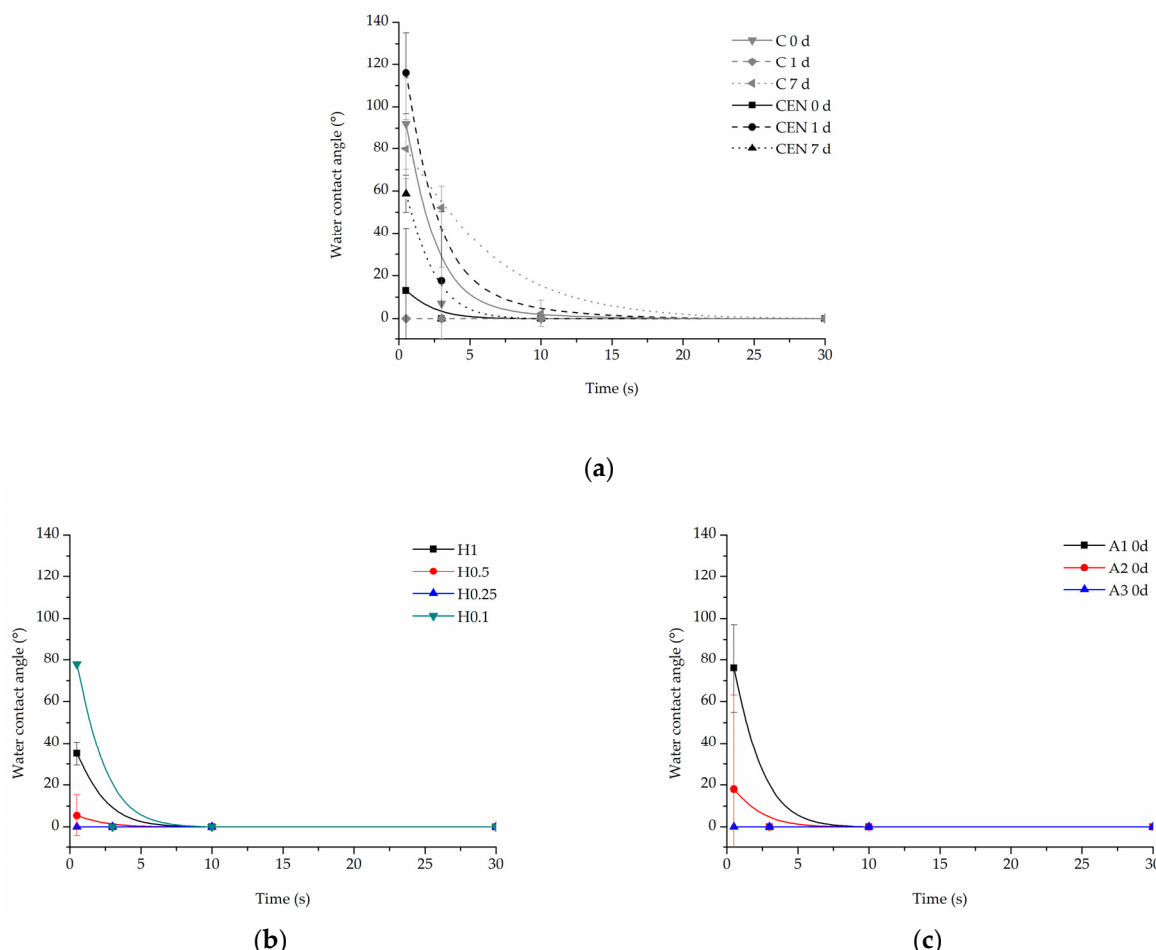


**Figure 12.** Water contact angle of PLCL nonwoven samples after surface functionalization: (a) reference samples after 0, 1, and 7 days of incubation in PBS, (b) hydrolysed samples after 7 days of incubation in PBS, and (c) aminolysed samples after surface functionalization before incubation in PBS.

Water drop on all hydrolysed samples before the degradation test was immediately absorbed, hence there is no dedicated graph. However, after incubation in PBS, the time of absorption slightly increased for hydrolysed samples (Figure 12b). There was no correlation between the amount of gelatin in these samples and the absorption time. At the 10 s time point, all hydrolysed samples have already absorbed the water drop.

In the case of aminolysed samples before the stability test, it was observed that the stronger the aminolysis parameters applied, the lower the initial contact angle value recorded. Interestingly, 7 day-incubation of PBS samples demonstrated higher wettability

with immediate absorption of the water drop, which is in contrast to the reference and hydrolysed samples (Figure 12c).

### 3.2.3. Mechanical Tests

The initial values of tensile strength and elongation at break for PLCL were equal to  $7.0 \pm 0.3$  MPa and  $427.6 \pm 28.0\%$ , respectively (Figure 13e,f). For both control samples, a significant decrease in tensile strength was observed after gelatin immobilisation (Figure 13a,e). This could be the effect of the applied temperature during gelatin immobilisation and the resulting change in the polymer structure. The plasma-treated samples demonstrated a slightly lower value of tensile strength in comparison to the reference samples (Figure 13b,e). In the case of the hydrolysed and aminolysed samples (Figure 13c–e), a gradual decrease in maximum load with the intensity of applied reaction conditions was observed. For the H1 sample, a dramatic decrease up to  $3.2 \pm 0.3$  MPa was noticed. In the case of the samples after aminolysis, this is the effect of the change in the molecular weight. It was discussed in our previous study with reference to the theoretical explanation [61]. For hydrolysed samples, this could result from the surface defects generating stress in the material.

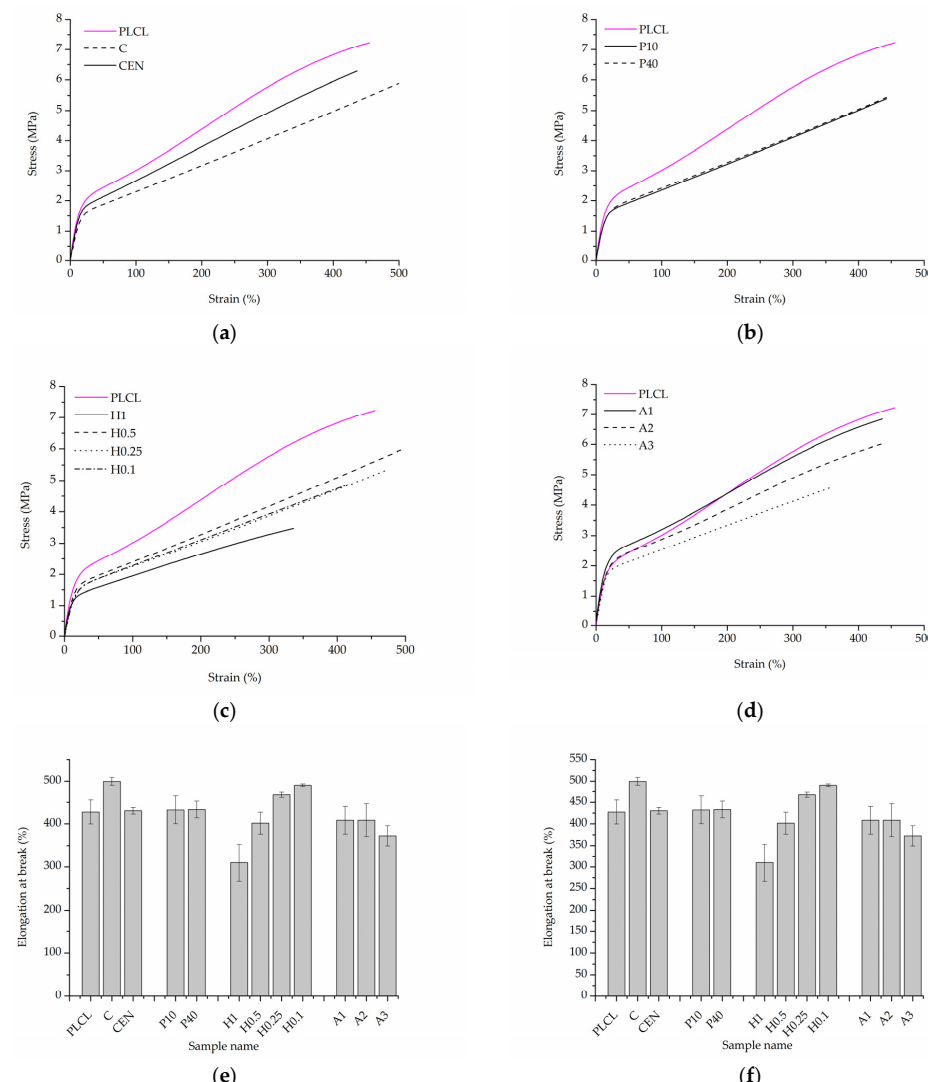


**Figure 13.** Uniaxial tensile stress test results. Stress–strain curves for: (a) control samples, (b) materials treated with plasma, (c) hydrolysis, and (d) aminolysis. Graphs comparing: (e) tensile strength, (f) elongation at break of investigated samples.

For the control sample with physically adsorbed gelatin, an increase in elongation at a break of  $499.8 \pm 9.1\%$  was observed (Figure 13f). However, that was an unexpected result and not the case for the control sample activated with EDC/NHS. In the case of plasma-treated samples, there was no change in elongation at break. The hydrolysed samples showed a slight increase in the elongation at break for lower concentrations of NaOH, and a decrease for higher concentrations, especially for the H1 sample, which is a result of surface defects as in the case of tensile strength. For A1 and A2 aminolysed samples, only a slight decrease was detected. A more significant decrease was observed for the A3 sample; however, the maximum extension value was still high being equal to  $372.8 \pm 23.5\%$ . Generally, a decrease in strain at break after aminolysis treatment is reported by other authors [62]. This is consistent with the results of the molecular weight change as a decrease in the M.W. results in a decrease in polymer chain entanglements and thus in the lower elongation at break.

### 3.2.4. Cellular Studies

The results of in vitro cytotoxicity test performed on materials' extracts showed some differences between the materials but did not indicate that any of the investigated samples were toxic to the cells (Figure 14a). All values were above 70% of the control. Plasma and NaOH treated materials (with the exception of the H1 sample) showed values above control which might mean some of the gelatin from the surface migrated to the medium and had a positive effect on the cells, but BCA test results do not prove this hypothesis.

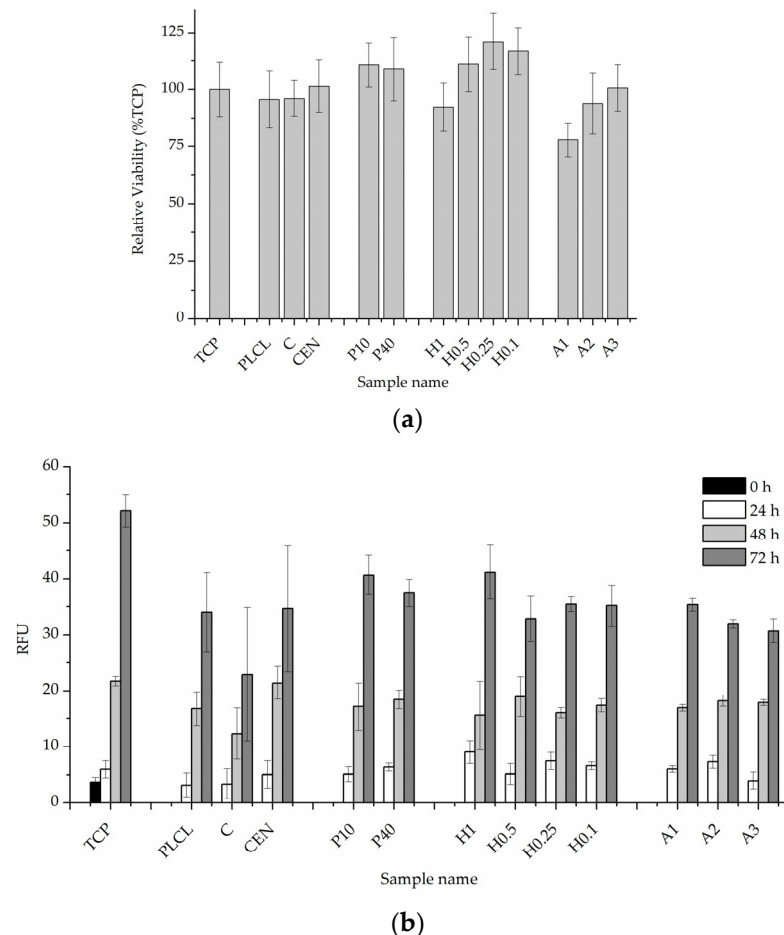


**Figure 14.** Quantitative in vitro test results, (a) 24-h cytotoxicity on material extracts, (b) 0–3 day viability, and proliferation test in direct contact with the material.

The 0–3 day experiment where cells were cultured directly on the materials' surfaces showed very similar and satisfactory results for all samples (Figure 14b). A slightly lower

value was recorded for a control material with gelatin attached only via physisorption which is difficult to explain while a pure PLCL material without any attached gelatin obtained a result on par with the rest of the functionalized nonwovens.

The observations conducted via both scanning electron and fluorescence microscopy of fibroblast cells cultured on the materials' surface showed some small differences in their morphology (Figures 15 and 16). L929 fibroblasts are a type of adherent, connective cell line that in a living tissue are responsible for the production of an extracellular matrix and a fibrous environment is their natural habitat. The less favourable the surface of the material is, the rounder a fibroblast becomes in order to minimize its contact with it. In contrast, the more native-like the surface they are seeded on is, the more likely they are to spread, extending their filopodia and lamellipodia to attach themselves to the surface [63,64].

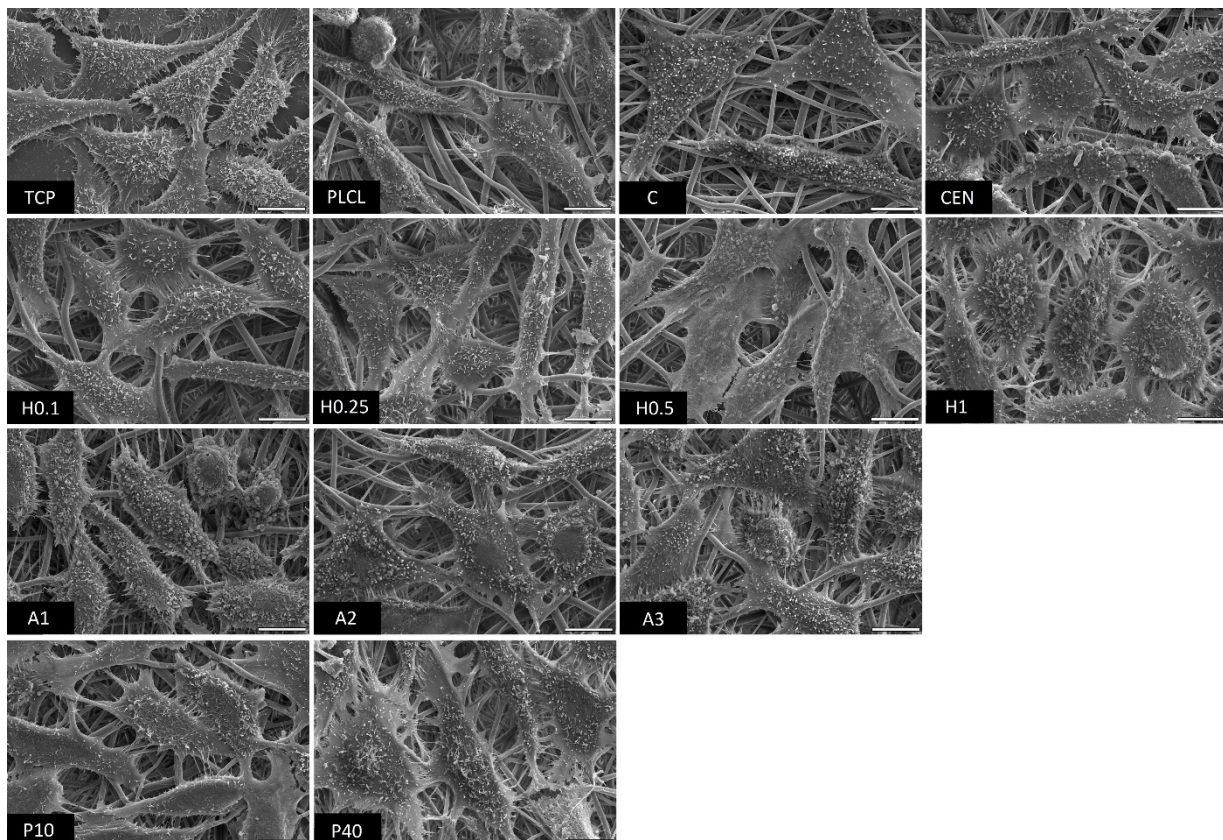


**Figure 15.** SEM microscopy images of L929 cells cultured the functionalized nonwoven materials and TCP. The marker is equal to 5  $\mu\text{m}$ .

Tissue culture polystyrene/plastic (TCP) that multiwell plates are made of is hydrophilic, and fibroblasts demonstrate flattened, spear-like or triangular, elongated shapes when cultured on its surface. The cells cultured on the PLCL and C control samples, from which one was not functionalized at all, the second had gelatin-only physisorbed and showed inferior cell morphology compared to the CEN sample or TCP. There could be seen cells in round form, or if spread, showing a visibly small number of filopodia. In the case of the rest of functionalized materials, fibroblasts showed an improved morphology and spreading with large numerous filopodia and lamellipodia in comparison to the control materials without gelatin. Among all tested samples, the fibroblast cells cultured on samples H1 and P40 showed the greatest amount of filopodia indicating these materials possessed the most attractive surface properties to the L929 cells. In the case of the H1 sample, it is believed that such a result is a consequence of increased surface area. The surface roughness of the fibres caused by hydrolysis, as was first stated in the last paragraph, is favourable by fibroblasts as it mimics native ECM and provides more sites for attachment.

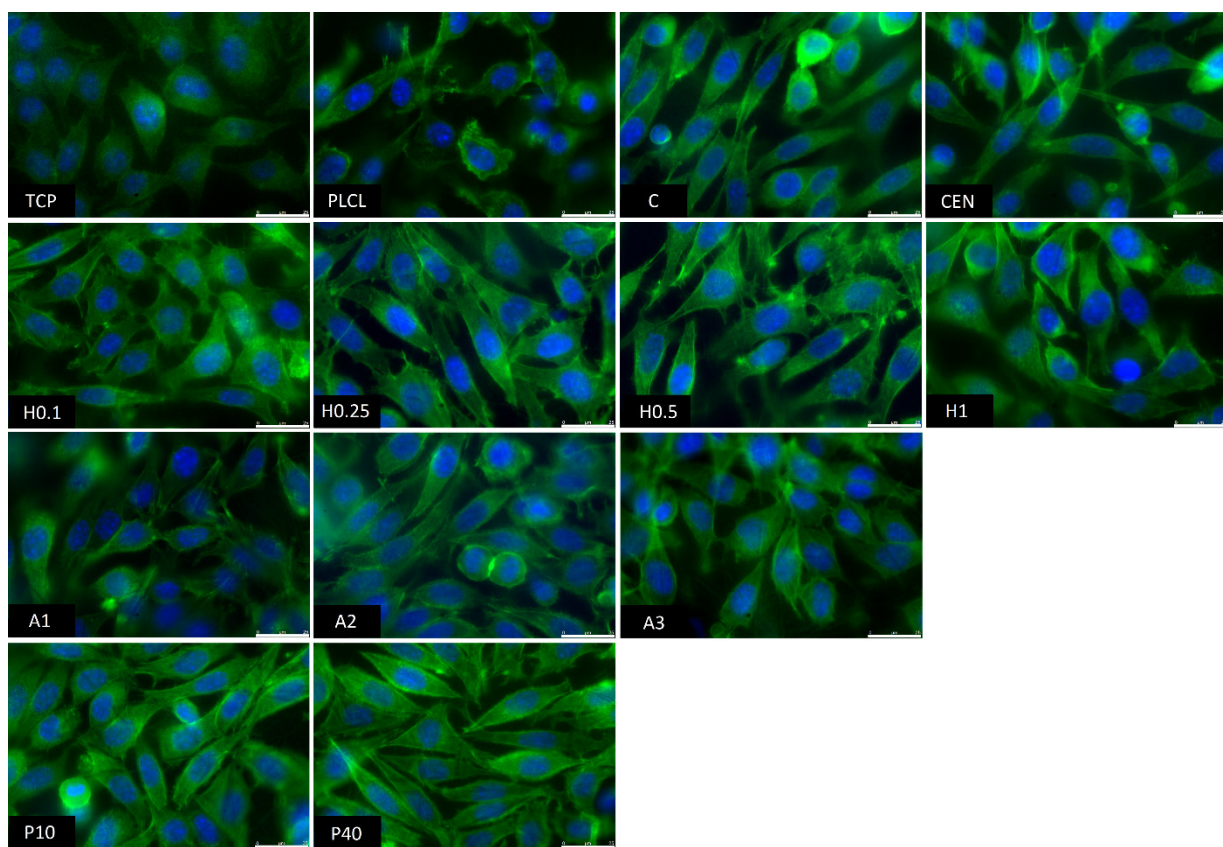


**Figure 16.** Fluorescence microscopy images of L929 cells cultured the functionalized nonwoven materials and TCP. The marker is equal to 25  $\mu$ m.

It is experimentally proven that surface chemistry modulates the conformation of adsorbed proteins [65,66]. Vallieres et al. [67] also reported differences in immobilised fibronectin conformation depending on the crosslinking method. In this study, as the -COOH groups of the polymer were activated during immersion in EDC/NHS solution after plasma and hydrolysis treatment, they were cross-linked with the -NH<sub>2</sub> groups of gelatin. Similarly, in the case of aminolysis and GTA activation, -NH<sub>2</sub> groups of gelatin were also involved in the cross-linking. Another thing to consider is if the -NH<sub>2</sub> group, which is involved in the crosslinking, originates from the RGD sequence, it could affect its further biological activity. Currently, suitable peptide exposure after immobilisation is the topic of many studies [68–70]. The proposed aminolysis-based modification differs from the hydrolysis and plasma-based methods, as in that case there is a spacer between the material surface and protein, consisting of diamine and glutaraldehyde chains. Other authors reported that this could improve the biological efficiency of the biomolecule [71,72]. However, such a positive effect of the spacer presence was not observed in this study.

#### 4. Conclusions

The main goal of this work was to compare three surface activation methods—hydrolysis, aminolysis, and cold oxygen plasma in terms of both their effect on PLCL material, as well as on enabling successful gelatin immobilization. The first part of the work consisted of the optimisation of the conditions of those processes. Discarding all samples with significantly altered morphology of the fibres and choosing the group with hydrophilic ones enabled the main part of the work to be conducted on a set of materials with more uniform properties, which facilitated the comparison of the final results of functionalized materials.

The results of all of the experiments indicated that all investigated surface activation methods were successful in being the first step of the gelatin immobilisation process. A

highly hydrophilic material with attached gelatin, which is more stable compared to the control samples, was achieved for all three tested methods.

Cellular studies showed improved morphology and spreading of cells cultured on functionalized materials compared to the untreated PLCL or the sample with physisorbed gelatin only.

A comprehensive examination of functionalized materials revealed differences in their properties that have to be taken into consideration when selecting which one of them is the most suitable for a specific medical application. A decision should be based on a specific function that the final scaffold material has to perform and the properties it needs to possess.

The most noticeable differences between the three surface activation methods were in how they affected the molecular weight of the polymer. Although both cold oxygen plasma and aminolysis caused polymer chain degradation in bulk, the hydrolysis induced damage on the surface of the material, whereas fibres' cores were barely affected.

The frayed surface of the fibres observed for samples hydrolysed with 1 M NaOH did help with gelatin attachment, as shown in the BCA test, but such harsh treatment resulted in the lack of mechanical properties and the loss of the almost 60% of material mass. Too many defects introduced to fibres' surfaces through hydrolysis weakened the material, making it prone to tearing. Aminolysis and plasma treatment with the loss of molecular weight increased brittleness.

These observations indicate that the use of any surface activation method should be limited to the lowest concentration/reaction time that enables subsequent satisfactory functionalization.

Future work following these findings should be focused on the optimisation of a surface activation method and subsequent attachment of a biologically active molecule for a specific application. Further biological studies conducted on functionalised materials must be performed with the use of cell types relevant to the chosen application.

**Author Contributions:** Conceptualization, methodology, analysis, and investigation, J.D. and O.J.; writing—original draft preparation, J.D. and O.J.; writing—review and editing, P.S., J.D. and O.J.; visualization, J.D. and O.J.; supervision, P.S.; funding acquisition, O.J., J.D. and P.S. All authors have read and agreed to the published version of the manuscript.

**Funding:** This research was funded by the POLISH NATIONAL SCIENCE CENTRE (NCN), grant number 2016/23/B/ST8/03409.

**Data Availability Statement:** The data presented in this study are available on request from the corresponding author.

**Conflicts of Interest:** The authors declare no conflict of interest.

## References

1. Gunatillake, P.A.; Adhikari, R.; Gadegaard, N. Biodegradable synthetic polymers for tissue engineering. *Eur. Cells Mater.* **2003**, *5*, 1–16. [[CrossRef](#)] [[PubMed](#)]
2. Bassani, F.; Liedl, G.L.; Wyder, P. Biological Structures. In *Encyclopedia of Condensed Matter Physics*; Ottenbrite, R.M., Javan, R., Eds.; Elsevier: Amsterdam, The Netherlands, 2005; pp. 99–108.
3. Richbourg, N.R.; Peppas, N.A.; Sikavitsas, V.I. Tuning the biomimetic behavior of scaffolds for regenerative medicine through surface modifications. *J. Tissue Eng. Regen. Med.* **2019**, *13*, 1275–1293. [[CrossRef](#)] [[PubMed](#)]
4. Qin, Y. A brief description of textile fibers. In *Medical Textile Materials*; Woodhead Publishing: Sawston, UK, 2016; pp. 23–42.
5. Dulnik, J.; Kołbuk, D.; Denis, P.; Sajkiewicz, P. The effect of a solvent on cellular response to PCL/gelatin and PCL/collagen electrospun nanofibres. *Eur. Polym. J.* **2018**, *104*, 147–156. [[CrossRef](#)]
6. Grémare, A.; Guduric, V.; Bareille, R.; Heroguez, V.; Latour, S.; L'heureux, N.; Fricain, J.C.; Catros, S.; Le Nihouannen, D.J. Characterization of printed PLA scaffolds for bone tissue engineering. *J. Biomed. Mater. Res. Part A* **2018**, *106*, 887–894. [[CrossRef](#)] [[PubMed](#)]
7. Budnicka, M.; Kołbuk, D.; Ruśkowski, P.; Gadomska-Gajadhur, A. Poly-L-lactide scaffolds with super pores obtained by freeze-extraction method. *J. Biomed. Mater. Res. Part B Appl. Biomater.* **2020**, *108*, 3162–3173. [[CrossRef](#)]

8. Felfel, R.M.; Poocza, L.; Gimeno-Fabra, M.; Milde, T.; Hildebrand, G.; Ahmed, I.; Scotchford, C.; Sottile, V.; Grant, D.M.; Liefeth, K. In vitro degradation and mechanical properties of PLA-PCL copolymer unit cell scaffolds generated by two-photon polymerization. *Biomed. Mater.* **2016**, *11*, 015011. [[CrossRef](#)]
9. Takayama, T.; Todo, M.; Tsuji, H. Effect of annealing on the mechanical properties of PLA/PCL and PLA/PCL/LTI polymer blends. *J. Mech. Behav. Biomed. Mater.* **2011**, *4*, 255–260. [[CrossRef](#)]
10. Kolbuk, D.; Jeznach, O.; Wrzecionek, M.; Gadomska-Gajadhur, A. Poly(Glycerol Succinate) as an Eco-Friendly Component of PLLA and PLCL Fibres towards Medical Applications. *Polymers* **2020**, *12*, 1731. [[CrossRef](#)]
11. Janmohammadi, M.; Nourbakhsh, M.S.; Bonakdar, S. Electrospun Skin Tissue Engineering Scaffolds Based on Polycaprolactone/Hyaluronic Acid/L-ascorbic Acid. *Fibers Polym.* **2021**, *22*, 19–29. [[CrossRef](#)]
12. Leal, B.B.J.; Wakabayashi, N.; Oyama, K.; Kamiya, H.; Braghierioli, D.I.; Pranke, P. Vascular Tissue Engineering: Polymers and Methodologies for Small Caliber Vascular Grafts. *Front. Cardiovasc. Med.* **2021**, *7*, 592361. [[CrossRef](#)]
13. Altun, E.; Aydogdu, M.O.; Togay, S.O.; Sengil, A.Z.; Ekren, N.; Haskoylu, M.E.; Oner, E.T.; Altuncu, N.A.; Ozturk, G.; Crabbe-Mann, M.; et al. Bioinspired scaffold induced regeneration of neural tissue. *Eur. Polym. J.* **2019**, *114*, 98–108. [[CrossRef](#)]
14. Kim, H.Y.; Chun, S.Y.; Lee, E.H.; Kim, B.; Ha, Y.S.; Chung, J.W.; Lee, J.N.; Kim, B.S.; Oh, S.H.; Kwon, T.G. Bladder Regeneration Using a Polycaprolactone Scaffold with a Gradient Structure and Growth Factors in a Partially Cystectomized Rat Model. *J. Korean Med. Sci.* **2020**, *35*, e374. [[CrossRef](#)] [[PubMed](#)]
15. Gentile, P.; Chiono, V.; Carmagnola, I.; Hatton, P.V. An Overview of Poly(lactic-co-glycolic) Acid (PLGA)-Based Biomaterials for Bone Tissue Engineering. *Int. J. Mol. Sci.* **2014**, *15*, 3640–3659. [[CrossRef](#)] [[PubMed](#)]
16. Erisken, C.; Zhang, X.; Moffat, K.L.; Levine, W.N.; Lu, H.H. Scaffold Fiber Diameter Regulates Human Tendon Fibroblast Growth and Differentiation. *Tissue Eng. Part A* **2013**, *19*, 519–528. [[CrossRef](#)] [[PubMed](#)]
17. Nakayama, K.H.; Batchelder, C.A.; Lee, C.I.; Tarantal, A.F. Decellularized rhesus monkey kidney as a three-dimensional scaffold for renal tissue engineering. *Tissue Eng. Part A* **2010**, *16*, 2207–2216. [[CrossRef](#)]
18. Gupta, S.K.; Mishra, N.C.; Dhasmana, A. Decellularization Methods for Scaffold Fabrication. *Methods Mol. Biol.* **2018**, *1577*, 1–10. [[CrossRef](#)]
19. Taylor, D.A.; Sampaio, L.C.; Ferdous, Z.; Gobin, A.S.; Taite, L.J. Decellularized matrices in regenerative medicine. *Acta Biomater.* **2018**, *74*, 74–89. [[CrossRef](#)]
20. Rhee, S.; Puetzer, J.L.; Mason, B.N.; Reinhart-King, C.A.; Bonassar, L.J. 3D Bioprinting of Spatially Heterogeneous Collagen Constructs for Cartilage Tissue Engineering. *ACS Biomater. Sci. Eng.* **2016**, *2*, 1800–1805. [[CrossRef](#)]
21. Choi, D.J.; Park, S.J.; Gu, B.K.; Kim, Y.J.; Chung, S.; Kim, C.H. Effect of the pore size in a 3D bioprinted gelatin scaffold on fibroblast proliferation. *J. Ind. Eng. Chem.* **2018**, *67*, 388–395. [[CrossRef](#)]
22. Irawan, V.; Sung, T.C.; Higuchi, A.; Ikoma, T. Collagen Scaffolds in Cartilage Tissue Engineering and Relevant Approaches for Future Development. *Tissue Eng. Regen. Med.* **2018**, *15*, 673–697. [[CrossRef](#)]
23. Dai, N.T.; Williamson, M.R.; Khammo, N.; Adams, E.F.; Coombes, A.G.A. Composite cell support membranes based on collagen and polycaprolactone for tissue engineering of skin. *Biomaterials* **2004**, *25*, 4263–4271. [[CrossRef](#)] [[PubMed](#)]
24. Mishra, R.; Varshney, R.; Das, N.; Sircar, D.; Roy, P. Synthesis and characterization of gelatin-PVP polymer composite scaffold for potential application in bone tissue engineering. *Eur. Polym. J.* **2019**, *119*, 155–168. [[CrossRef](#)]
25. Theodoridis, K.; Aggelidou, E.; Manthou, M.; Demiri, E.; Bakopoulou, A.; Kritis, A. Assessment of cartilage regeneration on 3D collagen-polycaprolactone scaffolds: Evaluation of growth media in static and in perfusion bioreactor dynamic culture. *Colloids Surf. B Biointerfaces* **2019**, *183*, 110403. [[CrossRef](#)] [[PubMed](#)]
26. Huettner, N.; Dargaville, T.R.; Forget, A. Discovering Cell-Adhesion Peptides in Tissue Engineering: Beyond RGD. *Trends Biotechnol.* **2018**, *36*, 372–383. [[CrossRef](#)] [[PubMed](#)]
27. D’Souza, S.E.; Ginsberg, M.H.; Plow, E.F. Arginyl-glycyl-aspartic acid (RGD): A cell adhesion motif. *Trends Biochem. Sci.* **1991**, *16*, 246–250. [[CrossRef](#)] [[PubMed](#)]
28. Khew, S.T.; Tong, Y.W. The specific recognition of a cell binding sequence derived from type I collagen by Hep3B and L929 cells. *Biomacromolecules* **2007**, *8*, 3153–3161. [[CrossRef](#)]
29. Ma, Z.; He, W.; Yong, T.; Ramakrishna, S. Grafting of Gelatin on Electrospun Poly(caprolactone) Nanofibers to Improve Endothelial Cell Spreading and Proliferation and to Control Cell Orientation. *Tissue Eng.* **2005**, *11*, 1149–1158. [[CrossRef](#)]
30. Paredes, J.A.U.; Polini, A.; Chrzanowski, W. Protein-based Biointerfaces to Control Stem Cell Differentiation. *RSC Smart Mater.* **2015**, *2015*, 3–29. [[CrossRef](#)]
31. He, L.; Shi, Y.; Han, Q.; Zuo, Q.; Ramakrishna, S.; Xue, W.; Zhou, L. Surface Modification of Electrospun Nanofibrous Scaffolds via Polysaccharide-Protein Assembly Multilayer for Neurite Outgrowth. *J. Mater. Chem.* **2012**, *22*, 13187–13196. [[CrossRef](#)]
32. Katti, D.; Vasita, R.; Shanmugam, K. Improved Biomaterials for Tissue Engineering Applications: Surface Modification of Polymers. *Curr. Top. Med. Chem.* **2008**, *8*, 341–353. [[CrossRef](#)]
33. Croll, T.I.; O’Connor, A.J.; Stevens, G.W.; Cooper-White, J.J. Controllable surface modification of poly(lactic-co-glycolic acid) (PLGA) by hydrolysis or aminolysis I: Physical, chemical, and theoretical aspects. *Biomacromolecules* **2004**, *5*, 463–473. [[CrossRef](#)] [[PubMed](#)]
34. Ma, Z.; Mao, Z.; Gao, C. Surface modification and property analysis of biomedical polymers used for tissue engineering. *Colloids Surf. B Biointerfaces* **2007**, *60*, 137–157. [[CrossRef](#)] [[PubMed](#)]

35. Durrieu, M.C.; Pallu, S.; Guillemot, F.; Bareille, R.; Amédée, J.; Baquey, C.; Labrugre, C.; Dard, M. Grafting RGD containing peptides onto hydroxyapatite to promote osteoblastic cells adhesion. *J. Mater. Sci. Mater. Med.* **2004**, *15*, 779–786. [CrossRef]
36. Barbosa, M.; Vale, N.; Costa, F.M.; Martins, M.C.L.; Gomes, P. Tethering antimicrobial peptides onto chitosan: Optimization of azide-alkyne “click” reaction conditions. *Carbohydr. Polym.* **2017**, *165*, 384–393. [CrossRef] [PubMed]
37. Qiu, Y.; Mao, Z.; Zhao, Y.; Zhang, J.; Guo, Q.; Gou, Z.; Gao, C. Polycaprolactone scaffold modified with galactosylated chitosan for hepatocyte culture. *Macromol. Res.* **2012**, *20*, 283–291. [CrossRef]
38. Gong, Y.; Zhu, Y.; Liu, Y.; Ma, Z.; Gao, C.; Shen, J. Layer-by-layer assembly of chondroitin sulfate and collagen on aminolyzed poly(l-lactic acid) porous scaffolds to enhance their chondrogenesis. *Acta Biomater.* **2007**, *3*, 677–685. [CrossRef]
39. Korogiannaki, M.; Zhang, J.; Sheardown, H. Surface modification of model hydrogel contact lenses with hyaluronic acid via thiol-ene “click” chemistry for enhancing surface characteristics. *J. Biomater. Appl.* **2017**, *32*, 446–462. [CrossRef]
40. Rasal, R.M.; Janorkar, A.V.; Hirt, D.E. Poly(lactic acid) modifications. *Prog. Polym. Sci.* **2010**, *35*, 338–356. [CrossRef]
41. Becker, J.M.; Pounder, R.J.; Dove, A.P. Synthesis of poly (lactide)s with modified thermal and mechanical properties. *Macromol. Rapid Commun.* **2010**, *31*, 1923–1937. [CrossRef]
42. Salhi, S.; Mahfoudh, J.; Abid, S.; Atanase, L.I.; Popa, M.; Delaite, C. Random poly( $\epsilon$ -caprolactone-L-alanine) by direct melt copolymerization. *Polym. Int.* **2020**, *69*, 1161–1168. [CrossRef]
43. Vilay, V.; Mariatti, M.; Ahmad, Z.; Pasomsouk, K.; Todo, M. Characterization of the mechanical and thermal properties and morphological behavior of biodegradable poly(L-lactide)/poly( $\epsilon$ -caprolactone) and poly(L-lactide)/poly(butylene succinate-co-L-lactate) polymeric blends. *J. Appl. Polym. Sci.* **2009**, *114*, 1784–1792. [CrossRef]
44. Hiljanen-Vainio, M.; Karjalainen, T.; Seppala, J. Biodegradable lactone copolymers. I. Characterization and mechanical behavior of  $\epsilon$ -caprolactone and lactide copolymers. *J. Appl. Polym. Sci.* **1996**, *59*, 1281–1288. [CrossRef]
45. Vieira, A.C.; Guedes, R.M.; Marques, A.T. Development of ligament tissue biodegradable devices: A review. *J. Biomech.* **2009**, *42*, 2421–2430. [CrossRef] [PubMed]
46. Hiljanen-Vainio, M.P.; Orava, P.A.; Seppala, J.V. Properties of  $\epsilon$ -caprolactone/DL-lactide ( $\epsilon$ -CL/DL-LA) copolymers with a minor  $\epsilon$ -CL content. *J. Biomed. Mater. Res.* **1997**, *34*, 39–46. [CrossRef]
47. Lu, X.L.; Cai, W.; Gao, Z.Y. Shape-memory behaviors of biodegradable poly(L-lactide-co- $\epsilon$ -caprolactone) copolymers. *J. Appl. Polym. Sci.* **2008**, *108*, 1109–1115. [CrossRef]
48. Laurent, C.P.; Vaquette, C.; Liu, X.; Schmitt, J.F.; Rahouadj, R. Suitability of a PLCL fibrous scaffold for soft tissue engineering applications: A combined biological and mechanical characterisation. *J. Biomater. Appl.* **2018**, *32*, 1276–1288. [CrossRef]
49. Eastoe, J.E. The amino acid composition of mammalian collagen and gelatin. *Biochem. J.* **1955**, *61*, 589–600. [CrossRef] [PubMed]
50. Jeznach, O.; Kolbuk, D.; Marzec, M.; Bernasik, A.; Sajkiewicz, P. Aminolysis as a surface functionalization method of aliphatic polyester nonwovens: Impact on material properties and biological response. *RSC Adv.* **2022**, *12*, 11303–11317. [CrossRef]
51. Gupta, B.; Plummer, C.; Bisson, I.; Frey, P.; Hilborn, J. Plasma-induced graft polymerization of acrylic acid onto poly(ethylene terephthalate) films: Characterization and human smooth muscle cell growth on grafted films. *Biomaterials* **2002**, *23*, 863–871. [CrossRef]
52. Nuutila, M. Gel Permeation Chromatography Methods in the Analysis of Lactide-Based Polymer. Master’s Thesis, University of Jyväskylä, Jyväskylä, Finland, 2018. Available online: <http://urn.fi/URN:NBN:fi:jyu-201811054624> (accessed on 15 June 2022).
53. Bu, Y.; Ma, J.; Bei, J.; Wang, S. Surface Modification of Aliphatic Polyester to Enhance Biocompatibility. *Front. Bioeng. Biotechnol.* **2019**, *7*, 1–10. [CrossRef]
54. Bhattacharjee, P.; Naskar, D.; Kim, H.W.; Maiti, T.K.; Bhattacharya, D.; Kundu, S.C. Non-mulberry silk fibroin grafted PCL nanofibrous scaffold: Promising ECM for bone tissue engineering. *Eur. Polym. J.* **2015**, *71*, 490–509. [CrossRef]
55. Monnier, A.; Al Tawil, E.; Nguyen, Q.T.; Valletton, J.M.; Fatyeyeva, K.; Deschrevel, B. Functionalization of poly (lactic acid) scaffold surface by aminolysis and hyaluronan immobilization: How it affects mesenchymal stem cell proliferation. *Eur. Polym. J.* **2018**, *107*, 202–217. [CrossRef]
56. Toledo, A.L.M.M.; Ramalho, B.S.; Picciani, P.H.S.; Baptista, L.S.; Martinez, A.M.B.; Dias, M.L. Effect of three different amines on the surface properties of electrospun polycaprolactone mats. *Int. J. Polym. Mater. Polym. Biomater.* **2021**, *70*, 1258–1270. [CrossRef]
57. Polini, A.; Petre, D.G.; Iafisco, M.; de Lacerda Schickert, S.; Tampieri, A.; van den Beucken, J.; Leeuwenburgh, S.C.G. Polyester Fibers Can Be Rendered Calcium Phosphate-Binding by Surface Functionalization with Bisphosphonate Groups. *J. Biomed. Mater. Res. Part A* **2017**, *105*, 2335–2342. [CrossRef]
58. Mistry, B.D. *A Handbook of Spectroscopic Data Chemistry (UV, JR, PMR, JCNMR and Mass Spectroscopy)*; Oxford Book Company: Oxford, UK, 2009.
59. Zhu, Y.; Mao, Z.; Shi, H.; Gao, C. In-Depth Study on Aminolysis of Poly( $\epsilon$ -Caprolactone): Back to the Fundamentals. *Sci. China Chem.* **2012**, *55*, 2419–2427. [CrossRef]
60. Weidner, S.; Kühn, G.; Decker, R.; Roessner, D.; Friedrich, J. Influence of Plasma Treatment on the Molar Mass of Poly(Ethylene Terephthalate) Investigated by Different Chromatographic and Spectroscopic Methods. *J. Polym. Sci. Part A Polym. Chem.* **1998**, *36*, 1639–1648. [CrossRef]
61. Jeznach, O.; Kolbuk, D.; Sajkiewicz, P. Aminolysis of Various Aliphatic Polyesters in a Form of Nanofibers and Films. *Polymers* **2019**, *11*, 1669. [CrossRef]
62. Oliveira, S.; Felizardo, T.; Amorim, S.; Mithieux, S.M.; Pires, R.A.; Reis, R.L.; Martins, A.; Weiss, A.S.; Neves, N.M. Tubular Fibrous Scaffolds Functionalized with Tropoelastin as a Small-Diameter Vascular Graft. *Biomacromolecules* **2020**, *21*, 3582–3595. [CrossRef]

63. Abercrombie, M. Fibroblasts. *J. Clin. Pathol. Suppl. (R. Coll. Pathol.)* **1978**, *12*, 1–6. Available online: <https://www.ncbi.nlm.nih.gov/pmc/articles/PMC1347118/> (accessed on 15 June 2022).
64. Kurashina, Y.; Miyata, S.; Komotori, J.; Koyama, T. Proliferation and Adhesion of L929 Fibroblasts on Surface with Different Microtopography. *Mater. Res. Soc. Symp. Proc.* **2014**, *1648*, 101. [CrossRef]
65. Stephansson, S.N.; Byers, B.A.; García, A.J. Enhanced expression of the osteoblastic phenotype on substrates that modulate fibronectin conformation and integrin receptor binding. *Biomaterials* **2002**, *23*, 2527–2534. [CrossRef] [PubMed]
66. Keselowsky, B.G.; Collard, D.M.; García, A.J. Surface chemistry modulates fibronectin conformation and directs integrin binding and specificity to control cell adhesion. *J. Biomed. Mater. Res. Part A* **2003**, *66*, 247–259. [CrossRef] [PubMed]
67. Vallières, K.; Chevallier, P.; Sarra-Bournet, C.; Turgeon, S.; Laroche, G. AFM imaging of immobilized fibronectin: Does the surface conjugation scheme affect the protein orientation/conformation? *Langmuir* **2007**, *23*, 9745–9751. [CrossRef] [PubMed]
68. Liu, Y.; Mahara, A.; Kambe, Y.; Hsu, Y.-I.; Yamaoka, T. Endothelial cell adhesion and blood response to hemocompatible peptide 1 (HCP-1), REDV, and RGD peptide sequences with free N-terminal amino groups immobilized on a biomedical expanded polytetrafluoroethylene surface. *Biomater. Sci.* **2021**, *9*, 1034–1043. [CrossRef] [PubMed]
69. Fischer, N.G.; He, J.; Aparicio, C. Surface Immobilization Chemistry of a Laminin-Derived Peptide Affects Keratinocyte Activity. *Coatings* **2020**, *10*, 560. [CrossRef]
70. Vida, Y.; Collado, D.; Najera, F.; Claros, S.; Becerra, J.; Andrade, J.A.; Perez-Inestrosa, E. Dendrimer surface orientation of the RGD peptide affects mesenchymal stem cell adhesion. *RSC Adv.* **2016**, *6*, 49839–49844. [CrossRef]
71. Yuan, L.; Yu, Q.; Li, D.; Chen, H. Surface Modification to Control Protein/Surface Interactions. *Macromol. Biosci.* **2011**, *11*, 1031–1040. [CrossRef]
72. Hern, D.L.; Hubbell, J.A. Incorporation of adhesion peptides into nonadhesive hydrogels useful for tissue resurfacing. *J. Biomed. Mater. Res.* **1998**, *39*, 266–276. [CrossRef]

**OŚWIADCZENIA DOKTORANTA  
O UDZIALE W PUBLIKACJACH  
NAUKOWYCH**



## Oświadczenie doktoranta o udziale w publikacji naukowej

Niniejszym potwierdzam, że mój wkład w przygotowanie **publikacji nr 1**, tj. Jeznach O., Kołbuk D., Sajkiewicz P., Aminolysis of various aliphatic polyesters in a form of nanofibers and films, Polymers, Vol.11, No.10, pp.1669-1-16, 2019, obejmował dyskusję i określenie koncepcji badań, wykonanie przeglądu literatury, otrzymanie włóknin poliestrowych metodą elektroprzędzenia i folii poliestrowych metodą odlewania z roztworu, przeprowadzenie reakcji aminolizy na włókninach i foliach poliestrowych, wykonanie badań stężenia przyłączonych grup aminowych za pomocą testu ninhydrynowego, wykonanie badań próbek metodą spektroskopii ATR-FTIR, przeprowadzenie 1-osiowej próby rozciągania próbek, wykonanie badań zwilżalności próbek, zebranie, opracowanie i dyskusję wyników przeprowadzonych badań, przygotowanie i redagowanie tekstu manuskryptu, przygotowanie odpowiedzi dla recenzentów. Jestem autorem korespondencyjnym niniejszej publikacji.

### Podpis doktorantki

A handwritten signature in blue ink, appearing to read "Olaśnia Jeznach".

### Podpis promotora

A handwritten signature in blue ink, appearing to read "Sajkiewicz".

### Podpis współautorów

- dr inż. Dorota Kołbuk-Konieczny D. Kołbuk



## Oświadczenie doktoranta o udziale w publikacji naukowej

Niniejszym potwierdzam, że mój wkład w przygotowanie publikacji nr 2, tj. Jeznach O., Kołbuk D., Marzec M., Bernasik A., Sajkiewicz P., Aminolysis as a surface functionalization method of aliphatic polyester nonwovens: impact on material properties and biological response, RSC Advances, Vol.12, No.18, pp.11303-11317, 2022, obejmował dyskusję i określenie koncepcji badań, wykonanie przeglądu literatury, otrzymanie włóknin poliestrowych metodą elektroprzędzenia, przeprowadzenie reakcji aminolizy na włókninach, wykonanie badań stężenia przyłączonych grup aminowych za pomocą testu ninhydrynowego, wykonanie obrazowania próbek za pomocą mikroskopii SEM, wykonanie badań zwilżalności próbek, wykonanie badań zmian średniej masy cząsteczkowej próbek za pomocą chromatografii żelowej, przeprowadzenie 1-osiowej próby rozciągania próbek, wykonanie badań próbek metodą spektroskopii ATR-FTIR, wykonanie obrazowania komórek metodą mikroskopii SEM, zebranie, opracowanie i dyskusję wyników przeprowadzonych badań, wykonanie analizy statystycznej, przygotowanie i redagowanie tekstu manuskryptu, przygotowanie odpowiedzi dla recenzentów.

Podpis doktorantki

A handwritten signature in blue ink, appearing to read "Olga Jeznach".

Podpis promotora

A handwritten signature in blue ink, appearing to read "Piotr Sajkiewicz".

Podpisy współautorów

- dr inż. Dorota Kołbuk-Konieczny D. Kołbuk
- dr inż. Mateusz Marzec M. Marzec
- prof. dr hab. inż. Andrzej Bernasik A. Bernasik



## Oświadczenie doktoranta o udziale w publikacji naukowej

Niniejszym potwierdzam, że mój wkład w przygotowanie **publikacji nr 3**, tj. Jeznach O., Kołbuk D., Reich T., Sajkiewicz P., Immobilization of Gelatin on Fibers for Tissue Engineering Applications: A Comparative Study of Three Aliphatic Polyesters, Polymers, Vol.14, No.19, pp.4154-1-21, 2022, obejmował dyskusję i określenie koncepcji badań, wykonanie przeglądu literatury, otrzymanie włóknin poliestrowych metodą elektroprzędzenia, przeprowadzenie reakcji aminolizy na włókninach, przeprowadzenie przyłączania żelatyny do powierzchni włókien, wykonanie obrazowania próbek za pomocą mikroskopii SEM, wykonanie badań stężenia przyłączonej żelatyny za pomocą testu BCA, wykonanie badań zmian odczynu pH roztworów żelatyny, wykonanie badań zwilżalności próbek, wykonanie badań swobodnej energii powierzchniowej próbek, przeprowadzenie 1-osiowej próby rozciągania próbek, wykonanie badań stabilności przyłączonej żelatyny, zebranie, opracowanie i dyskusję wyników przeprowadzonych badań, wykonanie analizy statystycznej, przygotowanie i redagowanie tekstu manuskryptu, przygotowanie odpowiedzi dla recenzentów. Jestem autorem korespondencyjnym niniejszej publikacji.

Podpis doktorantki

A handwritten signature in blue ink that reads "Olga Jeznach".

Podpis promotora

A handwritten signature in blue ink that reads "Paweł Sajkiewicz".

Podpisy współautorów

- dr inż. Dorota Kołbuk-Konieczny D. Kołbuk
- prof. Tobias Reich T. Reich



## Oświadczenie doktoranta o udziale w publikacji naukowej

Niniejszym potwierdzam, że mój wkład w przygotowanie **publikacji nr 4**, tj. Dulnik J., Jeznach O., Sajkiewicz P., A Comparative Study of Three Approaches to Fibre's Surface Functionalization, Journal of Functional Biomaterials, Vol.13, No.4, pp.272-1-23, 2022, obejmował dyskusję i określenie koncepcji badań, wykonanie przeglądu literatury, otrzymanie włóknin poliestrowych metodą elektroprzędzenia, przeprowadzenie reakcji aminolizy na włókninach, przeprowadzenie przyłączania żelatyny do powierzchni włókien poddanych aminolizie, wykonanie badań stężenia przyłączonej żelatyny za pomocą testu BCA, wykonanie badań stabilności przyłączonej żelatyny, zebranie, opracowanie i dyskusję wyników powyższych badań, interpretację wyników badań zwilżalności próbek po przyłączaniu żelatyny i wyników badań mechanicznych oraz udział w dyskusji innych wyników badań dotyczących metod przyłączania żelatyny, przygotowaniu i redagowaniu tekstu manuskryptu.

**Podpis doktorantki**

A handwritten signature in blue ink, appearing to read "Olga Jeznach".

**Podpis promotora**

A handwritten signature in blue ink, appearing to read "Piotr Sajkiewicz".

**Podpisy współautorów**

- mgr inż. Judyta Dulnik

A handwritten signature in blue ink, appearing to read "Judyta Dulnik".